

**Investigating cellular 2'-deoxyribonucleotide pools as
targets for non-small cell lung cancer therapy**

Thesis submitted for the degree of

Doctor of Philosophy

at the University of Leicester

by

Hussein Hadi Khairi Abbas

Radiation & Oxidative Stress Group

Department of Cancer Studies

University of Leicester

Supervisors

Dr. Steven S. Foster (Department of Genetics)

Prof. George DD Jones (Department of Cancer Studies)

2017

Abstract

Investigating cellular 2'-deoxyribonucleotide pools as targets for non-small cell lung cancer therapy

Hussein Hadi Khairi Abbas

Free 2'-deoxyribonucleotide triphosphates (dNTPs) are vulnerable to oxidation by reactive oxygen species (ROS) formed both as by-products of intracellular metabolism and from other exogenous oxidising agents. NUDT1 hydrolyses oxidised dNTPs to prevent their misincorporation into genomic DNA. Given that oxidative stress is a cancer hallmark, NUDT1 activity was proposed essential for cancer cell growth but non-essential in normal cells. Recently, potent and highly selective NUDT1 small molecule inhibitors have highlighted a new cancer therapeutic approach which could convert oxidative stress into cytotoxic DNA damage with eventual cancer cell death.

To assess the potential clinical relevance of NUDT1 inhibition for improving lung cancer cell targeting, this study aimed to test the genotoxic and cytotoxic effects of NUDT1 deficiency (siRNA-mediated knockdown or small-molecule inhibition) on H23, H522 and A549 non-small-cell lung cancer (NSCLC) cells relative to normal MRC-5 lung fibroblasts, and whether NUDT1 knockdown could augment current therapies.

The siRNA-mediated NUDT1 knockdown increased oxidatively damaged DNA levels and DNA damage signaling alterations in all lung cancer cell lines but not normal fibroblasts, despite no detectable differences in ROS levels between the lines. Unexpectedly, NUDT1 knockdown did not induce apoptosis in NSCLC cells, or enhance the effect of gemcitabine, cisplatin or radiation in combination treatments. We similarly studied the effects of NUDT1 inhibitors, TH287 and TH588. Inhibitor treatment increased oxidative DNA damage in H23 cells only, but induced apoptosis in H23 and H522 cells, indicating that they kill cells independently of DNA oxidation and seemingly via NUDT1-distinct mechanisms.

In conclusion, we show that NUDT1 has a specific role in lung cancer cells for suppressing oxidative DNA damage levels and genomic instability, though surprisingly the basis of this may not be related to ROS levels. However, targeting NUDT1 is not an effective therapeutic strategy; rather it induces non-cytotoxic DNA damage that could promote cancer heterogeneity and evolution.

Acknowledgments

Firstly, I would particularly like to thank my supervisors Dr. Steven S Foster and Prof. George DD Jones for their constant guidance, support, and encouragement through my PhD work, which has proven invaluable.

I would also like to extend my gratitude to my previous supervisors Dr. Mark D Evans and Prof. Marcus S Cooke who left the University of Leicester during the second year of my project.

My appreciation also extends to our Postgraduate tutor Dr. Don Jones for his support, encouragement and his following of this project. Big thanks also goes to everyone in the ROS group for their help and support. Many thanks also to Dr. Salvador Macip for his kind assistance with the apoptosis studies when I used the FACS machine.

Of course, I will not forget to thank all my friends in the UK, as well as the others in Iraq.

Also, I would like to thank the Ministry of Higher Education and Scientific Research of Iraq for sponsoring and funding my PhD study, and all the staff of Al-Mustansiriya University.

Finally, I would like to provide special thanks to my mother and brother for their continuous encouragement. Very special thanks to my wife, who has given me constant support and patience throughout the PhD study. I could not have done it without you!

I wish to dedicate this thesis to the soul of my father who died 18th of July 2009.

God bless him.

Table of contents

Abstract.....	II
Acknowledgments	III
Table of contents	IV
List of figures.....	IX
List of tables	XV
List of abbreviations	XVI
Chapter 1: Introduction	1
1.1 The association of oxidative stress and cancer cells -----	4
1.2 Nucleotide pool sanitization enzymes -----	5
1.3 De novo synthesis, catabolic and salvage pathways in dNTP pools regulation ---	8
1.4 Oxidation in dATP and dTTP pools -----	11
1.5 DNA repair mechanisms for oxidatively generated DNA lesions -----	12
1.5.1 Base excision repair -----	13
1.5.2 Nucleotide excision repair and transcription-coupled repair -----	15
1.5.3 Nucleotide incision repair -----	15
1.5.4 Mismatch repair -----	16
1.6 Replication stress and DNA damage response -----	18
1.6.1 Causes of DNA replicative stress -----	18
1.6.2 Consequences of DNA replication stress -----	20
1.6.3 DNA damage response -----	24
1.6.4 Replication stress relevance to cancer -----	28
1.7 NUDT1 and the impact of Nudix hydrolase family enzymes on carcinogenesis	29
1.8 Non-small cell lung cancer and its subtype -----	35
1.9 Gemcitabine and cisplatin as first-line treatment of NSCLC -----	35
1.10 The project aims and objectives -----	38
Chapter 2: Materials and methods.....	40

2.1 Materials	41
2.1.1 Cell lines	41
2.1.2 Cell culture reagents, chemicals, and supplies	41
2.1.3 Transfection reagent and small interfering RNA (siRNA)	42
2.1.4 Modified alkaline comet assay	42
2.1.5 Annexin V-FITC (fluorescein isothiocyanate) and propidium iodide (PI) Apoptosis Assay	42
2.1.6 Cellular proliferation-Water Soluble Tetrazolium (WST-1) assay	42
2.1.7 Intracellular ROS production measurement	42
2.1.8 Western blotting	43
2.2 Methods	44
2.2.1 Cell culture	44
2.2.2 NUDT1 knockdown and cell transfection using small interfering RNA (siRNA)	44
2.2.2.1 Forward transfection method of NUDT1 knockdown	44
2.2.2.2 Reverse transfection method of NUDT1 knockdown	45
2.2.3 Modified alkaline comet assay	45
2.2.3.1 Slides pre-coating	46
2.2.3.2 Cell treatments and irradiation	46
2.2.3.2.1 Hydrogen peroxide (H ₂ O ₂) exposure	46
2.2.3.2.2 Ionising radiation exposure	47
2.2.3.2.3 Small molecule NUDT1 inhibitors exposure	47
2.2.3.3 Cell-slides preparation and lysis	48
2.2.3.4 Alkaline unwinding/electrophoresis and staining steps	48
2.2.3.5 Comet visualisation and image analysis	49
2.2.4 Annexin V-FITC and PI Apoptosis Assay	49
2.2.5 Western blotting	51
2.2.5.1 Protein extraction and quantification from cultured cells	51
2.2.5.2 One dimensional SDS-Polyacrylamide gel electrophoresis (SDS- PAGE) preparation	51

2.2.5.3 Blotting-----	52
2.2.5.4 Immunolabelling and enhanced chemiluminescence (ECL) detection	53
2.2.5.5 Membrane stripping for re-probing-----	53
2.2.6 Cell counting and determination of growth rate-----	54
2.2.7 Cellular proliferation-Water Soluble Tetrazolium (WST-1) assay-----	54
2.2.8 Intracellular ROS production measurement-----	56
2.2.9 Data analysis and statistical tests-----	57
Chapter 3: Establishment of NUDT1 knockdown in normal human lung fibroblast and NSCLC cell lines	58
3.1 Optimization of siRNA delivery for NUDT1 knockdown-----	59
3.1.1 H23 cell knockdown using NUDT1 siRNA (s194633 or s9030)-----	61
3.1.2 H522 knockdown using NUDT1 siRNA (s194633 or s9030)-----	69
3.1.3 A549 knockdown using NUDT1 siRNA (s9030)-----	75
3.1.4 MRC-5 knockdown using NUDT1 siRNA (s9030)-----	75
3.2 The expression level of NUDT15 after NUDT1 knockdown-----	79
3.3 Discussion-----	81
Chapter 4: Genotoxic and cytotoxic effects of NUDT1 knockdown in NSCLC cell lines.....	84
4.1 Introduction-----	85
4.2 Determination of DNA damage induced by NUDT1 knockdown-----	88
4.3 Endogenous ROS levels of NSCLC lines relative to MRC-5 cells-----	94
4.4 DNA damage response following NUDT1 knockdown-----	95
4.5 Assessment of NUDT1 knockdown-induced apoptosis-----	100
4.6 Assessment of cellular viability following NUDT1 deficiency in NSCLC cell lines-----	106
4.7 Discussion-----	112
Chapter 5: Effect of NUDT1 knockdown on sensitization to current treatment agents.....	121
5.1 Introduction-----	122

5.2 Exposure to H ₂ O ₂ insult -----	123
5.2.1 Determination of apoptotic cell killing and sensitivity of NSCLC cells exposed to H ₂ O ₂ -----	123
5.2.2 Determination of H ₂ O ₂ -induced DNA damage in NSCLC cells with and without NUDT1 knockdown -----	129
5.3 Exposure to ionising radiation-----	139
5.3.1 Determination of ionising radiation-induced DNA damage in NSCLC cells with and without NUDT1 knockdown -----	139
5.4 Exposure to gemcitabine and cisplatin -----	142
5.4.1 Sensitivity of NSCLC cells to gemcitabine induced-apoptosis (cellular viability) -----	142
5.4.2 Sensitivity of NSCLC cells to cisplatin-induced apoptosis (cellular viability) -----	146
5.4.3 Potency of gemcitabine and cisplatin towards NSCLC cell lines -----	150
5.4.4 Determination of growth rate after cisplatin and gemcitabine exposure (growth inhibition) -----	152
5.4.5 Determination of apoptotic effect induced by gemcitabine or cisplatin when combined with NUDT1 knockdown in NSCLC cells -----	156
5.5 Discussion -----	162
Chapter 6: Genotoxic and cytotoxic effects of NUDT1 small molecule inhibitors on NSCLC cell lines.....	169
6.1 Introduction -----	170
6.2 Protein expression following treatment with small molecule NUDT1 inhibitors	172
6.3 Determination of small molecule NUDT1 inhibitors-induced DNA damage in NSCLC cell lines -----	175
6.4 Determination of apoptotic effect induced by small molecule NUDT1 inhibitors in NSCLC cell lines -----	181
6.5 Discussion -----	187
Chapter 7: General discussion and future directions.....	192
7.1 General discussion -----	193
7.2 Future directions-----	202

Appendix.....	204
References.....	208

List of figures

Figure 1-1 In vivo guanine oxidation products with the role of Nudix hydrolase family enzymes in nucleotide pool cleansing.	7
Figure 1-2 A schematic diagram of dNTP de novo synthesis and regulation within mammalian cells.	9
Figure 1-3 Salvage pathways that were proposed for 8-oxodG and 8-oxoGua.	11
Figure 1-4 Schematic models of the BER and NIR pathways for oxidatively damaged DNA.	14
Figure 1-5 A schematic illustration of DNA MMR pathway.	17
Figure 1-6 Overviews of the different sources of replication stress.	19
Figure 1-7 Overview of stalled replication fork restart/rescue pathways.	21
Figure 1-8 Mechanisms of stalled replication fork collapse.	23
Figure 1-9 Main DNA damage pathways for processing the replication intermediates.	25
Figure 1-10 Activation model of ATM and ATR in response to DNA damage lesion.	28
Figure 1-11 Diagrammatic representation of the human NUDT1 genomic structure, mRNAs transcripts, and their predicted translational products.	31
Figure 1-12 Mechanism of action of gemcitabine.	36
Figure 1-13 The proposed hypothesis of the effects of NUDT1 knockdown on lung cancer cells.	39
Figure 2-1 The principle mechanism of WST-1 assay.	55
Figure 2-2 The principle mechanism of DCFH (2, 7-dichlorodihydrofluorescein) assay for detection of intracellular ROS production.	57
Figure 3-1 The principle mechanism of siRNA action.	60
Figure 3-2 NUDT1 is slightly knocked down in H23 cell line after the forward transfection method with lower NUDT1 siRNA (s194633) concentrations.	62

Figure 3-3 Fast and robust knockdown of NUDT1 in H23 cell line after the reverse transfection method.....	63
Figure 3-4 Successful knockdown of NUDT1 in H23 cell line for up to 9 days after transfection with NUDT1 siRNA (s194633).....	65
Figure 3-5 NUDT1 is more efficiently knocked down in H23 cell line for up to 3 days after transfection with 15 nM siRNA (s9030).	67
Figure 3-6 Successful knockdown of NUDT1 in H23 cell line for up to 9 days after transfection with NUDT1 siRNA (s9030).	68
Figure 3-7 NUDT1 is slightly knocked down in H522 cell line after transfection with the lower NUDT1 siRNA (s194633) concentrations.....	71
Figure 3-8 NUDT1 is slightly knocked down in H522 cell line after transfection with 15 nM NUDT1 siRNA (s194633).	72
Figure 3-9 Efficient knockdown of NUDT1 in H522 cell line for up to 3 days after transfection with 20 nM NUDT1 siRNA (s9030).	73
Figure 3-10 Successful knockdown of NUDT1 in H522 cell line for up to 6 days after transfection with NUDT1 siRNA (s9030).	74
Figure 3-11 Successful knockdown of NUDT1 in A549 cell line for up to 6 days.....	77
Figure 3-12 Successful knockdown of NUDT1 in MRC-5 normal human lung fibroblasts cells for up to 6 days.	78
Figure 3-13 NUDT15 levels remain stable following transfection with NUDT1 siRNA for up to 6 days.	80
Figure 4-1 NUDT1 knockdown significantly increases Fpg sensitive sites of oxidised DNA bases within H23 cells.....	90
Figure 4-2 NUDT1 knockdown significantly increases Fpg sensitive sites of oxidised DNA bases within H522 cells.....	91
Figure 4-3 NUDT1 knockdown significantly increases Fpg sensitive sites of oxidised DNA bases within A549 cells.....	92
Figure 4-4 NUDT1 knockdown in MRC-5 cells does not lead to alteration level in Fpg sensitive sites of oxidised DNA bases	93

Figure 4-5 NSCLC cell lines generate endogenous ROS at levels similar to MRC-5 cells.	95
Figure 4-6 Alteration in phospho-Chk2 expression level 4 days after NUDT1 siRNA transfection in NSCLC cell lines.	98
Figure 4-7 Alteration in total Chk1 expression level 4 days after NUDT1 siRNA transfection in NSCLC cell lines.	99
Figure 4-8 Transient NUDT1 knockdown does not enhance apoptotic death in H23 non-small-cell-lung cancer cells.	101
Figure 4-9 Transient NUDT1 knockdown does not enhance apoptotic death in H522 non-small-cell-lung cancer cells.	102
Figure 4-10 Transient NUDT1 knockdown does not enhance apoptotic death in A549 non-small-cell-lung cancer cells.	104
Figure 4-11 Transient NUDT1 knockdown does not enhance apoptotic death in normal human lung fibroblast cell line (MRC-5 cells).	105
Figure 4-12 Transient NUDT1 knockdown reduces cell proliferation in H23 non-small-cell-lung cancer cells.	108
Figure 4-13 Transient NUDT1 knockdown does not reduce cell proliferation in H522 non-small-cell-lung cancer cells.	109
Figure 4-14 Transient NUDT1 knockdown does not reduce cell proliferation in A549 non-small-cell-lung cancer cells.	110
Figure 4-15 Transient NUDT1 knockdown does not reduce cell proliferation in normal human lung fibroblast cell line (MRC-5).	111
Figure 5-1 Bivariate plots of Annexin V-FITC and propidium iodide staining following H ₂ O ₂ treatment of H23 cell.	125
Figure 5-2 Apoptotic dose response curves in H23 cells following H ₂ O ₂ treatment.	126
Figure 5-3 Bivariate plots of Annexin V-FITC and propidium iodide staining following H ₂ O ₂ treatment of H522 cell.	127
Figure 5-4 H522 cell line displays an apoptotic resistance to high doses of H ₂ O ₂	128

Figure 5-5 Dose response curves of oxidised DNA bases and SSB/ALS in H23 cells following H ₂ O ₂ treatment.	130
Figure 5-6 Dose response curves of oxidised DNA bases and SSB/ALS in H522 cells following H ₂ O ₂ treatment.....	131
Figure 5-7 Transient NUDT1 knockdown does not lead to any alteration of oxidatively-modified DNA levels in H23 cells following H ₂ O ₂ treatment.....	133
Figure 5-8 Transient NUDT1 knockdown does not lead to any alteration of oxidatively-modified DNA levels in H522 cells following H ₂ O ₂ treatment.....	134
Figure 5-9 Transient NUDT1 knockdown in H23 cells does not alter oxidatively-modified DNA levels following both immediate and 24 h recovery of H ₂ O ₂ treatment.	137
Figure 5-10 Transient NUDT1 knockdown in H522 cells does not alter oxidatively-modified DNA levels following both immediate and 24 h recovery of H ₂ O ₂ treatment.	138
Figure 5-11 Transient NUDT1 knockdown in H23 cells does not alter oxidatively-modified DNA levels following both immediate and 24 h recovery of exposure to ionising radiation.	141
Figure 5-12 Bivariate plots of Annexin V-FITC and PI staining following gemcitabine treatment of H23 and H522 cell lines.	144
Figure 5-13 Apoptotic dose response curves to gemcitabine in H23 cells, while H522 cells are resistant to even high doses.	145
Figure 5-14 Bivariate plots of Annexin V-FITC and propidium iodide staining following cisplatin treatment of H23 and H522 cell lines.	148
Figure 5-15 Apoptotic dose response curves to cisplatin in H522 and H23 cell lines.	149
Figure 5-16 Dose-response curves for assessment of EC ₅₀ value of apoptosis.	151
Figure 5-17 The growth inhibitory response following cisplatin and gemcitabine treatment in H23 cells.	154
Figure 5-18 The growth inhibitory response following cisplatin and gemcitabine treatment in H522 cells.	155

Figure 5-19 Transient NUDT1 knockdown does not enhance the cytotoxicity of gemcitabine and cisplatin treatments in H23 cells.....	159
Figure 5-20 Transient NUDT1 knockdown does not enhance the cytotoxicity of gemcitabine and cisplatin treatments in H522 cells.....	160
Figure 5-21 Transient NUDT1 knockdown does not enhance the cytotoxicity of gemcitabine and cisplatin treatments, confirmed by transfecting H23 cells with other NUDT1 siRNA.	161
Figure 6-1 The chemical structure of small molecule NUDT1 inhibitors, (A) TH588 and (B) TH287 compounds. [The Figure adapted from (Gad et al., 2014).	170
Figure 6-2 TH287 and TH588 NUDT1 small molecule inhibitors do not alter the expression levels of NUDT1 protein.	174
Figure 6-3 TH287 and TH588 NUDT1 small molecule inhibitors increase the oxidised DNA bases levels in H23 cell line.	177
Figure 6-4 TH287 and TH588 NUDT1 small molecule inhibitors do not alter the oxidised DNA bases levels in H522 cell line.	178
Figure 6-5 TH287 and TH588 NUDT1 small molecule inhibitors do not alter the oxidised DNA bases levels in A549 cell line.	179
Figure 6-6 TH287 and TH588 NUDT1 small molecule inhibitors do not alter the oxidised DNA bases levels in MRC-5 cell line.	180
Figure 6-7 TH287 and TH588 NUDT1 small molecule inhibitors induce apoptotic death in H23 non-small-cell-lung cancer cells.	183
Figure 6-8 TH287 and TH588 NUDT1 small molecule inhibitors induce apoptotic death in H522 non-small-cell-lung cancer cells.	184
Figure 6-9 TH287 and TH588 NUDT1 small molecule inhibitors do not induce apoptotic death in A549 non-small-cell-lung cancer cells.....	185
Figure 6-10 TH287 and TH588 NUDT1 small molecule inhibitors do not induce apoptotic death in normal human lung fibroblast cell line (MRC-5 cells).	186
Figure 7-1 The model for targeting NUDT1 that does not induce apoptosis, but may lead to heterogeneity and cancer evolution.....	194

Figure 8-1 The metabolic kinetic of cell proliferation reagent WST-1 in MRC-5 cells cultured at a density of 1×10^4 cells.	204
Figure 8-2 The metabolic kinetic of cell proliferation reagent WST-1 in A549 cells cultured at a density of 1×10^4 cells.	205
Figure 8-3 The metabolic kinetic of cell proliferation reagent WST-1 in H23 cells cultured at a density of 1 or 2×10^4 cells.	206
Figure 8-4 The metabolic kinetic of cell proliferation reagent WST-1 in H522 cells cultured at a density of 1 or 2×10^4 cells.	207

List of tables

Table 2-1 The antibodies used for Western blot.	43
Table 2-2 The components of resolving and stacking gels for preparing SDS-Polyacrylamide Gel Electrophoresis (SDS-PAGE).....	52

List of abbreviations

ALS	Alkali-labile sites
AP	Apurinic-apyrimidinic
ATM	Ataxia telangiectasia mutated
ATR	Ataxia telangiectasia and Rad3-related protein
BER	Base excision repair
BSA	Bovine serum albumin
CDK	Cyclin dependent kinase
Chk1	Checkpoint kinase 1
Chk2	Checkpoint kinase2
DDR	DNA damage response
DMEM	Dulbecco's Modified Eagle
DMSO	Dimethyl sulfoxide
DSBs	Double-strand breaks
dATP	2'-deoxyadenosine 5'-triphosphate
(d)NTPs	(2'-deoxy) ribonucleotide triphosphates
dTTP	2'-deoxythymidine 5'-triphosphate
EC₅₀	50% increased effective concentration
ECL	Enhanced chemiluminescence
EDTA	Ethylenediaminetetraacetic acid
EMEM	Eagle's Minimum Essential Medium
ERCC1	Excision repair cross-complementation group 1
FBS	Fetal bovine serum
FITC	Flourescein isothiocyanate
Fpg	Formamidopyrimidine [fapy]-DNA glycosylase

GTP	Guanosine triphosphate
H2DCF-DA	2',7'-dichlorodihydrofluorescein diacetate
hMUTYH	Human mutY homolog E. coli
5-HMU	5-hydroxymethyluracil
h	Hours
hOGG1	Human 8-oxoGua DNA glycosylase 1
HOMO	Highest occupied molecular orbital
H₂O₂	Hydrogen peroxide
HRP	Horseradish peroxidase
IC₅₀	50% inhibitory concentration
LMP	Low melting point
min	Minutes
MMR	Mismatch repair
MRN	MRE11-Rad50-NBS1
MTH	Mut T homologue
NER	Nucleotide excision repair
NIR	Nucleotide incision repair
NMP	Normal melting point
NSCLC	Non-small cell lung cancer
Nudix	Nucleoside diphosphate linked moiety X
NUDT	Nudix (Nucleoside diphosphate linked moiety X)-type motif
2-OH-A	2-hydroxyadenine
2-OHdATP	2-hydroxy-deoxy-adenosine triphosphate
5-OHmdUTP	5-hydroxymethyl- deoxy-uridine triphosphate
8-oxodG	8-oxo-7,8-dihydro-2'-deoxyguanosine
8-oxodGDP	8-oxo-7,8-dihydro-2'-deoxyguanosine-5'-diphosphate

8-oxodGMP	8-oxo-7,8-dihydro-2'-deoxyguanosine-5'-monophosphate
8-oxodGTP	8-oxo-7,8-dihydro-2'-deoxyguanosine -5'-triphosphate
8-oxoGDP	8-oxo-7,8-dihydro- guanosine-5'-diphosphate
8-oxoGTP	8-oxo-7,8-dihydro-guanosine-5'-triphosphate
8-oxoGua	8-oxo-7,8-dihydroguanine
PARP	Poly(ADP-ribose) polymerase
PBS	Phosphate-buffered saline
PI	Propidium iodide
PNP	Purine nucleoside phosphorylase
PPi	Inorganic pyrophosphate
PVDF	Polyvinylidene difluoride
RISC	RNA-induced silencing complex
RNR	Ribonucleotide reductase
ROS	Reactive oxygen species
RPA	Replication protein A
<i>RRM1</i>	Ribonucleotide reductase subunit M1
SA-beta-gal	Senescence associated beta-galactosidase
S.D	Standard deviation
SDS	Sodium dodecyl sulfate
SDS-PAGE	SDS-Polyacrylamide gel electrophoresis
siRNA	Small interfering RNA
SSBs	Single-strand breaks
TBST	Tris-Buffer saline and Tween 20
TCR	Transcription couple repair
TEMED	N,N,N',N'-tetramethylethylenediamine
WST-1	Water Soluble Tetrazolium

Chapter 1: Introduction

A major focus of current cancer research is to develop therapeutic strategies that improve cancer cell targeting. Many of these strategies are based on exploiting cancer-cell-specific genetic features or phenotypic traits that are not expressed in normal cells but that are acquired during carcinogenesis or tumour evolution (Hanahan and Weinberg, 2011, Helleday, 2014). One such strategy is synthetic lethality, which is acquired when a defect in a particular factor or pathway renders a cancer cell sensitive to inhibition of another second specific factor. Still, this approach is often limited to a certain context or cancer type, for example, inhibiting poly(ADP-ribose) polymerase (PARP) in BRCA1- and BRCA2-deficient breast and ovarian cancers (Bryant et al., 2005, Farmer et al., 2005). An alternative though related strategy that may be more effective in treating a wider range of cancers is cancer phenotypic lethality (Helleday, 2014), which is the targeting of factors and cell processes that are non-essential in normal cells but that become essential for cell growth following the acquisition of hallmark cancer traits (Helleday, 2014, Liou and Storz, 2010, Toledo et al., 2011, Puigvert et al., 2016). However, until such ‘conditionally essential’ pathways are discovered and the mechanisms of their interactions with cancer traits are elucidated, radiotherapy- and chemotherapy-based treatments that are often associated with side-effects and resistance will remain the mainstay of cancer treatment.

Oxidative stress essentially arises from an imbalance between the reactive oxygen species (ROS) production and the ability of a cellular body to counteract their levels or harmful effects through detoxification by antioxidants. It has become a hallmark cancer trait (Liou and Storz, 2010), that can contribute to both carcinogenesis and continuing tumour evolution (Liou and Storz, 2010, Kumar et al., 2008). Paradoxically, the ROS are regarded as the basis of several cytotoxic chemotherapy and radiotherapy treatments. Thus, several normally non-essential oxidative stress response factors and pathways may become essential in cancerous cells and/or affect therapy responses in a significant way.

It is well known that cellular components within any living organism are constantly exposed to potentially damaging ROS as a by-product of intracellular metabolism or via exogenous agents such as radiation, therapeutic drugs, and environmental toxicants (Evans et al., 2004). The cell’s nucleic acid components, including DNA, RNA and their synthetic precursor nucleotides, are regarded as important targets for not only the potentially mutagenic, but also for the cytotoxic actions of ROS (Youn et al., 2008). It

has been implicated that ROS and the generation of oxidized DNA lesions have important mechanistic roles in the development of cancer, neurodegenerative diseases, cardiovascular diseases, atherosclerosis, acquired immunodeficiency syndrome and aging (Youn et al., 2008, Speina et al., 2005, Satou et al., 2007b, Rai, 2010). Despite ROS-induced DNA damage directly being widely reported in terms of causing mutations and tumorigenesis, the free 2'-deoxyribonucleotide triphosphates (dNTPs) pools are reported to be 190-13,000 times more susceptible to modification than DNA (Topal and Baker, 1982). To a great extent, this suggests that oxidative stress-induced DNA damage can arise through misincorporation of oxidised dNTPs during DNA replication process rather than direct DNA damage. Previously, oxidative modification of DNA and RNA synthesis precursors, dNTPs and ribonucleotide triphosphates (NTPs) has received less attention than DNA oxidation. However, the oxidised dNTPs could induce mutation, invoke DNA damage response (DDR) and promote apoptosis or senescence by virtue of their being mis-incorporated into DNA and RNA by polymerases.

Oxidation of guanine (the most easily oxidized nucleobase in the genome) to 8-oxo-7,8-dihydroguanine (8-oxoguanine, 8-oxoGua) has been considered extensively, though the spectrum of oxidation-derived DNA lesions exceeding 100 different types (Tsuzuki et al., 2001). There are two distinctive pathways for 8-oxoGua generation, one of which is the direct oxidation of guanine bases within DNA, or oxidation of guanine nucleotide precursors with mis-incorporation of 8-oxo-7,8-dihydro-2'-deoxyguanosine-5'-triphosphate (8-oxodGTP) into the nascent DNA strand by DNA polymerases during replication events opposite adenine and cytosine with nearly equal efficiency (Youn et al., 2008, Tsuzuki et al., 2001). The latter pathway is more vulnerable to oxidation processes, as nucleotide precursors are free in nucleotide pools and not present in double-stranded DNA nor bound to protecting histone proteins (Youn et al., 2008). The mis-pairing events are likely to elicit A:T to G:C or GC: to TA transversion mutations (Nakabeppu, 2001, Setoyama et al., 2011). In addition, an adequate dNTPs amount along with appropriate balanced dNTP pools could determine the fidelity of DNA synthesis that affects genetic stability (Rampazzo et al., 2010). Similarly, oxidation of guanine in cellular ribonucleotide pools [8-oxo-7,8-dihydro-guanosine-5'-triphosphate (8-oxoGTP)] can lead to mis-incorporation into messenger RNA, inducing errors in transcription, translation processes and protein synthesis especially during codon-

anticodon pairing (Setoyama et al., 2011, Bialkowski et al., 2009). Thus, indeed, both deoxyribonucleotide and ribonucleotide pools are potentially subjected to oxidation by ROS with resulting mis-incorporation of the oxidized forms.

The oxidised DNA bases do not majorly disrupt DNA structure. Accordingly, they can result in secondary types of DNA lesion, including DNA single-strand breaks (SSBs) that produce by damaged bases removal during base excision repair (BER) or mis-pairing events (Shibutani et al., 1991). Double-strand breaks (DSBs) (Rai et al., 2009) could also arise through poorly defined mechanisms, perhaps due to DNA replication stress. In particular, the DSBs are highly genotoxic and cytotoxic if not repaired correctly. Collectively, by this way, it is predicted that the pathways involved in the prevention of oxidised DNA base misincorporation could be critical in either eliciting or suppressing tumour development and evolution relying on context (Olinski et al., 2003). In particular, routes act to prevent cellular death during oxidative stress and when there is elevation of oxidised dNTPs levels, this raises the possibility that the factors involved in such pathways are 'conditionally essential' in cancer, highlighting potential new therapeutic targets.

Supporting this idea, some previous works regarding Nudix (Nucleoside diphosphate linked moiety X) hydrolase family enzymes, especially Nudix-type motif 1 (NUDT1) [also known as Mut T homologue 1, MTH1], suggest that it is required to maintain genome integrity and cell viability specifically in premalignant and malignant cells. These family enzymes have dNTP sanitizing activity, acting to hydrolyse selected oxidised dNTP and NTP substrates to the corresponding mono-phosphate products and inorganic pyrophosphate (PPi) to prevent their misincorporation into DNA and RNA respectively (Sakumi et al., 1993, Fujikawa et al., 2001, Nissink et al., 2016).

1.1 The association of oxidative stress and cancer cells

Oxidative stress, which arises when there is an imbalance between the production of ROS and the cellular ability to counteract their levels or effects, is often detected in almost all cancer cells and hence has become a hallmark cancer trait (Liou and Storz, 2010, Luo et al., 2009). Oxidative stress may significantly contribute to both initial malignant transformation and disease progression (Liou and Storz, 2010, Kumar et al., 2008). Oxidative stress can emerge in cancers through various ways, including oncogene-induced effects (Irani et al., 1997, Moiseeva et al., 2009), altered metabolic

activity (Hanahan and Weinberg, 2011) and mitochondrial dysfunction (Petros et al., 2005). Paradoxically, ROS are the basis of much of the cytotoxicity of radiotherapy and several chemotherapy treatments (Borek, 2004, Lomax et al., 2013, Conklin, 2004). Given that ROS accumulation within the cancer cell requires counteracting scavenging mechanisms to enable cell survival (Gorrini et al., 2013), this suggests there may be several normally non-essential oxidative stress response factors and pathways that become essential in cancer cells and/or significantly affect responses to cancer therapies.

Various ROS can react with all DNA components to cause numerous types of lesions (Dizdaroglu and Jaruga, 2012). This means that cancer-associated oxidative stress is potentially a major source of mutations as cancers initiate and evolve (Olinski et al., 2003, Valko et al., 2006). Moreover, ROS alter intracellular signaling cascades that are linked to tumor cell growth and survival. At low to moderate levels ROS by act as signaling molecules (Valko et al., 2006, Gorrini et al., 2013), causing phosphorylation of mitogen-activated protein kinase (MAPK) and extracellular signal-regulated kinase (ERK), and activation of cyclin D1 expression and JUN N-terminal kinase (JNK) pathways. They may also reversibly inactivate phosphatase and tensin homolog (PTEN) and protein tyrosine phosphatases (PTPs) due to the existence of residues of the redox-sensitive cysteine in their catalytic centre (Gorrini et al., 2013). ROS also modify other important cellular components such as protein, lipids, NTPs and dNTPs. As previously mentioned, the free dNTP pool is 190-13,000 times more susceptible to modification than genomic DNA (Topal and Baker, 1982), suggesting that cellular NTP and dNTP pools are more vulnerable to oxidative stress than the components of genomic DNA (Topal and Baker, 1982). If not removed from the pool, oxidised dNTPs can be misincorporated into nascent DNA strands by DNA polymerases (Kamiya and Kasai, 1995, Shimizu et al., 2003). This raises the possibility that a significant amount of oxidatively modified bases within cancer cell genomes is via misincorporation of oxidised dNTPs rather than direct modification of genomic DNA by ROS.

1.2 Nucleotide pool sanitization enzymes

An increase in oxidised dNTPs misincorporation during oxidative stress has the potential to induce DNA-replication-associated genomic instability and/or cell death (Mazouzi et al., 2014, Zeman and Cimprich, 2014, Gad et al., 2014). This means that

the pathways that act to sanitise the dNTP pool and prevent the accumulation of oxidised DNA bases within the genome could be critical in either promoting or suppressing cancer cell growth and continuing tumour evolution depending on circumstances. During oxidative stress state, if particular pathways act to prevent cell death in the presence of increased levels of oxidised dNTPs, there is much likelihood that the factors involved in such pathways are ‘conditionally essential’ in cancer cells, highlighting potential new therapeutic approaches.

A protective mechanism with Nudix hydrolase family enzymes exists to cleanse oxidatively modified dNTPs and NTPs from the nucleotide pools and prevent their misincorporation into DNA genome or RNA by converting them into a mono-phosphate product and PPi, respectively. To date, 24 hydrolase genes and at least 5 pseudogenes have been described in the human genome (McLennan, 2006, Carter et al., 2015).

As shown in Figure 1-1., NUDT1 (also known as MTH1); and NUDT15 (MTH2) have the ability to hydrolyze 8-oxodGTP to 8-oxo-7,8-dihydro-2'-deoxyguanosine-5'-monophosphate (8-oxodGMP) and PPi products. Subsequently, processing to 8-oxodGMP by 3'(5')-deoxynucleotidases may ultimately give rise to 8-oxo-7,8-dihydro-2'-deoxyguanosine (8-oxodG). Otherwise, 8-oxo-7,8-dihydro-2'-deoxyguanosine-5'-diphosphate (8-oxodGDP) could be likely hydrolysed to monophosphate products by NUDT18 (MTH3) and NUDT15 (Takagi et al., 2012). To a lesser extent, it has also been found that NUDT5 may possibly degrade 8-oxodGDP to 8-oxodGMP, although the 8-oxodGDPase activity of this enzyme reaction is probably irrelevant at physiological pH (Ishibashi et al., 2003).

Recently, the role of NUDT18 as a ribonucleotide defensive action has been described, when Takagi et al. reported that it could hydrolyze 8-oxo-7,8-dihydro-guanosine-5'-diphosphate (8-oxoGDP) as efficiently as 8-oxodGDP; in contrast to NUDT1 and NUDT15 which exhibit limited activity towards 8-oxoGTP (Takagi et al., 2012).

Other than guanine deoxyribonucleotide DNA precursors, NUDT1 catalyses the hydrolysis of 2-hydroxy-dATP, 2-hydroxy-ATP, 8-oxodATP. Hence, it is named “oxidized purine nucleoside triphosphatase” (Yoshimura et al., 2003, Bialkowski and Kasprzak, 2004). It is probable that the functional groups of the purine ring at the 2 and 6 positions have an important effect on the affinity of the compound for NUDT1 protein (Kamiya et al., 2006).

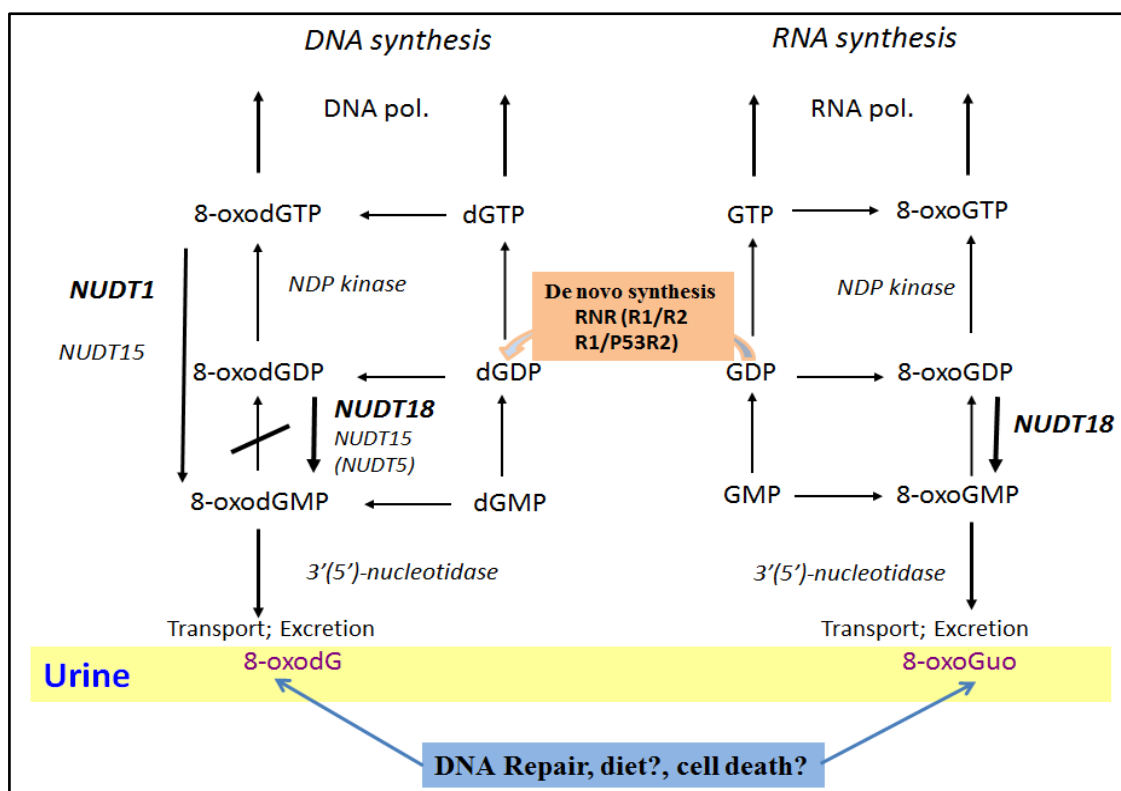


Figure 1-1 In vivo guanine oxidation products with the role of Nudix hydrolase family enzymes in nucleotide pool cleansing.

The protective mechanism of Nudix hydrolase prevent mis-incorporation of oxidized guanine products; 8-oxodGTP and 8-oxoGTP; during DNA and RNA synthesis, initiated by related polymerase (pol.) enzymes, respectively. NUDT1 and NUDT15 hydrolyse 8-oxodGTP to 8-oxodGMP which ultimately produces 8-oxodG by 3'(5')-nucleotidases, while NUDT18 (MTH3) is more likely to degrade (2'-deoxy) ribonucleotide diphosphates to monophosphates products. Moreover, ribonucleotide reductase (RNR) is responsible for a reduction of GDP to dGDP. 8-oxo(d)GDP is further phosphorylated by nucleotide diphosphate (NDP) kinase to related triphosphate products, serve as a substrate for DNA or RNA synthesis. Additional phosphorylation steps to monophosphate products might occur to give rise to related triphosphates (d)NTPs substrates. However, guanylate kinase enzyme is entirely inactive for 8-oxoguanine containing nucleotides (8oxodGMP). In contrast to DNA repair, evidence suggesting that diet and cell turn over role seems to be negligible or minimal, at least, for the urinary 8-oxodG level (Cooke et al., 2009).

NUDT1 has substrate preference in the order: 2-hydroxydATP > 2-hydroxyATP > 8-hydroxydGTP ~ 8-hydroxydATP >> 2'-deoxyguanosine 5'-triphosphate (dGTP) > 8-hydroxyGTP > 8-hydroxyATP (Fujikawa et al., 2001).

In addition, NUDT18 can hydrolyse other oxidized nucleotide diphosphates, namely, 2-hydroxy-dADP and 8-hydroxy-dADP (Takagi et al., 2012). Moreover, Kamiya et al. reported that NUDT5 degrades 8-hydroxy-dGDP and 8-hydroxy-dADP with nearly similar high kinetic efficiency, and lower efficiency for 2-hydroxy-dADP and 5-formyl-dUDP (the dNTP analogues of these compounds are very poor substrates for NUDT5); although again, these reactions may be irrelevant at physiological pH (Kamiya et al., 2009).

In addition, it has been proposed that several DNA repair pathways may contribute to the production of 8-oxodG, the most logical of which is the activity of selected members of the Nudix hydrolase family of enzymes, NUDT1, NUDT15 and NUDT18 (Evans et al., 2010). Therefore, understanding the origins of 8-oxodG is important to meaningful interpretation of changes in excretion.

1.3 De novo synthesis, catabolic and salvage pathways in dNTP pools regulation

In order to control the levels of (d)NTP pools during de novo synthesis, ribonucleotide reductase (RNR) is responsible for reduction of ribonucleotide diphosphates to their related deoxynucleotides, with further phosphorylation step by nucleotide diphosphate kinase to triphosphate products, to serve as a substrate for DNA polymerase to incorporate into DNA during synthesis (Rampazzo et al., 2010, Evans et al., 2010) (Figure 1-2). The RNR active form is a heterotetramer with two large subunits, R1 protein, and other two small ones, R2 or p53R2 (Rampazzo et al., 2010) (Figure 1-1, and 1-2). The ribonucleotide reductase isoform, R1/R2, is responsible for catalysing the reduction of ribonucleoside diphosphates during the S phase of the cell cycle; while the R1/p53R2 isoform operates in all phases of the cell cycle and also in non-dividing cells (Rampazzo et al., 2010) (Figure 1-1). It is interesting to note that mitochondrial and cytosolic dNTP pools are not isolated from each other, as there are certain carriers for deoxynucleosides and deoxynucleotides within an inner mitochondrial membrane which are responsible for intercommunication between the pools (Rampazzo et al., 2010).

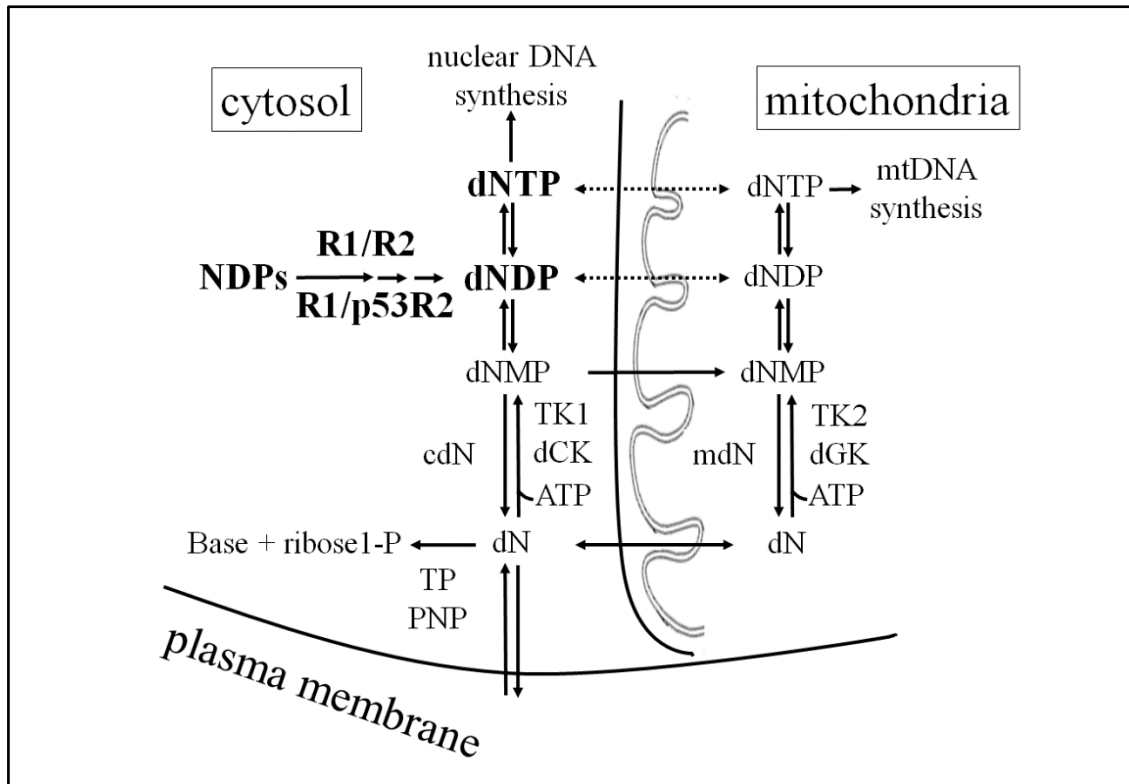


Figure 1-2 A schematic diagram of dNTP de novo synthesis and regulation within mammalian cells.

De novo synthesis of deoxynucleotides in the cytosol (the bold symbols) occurs in parallel with two salvage pathways in both cytosol and mitochondria. The deoxynucleotides (dN) are phosphorylated into monophosphate product (dNMP) in the cytosol by deoxycytidine kinase (dCK) and thymidine kinase 1 (TK1); while in mitochondria, deoxynucleoside kinases [deoxyguanosine kinase (dGK) and thymidine kinase 2 (TK2)] appear to be involved in such phosphorylation process. Subsequently, the formed dNMP are either subjected to further two phosphorylation steps to convert into dNTP, or could be dephosphorylated by the action of cytosolic or mitochondrial 5'-deoxynucleotidases (cdN and mdN). The deoxynucleotides are capable of maintaining in exchange between cytosolic and mitochondrial compartments, as they cross the cellular membrane and the inner mitochondrial via certain equilibrative or nucleoside carriers. Alternatively, throughout the catabolic pathway, the deoxynucleosides are degraded by nucleoside phosphorylases such as purine nucleoside phosphorylase (PNP) or thymidine phosphorylase (TP) enzymes that able to convert deoxynucleoside into 2'-deoxyribose-1-phosphate and nucleobase. [This Figure modified from (Rampazzo et al., 2010)].

Furthermore, deoxynucleosides are rationally subjected to phosphorylation or hydrolysis during salvage and catabolic pathways, respectively. During the formal route, monophosphates (dNMPs) may be formed by the action of cytosolic thymidine kinase 1 and deoxycytidine kinase towards deoxynucleoside, whereas in mitochondria, deoxynucleoside kinases (thymidine kinase 2 and deoxyguanosine kinase) appear to be involved (Rampazzo et al., 2010, Henderson et al., 2010) (Figure 1-2). Similar to R2 subunit, thymidine kinase 1 is only considered as cell cycle regulator among other deoxynucleoside kinases (Rampazzo et al., 2010). Two additional phosphorylation steps are required to give rise to dNTP substrates which, as mentioned above, are suitable for incorporation into DNA by DNA polymerases (Rampazzo et al., 2010) (Figure 1-2). However, it has been stated that the usage of 8-oxodGMP for DNA synthesis is not applicable, as cellular guanylate kinase enzyme is entirely inactive for 8-oxoguanine containing nucleotides (Ishibashi et al., 2003).

Throughout the catabolic pathway, the deoxynucleosides are degraded by purine nucleoside phosphorylase (PNP) or thymidine phosphorylase enzymes, that convert deoxynucleoside into 2'-deoxyribose-1-phosphate and the nucleobase (Rampazzo et al., 2010, Henderson et al., 2010) (Figure 1-2). In this case, it is assumed that 8-oxoGua could be produced as a consequence of the action of PNP on 8-oxodG. The former is a substrate for hypoxanthine-guanine phosphoribosyltransferase activity, resulting in 8-oxoGMP production (Henderson et al., 2010) (Figure 1-3). Successive serial phosphorylations are undertaken to yield ribonucleotide triphosphates acting as a substrate for RNA polymerase to incorporate into RNA synthesis (Henderson et al., 2010) (Figure 1-3). However, 8-oxoGDP might also be prone to RNR activity, as mentioned above, to yield 8-oxodGDP with subsequent phosphorylation forming 8-oxodGTP that serves as a substrate for DNA polymerase to incorporate into DNA during synthesis (Figure 1-3). Thus, it is argued that such phosphorolytic degradation could further contribute to dNTP pool expansion.

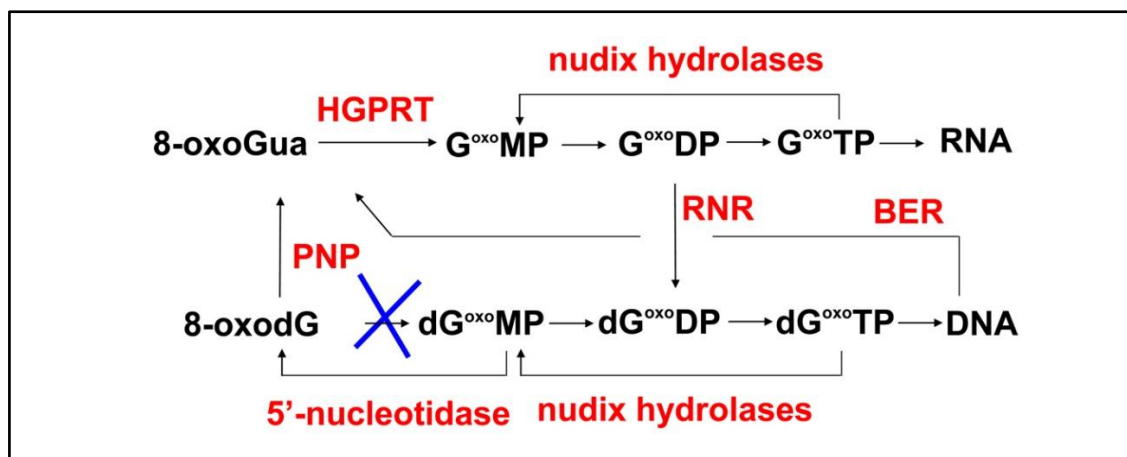


Figure 1-3 Salvage pathways that were proposed for 8-oxodG and 8-oxoGua.

It assumes the metabolism of 8-oxodG into 8-oxoGua occur through the purine nucleoside phosphorylase (PNP)-mediated pathway. Under the influence of hypoxanthine-guanine phosphoribosyltransferase (HGPRT), 8-oxoGua is converted into 8-oxoGMP that undertaken consecutive serial phosphorylations to yield ribonucleotide triphosphates, acting as a substrate for RNA polymerase to incorporate into RNA synthesis. However, 8-oxoGDP might also be prone to ribonucleotide reductase (RNR) activity, to generate 8-oxodGDP that phosphorylate to 8-oxodGTP and then misincorporated into DNA by DNA polymerase. The complexity of 8-oxodG salvage is possibly caused by the contribution of BER pathway, cleansing of nucleotide pool via nudix hydrolases and the role of 5'-nucleotidase activity. [The Figure adapted from (Henderson et al., 2010)].

1.4 Oxidation in dATP and dTTP pools

After exposure to an oxidative stress insult, 2'-deoxyadenosine 5'-triphosphate (dATP) and 2'-deoxythymidine 5'-triphosphate (dTTP) pools could experience oxidation with formation of 2-hydroxy-dATP (2-OHdATP) and 5-hydroxymethyl-dUTP (5-OHmdUTP), respectively; with ultimate production of their corresponding 2'-deoxyribonucleoside products, albeit other oxidized products could also form from oxidation of DNA such as thymidine glycol.

A recent speculation has been raised for the possible mis-incorporation of 5-OHmdUTP precursors into DNA as the main source of 5-hydroxymethyluracil base (5-HMU) formation in DNA, other than direct ways of its production via either deamination/oxidation of 5-methylcytosine or oxidation of thymine (Evans et al., 2010). Thereby, 5-HMU could pair with adenine or guanine bases, and the latter may result in C to T transition mutation (Evans et al., 2010). As a rational contribution for

extracellular 5-HmdU, it is proposed that Nudix hydrolase family enzymes might be a logical source via enzyme activity against oxidized dTTP, including 5-OHmdUTP. This, however, remains to be proven (Evans et al., 2010).

Regarding 2-OHdATP, its mutagenicity is perceived in a dose-dependent manner, and enhanced by the presence of corresponding diphosphate product (2-hydroxy deoxyadenosine 5'-diphosphate) as a potent inhibitor of NUDT1 protein. It could elicit a G:C to A:T transition mutation, when incorporated opposite cytosine, including tandem CC to TT mutations (Satou et al., 2003). However, once 2-OHdATP is incorporated opposite guanine, it is also likely to elicit G:C to T:A transversion mutation with higher mutagenic affinity than 8-OHdGTP *in vivo* (Fujikawa et al., 1999). Similarly, more efficient protective ability of NUDT1 was also recognized in nucleotide pool, nearly 5-fold, to hydrolyse 2-OHdATP compared to 8-OHdGTP; even 2-OHdATP is apparently hydrolysed in an effective way by NUDT1 (Fujikawa et al., 1999, Fujikawa et al., 2001). In terms of the accumulation of 2-hydroxyadenine (2-OH-A) in DNA, the oxidation of dATP nucleotide pool represents the predominant way for its generation rather than the direct oxidation of adenine in DNA, unlike 8-oxoGua formation (Ushijima et al., 2005). The contribution of human mutY homolog *E. coli* (hMUTYH) in 2-OH-A excision could be easily explained when 2-OH-A is present opposite guanine, perhaps, it might interact with MSH2, and both would co-operate for post-replicative DNA repair of such mis-incorporation during the replication process (Ushijima et al., 2005). Furthermore, in contrast to 8-oxoGua, the adenine oxidized base (2-OH-A) might critically reduce the catalytic property of several DNA polymerases with error-free bypass in concert with proliferating cell nuclear antigen (PCNA) and replication protein A (RPA), thus, slows down replication fork progression, generating signals to recruit a specialized translesion synthesis DNA polymerases (Crespan et al., 2007).

1.5 DNA repair mechanisms for oxidatively generated DNA lesions

The oxidised dNTPs can be misincorporated into nascent DNA strands by DNA polymerase, if they are not removed from the pool (Kamiya and Kasai, 1995, Shimizu et al., 2003). However, the ROS can also directly react with DNA genome lead to induce numerous types of lesions (Dizdaroglu and Jaruga, 2012). Accordingly, the cells identify and correct DNA damage to avoid the occurrence of genome instability and

malignant transformation. In addition, if the damaged DNA is not removed, the induction of cellular senescence or apoptosis is possibly considered to take place (Campisi and di Fagagna, 2007).

Depending on the inflicted type of DNA damage, there are variety of repair pathways that evolved to restore the genome integrity. Recently, it seems that BER is the most prevalent repair pathway for removal of the majority of oxidatively derived DNA lesions (Cooke et al., 2005, Henderson et al., 2010).

1.5.1 Base excision repair

DNA glycosylase activity of BER is responsible for the cleavage of N-glycosylic bond between a modified base and deoxyribose, forming an abasic [apurinic-apyrimidinic (AP)] site or SSB (Evans and Cooke, 2007) (Figure 1-4). Depending on its AP lyase activity, it is either denoted as short or long patch repair with a removal of one or 2-6 nucleotides, respectively; followed by gap filling and ligation of DNA (Evans et al., 2004, Henderson et al., 2010). The short-patch BER pathway accounts for the repair of more than 80% of DNA bases modification (Nickson and Parsons, 2014). Recently, eleven human DNA glycosylases have been identified, that differ in their substrate specificity towards the oxidised base products and the DNA lesion types recognition (Nickson and Parsons, 2014, Krokan et al., 2000). For example, Human 8-oxoGua DNA glycosylase 1 (hOGG1) is one of the BER enzymes that has a DNA glycosylase activity towards 8-oxoGua paired with cytosine in double-stranded DNA (Zheng et al., 2009). Furthermore, during the mis-incorporation of 8-oxodGTP into DNA a complementary enzyme; hOGG2; is accountable for the excision of 8-oxoGua paired opposite adenine or guanine (Henderson et al., 2010, Cooke et al., 2005). Other reported enzymes also have notable activities for the elimination of 8-oxoGua including MYH; which removes adenine mis-paired with 8-oxoGua in template DNA (Oka et al., 2008); NEIL1, NEIL2, NTH1, N-methylpurine-DNA glycosylase, and ribosomal protein S3 (Henderson et al., 2010, Cooke et al., 2005).

Rozalski et al. showed that in 8-oxo-guanine glycosylase 1 (OGG1) knockout mice there was a 26% reduction of urinary 8-oxoGua level, while no significant difference was observed for urinary excretion of 8-oxodG in comparison with wild-type (Rozalski et al., 2005). Therefore, it is proposed that compensatory mechanism with glycosylase

activity does occur, although less efficient, to substitute for such reduction in excretion of urinary 8-oxoGua (Rozalski et al., 2005, Evans et al., 2010, Henderson et al., 2010).

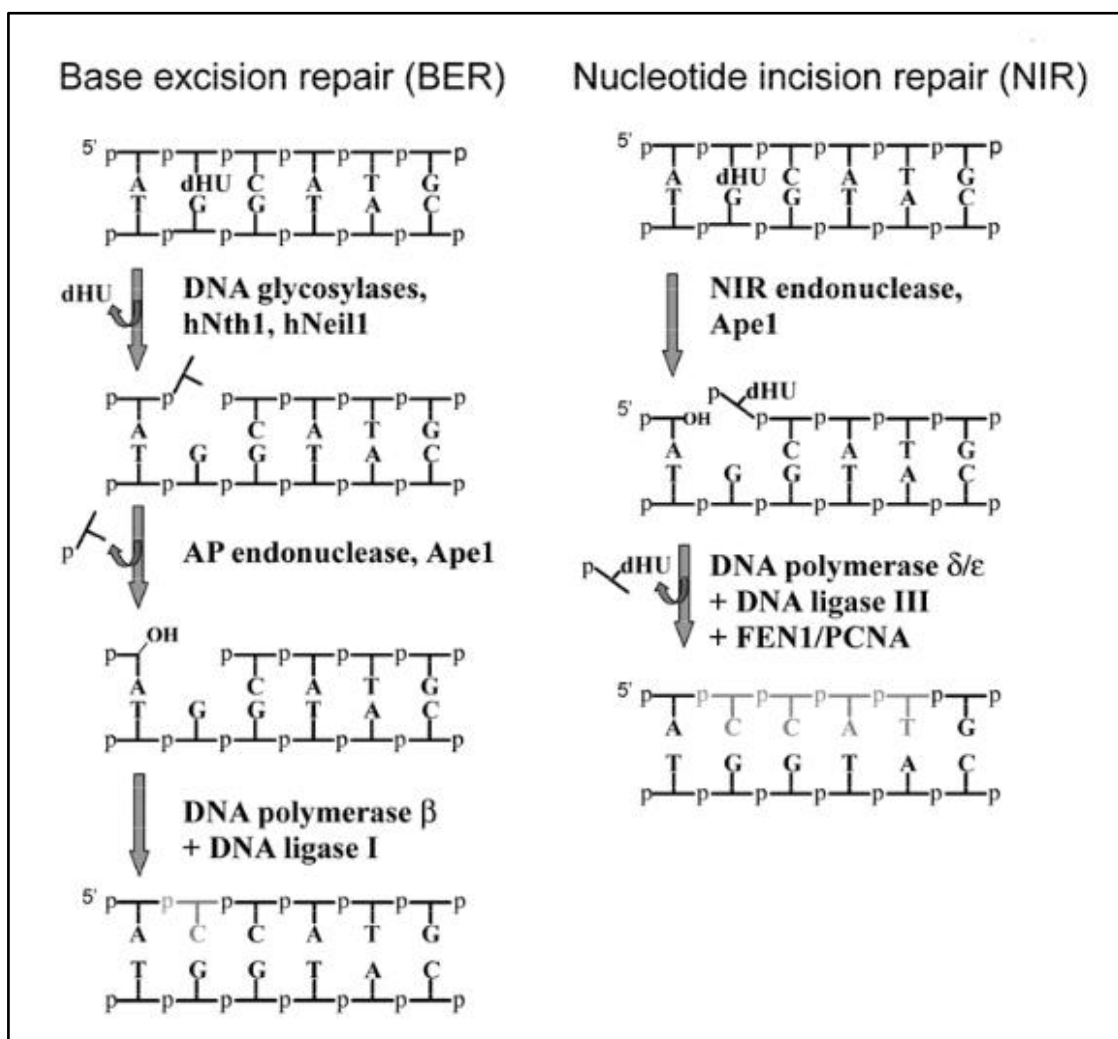


Figure 1-4 Schematic models of the BER and NIR pathways for oxidatively damaged DNA.

DNA glycosylase activity of BER pathway involves in the early step to excise the damaged base by cleavage of the N-glycosylic bond between a modified base and the sugar phosphate backbone (deoxyribose) forming an abasic [apurinic-apyrimidinic (AP)] site or single-strand break (SSB). Alternatively, during NIR route, the oxidatively damaged DNA is incised by an apurinic/apyrimidinic endonuclease (ApeI), on the 5' side. This occurs in a DNA-glycosylase-independent mechanism to provide 3'-hydroxyl and 5'-phosphate correct ends for DNA synthesis. [The Figure adapted from (Evans and Cooke, 2007)].

1.5.2 Nucleotide excision repair and transcription-coupled repair

The activity of nucleotide excision repair (NER) is primarily directed to bulky DNA adducts, for instance, cyclobutane thymine dimers. However, its contribution in excision of smaller non-bulky lesions has also been reported especially 8-oxoGua and thymine glycol (Tg) (Cooke et al., 2005). There is evidence suggesting that NER could presumably yield oligomer containing lesion products 24-32 nucleotides long, which could be degraded by intra/extracellular 5'-3'-exonucleolytic digestion to produce eventual shorter lesion containing oligomer with 6-7 nucleotides in length (Cooke et al., 2005, Evans et al., 2004). It is suggested that, perhaps, further processes might occur that degrade such oligomers to appear in urine as 8-oxodG, for example (Evans et al., 2010). Although the main role of XPA and XPC in repairing 8-oxoGua is not entirely via their function in NER, the exact role is still unidentified. Possibly, XPA and XPC may aid in lesion recognition and/or stimulating glycosylase activity (Evans et al., 2010).

Transcription couple repair (TCR) could also theoretically participate in the production of lesion-containing oligonucleotide products. By this way, the TCR could recruit NER to the genome at a transcriptionally active region with subsequent generation of such oligonucleotide products lesion, although the exact situation for its enrolment in 8-oxoGua removal is uncertain (Evans et al., 2010). The repair rate of oxidatively induced monomeric base lesion such as Tg or 8-oxoGua are more rapidly removed in transcribed genome region in comparison to non-transcribed one (Evans et al., 2004).

1.5.3 Nucleotide incision repair

Nucleotide incision repair (NIR) is identified as a DNA-glycosylase-independent mechanism in which an incision is achieved by apurinic/apyrimidinic endonuclease (Ape1), on the 5' side of oxidatively damaged DNA, with producing 3'-hydroxyl and 5'-phosphate correct ends ready for DNA synthesis, and also coupled to the repair of the outstanding 5'-dangling modified nucleotide (Evans and Cooke, 2007) (Figure 1-4). In fact, its end result, an oxidized 2'-deoxyribonucleoside-3'-monophosphate, could be further progressed by 3'(5')-nucleotidase into urinary 8-oxodG (Evans et al., 2010).

It is apparent that certain oxidized nucleobases are recognized and removed by the NIR pathway. These oxidised nucleobases, including 5,6-dihydrothymine, 5,6-dihydrouracil,

5-hydroxyuracil and 5-hydroxycytosine, could act as substrates for NIR, and they are also recognised and removed by DNA glycosylases. By this means, it is suggested that NIR could act as a compensatory pathway to counteract the oxidation of DNA (Evans et al., 2010). It is noted that NIR and BER could share common substrates and this suggests that both routes work in concert for cleansing the genome of lesions with potential mutagenic and cytotoxic effects (Evans and Cooke, 2007). In addition, under specific structural situations a gap containing a 3'-terminal 8-oxodG or single-strand nick, 8-oxoGua could also be a substrate for apurinic/apyrimidinic endonuclease (Ape1) in NIR (Evans et al., 2010). Such a structural context possibly emerges during misincorporation of 8-oxodGTP at some stage of DNA replication, gap filling after DNA repair or even following ionizing radiation-induced DNA damage with clustered lesion formation (Evans et al., 2010). It is possible that tandem lesions refractory to repair by BER, with oxidized pyrimidine and 8-oxoGua constituents, could feasibly be repaired by the NIR route (Evans et al., 2010).

1.5.4 Mismatch repair

During DNA replication, mismatch repair (MMR) might provide additional defence ability for any mismatches evading the proofreading process, and perhaps, 8-oxodGTP mis-incorporation following Nudix hydroxylase activity escape (Russo et al., 2004, Evans et al., 2010). Error correction is started by heterodimeric recognition factors hMutS α (hMSH2/hMSH6) and hMutS β (hMSH2/hMSH3) which preferentially distinguish (base-base mismatches and small insertion-deletion loops) and (large insertion-deletion loops), respectively (Russo et al., 2004). For that reason, hMutS β seems neither to bind DNA substrates with 8-oxodG nor induce ATPase activity (Mazurek et al., 2002). Subsequently, the process is preceded by binding ATP, recruitment of hMutL α (hMLH1/hPMS2) into recognition complex, then nicking 3' or 5' of the lesion by the endonuclease activity of hMutL α , and probably further resection performed by the 5' to 3' exonuclease I (hEXO1) (Wang and Hays, 2007, Evans et al., 2010) (Figure 1-5). The latter removes the mismatch, producing an associated 8-oxodGMP, which acts as a substrate for nucleotidase enzyme activity to dephosphorylate into 8-oxodG (Evans et al., 2010). Colossi and colleagues proposed the role of MMR in excision of incorporated 8-oxodGMP from newly synthesized nascent DNA (Colussi et al., 2002). Moreover, the mammalian MutS α displays lower recognition potential into the context of 8-oxoG:C and 8-oxoG:A base pairs following

an oxidation insult, whereas its highest preferential is subjected towards 8-oxoGua:T and 8-oxoGua:G pairs (Macpherson et al., 2005).

It is also worth noting that the exonuclease proofreading function of DNA polymerase, particularly when participating in the elimination of faulty 8-oxodGTP incorporation in daughter DNA, generates 8-oxodGMP which eventually might result in 8-oxodG (Evans et al., 2010).

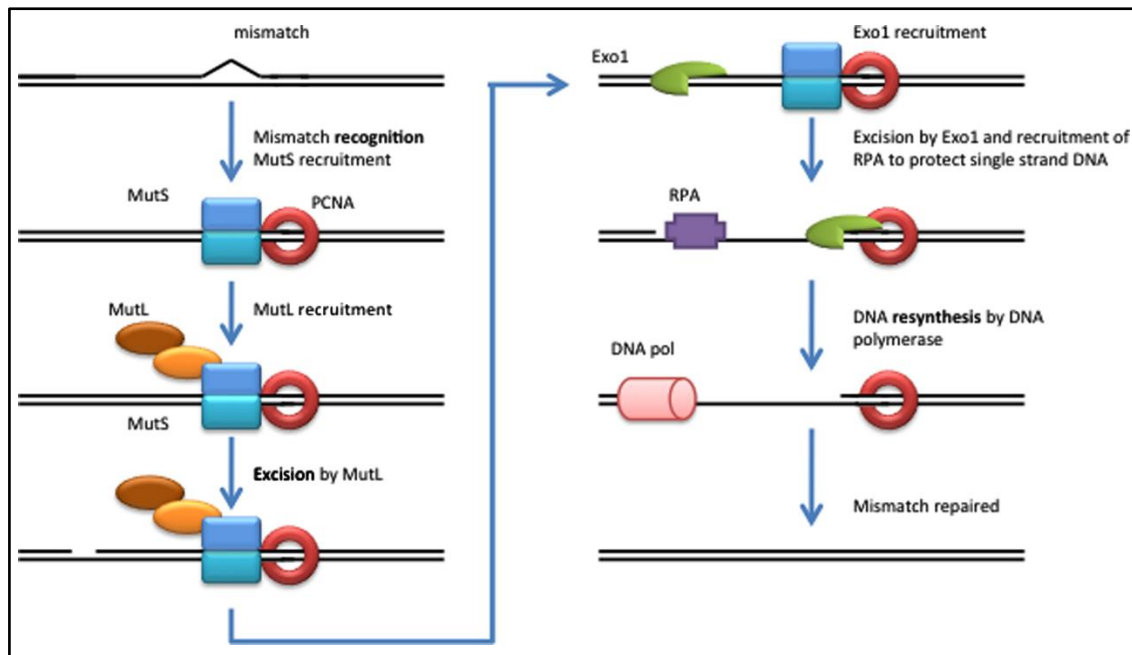


Figure 1-5 A schematic illustration of DNA MMR pathway.

During DNA replication, base-base mismatches and insertion-deletion loops could be recognized by the MMR pathway. Three steps are responsible for repairing these errors, including lesion recognition, lesion excision and finally DNA resynthesis by DNA polymerase [The Figure adapted from (Guillot and Martin, 2014)].

1.6 Replication stress and DNA damage response

DNA replication is regarded as a crucial cellular mechanism and is tightly controlled to ensure full transmission of genetic materials into the next offspring cells. In that case, the cellular division has to happen once in each cell cycle with accurate DNA duplication, otherwise, genomic instability and genetic aberrations might accumulate; encouraging certain diseases and cancer establishment (Boyer et al., 2016).

The oxidised DNA bases within the genome do not majorly disrupt DNA structure. However, they have the potential to subsequently induce mutations via mis-pairing events during DNA replication (Shibutani et al., 1991, Tkeshelashvili et al., 1991, Sekiguchi, 2006, Fotouhi et al., 2011). They can also lead to the generation of secondary types of DNA damage such as DNA SSBs that arise when DNA glycosylases remove damaged bases during BER (Oka et al., 2008). Oxidised DNA bases may also lead to a production of DNA DSBs (Rai et al., 2009, Rai et al., 2011, Gad et al., 2014), though the mechanisms for how this occurs remain undefined. One proposed model is that oxidised DNA bases induce DNA replication stress, and that this somehow subsequently leads to DSBs (Gad et al., 2014, Huber et al., 2014).

Challenging the replication fork with different obstacles may perhaps lead to so-called “replication stress”. The latter is a condition of slowing down or stalling in the progression of DNA replication fork and in turn altered DNA synthesis (Mazouzi et al., 2014, Zeman and Cimprich, 2014).

1.6.1 Causes of DNA replicative stress

There are numerous recognized sources of replication stress among which unrepaired DNA lesions are considered as the most common obstacle (Figure 1-6). However, such DNA damage could be bypassed by DNA damage tolerance pathways. Misincorporation of ribonucleotides is another replication fork barrier which has been identified, which are removed by RNase H2, a specialized enzyme in ribonucleotide excision repair (Zeman and Cimprich, 2014). In addition, repetitive DNA sequences with secondary DNA structure formation, including hairpins, triplexes, cruciforms, H-DNA, Z-DNA and G4, might be obstructive for normal DNA synthesis with subsequent threatening for genome stability (Mazouzi et al., 2014) (Figure 1-6).

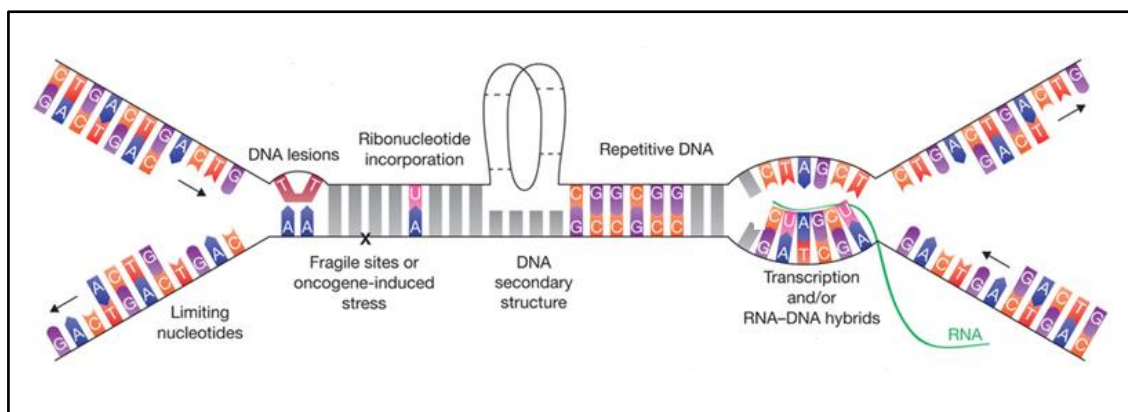


Figure 1-6 Overviews of the different sources of replication stress.

Several obstacles or conditions are shown with the ability to slow or stall DNA replication fork, such as limiting nucleotides, DNA lesions (DSBs and SSBs), ribonucleotide incorporation, repetitive DNA sequences, transcription complexes and/or RNA–DNA hybrids, DNA secondary structure, fragile sites, and oncogene-induced stress. [The Figure adapted from (Zeman and Cimprich, 2014)].

Replication fork and transcription machinery are coordinated processes and work in spatially separated sites. Once a collision occurs, DNA–RNA hybrids (R-loops) (Figure 1-6) are problematic for replication; because this genomic region could be susceptible to DSB and early replicating fragile sites formations. Furthermore, topological stress could interfere with DNA replication, even before replication–transcription complex collision has taken place, and is likely due to tethering of newly formed RNA transcripts to the nuclear pore. This process is counteracted in ataxia telangiectasia and Rad3-related protein (ATR)-mediated manner to ensure the ordinary progression of the replication fork (Zeman and Cimprich, 2014, Mazouzi et al., 2014).

Moreover, there are other genomic loci that are denoted as common fragile sites; enriched with A/T content, have condensed chromatin structure and exhibiting late replication (Figure 1-6). In the human genome, more than 200 common fragile sites are present with quite a large size, around 1–10 Mb. These regions are also prone to DNA DSBs induced by replication stress (Zeman and Cimprich, 2014, Mazouzi et al., 2014).

Expression of oncogenes promotes cell proliferation through controlling cell cycle regulatory pathways. Recently, overexpression or activation of oncogenes has appeared as a source of replication stress in response to deregulation of origin firing. Cyclin E and overexpression RAS could alter cyclin-dependent kinase (CDK) with subsequent increasing in origin firing and reduction in inter-origin distances. As a consequence,

DNA replication fork stalling and collapse might occur, resulting in DSBs as well as genomic instability. In addition, reduction in replication origin licensing could also observe following overexpression of cyclin E. such event leads to under-replicated DNA (Boyer et al., 2016, Gaillard et al., 2015). After oncogene activation, licensing factors such as chromatin licensing and DNA replication factor 1 (Cdt1) and cell division cycle 6 (CDC6) might aberrantly be upregulated and lead to DNA re-replication, by re-licensing and origin firing for more than one time during an individual cell cycle (Boyer et al., 2016). Moreover, it has been stated that ROS generation is an indirect effect of oncogene activation, such as MYC, with DNA damage outcome that might act as a potential for replication fork progression impairment (Gaillard et al., 2015).

1.6.2 Consequences of DNA replication stress

Cells respond to stalled fork during replicative stress, in order to rescue the fork progression. However, if stabilization of stalled forks does not occur or they persist for a long time, a collapse of DNA replication machinery is the ultimate outcome with associated genome instability. Activation of ATR pathway can stabilize and restart replication forks following the removal of the cause of the stress (Zeman and Cimprich, 2014). Upon stalling of the replication fork, stretches of single-stranded DNA coated with RPA can form as a result of uncoupling between DNA polymerase and the helicase. This acts as a signal for replication stress response with a recruitment of ATR into the region, through the interaction of RPA and ATR-interacting protein (ATRIP). Prevention of late origin firing and cell cycle progression are also induced following ATR/checkpoint kinase1 (Chk1) signaling cascade activation (Boyer et al., 2016, Gaillard et al., 2015). Other pathways are responsible for restarting replication process in case of unrepaired DNA lesion (Zeman and Cimprich, 2014) (Figure 1-7).

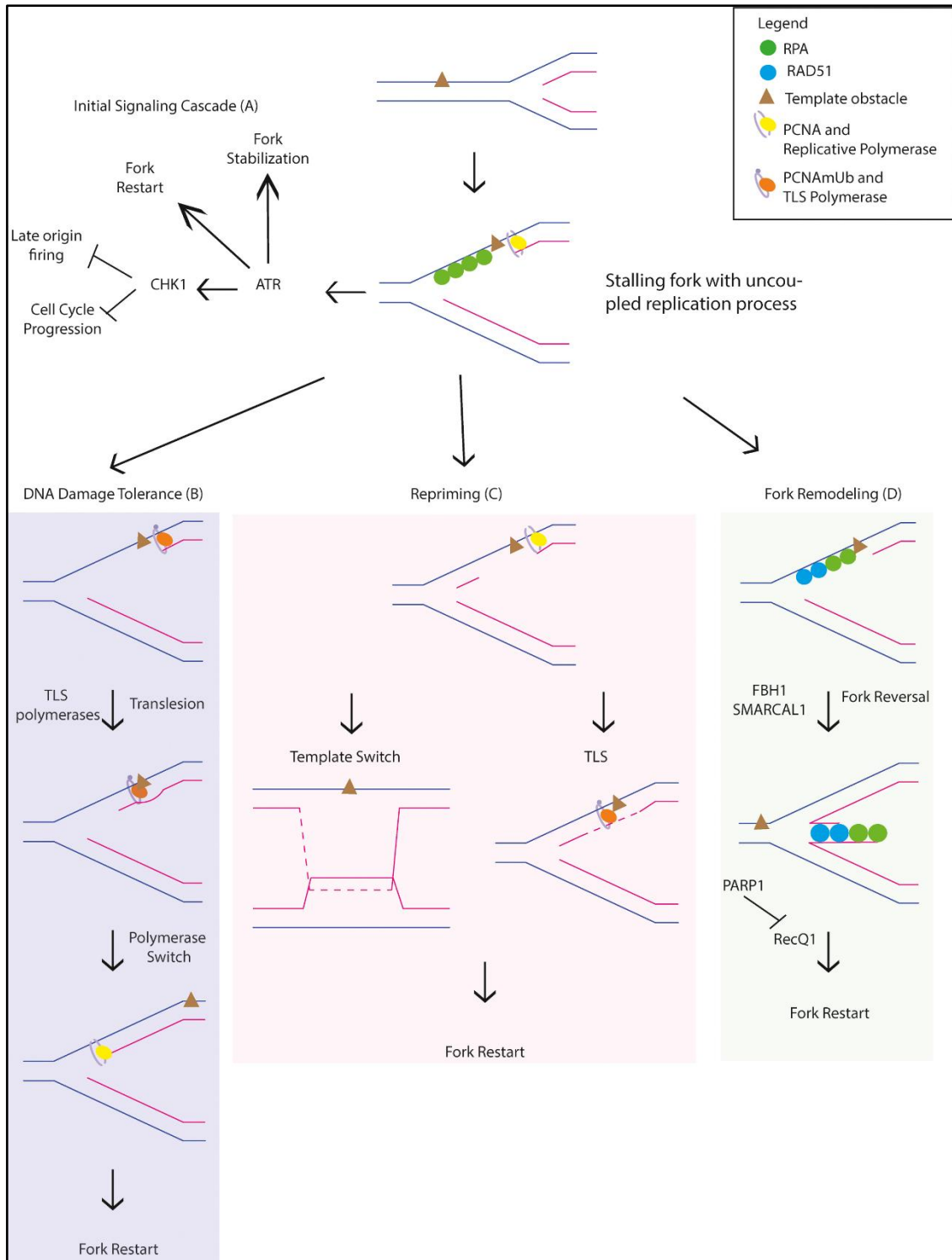


Figure 1-7 Overview of stalled replication fork restart/rescue pathways.

Stalled replication fork might occur at a template obstacle (represented as a brown triangle) that lead to an uncoupling between the polymerase and the helicase. The accumulation of single-stranded DNA is protected by RPA and this act as a signal for replication stress response initiation with (A) recruitment of ATR into the region and activation of effector kinase Chk1 to stabilize the forks and prevent cell cycle progression. Several mechanisms can restart replication forks as indicated (B, C, and D). [The Figure adapted from (Boyer et al., 2016)].

DNA damage tolerance is an alternative route to avoid fork stalling during S phase. It can be achieved by specialized translesion polymerases, a member of Y polymerase family (Pol η , Polk, Polt and Rev1), that demonstrate a lower fidelity towards continuing DNA synthesis (Boyer et al., 2016) (Figure 1-7). In addition, repriming replication could bypass DNA lesions and reinitiate replication machinery further down the DNA template (Figure 1-7). This, in turn, produces a gap which necessitates an involvement of post-replicative DNA repair, mainly by translesion (TLS) DNA synthesis or homologous recombination mediated template switch (Boyer et al., 2016, Gaillard et al., 2015). The former reinitiating activity has been attributed to a recently found DNA polymerase, termed Primpol (Boyer et al., 2016). Fork remodeling with a formation of fork reversal is another facilitating pathway for fork restart (Figure 1-7). There are certain helicases proteins which are involved in the promotion of fork reversal such as FBH1, SMARCAL1 along with other enzymes. Transient inhibition of RECQ1 following PARP1 activation has also been viewed as a key factor for fork stabilization and remodeling to restart (Boyer et al., 2016) (Figure 1-7).

In the perseverance of replication stress or loss of replication components, failure to restart stall forks with sequential fork collapse might occur, despite the presence of a complex cellular response to stabilize and restart a stalled fork (Zeman and Cimprich, 2014). The exact mechanism of replication fork collapse is still not well established, and one of the potentials are replisome dissociation or involvement of unfunctional and improper positioned replisome (Figure 1-8). Formation of a DSB at the site of fork blockage is another likely possibility. Such process could be attributed to an endonucleolytic digestive effect on vulnerable products (reversed fork, stalled fork, or single-stranded DNA), or replication run-off (Zeman and Cimprich, 2014) (Figure 1-8).

Furthermore, single-stranded DNA gaps left after the fork could passively convert to fork breakage, promoting the formation of single-ended DSBs or double-ended DSBs (Cortes-Ledesma and Aguilera, 2006). DSBs exhibit cellular genotoxic influence, although single-ended DSB repair is mediated by the break-induced replication pathway of homologous recombination (Aguilera and Gomez-Gonzalez, 2008).

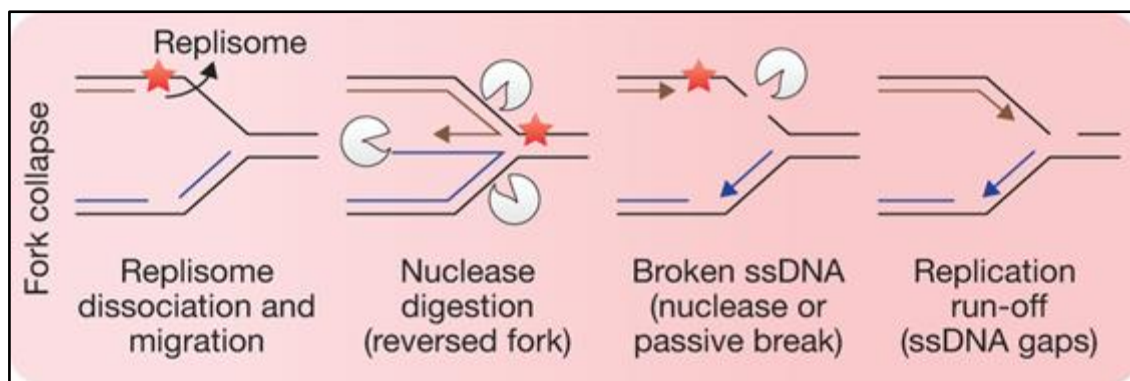


Figure 1-8 Mechanisms of stalled replication fork collapse.

When stalled replication forks at DNA lesions (red star) are not stabilized or persisted for a longer time, the replication forks will collapse and subsequently prevent the restart of replication. The exact mechanism that provokes replication fork collapse is still undefined. However, there are a number of possibilities that exist such as dissociation of replisome components, nuclease digestion of a reversed or stalled fork, or replication run-off (single-stranded DNA gaps). [The Figure adapted from (Zeman and Cimprich, 2014)].

Taken together, the proposed model as to how oxidised DNA bases induce DNA replication stress and that leads to the production of DSBs remains undefined and the mechanisms are unclear. It is possible that DSBs can arise from replication fork run-off at BER-induced SSBs, which would lead to the generation of one-ended broken DNA replication forks in a mechanism analogous to DSBs arising from Top1-DNA adducts (Strumberg et al., 2000). Alternatively, DNA replication forks may stall at sites of oxidatively damaged DNA and be cleaved by endonucleases to also generate one-ended broken replication forks (Hanada et al., 2007, Regairaz et al., 2011). No matter how they arise, DSBs are potentially highly genotoxic or cytotoxic due to loss of chromosome integrity. In particular, one-ended DSBs on replicating chromosomes may be very difficult to resolve and are linked to various types of mutations (Lee et al., 2007, Zhang et al., 2009, Hastings et al., 2009, Liu et al., 2011).

The data described above would indicate that increased misincorporation of oxidised dNTPs during oxidative stress has the potential to induce DNA-replication-associated genomic instability and/or cell death. This means that the pathways that act to sanitise the dNTP pool and prevent the accumulation of oxidised DNA bases within the genome could be critical in either promoting or suppressing cancer cell growth and continuing tumour evolution depending on circumstances and context.

1.6.3 DNA damage response

The DDR is a complex web of interacting pathways to counteract and detect DNA damage and replication stress, transduce the signals to maintain a proper cellular reaction (Ciccio and Elledge, 2010). This coordinated network can be achieved by certain sensors, signal transducers and effector proteins (Jackson and Bartek, 2009). Among the primary mediators of DDR, ataxia telangiectasia mutated (ATM) and ATR belong to phosphatidylinositol 3-kinase-like protein kinase family with different response to various stimuli (Mazouzi et al., 2014).

ATM is activated on account of DSBs, whereas, ATR responds to single-strand DNA creation following stalled replication forks (Gaillard et al., 2015). As described above in section 1.6.2., RPA coating of single-stranded DNA can act as a platform to recruit ATR into the fork site. It can also recruit Rad17-RFC2-5 to load the Rad9-Hus1-Rad1 (9-1-1) complex which can bind and recruit TOPBP1 protein, resulting in stimulation of ATR kinase activity (Ciccio and Elledge, 2010, Mazouzi et al., 2014) (Figures 1-9, and 1-11B). This, in turn, is translated through activation and phosphorylation of Chk1, to suppress late origin firing as well as stimulate S-phase checkpoint necessary for modulating recovery of the cell (Mazouzi et al., 2014) (Figure 1-9). Stabilization of replication fork is supported by TIM/TIPIN complex and claspin, allowing Chk1 kinase to accumulate at the site of RPA coated single-stranded DNA. Moreover, the stalled replication fork is restarted in a way which depends on numerous DNA helicases, such as BLM, WRN, FANCM, HLTF, and SMARCAL1; that many of which are recruited and/or interact with PRA at the fork region (Ciccio and Elledge, 2010). It has been suggested that MRE11-Rad50-NBS1 (MRN) complex and RAD51 are also accumulated at single-stranded DNA following replication stressful conditions, although the role of ATM in activation of MRN in early replication stress is not entirely revealed (Mazouzi et al., 2014) (Figure 1-9). In addition, the replication intermediates can be resolved by activation of BLM helicase by ATM (Mazouzi et al., 2014) (Figure 1-9).

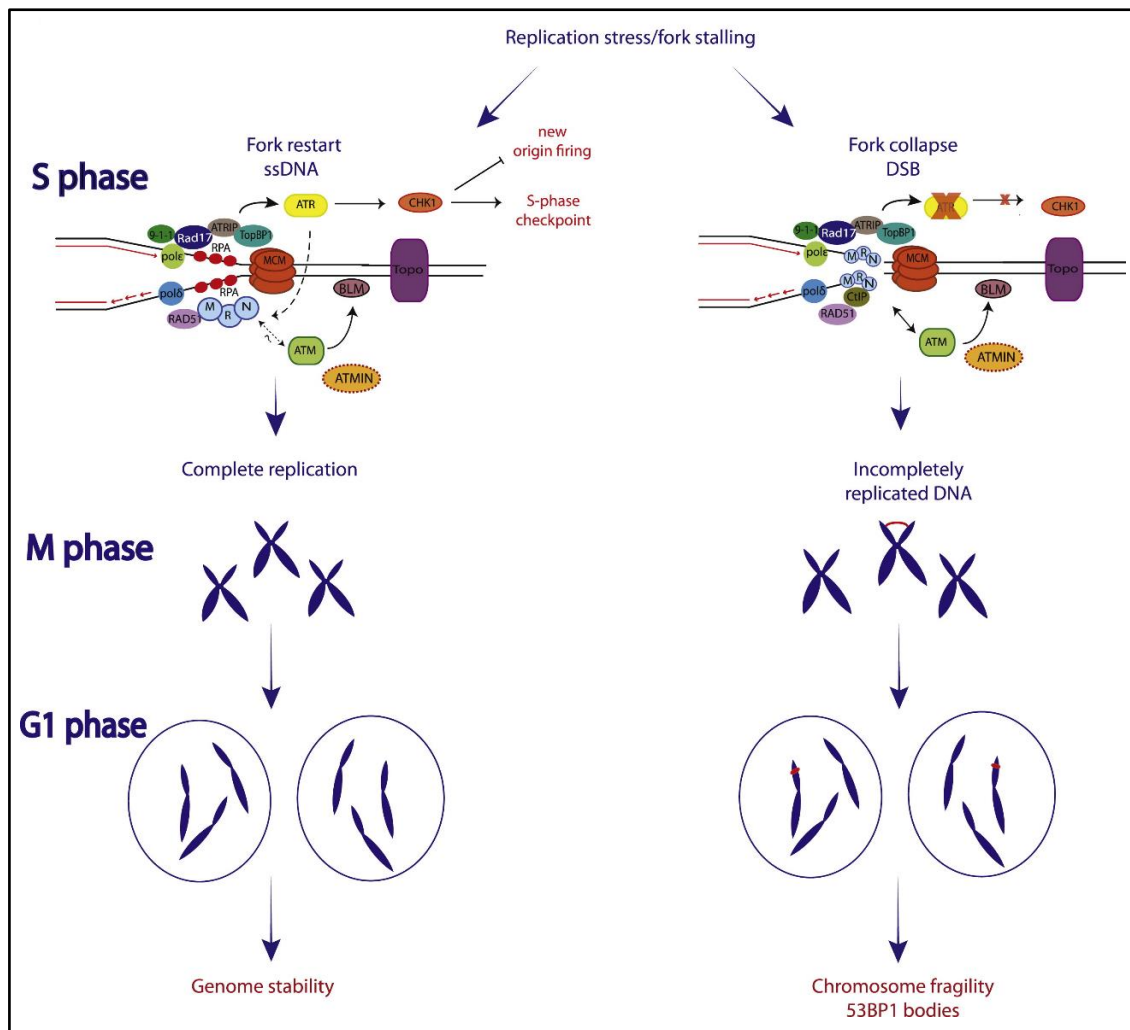


Figure 1-9 Main DNA damage pathways for processing the replication intermediates.

Replication stress leads to the production of single-strand DNA coated by RPA. The latter protein is able to recruit ATRIP, Rad17 and 9-1-1 complex that together with TOPBP1 cause ATR kinase activation. This, in turn, is responsible for phosphorylation of Chk1, to suppress late origin firing as well as stimulate S-phase checkpoint necessary for modulating recovery of the cell. The MRN complex and RAD51 are also accumulated at sites of single-strand DNA following replication stress and necessary for fork restart. Though the role of ATM in activation of MRN in early replication is not entirely identified, ATMIN might have a role in the ATM activation in response to replication stress. In addition, ATM can stimulate BLM helicase, contributing to the resolution of replication intermediates. Defective checkpoint activation induced by compression of ATR cascade might lead to fork collapse into DSBs. These lesions may subsequently resolve by homologous recombination via CtIP and RAD51 recruitment. However, replication stress in the absence of ATR can cause incompletely replicated genome with abnormal DNA structures formation that probably transmitted to the next generation, if not resolved in a proper way, and leading to genome instability. [The Figure adapted from (Mazouzi et al., 2014)].

Upon fork collapse, and DSBs formation, there will be a recruitment of MRN/ATM at the breakage site to mediate homologous recombination repair. The activation of ATM kinase results in phosphorylation of checkpoint kinase2 (Chk2) and p53, as well as enabling γ H2AX-dependent signaling cascade induction, triggering further recruitment of MDC1, RNF 168, BRCA1, and 53BP1 into the DSBs site (Ciccio and Elledge, 2010) (Figure 1-10A). However, if the replication intermediates are unresolved, 53BP1 nuclear bodies can bind DSBs and shield the unrepaired DNA lesions in the subsequent G1 stage of the cell cycle (Mazouzi et al., 2014).

ATR/Chk1 together with ATM/Chk2, act in a way to decrease the activity of CDK, presumably by transcription factor p53 activation or Cdc25 interaction. Such inhibition arrests the cell or slows down the cell cycle progression (Jackson and Bartek, 2009, Jossen and Bermejo, 2013). Simultaneous enhancement of DNA repair could also occur following ATR/ATM signal inducing cascades; via recruitment and activation of DNA repair proteins in the damaged region with modulation of their phosphorylation, acetylation, ubiquitylation or SUMOylation. However, DDR could elicit cellular senescence or apoptotic cell death in the case of deficiencies or difficulties in the removal of DNA damage (Jackson and Bartek, 2009).

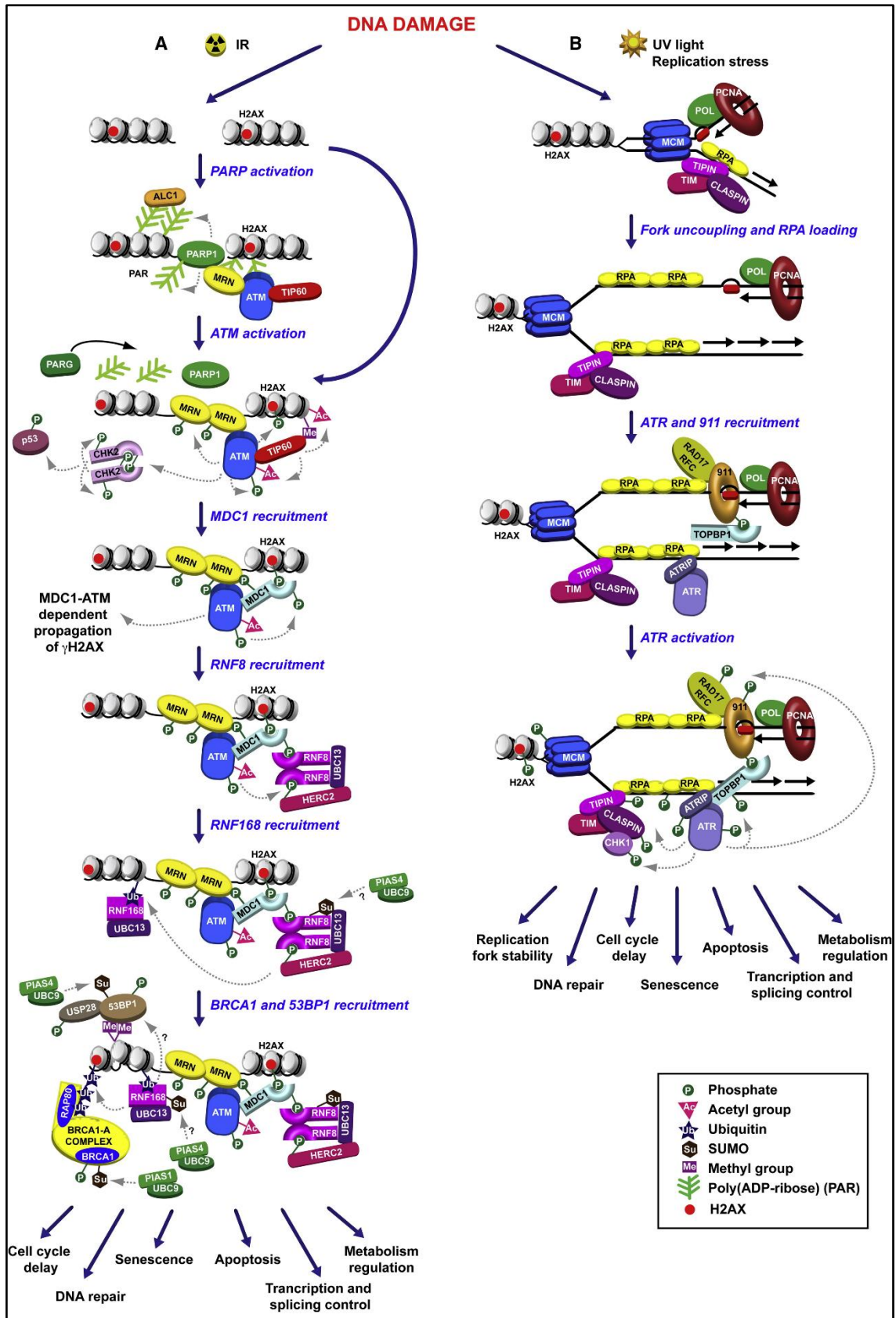


Figure 1-10 Activation model of ATM and ATR in response to DNA damage lesion.

(A) DSBs formation activates PARP1 that leads to recruitment of MRN/ATM complex at DSBs sites. Subsequently, ATM kinase activation by MRN and TIP60 results in phosphorylation of Chk2 and p53, in addition, to enable γ H2AX-dependent signaling cascade induction, and triggers further recruiting of MDC1, RNF 168, BRCA1, and 53BP1 into the DSBs region. (B) stalled Replication fork and accumulation of RPA-coated single-stranded DNA, leading to recruitment of ATR/ATRIP and the RAD17/RFC2-5 complexes. The latter promotes 9-1-1 complex loading and that can bound and recruit TOPBP1 protein, resulting in stimulation of ATR kinase activity and phosphorylation of Chk1. [The Figure adapted from (Ciccia and Elledge, 2010)].

1.6.4 Replication stress relevance to cancer

In the early tumorigenesis, activation of ATR/ATM-dependent DDR signaling is detectable in precancerous lesions, which presumably acts to suppress cancer. The cell could stimulate DNA damage checkpoints before the occurrence of a defective p53 pathway or genomic instability. Any mutation in such DNA damage checkpoints might allow the ongoing of cellular proliferation and survival with tumor development (Bartkova et al., 2005, Gorgoulis et al., 2005). Epigenetic effects of environment or other molecular factors might also harbor a burden for inactivation of DDR components during carcinogenesis (Jackson and Bartek, 2009).

One of the hallmarks of cancer is a genomic instability, and it is stated DNA replication as the most vulnerable cell process that can lead to it (Gaillard et al., 2015). The situation that elicits high DNA damage levels will possibly lead to replication stress, and to some extent, this is regarded as a genome instability source, as well as, a feature of premalignant and malignant cells (Gaillard et al., 2015). Therefore, it is crucial to understand the molecular basis of replication to realize the aspect of tumorigenesis (Gaillard et al., 2015). There is evidence that colorectal cancer cells harbouring sufficient cancer chromosomal instability could exhibit an impairment in replication fork progression with increased DNA replication stress, and largely accompanied by structural chromosomal abnormalities that missegregate during mitosis (Burrell et al., 2013a). By this mean, a raised level of numerical and structural chromosome alterations have been greatly observed during the status of replication stress and might cause inter and/or intra-tumor heterogeneity (Burrell et al., 2013a, Burrell et al., 2013b). The latter

allows the tumor to attain new characteristic features with therapeutic resistance and poor prognosis (Burrell et al., 2013a).

Chromosome segregation errors arise as a consequence of incomplete DNA replication or unresolved repair intermediates; and they are typically started at or before the onset of a mitotic stage of the cell cycle (Gaillard et al., 2015). The most common missegregating chromosomes include pre-mitotic acentric and anaphase bridge defects. However, mitotic dysfunction accounts for the less frequent abnormality such as lagging chromosomes (Burrell et al., 2013a). Upon breakage of this missegregating chromatids, it potentially provokes breakage-fusion-bridge formations, events usually identified in cancer cells (Gaillard et al., 2015). In addition, micronuclei could be generated from lagging chromosomes in the progeny cells. Defective DNA replication in the micronuclei occurs with widespread DNA damage and fragmentation, resulting in massive genomic rearrangements which might reintegrate into to nucleus during the successive cell cycle. Thus, such micronuclei might contribute to the development of cancer (Gaillard et al., 2015).

1.7 NUDT1 and the impact of Nudix hydrolase family enzymes on carcinogenesis

The oxidised dNTPs are cleared from nucleotide pools by Nudix hydrolase family enzymes; such as NUDT1, to prevent their mis-incorporation into DNA genome or RNA by converting them into a mono-phosphate product and PPi (Mildvan et al., 2005).

The hNUDT1 gene, located on chromosome 7p22, has five exons and can ultimately produce seven mRNAs types namely type 1, 2A, 2B, 3A, 3B, 4A and 4B with different 5' sequences (Figure 1-11). The differences in location of transcription initiation as well as alternative splicing process were mainly responsible for such variants (Nakabeppu, 2001, Oda et al., 1999). During the translation process, the main isoform of NUDT1 (p18) is encoded by type 1, 2A, 3A and 4A mRNA; whereas the production of three forms of NUDT1 polypeptides (p21, p22, and p18) were undertaken by B-type transcripts and recognized by Western blot analysis of human cells extracts (Nakabeppu, 2001). In addition, polymorphism at exon 4 of NUDT1 gene could exist in association with codon 83 of p18 NUDT1 protein (ATG⁸³ and GTG⁸³ codons), that encode Met83-MTH1 and Val83-MTH1, respectively. The former is exclusively being linked with another single nucleotide polymorphism at exon 2c (GC) with consequent

formation of Met83-MTH1 (p26). The association between Val83 and polymorphism (GT) at exon 2c can also occur, but without p26 synthesis (Nakabeppu, 2001).

The structure of NUDT1 gene possesses binding sites for particular regulatory transcriptional activators such as NF- κ B, AP-1, and ETs family proteins. The latter is involved in the induction of gene expression especially during proliferative activation of cells and cancer progression, whereas NF- κ B and AP-1 upregulate NUDT1 gene expression in the situation of oxidative stress (Nakabeppu, 2001). Other binding sequences also occur for Sp1 and c-Myc proteins. Moreover, NF- κ B transcription factor has a functional role for induction of premature senescence in normal human lung fibroblasts (HDF cell line) or even as an apoptotic outcome in lung cancerous cell line, following ROS-mediated DDR through the p53-p21 pathway. However, the linkage between signaling of NF- κ B and NUDT1 for inducible cellular senescence needs to be determined (Sfikas et al., 2012).

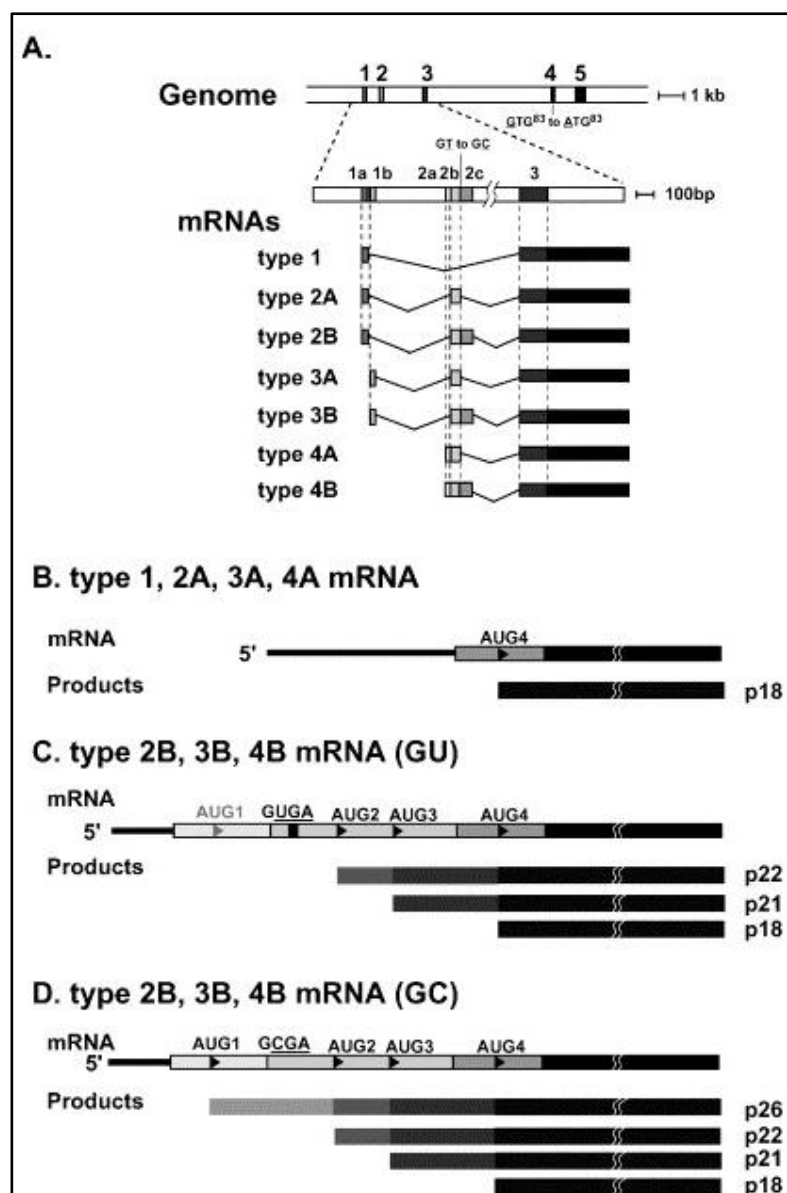


Figure 1-11 Diagrammatic representation of the human NUDT1 genomic structure, mRNAs transcripts, and their predicted translational products.

(A) Genome structure along with alternative splicing process of NUDT1 gene. The overall human NUDT1 gene structure, located on chromosome 7p22, is shown in the upper part, in which each hatched box represents an exon. Throughout the lower part, seven types of NUDT1 mRNA and a portion of their genome are depicted. The former is generated by alternative transcription initiation and splicing in exons 1 and 2, but not 3-5. Polymorphic alteration (GT to GC located at the beginning of exon 2c segment; GTG⁸³ to ATG⁸³ in exon 4) are also shown. (B) Type 1, 2A, 3A, and 4A NUDT1 mRNAs with their translation product, p18. (C) B-type NUDT1 mRNAs along with GU polymorphism at the beginning of exons 2c and their translation products (p18, p21, and p22). (D) B-type NUDT1 mRNAs along with GC polymorphism at the beginning of exons 2c and their translation products (p18, p21, p22, and p26). This polymorphic site abolishes the UGA stop codon, hence, AUG1 can be utilized as an initiation codon. [The Figure adapted from (Nakabeppu, 2001)].

Evidence exists for oxidative stress; in particular oxidatively damaged DNA, having a crucial role to form specific mutations during initiation of cell transformation and cancer development (Olinski et al., 2003).

The analysis of mutation frequency at *Hprt* gene in DK1 and DK7 cells with deficient NUDT1 alleles (NUDT1^{-/-} cells) revealed 2-fold rise of the mutation rate in comparison to those expressing NUDT1 (NUDT1^{+/+} cells), suggesting a potential role for NUDT1 in prevention the mutations occurrence under normal growth conditions (Tsuzuki et al., 2002). In addition, the mutagenicity of 8-oxodGTP was enhanced by 2-OHdATP as the A:T to C:G transversion mutations were elevated when both oxidised dNTPs existed in the reaction during in vitro replication system with a HeLa extract (Satou et al., 2007a). This mutation enhancement was attributed to the suppression of 8-oxodGTP hydrolysis by the presence of 2-OHdATP, suggesting that depletion of NUDT1 protein might have a major role for such induced mutations rate (Satou et al., 2007a). It has also been revealed that triple knockdowns of NUDT1, NUDT15, and NUDT5 by small interfering RNA (siRNAs) in human embryonic kidney (293T cells), leads to an increased frequency of A:T to C:G transversion mutations than a single knockdown. This mutation was initiated by 8-oxodGTP, suggesting mutual complementary roles of the three Nudix hydrolase enzymes during removal of 8-oxodGTP from the dNTP pool (Hori et al., 2010). In addition, it was noted that hydrogen peroxide (H₂O₂) treatment leads to the accumulation of genomic 8-oxoGua and cell death in *NUDT1*^{-/-} mouse embryonic fibroblasts (Yoshimura et al., 2003), demonstrating that oxidative stress can be cytotoxic in a NUDT1-deficient background. The role of NUDT1 in cancer is also strengthened in other studies, as lower NUDT1 levels are associated with higher 8-oxoGua in the genomic DNA of U2O2 osteosarcoma cells and non-small cell lung cancer (NSCLC) samples (Gad et al., 2014, Speina et al., 2005).

Previously, knockout mice models have shown accumulation of 8-oxoGua in their DNA genomes. Sakumi et al. noted that 18-month-old *Ogg1* knockout mice have a 5-fold higher chance of developing spontaneous lung adenomas and carcinomas compared to wild-type animals with the accumulation of 8-oxoGua in their DNA genomes (Sakumi et al., 2003). Similar elevation in the genome accumulation level of 8-oxoGua was observed for double *Ogg1* and NUDT1 deficient mice, suggesting the direct guanine base oxidation much more frequently occurs than the DNA misincorporation of 8-oxodGTP and it also indicated that maintaining low level of 8-oxodG in DNA is mostly

attained by Ogg1 (Sakumi et al., 2003). Interestingly, no lung tumour was observed in these double knockout mice, suggesting disrupted NUDT1 gene might possibly decrease tumorigenesis of Ogg1 deficiency (Sakumi et al., 2003). The author argued that oxidized forms of dATP or ATP accumulation might be responsible for this suppression of tumorigenesis, as NUDT1 is actually able to hydrolyze other oxidized purine nucleotide triphosphates besides 8-oxodGTP. Another possibility is the existence of another tumour suppressor gene that acted in close proximity and co-transmitted with NUDT1 knockout allele. In addition, double knockout of Ogg1 and NUDT1 might induce tumour cell death, resulting from the excessive buildup of 8-oxoGua in nuclear DNA with no lung tumour formation (Sheng et al., 2012). Earlier studies also demonstrated more development of adenoma/adenocarcinoma in lung, liver, and stomach of 18-month-old NUDT1 knockout mice relative to wild-type animals (Tsuzuki et al., 2002, Tsuzuki et al., 2001).

However, NUDT1 overexpression may be necessary for tumour cell proliferation and survival once a tumour has developed in order to compensate for oncogenic RAS-mediated DDR and ROS formation, leading to avoidance of RAS-induced senescence outcome (Rai et al., 2011). Supporting the idea of a role in cancer cell maintenance, NUDT1 expression increases in different types of cancer at messenger RNA or protein levels. It was mentioned that the rise in NUDT1 expression may be at the mRNA level in human renal cell carcinoma (Okamoto et al., 1996), breast tumours (Wani et al., 1998), and pancreatic adeno-carcinoma (Rai et al., 2011); or in NUDT1 protein levels in brain tumours (Iida et al., 2001), and non-small cell lung carcinoma (Kennedy et al., 2003). The latter malignancy along with pancreatic adeno-carcinoma and transitional cell carcinoma of the urinary bladder are well-known tumours with a mutation in RAS gene (Rai et al., 2011, Li et al., 2005), which are small GTPases that can bind and hydrolyse guanosine triphosphate (GTP) (de Castro Carpeño and Belda-Iniesta, 2013). Interestingly, such NUDT1 elevation continues in high-grade NSCLC adenocarcinoma with KRAS mutation compared to surrounding normal tissue. This is in favour, perhaps, of the adaptive mechanism during cancer progression rather than compensatory effect to counteract oxidative stress induced by RAS oncogene (Rai, 2010). NUDT1 overexpression in oncogene-expressing human cells promoted transformation (Rai et al., 2009, Rai et al., 2011, Patel et al., 2015). Furthermore, the

NUDT1 levels correlate with ROS levels in NSCLC tumours (Patel et al., 2015), suggesting that higher ROS levels lead to a requirement for higher NUDT1 activity.

These studies imply that as cells undergo malignant transformation and acquire the trait of oxidative stress, the NUDT1 activity does indeed consequently become essential for continued cell growth. Accordingly, NUDT1 knockdown leads to DDR activation and increased senescence levels in oncogene-expressing human epithelial cells (Giribaldi et al., 2015). The basis of this DDR activation was at least partially linked to oxidative stress and DNA replication stress as culturing in a low oxygen or inhibiting DNA replication with aphidicolin suppressed senescence induction in NUDT1-deficient cells (Rai et al., 2009). Conversely, NUDT1 overexpression promoted transformation in human fibroblasts and epithelial cells by alleviating oncogene-induced DDR activation and premature senescence (Rai et al., 2009, Rai et al., 2011, Patel et al., 2015), and repressed the DNA-replication-dependent mutator phenotype in mismatch-repair-defective colorectal cancer cells (Russo et al., 2004).

Collectively, these data indicate that NUDT1 compensates for the cancer-associated trait of high oxidative stress, suppressing oxidative DNA damage levels to prevent secondary cytotoxic DNA damage and cell death. It is improbable that normal untransformed cells display a similar reliance on NUDT1 activity, though this may depend on context (e.g. cell type, environment, etc.) as NUDT1 knockdown has been observed to have effects in early-passage primary human skin fibroblasts (Rai et al., 2009). Nonetheless, high tumour cell selectivity and sensitivity may be observed with a therapeutic NUDT1 inhibitor. However, results with NUDT1 inhibitors have so far been contradictory. The first developed NUDT1 inhibitors appear to selectively inhibit cancer cell growth (Gad et al., 2014, Huber et al., 2014), but subsequently developed NUDT1 inhibitors from other laboratories display only a weak cancer cell cytotoxicity (Kettle et al., 2016, Kawamura et al., 2016, Petrocchi et al., 2016). Furthermore, these very recently published studies suggest that NUDT1 deficiency induced by either siRNA knockdown or CRISPR-mediated knockout does not hinder the growth of HeLa, SW480 or U2OS cells (Kettle et al., 2016, Kawamura et al., 2016), opposing several previous observations and conclusions (Helleday, 2014, Gad et al., 2014, Patel et al., 2015). Thus, further work must be done to determine the therapeutic potential of targeting NUDT1.

1.8 Non-small cell lung cancer and its subtype

Primary lung cancer is regarded as one of leading cause of cancer death worldwide (Coleman et al., 2011). It has two main types: small cell lung cancer (SCLC) and NSCLC. The latter accounts for 80-85% of lung cancer, and it is further subdivided into adenocarcinoma, squamous cell carcinoma, large cell carcinoma, and other subtypes (Reck et al., 2014, Lechevalier et al., 1994). Despite improvements in survival rates for many other cancer types in recent years, NSCLC therapeutic responses and patient outcomes have not significantly improved (Coleman et al., 2011, Haslett et al., 2014). Consequently, there is a critical need to identify new NSCLC therapeutic targets and strategies (Besse and Reck, 2014).

The most common subtype is adenocarcinoma which represents almost 40% of NSCLC (Raponi et al., 2006). It is more prevalent in female and young age group than other types of lung cancer (Toyooka et al., 2003). In addition, this malignant tumour tends to locate in outer part of the lung, while, squamous cell carcinoma (25-30% of NSCLC) is often found at central lung region near the bronchi (Langer et al., 2010). For the large cell carcinoma, it is the least subtype, accounts for 10-15% of NSCLC, and could appear in any lung area. There are also other rare subtypes of NSCLC, for example, adenosquamous carcinoma and sarcomatoid carcinoma (Hirsch et al., 2008). The treatment base strategy of NSCLC depends mainly on the cancer staging, molecular cancer aspect, patient age, his general wellbeing and preference (Reck et al., 2014).

1.9 Gemcitabine and cisplatin as first-line treatment of NSCLC

Gemcitabine (2', 2'-difluorodeoxycytidine, dFdC) is a chemical antimetabolite and analogue of deoxycytidine. It has been applied as the first-line treatment of NSCLC along with cisplatin. As shown in Figure 1-12, the prodrug once taken up by a cell through specific carriers is phosphorylated by deoxycytidine kinase into difluorodeoxycytidine monophosphate. Further metabolism occurs for the latter to give rise to active nucleosides, diphosphate (dFdCDP) and triphosphate (dFdCTP) forms. These active metabolites are integrated in such way to afford gemcitabine cytotoxicity and inhibition of DNA synthesis in S phase stage during cell division. Initially, Gemcitabine diphosphate inhibits an enzyme RNR, leading to a reduction in the available deoxyribonucleotides required for DNA synthesis. Moreover, a competition of the active gemcitabine triphosphate with deoxycytidine triphosphate, for incorporation

into DNA, is responsible for chain termination with an addition of only single deoxynucleotide (Oguri et al., 2006, Bepler et al., 2006, Toschi and Cappuzzo, 2009).

There is evidence suggesting that the cytotoxic action of gemcitabine to inhibit cell growth is also mediated in a ROS-dependent manner (Donadelli et al., 2007). However, according to a recent study, induction of ROS production by gemcitabine could up-regulate chemokine receptor (CXCR4/CXCL12) signaling, resulting in an enhancement of the drug resistance and invasiveness in pancreatic cancer cell via NF- κ B and hypoxia-inducible factor 1 α expression (Arora et al., 2013). These two observations were diminished with prior exposure to N-acetyl cysteine to scavenge free radicals. Thereby, the role of gemcitabine-induced ROS effects remains to be determined.

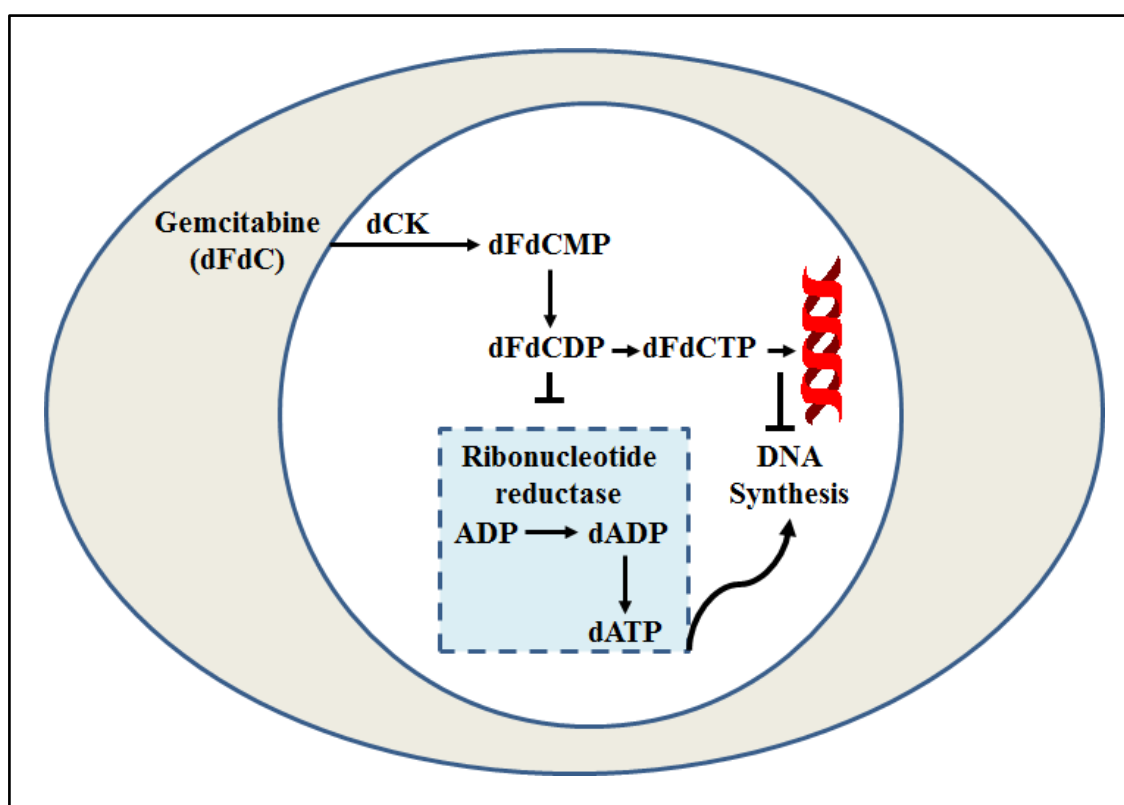


Figure 1-12 Mechanism of action of gemcitabine.

Once gemcitabine (dFdC) incorporates into the cell, it undergoes phosphorylation by deoxycytidine kinase (dCK) into difluorodeoxycytidine monophosphate (dFdCMP). Further metabolism give rise to active nucleosides, diphosphate (dFdCDP) and triphosphate (dFdCTP) forms. dFdCDP is a direct inhibitor of ribonucleotide reductase (RNR), resulting in a reduction in the available deoxyribonucleotides required for DNA synthesis, mainly dATP. In addition, dFdCTP competes with deoxycytidine triphosphate for incorporation into DNA during synthesis and contribute to termination of chain elongation. [The Figure modified from (Morgan et al., 2008)].

The combined chemotherapy of gemcitabine with platinum-based agents might be based on the interference of the former with inhibition of repair of DNA damage provoked by platinum compounds (Toschi and Cappuzzo, 2009). Once inside the cell, cisplatin undergoes an aquation reaction process with a displacement of its chloride groups by water. This facilitates platinum atom to bind with N⁷ position purine bases, with ultimate formation of mainly 1,2- or 1,3- intrastrand adducts, or interstrand crosslinked to a lower extent (Basu and Krishnamurthy, 2010, Un, 2007). However, in fact, the interaction of a small proportion of cisplatin could occur with DNA. The detection and cellular response to such induced DNA damage might contribute to the efficacy of chemotherapeutic agents by activating different signaling pathways for avoidance or promotion of cell death (Basu and Krishnamurthy, 2010). In addition, cisplatin can increase intracellular ROS levels which might occur via activation of NADPH oxidase, up-regulation of the latter produces superoxide and therefore other ROS formation (Itoh et al., 2011, Casares et al., 2012). Recently, it has been stated that the ROS might be created independently from the actual amount of nuclear DNA damage following cisplatin treatment; arising as a consequence of mitochondrial DNA adduct formation with impairment in protein synthesis responsible for electron transport chain. The cellular response to cisplatin-enhanced mitochondrial dysfunction, in that case, perhaps determines the cisplatin cytotoxic outcome and likely depends on redox status, the integrity of DNA as well as the metabolic activity of mitochondria (Marullo et al., 2013).

Overall, the mechanisms of action of several current lung cancer therapeutic agents such as radiotherapy, gemcitabine and cisplatin, suggests that combining them with the effects of NUDT1 inhibition could lead to additive or synergistic effects that would improve patient outcomes. In particular, radiotherapy is used as a front-line therapy for lung cancer (Haslett et al., 2014), largely inducing cell death via the generation of free radicals (Borek, 2004, Lomax et al., 2013). Additionally, as discussed thoroughly above, gemcitabine is a chemical antimetabolite and analogue of deoxycytidine that induces DNA replication stress (Oguri et al., 2006, Bepler et al., 2006, Toschi and Cappuzzo, 2009); and cisplatin leads to DNA replication defects via the formation of DNA crosslinks (Basu and Krishnamurthy, 2010, Un, 2007) and can increase intracellular ROS levels possibly through mitochondrial dysfunction and activation of

NADPH oxidase and superoxide production (Itoh et al., 2011, Casares et al., 2012, Marullo et al., 2013).

1.10 The project aims and objectives

This study was aimed to clarify the contradictory data relating to the role of NUDT1 in cancer. Specifically, it was focused on defining the role of NUDT1 in NSCLC, and on determining if targeting NUDT1 is an effective ‘cancer phenotypic lethality’ strategy for treating NSCLC either as a single-agent treatment or for enhancing the effectiveness of current therapies. This work is considered significant to the cancer field as, despite the presence of improvements in survival rates for many other cancer types in recent years, NSCLC therapy responses and patient outcomes have not significantly improved (Coleman et al., 2011, Haslett et al., 2014). Consequently, there is a critical need to identify new NSCLC therapeutic targets and strategies (Besse and Reck, 2014).

Therefore, it was investigated the effect of siRNA-mediated NUDT1 knockdown in both NSCLC and normal lung cells, whether this could lead to any cellular alteration in respect to DNA damage and/or apoptotic death pattern, Figure 1-13. It was also assessed if NUDT1 depletion by siRNA could increase the cytotoxicity of radiation or chemotherapy treatments. In addition, this study examined the effects of small molecule NUDT1 inhibitors that have been recently suggested as highly effective for cancer cell killing due to NUDT1 inhibition, and indicated also as a new therapeutic approach, converting the oxidative stress into cytotoxic DNA damage with eventual cancer cell death (Gad et al., 2014, Huber et al., 2014). This will enable us for further understand their role in regard to oxidatively damaged DNA and cytotoxicity of NSCLC.

For this purpose, this project has three interrelated objectives:

1. To investigate the effects of NUDT1 knockdown on genome stability and cell viability in cancer and normal cells.
2. To investigate the effects of NUDT1 knockdown on the response of lung cancer cells to ionising radiation, cisplatin, and gemcitabine.
3. To determine the therapeutic potential of NUDT1 small molecules inhibitors, TH287 and TH588 (Gad et al., 2014), for treating lung cancers.

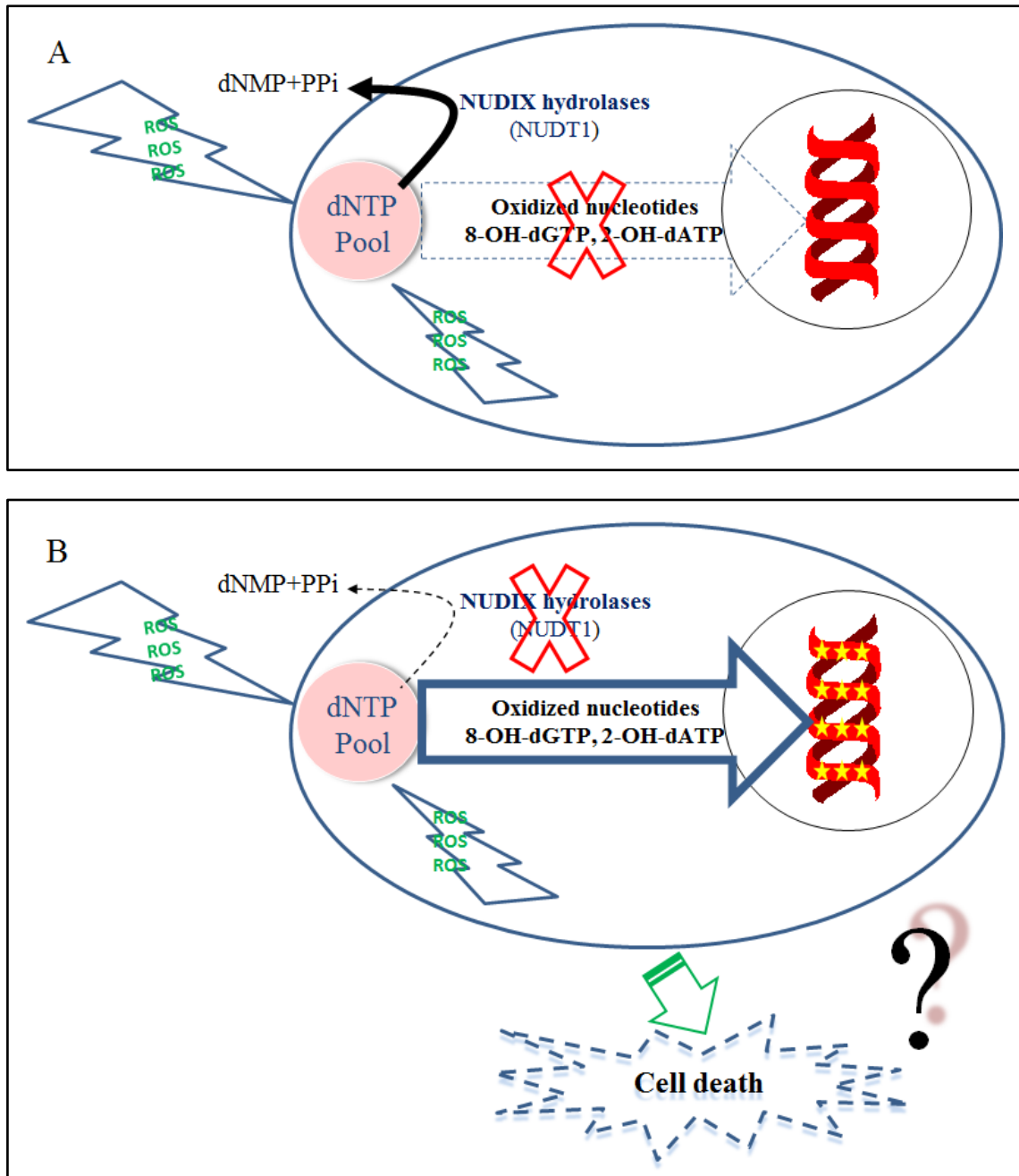


Figure 1-13 The proposed hypothesis of the effects of NUDT1 knockdown on lung cancer cells.

Lung cancer cells are under high levels of oxidative stress relative to normal cells; which is due to increased reactive oxygen species (ROS) from endogenous and exogenous sources, including therapeutic agents. (A) There is an existence of a protective mechanism with nudix hydrolases enzymes that convert oxidised dNTPs to dNMP products with a generation of inorganic pyrophosphate (PPi). (B) In the presence of NUDT1 deficiency, the oxidised nucleosides precursors might be mis-incorporated into DNA, which could ultimately lead to cell death through poorly defined mechanism(s). Yellow stars indicate increased levels of oxidatively damaged DNA.

Chapter 2: Materials and methods

2.1 Materials

2.1.1 Cell lines

A549 (CCL-185) cells were kindly obtained from Prof. G D D Jones (Dept. Cancer Studies and Molecular Medicine, University of Leicester, UK), while H522 (CRL-5810), H23 (CRL-5800) and MRC-5 (CCL-171) cells were purchased from American Type Tissue Culture Collection (ATCC, LGC Standards, Teddington, Middlesex, UK). All cell lines were maintained at a low passage as laboratory stocks.

H522, H23, and A549 cell lines are denoted as a human non-small cell lung cancer (NSCLC). All carry the K-RAS 12 mutation that leads to loss of intrinsic GTPase function with the protein being continuously bound to GTP in an active state with constant cell growth signaling. In addition, H522 cell line has a frame shift codon 191 with P deletion (p.P191fs*57) of p53 gene. H23 cell also has a p53 mutation in codon 246 (ATC -> ATG, isoleucine -> methionine); whereas, A549 cell line is regarded as p53 competent. Moreover, H23 cell line expresses C-myc, L-myc, v-src, v-abl, v-erb B, c-raf 1, Ha-ras, Ki-ras and N-ras RNAs. The other cell line used in this project is normal human lung fibroblast (MRC-5), derived from 14 weeks gestation Caucasian male.

2.1.2 Cell culture reagents, chemicals, and supplies

RPMI 1640 Medium (ATCC modification), Opti-MEM[®] Medium, Dulbecco's Modified Eagles Medium-high glucose (DMEM), with the supplement fetal bovine serum (FBS) were all supplied by Invitrogen (Gibco, Life Technologies Ltd, Paisley, UK). Eagle's Minimum Essential Medium (EMEM) was obtained from American Type Tissue Culture Collection (ATCC, LGC Standards, Teddington, Middlesex, UK). Cell culture flasks were from Greiner Bio-One GmbH (CELLSTAR, Frickenhausen, Germany). Cisplatin, gemcitabine, etoposide, phleomycin, hydroxyurea and NUDT1 small molecule inhibitors (TH287, TH588) were purchased from Sigma-Aldrich Company Ltd. (Dorset, UK). All other materials and chemical reagents were from Sigma-Aldrich Company Ltd. (Dorset, UK) or Fisher Scientific (Loughborough, UK) unless stated otherwise.

2.1.3 Transfection reagent and small interfering RNA (siRNA)

DharmaFECT 1 Transfection Reagent was purchased from GE Healthcare, Dharmacon Inc., UK. Silencer® Select Validated siRNA for NUDT1 as well as Silencer® Select Negative Control 1 siRNA were obtained from Ambion (Life technologies, Carlsbad, CA, USA). The specific sequences (5'→3') of siRNA-NUDT1 oligonucleotides were as follow:

NUDT1 siRNA ID s194633: sense UUAACUGGAUGGAAGGGAAAtt; antisense UUCCCUUCCAUCCAGUUAAtt.

NUDT1 siRNA ID s9030: sense CAUCUGGAAUUAACUGGAUtt; antisense AUCCAGUAAAUUCCAGAUGaa.

2.1.4 Modified alkaline comet assay

Formamidopyrimidine [fapy]-DNA glycosylase (Fpg) enzyme was bought from New England Biolabs (Hitchin, UK).

2.1.5 Annexin V-FITC (fluorescein isothiocyanate) and propidium iodide (PI) Apoptosis Assay

Annexin V-FITC/PI apoptosis detection kit was purchased from Affymetrix (eBioscience, Vienna, Austria). In addition, FACS tubes were from Bdbiosciences, Durham, USA.

2.1.6 Cellular proliferation-Water Soluble Tetrazolium (WST-1) assay

The ready-to-use Cell Proliferation Reagent WST-1 was obtained from Roche Diagnostics GmbH, Roche Applied Science, Mannheim, Germany.

2.1.7 Intracellular ROS production measurement

2',7'-dichlorodihydrofluorescein diacetate (H2DCF-DA) was obtained from Thermo Fisher Scientific, Loughborough, UK. Moreover, Black 96 well plates were purchased from Porvair Sciences, Norfolk, UK.

2.1.8 Western blotting

The antibodies used are listed in Table 2-1. Rabbit polyclonal antibodies (anti-NUDT1 and anti-NUDT15), as well as mouse monoclonal anti-alpha tubulin antibody, were purchased from Abcam (Cambridge, UK). Antibodies against Phospho-Chk1 (Ser345), Phospho-Chk1 (Ser317), Chk1 (2G1D5), Phospho-Chk2 (Thr68) were supplied by Cell Signaling Technology (Leiden, The Netherland). Secondary antibody conjugated with horseradish peroxidase (HRP), goat polyclonal anti-rabbit IgG, was also obtained from Abcam (Cambridge, UK), whereas polyclonal goat anti-mouse immunoglobulins/HRP was from Dako (Glostrup, Denmark). Dried skimmed milk powder (Marvel®) was purchased locally.

Table 2-1 The antibodies used for Western blot.

	Antibody	Description	Host	Dilution	Supplier
Primary	Anti-NUDT1	polyclonal	rabbit	1:1000	Abcam
	Anti-NUDT15	polyclonal	rabbit	1:250	Abcam
	Anti-alpha tubulin	monoclonal	mouse	1:15000	Abcam
	Phospho-Chk1 (Ser345)	polyclonal	rabbit	1:500	Cell Signaling Technology
	Phospho-Chk1 (Ser317)	polyclonal	rabbit	1:500	Cell Signaling Technology
	Chk1 (2G1D5)	monoclonal	mouse	1:1000	Cell Signaling Technology
	Phospho-Chk2 (Thr68)	polyclonal	rabbit	1:500	Cell Signaling Technology
Secondary	Anti-rabbit IgG/HRP	polyclonal	goat	1:5000	Abcam
	Anti-mouse immunoglobulins/HRP	polyclonal	goat	1:5000	Dako

Protein standard bovine serum albumin (Pierce® BCA Protein Assay Kit), PageRuler™ Plus Prestained Protein Ladder, the enhanced chemiluminescence detection kit (Pierce®

ECL Western Blotting Substrate), and CL-XPosure™ Film were all obtained from Thermo Scientific (Rockford, IL, USA). In addition, ProtoGel (30% Acrylamide/0.8% bis-Acrylamide) and Immobilon®-P transfer membrane (PVDF 0.45 µm) were supplied by Geneflow (Lichfield, UK) and EMD Millipore (Bedford, MA, USA), respectively.

2.2 Methods

2.2.1 Cell culture

Normal human lung fibroblast (MRC-5) and A549 cell lines were grown in EMEM and DMEM-high glucose media, respectively, supplemented with 10% (v/v) FBS. In addition, the other two NSCLC cells (H522 and H23) were cultured in RPMI 1640 medium (ATCC modification) supplemented with 10% (v/v) FBS.

Subculture was usually performed every 3-4 days when the cells were 80-90% confluent. During the routine passaged of cells, the medium was removed, washed with pre-warmed (37°C) phosphate-buffered saline (PBS), and incubation of cells with 1 x 0.5% trypsin- Ethylenediaminetetraacetic acid (EDTA) (0.1% trypsin, 0.4% EDTA) for 4-5 minutes (min) in order to detach them from the flask. Trypsin-EDTA was neutralized by addition of culture medium. The cell suspension was then centrifuged at 400 X g for 4 min, and the pellet was re-suspended in an appropriate amount of culture medium to make T-75 cm² flasks at ratio 1:4, 1:5, and 1:6 for (H522 and H23), MRC-5 and A549 cell lines, respectively. Finally, all cells were maintained at 37°C with humidified atmosphere, 95% air/5% CO₂.

2.2.2 NUDT1 knockdown and cell transfection using small interfering RNA (siRNA)

The transfection procedures were performed according to manual instruction protocol (Ambion, Life technologies, Carlsbad, CA, USA). Stock working solutions (5 µM) of NUDT1 siRNA and silencer select -ve control (scramble) were prepared, by re-suspending of 1 nmole dried siRNA in 200 µl nuclease free water, and stored at -20°C.

2.2.2.1 Forward transfection method of NUDT1 knockdown

To start with, the cells were seeded in 6-well plates (3 x 10⁵ per well) and allowed to grow in 2.5 ml complete media for 24 hours (h) at 37°C in humidified atmosphere, 95% air /5% CO₂. Once the cells were 50-60% confluent, the media were removed, washed

with 2 ml PBS, and finally, Opti-MEM[®] Medium (2.25 ml) was added to each well with 250 μ l of transfection complex. The latter was made by dilution of 7.5 μ l of DharmaFECT 1 Transfection Reagent in 125 μ l Opti-MEM[®] Medium and incubated with diluted siRNA for 10 min at room temperature. Herein, the diluted siRNA concentrations (2, 4, 8 or 15 nM) were prepared from 5 μ M stock solution by dilution in 125 μ l Opti-MEM[®] Medium. In the same way, a transfection complex of silencer select -ve control (scramble) was also need to be prepared using the above concentrations. The cells were then maintained at 37°C, 95% air/5% CO₂ for 24 h, after which the existing medium was replaced with fresh complete medium and continued incubation for further 24 or 48 h transfection time points. Finally, in order to validate the efficiency of the process during the indicated transfection periods, cell lysates were also collected for Western blot, as mentioned in section 2.2.5.

2.2.2.2 Reverse transfection method of NUDT1 knockdown

The three components of transfection procedure (siRNA, lipid, and cells) were added to each well of 6-well plates at essentially the same time. The transfection complex was prepared by dilution of 7.5 μ l of DharmaFECT 1 Transfection Reagent in 125 μ l Opti-MEM[®] Medium and incubated with diluted siRNA for 10-20 min at room temperature. Herein, the diluted siRNA concentrations (2, 4, 8, 10, 15 or 20 nM) were prepared from 5 μ M stock solution by dilution in 125 μ l Opti-MEM[®] Medium. Subsequently, cell solutions at a density of (3×10^5 cells) were added to each well which contained siRNA transfection complex and topped up with Opti-MEM[®] Medium at a final volume of 2.5 ml per well. In the same way, the control sample (scramble) were also included in every transfection experiments. The cells were then maintained at 37°C, 95% air/5% CO₂ for 24 h, after which the existing medium was removed, replaced with fresh complete medium and incubated back according to transfection time points. Cell subculture was carried out every 3 days up to 9 days to allow cell growth and prevent over confluence. Finally, in order to validate the efficiency of the process during the indicated transfection periods, cell lysates were also collected for Western blot, as mentioned in section 2.2.5.

2.2.3 Modified alkaline comet assay

Alkaline single cell gel electrophoresis was carried out with refinement of the originally described method (Singh et al., 1988). It detects DNA lesions induced by various

genotoxic insults. Essentially, the cells were embedded in low melting point (LMP) agarose gel on fully frosted slides. The latter are pre-coated with a normal melting point (NMP) agarose gel. The prepared slides were then immersed overnight in a lysis buffer to remove cell membranes and histones with a formation of supercoiled DNA as nucleoids. Herein, specific repair enzyme, namely Fpg, is introduced at post-lysis step. Fpg possesses N-glycosylase activity to release oxidatively damaged purine lesions from double stranded DNA, leaving an apurinic (AP) site. In addition, it has the AP-lyase activity which generates a one base gap by cleaving both 3' and 5' ends of AP site. The Fpg enzyme detects and removes 8-oxoGua, 8-oxoadenine, fapy-guanine, methy-fapy-guanine, fapy-adenine, aflatoxin B₁-fapy-guanine, 5-hydroxy-cytosine, and 5-hydroxy-uracil (Tchou et al., 1994, Hatahet et al., 1994).

The formed nucleoids were unwound and electrophoresed in alkaline conditions at which strand breaks would relax the supercoiled DNA loops and then move towards positive electrode, creating “the comet”. At this point, the slides were neutralized, stained by fluorescent DNA binding dye, and finally analysed using computerized detection system. The subdued light was required during the above technique steps in order to minimize any additional DNA damage.

2.2.3.1 Slides pre-coating

1% NMP agarose in double-distilled water was used to pre-coat microscope slides by dipping them into the agarose and left to dry overnight at room temperature. The agarose was prepared by adding 0.5 g NMP agarose to 50 ml ultra-pure water and dissolved in a microwave oven.

2.2.3.2 Cell treatments and irradiation

Both non-transfected and transfected cells (section 2.2.2.2) were seeded at a density of 3×10^4 cells in 12-well plates (Greiner Bio-One GmbH, CELLSTAR, Frickenhausen, Germany) and incubated overnight with 1 ml of a corresponding complete medium in a humidified atmosphere, 95% air/5% CO₂ at 37°C.

2.2.3.2.1 Hydrogen peroxide (H₂O₂) exposure

After removal of the existing media, grown cells were washed in 1 ml PBS, pH 7.4, and then exposed to freshly prepared H₂O₂.

H₂O₂ solution 30% (w/w) was diluted with distilled water to make 9.8 mM stock. The seeded cells were treated with H₂O₂ in serum-free medium at final concentrations of 0, 50, 100 and 200 µM for 30 min on ice or at 37°C in 5% CO₂. Such treatment on ice minimises the possibility of cellular DNA damage processing that occurs after oxidant exposure. Subsequently, a removal of oxidant treatments and further wash with PBS were performed.

The repair of oxidative DNA damage was also assessed after exposure to 100 µM, H₂O₂ in serum-free medium. Similarly, after treatment for 30 min incubation on ice, the existing media was taken out and washed twice with 1 ml PBS to remove any remaining oxidant. The exposed cells were then incubated for 24 h in complete medium containing serum at 37°C in a humidified atmosphere with 95% air/5% CO₂.

At that point, the treated cells were harvested by 0.5% trypsin-EDTA and stored on ice to proceed with slide preparation.

2.2.3.2.2 Ionising radiation exposure

X-ray treatments were carried out using Xstrahl RS320 X-Ray Irradiator system (Xstrahl LTD, Surrey, UK). For assessments of immediate DNA damage, the slides containing embedded cells in low melting point agarose were X-irradiated on ice with 10 Gy dose or left untreated prior to overnight incubation in a lysis buffer (see section 2.2.3.3).

For recovery samples (repair of DNA damage process), cells in suspensions were irradiated on the ice with 10 Gy or left untreated, and then incubated for 24 h in complete medium at 37°C in a humidified atmosphere, 95% air/5% CO₂. Afterward, the adherent cells were trypsinized and collected on ice prior to preparing comet assay sample slides as described below.

2.2.3.2.3 Small molecule NUDT1 inhibitors exposure

NUDT1 small molecule inhibitors (TH287, TH588) were dissolved in DMSO (dimethyl sulfoxide) to form 15 mM stock solution and stored at 4°C. The growing cells in T25 cm² culture flasks were treated with 10 µM of TH287 or TH588 in complete medium with a humidified atmosphere, 95% air/5% CO₂ at 37°C for 24 h. DMSO (0.066% v/v) control sample was also included together with the above treatment. The existing media

were then taken out, washed once with 5 ml PBS to remove any remaining drugs, trypsinized and counted by using C-chip disposable haemocytometer (Labtech International Ltd, East Sussex, UK). After thorough mixing of equal volumes of cell solution and 0.4% trypan blue stain, 30,000 cells were obtained per-slide. The required cell suspension was subsequently suspended, in an Eppendorf, by an addition of PBS to make 500 μ l and collected on ice.

2.2.3.3 Cell-slides preparation and lysis

The trypsinized collected samples were centrifuged at 400 g for 4 min at 4°C, and the cell pellets were then re-suspended in 200 μ l of pre-warmed 0.6% LMP agarose. From the latter, 80 μ l of the cell resuspension was dispensed directly onto each half of a microscopic slide pre-coated with dried 1% NMP agarose, forming two gels per slide with the aid of 22 x 22 mm cover slips. The gels were allowed to set on a cold metal plate for approximately 10 min, and once solidified, the cover slips were carefully removed. The slides with embedded cells were prepared in duplicate for each sample and incubated overnight at 4°C in Coplin jar containing lysis buffer [2.5M NaCl, 100mM Na₂EDTA, 10 mM Tris-Base, pH 10 adjusted by NaOH] along with freshly added 1% Triton X-100.

2.2.3.4 Alkaline unwinding/electrophoresis and staining steps

After an overnight lysis step, the slides were washed once for 10 min with cold double-distilled water, and rinsed with further two changes of an enzyme reaction buffer [40 mM Hepes, 0.1 M KCl, 0.5 mM Na₂EDTA, 0.2 mg/ml bovine serum albumin (BSA), pH 8 adjusted with KOH], each for 10 min at room temperature. The enzyme reaction buffer was prepared as a 10 X stock and frozen at -20°C in aliquots. Here, in order to recognise an oxidatively damaged purine lesions, Fpg enzyme was added at final concentration of 0.8 U/gel (1:500) in 50 μ l enzyme reaction buffer (The optimal condition was previously established in our laboratory). To another gel slide, an enzyme reaction buffer alone was also poured using above volume. The cells then incubated under 22 x 22 mm cover slips for 30 min at 37°C in a humidified atmosphere, comprising 95% air/5% CO₂. The applied cover slips were gently removed, and the slides were next laid lengthwise in the same direction into an ice surrounded electrophoresis tank, filled with a freshly prepared cold alkaline electrophoresis buffer

[300 mM NaOH, 1 mM Na₂EDTA, pH \geq 13] to allow DNA unwinding for 20 min before running electrophoresis in the same buffer, at a constant 30 V and 300 mA for a further 20 min. The electrophoresis buffer was made up to 1 L by an addition of 30 ml of 10 M NaOH and 5 ml of 200 mM Na₂EDTA to 965 ml of chilled double-distilled water. Subsequently, every single slide was flooded with 1ml of neutralization buffer [0.4 M Tris-Base, pH 7.5], immersing in cold double-distilled water each for 20 min, and then left to dry at 37°C for 3 h or overnight at room temperature. The slides were then rehydrated in cold double distilled water for 30 min prior to stain with 2.5 μ g/ml PI for another 20 min at room temperature. A Further wash with cold double-distilled water was next performed for 30 min. Finally, the slides were dried overnight at 37°C and stored for later visualisation by fluorescent microscope.

2.2.3.5 Comet visualisation and image analysis

For each sample, a total of 200 consecutive cells (fifty comets per each of two gels on duplicate slides) were randomly selected with care to avoid borders and overlapped comets. The visualisation of comets was accomplished by using a fluorescent microscope (Olympus model BH-2-RFL-T2, Olympus Optical Co., LTD., Tokyo, Japan), fitted with an excitation filter of 515-535 nm and a 590 nm barrier filter at X 200 magnification. The images were captured via a high performance charged-coupled device camera (COHU MOD 4912-5000/0000, Cohu, Inc. / Electronic Division, San Diego, CA, USA) and analysed by Komet software (Version 5.5, Andor Technology, Belfast, UK); at which % tail DNA for each cell was recorded as a parameter of DNA damage.

2.2.4 Annexin V-FITC and PI Apoptosis Assay

Annexin V-FITC/PI assay was carried out to detect apoptosis by targeting phosphatidylserine on the outer leaflet of the cell membrane using flow cytometry. In early apoptotic stage, the membrane structure is changed with the loss of its lipid asymmetry while the membrane integrity is lost during late-stage of apoptosis. Simultaneously, PI (a membrane impermeable DNA stain) is applied to discriminate between vital, apoptotic and dead cells, as those cells with lost membrane integrity allow annexin V binding to cytosolic phosphatidylserine, as well as cell uptake of PI (van Engeland et al., 1998).

The procedure was performed according to the Annexin V-FITC apoptosis detection kit manual at which cell density should be $2-5 \times 10^5/\text{mL}$. In brief, cells were grown in T25 cm^2 flasks until 40% confluence. For the transfected cells in section 2.2.2.2., the procedure was carried out in 6-well plates. Fresh medium was then added (with or without treatment of cells with a chemotherapeutic drug). Cells exposed to 50-150 μM etoposide [dissolved in DMSO, at a final concentration of 0.5-1.5% v/v in cell culture medium] was used as a positive control for apoptosis, whereas untreated cells were regarded as a negative control. In addition, the cells were treated with different concentrations of chemotherapeutic agents namely cisplatin and gemcitabine which were dissolved in ddH₂O, to form a stock solution of 5 mM, stored at 4°C and protected from light. Drugs were then diluted with 5 mL of corresponding complete media prior to cell treatment to get concentrations of 1, 2, 5, 10, 20 and 50 μM for cisplatin and 0.001, 0.01, 0.05, 0.1, 1, 5, 10, 20, 40, 80, and 120 μM for gemcitabine. Treatment with freshly prepared H₂O₂ (section 2.2.3.2.1) was also performed at final concentrations of 50, 100, 200, 400, 600, and 800 μM in serum-free medium at 37°C in 5% CO₂. Similarly, the growing cell lines were exposed to NUDT1 small molecule inhibitors (TH287, TH588) (section 2.2.3.2.3.) at a final concentration of 10 μM . The cells were incubated for time points 24 or 48 hr at 37°C in 9 % air/5% CO₂.

Subsequently, the cells were trypsinized and collected together with any floating cells. The isolated cells were then pelleted, washed with PBS and re-suspended in 200 μL annexin V binding buffer (10 mM HEPES/NaOH, pH 7.4, 140 mM NaCl, 2.5 mM CaCl₂). Annexin V-FITC 5 μL was added to the cell suspension and incubated in the dark for 10 min at room temperature. After washing cells with annexin V binding buffer, PI dye (10 μL of 20 $\mu\text{g}/\text{mL}$) was also added to each sample. During samples processing, preparation of four untreated negative control cells was under taken for instrumental compensation and gating; no stain, PI only, annexin V-FITC only and both PI and annexin V-FITC stain. Finally, the samples were analysed on a BD FACSCanto™ II flow cytometer (BD Biosciences, San Jose, CA, USA) using BD FACSDiVa™ v6.1.3 software. At least 10000 events were acquired per sample.

EC₅₀ values for apoptosis were determined by GraphPad Prism software, version 6.05, using a nonlinear curve fit with response-variable slope (four parameters), a response (three parameters), or a normalized response model.

2.2.5 Western blotting

2.2.5.1 Protein extraction and quantification from cultured cells

Cells were grown in a Petri dish to 60% confluence, the medium was removed and the cell layer then washed twice with PBS prior to the addition of 0.5 mL boiled Laemmli buffer (2% Sodium dodecyl sulphate (SDS), 10% glycerol, 50mM Tris-HCl pH 6.8) with scraping of cells to one side of the plate. Subsequently, the cell lysates were heated at 95°C for 5 min in a water bath, cooled to room temperature, and sonicated for 15 seconds at 14µm to shear the DNA, using Soniprep 150 (MSE, Crawley, UK). The bicinchoninic acid protein assay was used, in which determination of protein sample concentration was obtained from a standard curve, constructed from the absorbance at 562 nm using a microplate reader (Bio-Tek Instruments Inc., Winooski, Vermont, USA) against a series of BSA protein standards of known concentration.

For Western blotting, a final protein concentration of 1mg/mL of cell lysate is required. The cell lysates were appropriately diluted by addition of 2-mercaptoethanol (1% v/v), bromophenol blue (0.005% w/v) and Laemmli buffer up to a final volume of 200 µL, then stored at -20°C.

2.2.5.2 One dimensional SDS-Polyacrylamide gel electrophoresis (SDS-PAGE) preparation

As shown in Table 2-2, the resolving and stacking gels with 10% and 5% respectively, were utilised for SDS-PAGE preparation in order to separate proteins. Here, the required solution volumes of 30% w/v acrylamide, 1.5 M Tris-base (pH= 8.8), 1.0 M Tris-HCl (pH= 6.8), 10% w/v SDS and ultra-pure water were all mixed together prior to the addition of freshly made 10% w/v ammonium persulphate to quickly set a gel and N,N,N',N'-tetramethylethylenediamine (TEMED) to initiate polymerisation.

The resolving gel was loaded into the gel casting unit, followed by pipetting 150 µL of 2-propanol over the top to prevent evaporation during gel setting and to ensure a level gel interface. Once the gel had set the 2-propanol on top was removed and then the gel was rinsed with sterile ultra-pure water. Subsequently, the 5% stacking gel was poured over resolving gel, a gel comb inserted into stacking layer, and allowed to set at room temperature. Once set, the gel comb was removed and the gel used, or wrapped in damp paper towels and surrounded with saran wrap and stored at 4°C until required.

Before loading 20 μL (20 μg) of each dilute cell lysate in separate wells, the protein samples were denatured at 99°C for 5 min in a water bath and then stored in ice. When the molecular weight marker, 4 μL , was also loaded onto the gel, the gel was ready to run in running buffer (0.3% w/v Tris-HCL, 1.4% w/v glycine, 0.1% w/v SDS) at 170 V for 1 h till the sample front had run the required distance.

Table 2-2 The components of resolving and stacking gels for preparing SDS-Polyacrylamide Gel Electrophoresis (SDS-PAGE).

Solution components	10% resolving gel (mL)	5% stacking gel (mL)
Ultra-pure H ₂ O	1.9	3.4
30% w/v acrylamide	1.7	0.83
Gel buffer (1.5 M Tris-base, pH 8.8)	1.3	-----
Gel buffer (1.0 M Tris-HCl, pH 6.8)	-----	0.63
10% w/v SDS	0.05	0.05
10% w/v ammonium persulphate (APS)	0.05	0.05
TEMED	0.002	0.005
Total	5 mL	5 mL

2.2.5.3 Blotting

The proteins separated by SDS-PAGE were blotted onto polyvinylidene difluoride (PVDF) membrane using BioRad Mini Protean 3 Western transblot system. The membrane was activated by washing with methanol for few min. Carefully the gel was removed, washed for a few min in transfer buffer (0.3% w/v Tris-HCL, 1.4% w/v Glycine, 20% v/v Methanol) to take away any residual SDS. Four filter papers, gel, and membrane, with almost similar size, were soaked in transfer buffer and placed into transfer cassette in the following order towards anode: 2 filter paper-gel-PVDF membrane-2 filter paper. Once the transfer apparatus was filled with transfer buffer, the transfer electrophoresis was set with constant voltage, 25V, for 16 hr at room temperature or 100V for 1 hr at 4°C.

2.2.5.4 Immunolabelling and enhanced chemiluminescence (ECL) detection

After transfer, protein bands were visualized to determine the success of transfer process, using a Ponceau S red stain (0.1% w/v Ponceau S in 5% v/v acetic acid). Subsequently, the membrane was either left as a whole or cut with a scalpel blade between 55 kDa and 35 kDa molecular weight identified by the marker colours. The membrane was de-stained to remove Ponceau S by washing with deionised water. The membrane portions were then blocked with 5% w/v milk-TBST (Tris-Buffer saline and Tween-20) [50 mM Tris-base pH 7.65, 150 mM NaCl, 0.1% v/v Tween-20] for 1-2 hr at room temperature to block nonspecific antibody binding. Following three serial washes with TBST, each for 5 min, the membranes were probed with primary antibody (indicated in Table 2-1) against NUDT1, NUDT15, Phospho-Chk1 (Ser345), Phospho-Chk1 (Ser317), Phospho-Chk2 (Thr68), Chk1 (2G1D5), and α -tubulin at a dilution of 1:1000, 1:250, 1:500, 1:500, 1:500, 1:1000, and 1:15000; respectively, in TBST-BSA for 1 hr at room temperature. Further membrane washes were performed four times for 5 min each. Species-specific HRP conjugated goat secondary antibodies (polyclonal goat anti-rabbit or polyclonal goat anti-mouse 1:5000 diluted in 5% milk-TBST, as indicated in Table 2-1, were then applied prior to thorough washing with TBST. Finally, protein was detected by ECL kit according to manufacturer's instructions and was exposed to X-ray film (CL-XPosure™ film) with different time points. The film was developed with X-ray film processor (Agfa Curix-60, Mortsel, Belgium). The band intensities were quantified by using densitometry GeneSnap software (Syngene, UK) or Image J 1.49 version software (W. S. Rasband, U.S. National Institutes of Health), normalized with the loading control α -Tubulin, and established relative to media without transfection reagent.

2.2.5.5 Membrane striping for re-probing

After washing twice with TBST each for 5 min, the blotted membranes were stripped, whenever necessary, using a striping buffer (0.5% SDS, 0.2 M glycine, and 1% Tween-20 pH 2.5) with a volume that covered the membrane for 20 min at room temperature. Subsequently, the solution was removed and further washed three times with TBST each for 5 min. At this point, the membrane was ready for blocking stage and re-probed to proceed (section 2.2.5.4).

2.2.6 Cell counting and determination of growth rate

Cell counting was performed to verify the proliferative ability of cells after exposure to various drug concentrations. Both cisplatin and gemcitabine were used at concentrations of (0.25, 0.5, 1, 2, 5, 10, and 20 μM) and (0.001, 0.01, 0.05, 0.1, 1, 10, 20, 40, and 80 μM), respectively. In brief, H522 and H23 cells were seeded at 5×10^4 in 12-well plates containing 2 mL RPMI 1640 medium with 10% FBS and incubated at 37°C, 95% air/5% CO₂ for 24 h. Subsequent treatment with indicated concentration of gemcitabine or cisplatin was maintained for 24, 48 and 72 h along with untreated cells as a control. On the day of analysis, the media was removed prior to washing twice with PBS, cells trypsinized with 1 x 0.5% trypsin-EDTA and 10 μL of the cell suspension re-suspended in 9.990 mL Isoton® II diluent (Beckman Coulter, USA), at 1:1000 dilution. The cells were then counted using Z2 Coulter particle count and size analyzer (Beckman Coulter, Fullerton, CA, USA); with an aperture size 70 μm and setting the diameter of counted cells to range between 8-26 μm .

IC₅₀ values for growth inhibition were determined by GraphPad Prism software, version 6.05, using nonlinear curve fit with response-variable slope (four parameters) or normalized response model.

Cell doubling times were determined by the following formula:

$$\text{Doubling time} = \ln 2 / k$$

In which (k) is the growth rate and can be calculated as:

$$k = \ln (N(t) / N(0)) / t$$

In which N(t) is the number of cells at t time, whereas, N(0) is the number of cells at time 0. The time (t) is usually in hours.

2.2.7 Cellular proliferation-Water Soluble Tetrazolium (WST-1) assay

The WST-1 assay was used according to the manufacturer's instructions (Roche Diagnostics GmbH, Roche Applied Science, Mannheim, Germany). In this technique, the Cell Proliferation Reagent WST-1 is a non-radioactive, spectrophotometric assessment of cellular proliferation, growth, viability, as well as chemosensitivity in cell populations. The test is based on the cleavage of tetrazolium salts, slightly red, into dark

red coloured dye formazan by certain cellular enzymes. Such application using 96-well-plate format allows an expansion in viable cells number, leading to an elevation in the overall mitochondrial dehydrogenases activity, which reduce WST-1 reagent with a formation of formazan dye in the presence of intermediate electron acceptor (Figure 2-1). By this way, the rate of WST-1 cleavage is directly proportional to the number of metabolic active viable cells within the culture.

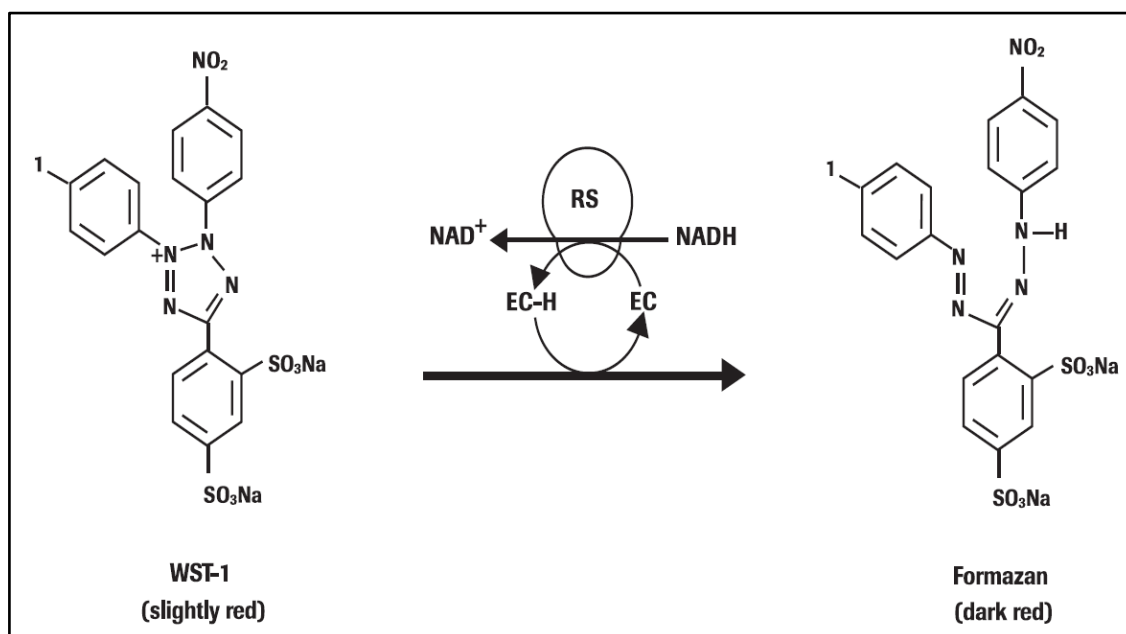


Figure 2-1 The principle mechanism of WST-1 assay.

Reduction of tetrazolium salt WST-1 into dark red coloured dye formazan by cellular enzymes. EC and RS stand for electron coupling reagent and mitochondrial succinate-tetrazolium-reductase system, respectively. The Figure adapted from Cell Proliferation Reagent WST-1 assay manual (Roche Diagnostics GmbH, Roche Applied Science, Mannheim, Germany).

In brief, the indicated cells (H23, H522, A549, and MRC-5) were transfected, as mentioned above in section 2.2.2.2, with the appropriate concentration (15 or 20 nM) of NUDT1 siRNA, negative control scramble siRNA or media without transfection reagent using 6-well plates. Two days after transfection process, the cells (1×10^4 and/or 2×10^4) per well were seeded in triplicate into clear flat bottom 96-well plates and incubated overnight in 100 μ l of corresponding complete media at 37°C with humidified atmosphere, 95% air/5% CO₂. Subsequently, the cell growth continued for the remaining 48 h; or etoposide (VP-16) in final concentrations of (100-150 μ M) were added to the appropriate cultures for the same indicated period time as a positive

control. Finally, direct addition of 10 μ l volume of Cell Proliferation Reagent WST-1 was applied into each well with cells already cultured in 100 μ l media (final dilution of 1:10 as a working concentration) and then incubated for 30 min to 4 h in a humidified chamber with 95% air/5% CO₂ at 37°C. The latter ready-to-use colorimetric solution consists of WST-1 and an electron coupling reagent, diluted in PBS. Background control (blank) without seeded cells were also included. After 1 min of thorough shaking, samples absorbance were immediately measured against a blank control in an ELx808 micro plate reader (BIO-TEK Instruments, Inc., Winooski, Vermont, USA) at a wavelength of 450 nm.

All of the assays were repeated at least in triplicate, and the determination of cell viability was expressed as a percentage of an optical density, by comparison, mean absorbance of transfected or etoposide (VP-16) treated samples against that of control un-transfected cells exposed to media without transfection reagent, using the following equation:

$$\text{Cell viability (\%)} = (\text{Mean absorbance of sample} / \text{Mean absorbance of control}) \times 100.$$

2.2.8 Intracellular ROS production measurement

The internal background level of ROS production was determined in NSCLC and normal human lung fibroblast cell lines, using H₂DCF-DA. It is a non-fluorescent probe and chemically reduced form. Once permeating the cell membrane, the cleavage of the acetate groups by intracellular esterases is taken place and further oxidized in the presence of ROS to become green highly fluorescent 2',7'-dichlorofluorescein (DCF) (Figure 2-2) (Aula et al., 2015).

In brief, 3 x 10⁴ cells per well were seeded in triplicate in black 96-well plates and cultured for 24 h with 200 μ l corresponding media in a humidified atmosphere, 95% air/5% CO₂ at 37°C. The next day, the media was removed and the cells were washed with 200 μ l PBS prior to the addition of 1 μ l of H₂DCF-DA stock (20.5 mM, dissolved in DMSO) and incubation in the dark for 30 min in a humidified atmosphere, 95% air/5% CO₂ at 37°C. 200 μ l of PBS was then added to the wells or freshly prepared H₂O₂, 9.8 mM at room temperature, for the positive control. Blank samples without seeded cells were also included. The relative fluorescence intensity of samples was

immediately measured in FLUOstar OPTIMA microplate reader (BMG LABTECH, Offenburg, Germany) with 485 nm excitation and 520 nm emission wavelengths.

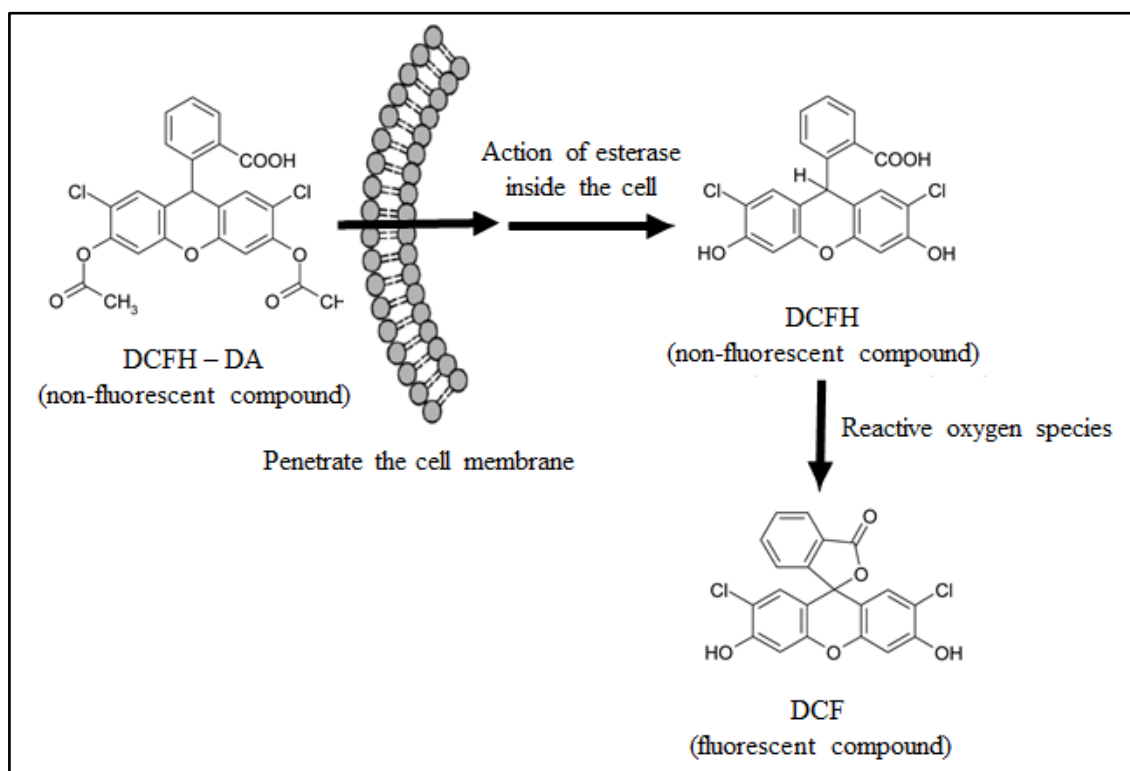


Figure 2-2 The principle mechanism of DCFH (2, 7-dichlorodihydrofluorescein) assay for detection of intracellular ROS production.

Once permeating the cell membrane, the reagent DCFH-DA (2', 7'-dichlorofluorescein diacetate) converts to DCFH by cellular esterases, and consecutive oxidation of DCFH with intracellular reactive oxygen species leads to the formation of highly fluorescent DCF (2', 7'-dichlorofluorescein). [The Figure modified from (Aula et al., 2015)].

2.2.9 Data analysis and statistical tests

Statistical analyses were performed using GraphPad Prism software, version 6.05, to measure mean \pm standard deviation (S.D) or standard error mean (SEM). The data were evaluated by one-way ANOVA with post-hoc Tukey's multiple comparison test; in which P-value < 0.05 was considered as statistical significant. The experiments were carried out at least in triplicate or as indicated.

Chapter 3: Establishment of NUDT1 knockdown in normal human lung fibroblast and NSCLC cell lines

3.1 Optimization of siRNA delivery for NUDT1 knockdown

Transient transfection with siRNA was applied in this project to demonstrate the short-term impact of gene expression changes. The siRNA is termed as a double-stranded RNA molecule, around 21-23 base pair in length with 3'-overhangs of two nucleotides and 5'-phosphate ends. Usually, the siRNA is incorporated into a protein complex called the "RNA-induced silencing complex" (RISC) with subsequent unwinding and cleavage of its sense strand (Figure 3-1). The remaining antisense strand-RISC complex produces a sequence specific structure to facilitate a recognition of complementary mRNA. By this way, the activated siRNA cleaves the targeted mRNA at the middle of the attachment region with subsequent degradation, resulting in gene silencing and disruption of translation process (Ovcharenko et al., 2005) (Figure 3-1).

As the nucleic acid sequence of siRNA is not integrated into the cell genome, a temporary action is observed. Here, siRNA is introduced into the cells by liposome-mediated transfection, a technique called lipofection. This involves the formation of liposome cationic lipids or non-lipid polymers, which can merge with the cellular membrane to enable the delivery of molecules (Wu et al., 2000). To address this technique, two different approaches were performed, forward and reverse transfection. The occurrence of the latter strategy was through a concurrent mixing of the main transfection elements (siRNA, transfection reagent, and cells), while the forward method required cell plating 24 h prior to addition of transfection complex (Ovcharenko et al., 2005). In addition, it is essential to carefully optimize the appropriate conditions of such transfection practice.

Lipofection is a widely-used process to transfect populations of cells. A robust uptake and delivery of siRNA into the cultured cells of interest are necessary to obtain a successful gene silencing following siRNA transfection. It was the aim of this chapter to establish an efficient knockdown of NUDT1, in a panel of NSCLC cell lines and normal human lung fibroblast. NUDT1 was targeted in H23 and H522 adenocarcinoma (both with mutated p53) as well as A549 lung carcinoma (wild-type p53) NSCLC cell lines to determine if any detectable outcomes are applicable to NSCLC in general or are dependent on the p53 state of the cells. In addition, it is essential to consider MRC-5 normal lung cells, acting as a control to assess if the consequent influences are cancer specific.

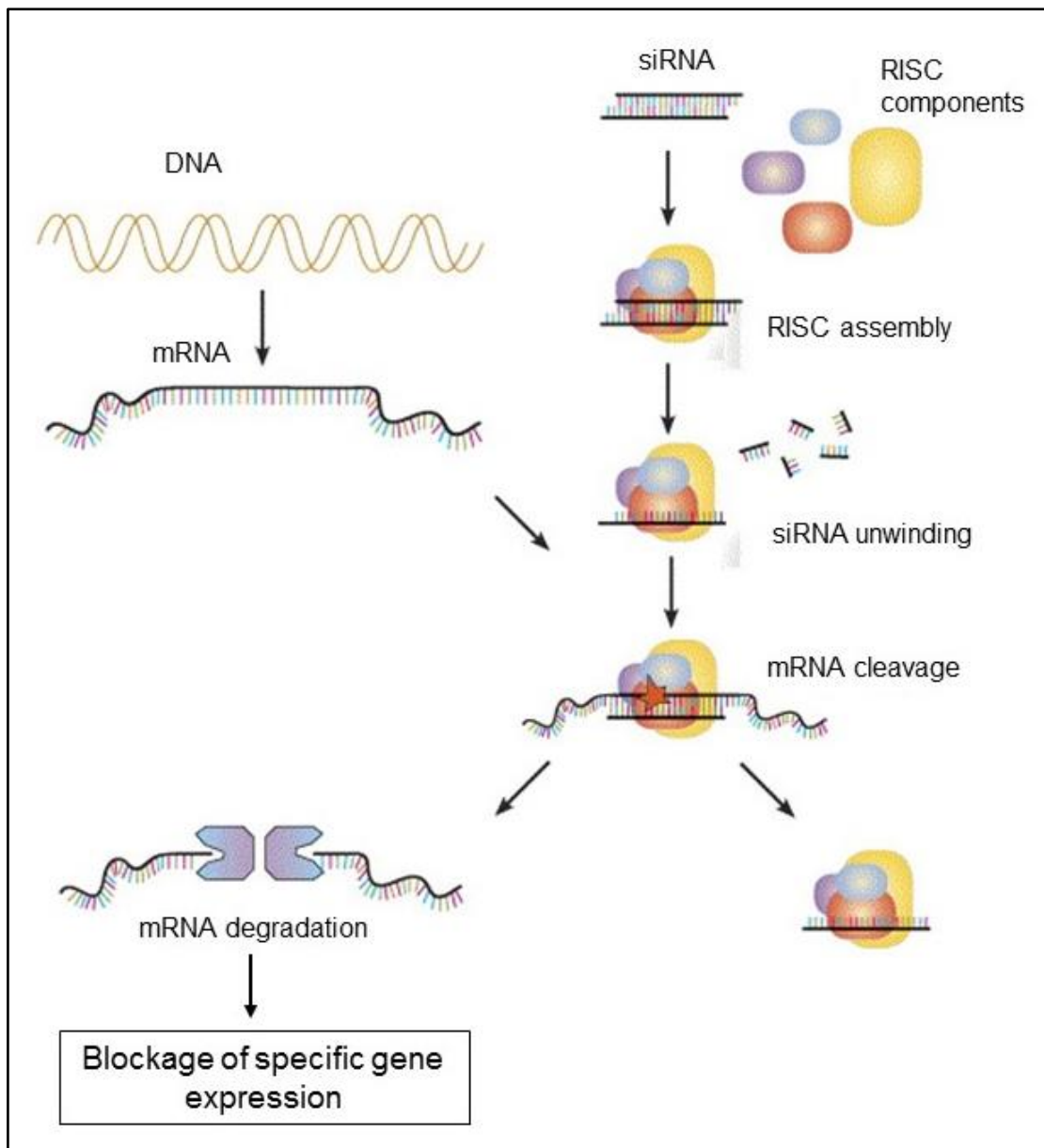


Figure 3-1 The principle mechanism of siRNA action.

Double-stranded siRNA molecules are incorporated into RNA-induced silencing complex (RISC) followed by siRNA unwinding and binding of its antisense strand to the target complementary mRNA. By this way, the activated siRNA cleaves the middle region of targeted mRNA with subsequent degradation of mRNA by an endonuclease, resulting in blockage of gene expression [The Figure modified from (Wacheck and Zangemeister-Wittke, 2006)].

3.1.1 H23 cell knockdown using NUDT1 siRNA (s194633 or s9030)

First of all, the H23 cell line was transfected with NUDT1 siRNA (s194633) using a forward plated method. In order to obtain a reliable and effective knockdown, the delivered siRNA amount needs to be optimized. As shown in Figure 3-2, the transfection method was performed with different concentrations of NUDT1 siRNA (s194633) (2, 4 and 8 nM). Silencer select -ve control siRNA 8 nM (Scramble siRNA), and untreated samples with media (M) without transfection reagent or siRNA were also included as a control. For all used concentrations, there was an almost similar reduction of about 50% in NUDT1 expression up to 3 days after the knockdown when assessed by Western blot. Specifically, on day 3 for instance, the average levels of NUDT1 knockdown after the forward transfection method with 2, 4 or 8 nM NUDT1 siRNA were 72%, 45%, and 46%, respectively.

However, higher transfection efficiency was obtained with 15 nM NUDT1 siRNA (s194633) using both forward and reverse transfection, Figure 3-3. The rationale of this experiment was to estimate the delivery efficacy of both stated methods. On day 1, the reverse transfection process induced an earlier NUDT1 knockdown than the forward procedure with relative NUDT1 expression levels of 63% and 27%, respectively. These relative expression levels remained low on the consecutive days. Specifically, the levels of NUDT1 knockdown on day 2 were 92% for forward, and 94% for reverse methods; while on day 3 they were 86% for forward, and 96% for reverse methods. Therefore, NUDT1 siRNA (s194633) at 15 nM was more successfully knockdown in the H23 cell line than other above-tested concentrations. In addition, this result also suggests higher robust uptake of siRNA via lipofection with reverse transfection method, as both earlier and greater inhibition levels of NUDT1 protein were observed during such method relative to the forward transfection approach. Thereby, the reverse process was used in all subsequent experiments for all tested cell lines. The scrambled samples (silencer select -ve control siRNA) and media without transfection reagent or siRNA were also used in this project as a control.

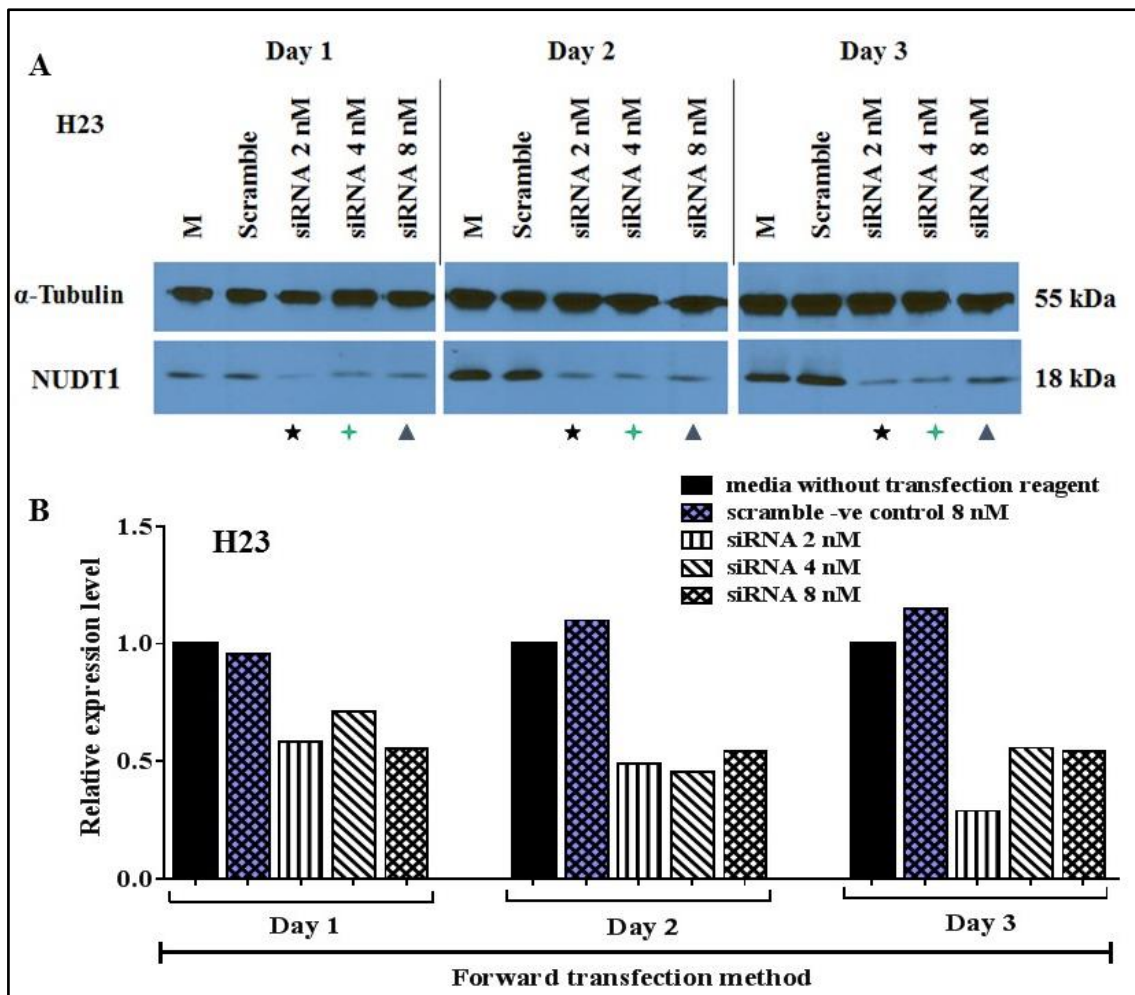


Figure 3-2 NUDT1 is slightly knocked down in H23 cell line after the forward transfecion method with lower NUDT1 siRNA (s194633) concentrations.

Western blots to determine NUDT1 protein levels. [A] H23 cells were grown in media (M) without transfecion reagent/siRNA, or transfected for 3 days with NUDT1 siRNA (s194633) (2 [★], 4 [+], or 8 [▲] nM), or silencer select -ve control siRNA 8 nM (Scramble), using forward transfecion methods. [B] Bands intensities of Western blot were initially quantitated, normalized with the corresponding loading control α -Tubulin bands, and then siRNA samples for each day were normalized to the corresponding band of media without transfecion reagent or siRNA. The number of individual experiments (n) = 1.

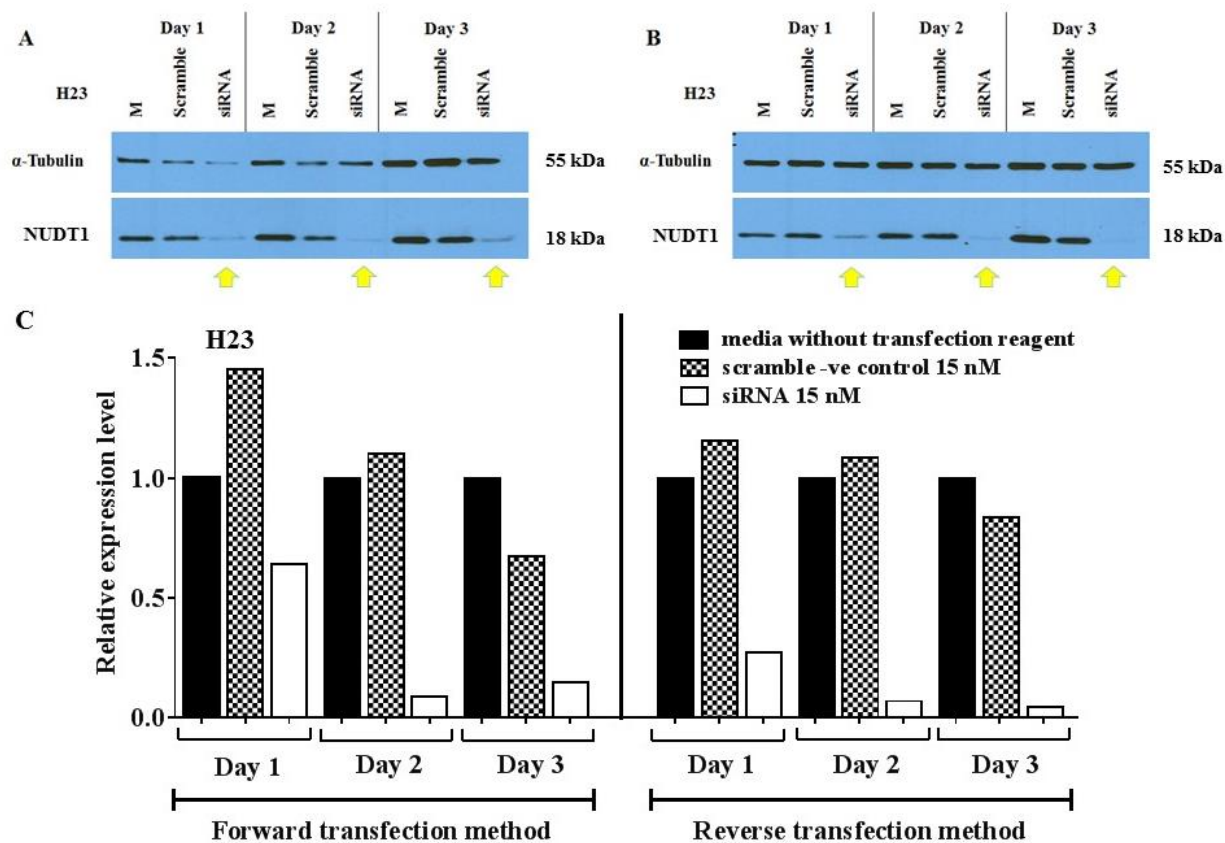


Figure 3-3 Fast and robust knockdown of NUDT1 in H23 cell line after the reverse transfection method.

Western blots to determine NUDT1 protein levels. H23 cells were grown in media (M) without transfection reagent/siRNA, or transfected for 3 days with NUDT1 siRNA (s194633) (15 nM [▲]), or silencer select -ve control siRNA 15 nM (Scramble), using both [A] forward and [B] reverse transfection methods. [C] Bands intensities of Western blot were initially quantitated, normalized with the corresponding loading control α -Tubulin bands, and then siRNA samples for each day were normalized to the corresponding band of media without transfection reagent nor siRNA. The number of individual experiments (n) = 1. For other experiments, the reverse process was used.

In order to determine the duration of gene silencing due to siRNA, H23 cells were allowed to continue to grow and subcultured every 3 days following NUDT1 knockdown. As depicted in Figure 3-4, there was a dramatic decrease in the expression of NUDT1 by at least 75% only four days after 15 nM NUDT1 siRNA (s194633) transfection, and remained low for up to 9 days compared to untreated samples. Specifically, the highest range of transfection efficiency was observed on day 4 (83%), and then gradually decreased reaching 75% on day 7. By day 9, it achieved an efficiency of 88%. Nevertheless, no reduction in the levels of NUDT1 expression were observed in the consecutive days, as the NUDT1 expressions returned to the original levels before transfection of cells (data not shown). This observation suggests an efficient transfection of H23 cell line with 15 nM NUDT1 siRNA (s194633) for up to 9 days. Thus, siRNA could be used to study the role of NUDT1 in H23 cell line.

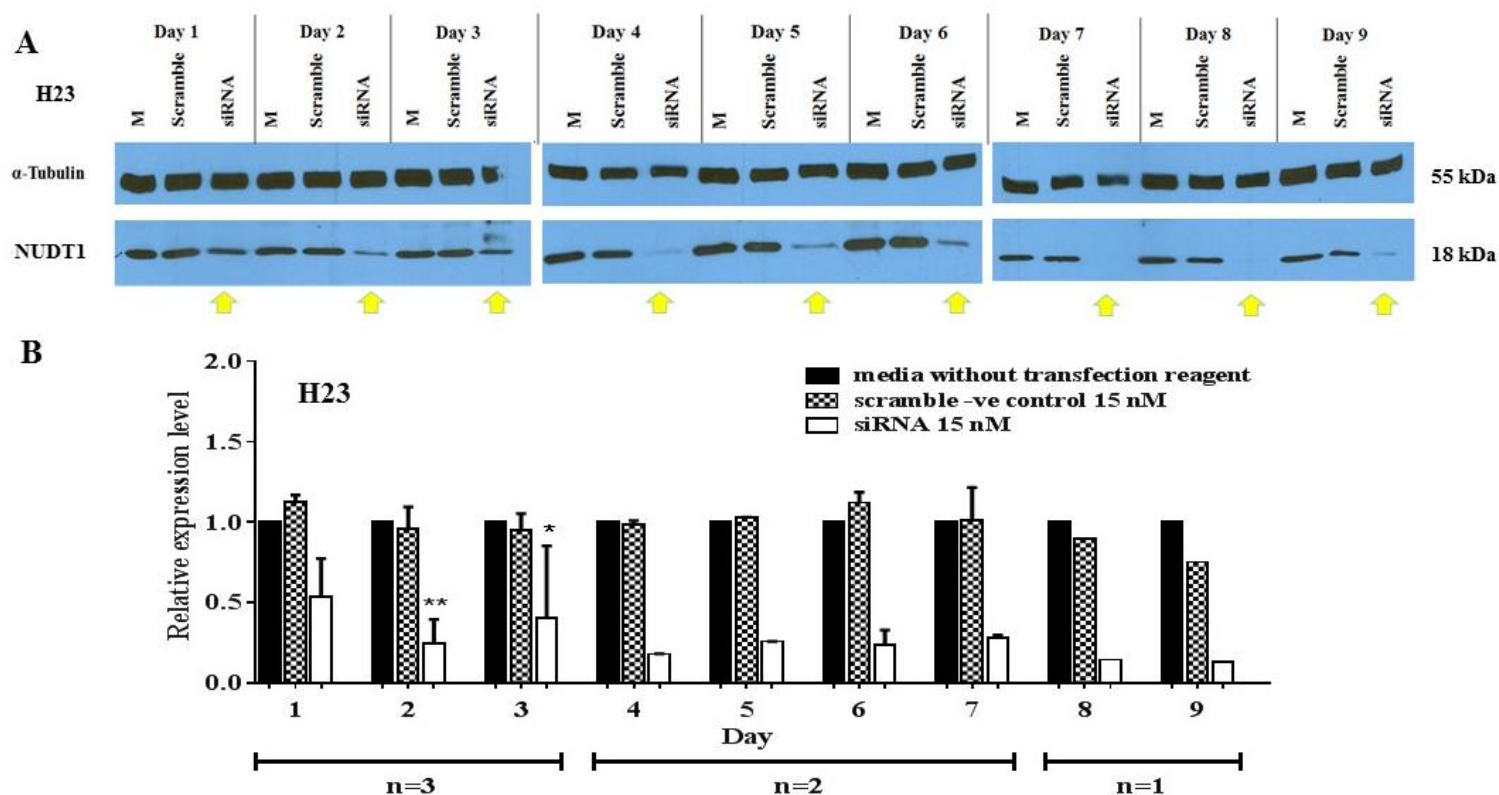


Figure 3-4 Successful knockdown of NUDT1 in H23 cell line for up to 9 days after transfection with NUDT1 siRNA (s194633).

Western blots to determine NUDT1 protein levels. [A] H23 cells were grown in media (M) without transfection reagent/siRNA, or transfected for 9 days in total with NUDT1 siRNA (s194633) (15 nM [▲]), or silencer select -ve control siRNA 15 nM (Scramble). [B] Bands intensities were initially quantitated, normalized with the corresponding loading control α -Tubulin bands, and then siRNA samples for each day were normalized to the corresponding band of media without transfection reagent nor siRNA. Asterisks represent a significant difference relative to corresponding untransfected (no transfection reagent/siRNA) control cells (** $P < 0.01$, and * $P < 0.05$). The number of individual experiments (n) are indicated.

Another siRNA was also used to deplete NUDT1 protein to confirm the result of knockdown and whether more efficient siRNA delivery into the cells could be attained. In this experiment, different concentrations of NUDT1 siRNA (s9030), 10 and 15 nM, were tested. According to the data displayed in Figure 3-5, the optimal concentration of such siRNA was 15 nM for H23 cells, as after 3 days of transfection a greater decline in the level of relative NUDT1 expression (14%) was found compared to 22% by using the lower concentration (10 nM siRNA).

Afterward, H23 cells were allowed to continue to grow and subcultured every three days following siRNA transfection with 15 nM concentration, in order to determine the interval length of gene silencing. As shown in Figure 3-6, NUDT1 expression was consistently downregulated by about 80% only 3 days after NUDT1 siRNA transfection, and this was maintained for at least 9 days. Specifically, this trend reduction reached 88% on day 3, then slight fluctuations in its level were observed in the consecutive days (between day 4-8), with the lowest level of NUDT1 knockdown was 66% on day 7. However, the NUDT1 knockdown efficiency on day 9 was retained to 93%. This observation suggests an efficient transfection of H23 cell line with 15 nM NUDT1 siRNA (s9030) up to 9 days. Thus, by using siRNA it was able to later study the role of NUDT1 in H23 cell line.

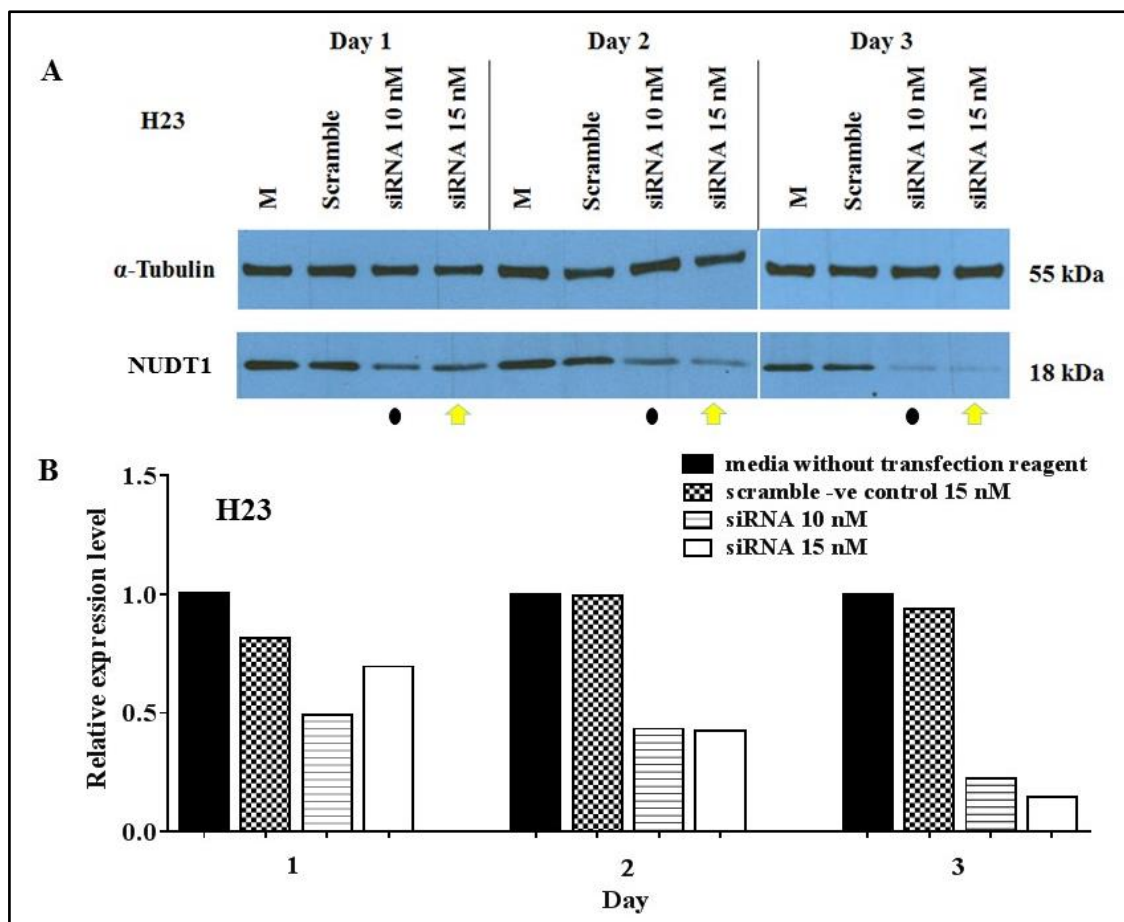


Figure 3-5 NUDT1 is more efficiently knocked down in H23 cell line for up to 3 days after transfection with 15 nM siRNA (s9030).

Western blots to determine NUDT1 protein levels. [A] H23 cells were grown in media (M) without transfection reagent/siRNA, or transfected for 3 days with NUDT1 siRNA (s9030) (10 [●] or 15 [▲] nM), or silencer select -ve control siRNA 15 nM (Scramble). [B] Bands intensities were initially quantitated, normalized with the corresponding loading control α -Tubulin bands, and then siRNA samples for each day were normalized to the corresponding band of media without transfection reagent nor siRNA. The number of individual experiments (n) = 1.

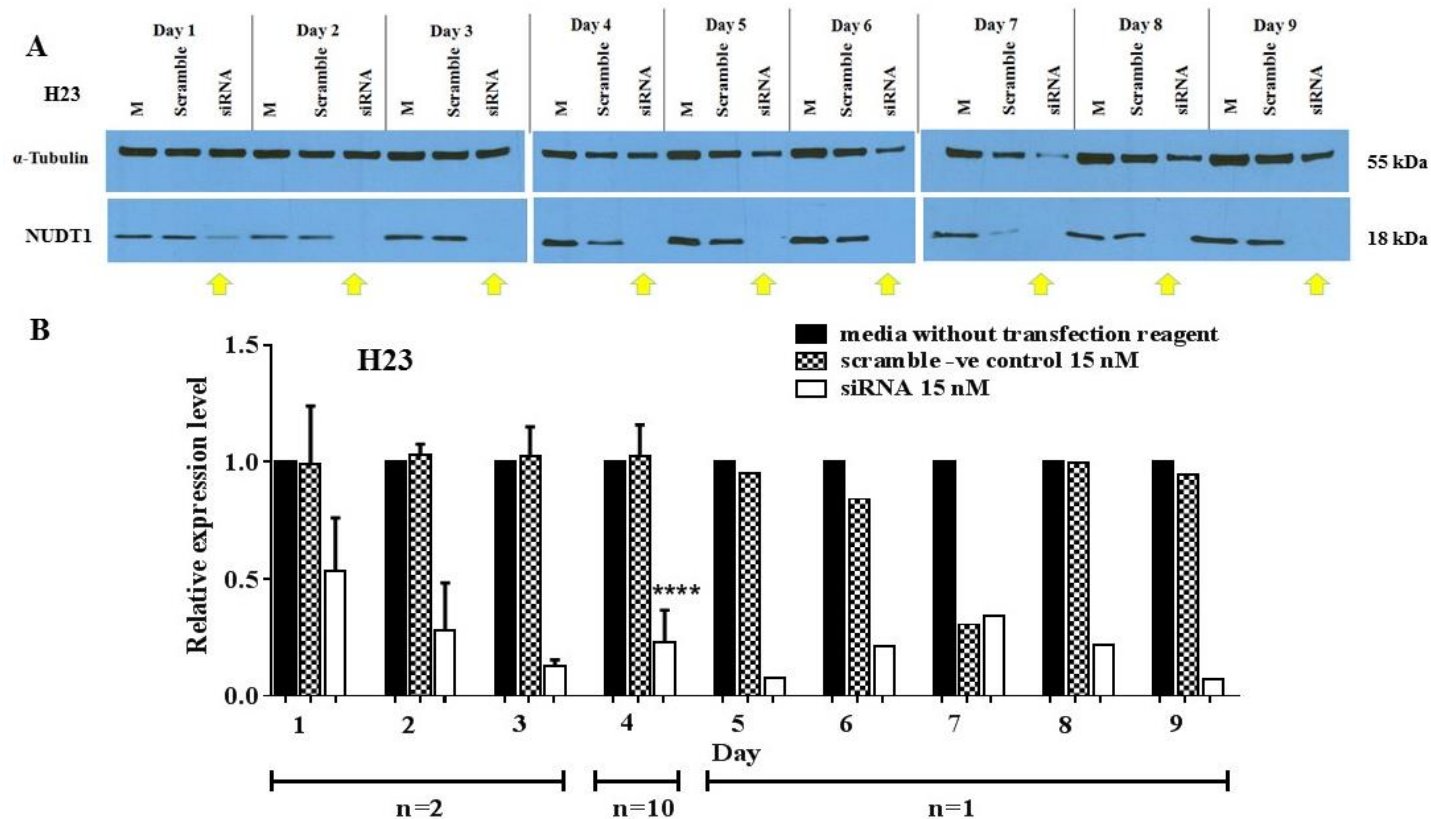


Figure 3-6 Successful knockdown of NUDT1 in H23 cell line for up to 9 days after transfection with NUDT1 siRNA (s9030).

Western blots to determine NUDT1 protein levels. [A] H23 cells were grown in media (M) without transfection reagent/siRNA, or transfected for 9 days in total with NUDT1 siRNA (s9030) (15 nM [\blacktriangledown]), or silencer select -ve control siRNA 15 nM (Scramble). [B] Bands intensities were initially quantitated, normalized with the corresponding loading control α -Tubulin bands, and then siRNA samples for each day were normalized to the corresponding band of media without transfection reagent nor siRNA. Asterisks represent a significant difference relative to corresponding untransfected (no transfection reagent/siRNA) control cells (**** $P < 0.0001$). The number of individual experiments (n) are indicated.

3.1.2 H522 knockdown using NUDT1 siRNA (s194633 or s9030)

For H522 cells, the delivered siRNA amount also needs an adjustment in order to maintain a reliable and effective knockdown. To start with, the cells were transfected with NUDT1 siRNA (s194633) using 2, 4 and 8 nM concentrations, Figure 3-7. Silencer select -ve control siRNA (scramble siRNA), and untreated samples with media (M) without transfection reagent or siRNA were also included as a control. There was a slight decrease in NUDT1 expression with the indicated concentrations up to 3 days (Figure 3-7), as revealed by Western blot. Despite applying a higher amount of siRNA (15 nM), the reduction in NUDT1 protein was still less than 50% on day 3, Figure 3-8, indicating its lower efficiency NUDT1 knockdown in H522 cells relative to H23 cell line.

Therefore, another siRNA (s9030) was also applied in order to achieve better NUDT1 knockdown efficacy in H522 cells. Herein, the transfection was carried out with different concentrations of siRNA including 10, 15 and 20 nM. As shown in Figure 3-9, the reduction in gene expression was seen after 24 h with the higher used siRNA concentrations (15 and 20 nM). This drop sustained to highpoint levels on day 3, reaching 76%, 81%, and 79% NUDT1 knockdown efficiency for 10, 15, and 20 nM siRNA (s9030), respectively, which are much higher levels of NUDT1 knockdown than what was established with the above-mentioned NUDT1 siRNA (s194633) at 15 nM concentration, Figure 3-8. Indeed, the data suggests robust depletion of NUDT1 protein following siRNA (s9030) transfection of H522 compared to NUDT1 siRNA (s194633). In addition, it was considered the usage of 20 nM NUDT1 siRNA (s9030) for further transfection of H522 cells.

In order to determine the duration of gene silencing due to siRNA, H522 cells were allowed to continue to grow and subcultured every 3 days following transfection with 20 nM NUDT1 siRNA (s9030).

As shown in Figure 3-10, the NUDT1 level was consistently reduced about 70% only 4 days after NUDT1 siRNA (s9030) transfection, and remained low for up to 6 days. Specifically, the average level of NUDT1 knockdown on day 3 was 49%; while on day 4 it was 70%. NUDT1 knockdown was extended up to 6 days, albeit with lower extent (48% and 50% on day 5 and 6, respectively) (Figure 3-10). However, on the

consecutive days, no reduction in the levels of NUDT1 expression were observed as the NUDT1 expression returned to the original levels before transfection of cells.

Collectively, by using 20 nM NUDT1 siRNA (s9030) for transfection of H522 cell line, the NUDT1 knockdown efficiency was at a lower degree to some extent and slightly delayed until day 4 relative to other tested cell lines. By this way, the above result still suggests an efficient transfection of H522 cells following the intake of 20 nM NUDT1 siRNA (s9030), although at a lower degree, and able to later study the role of NUDT1 in H522 cell line.

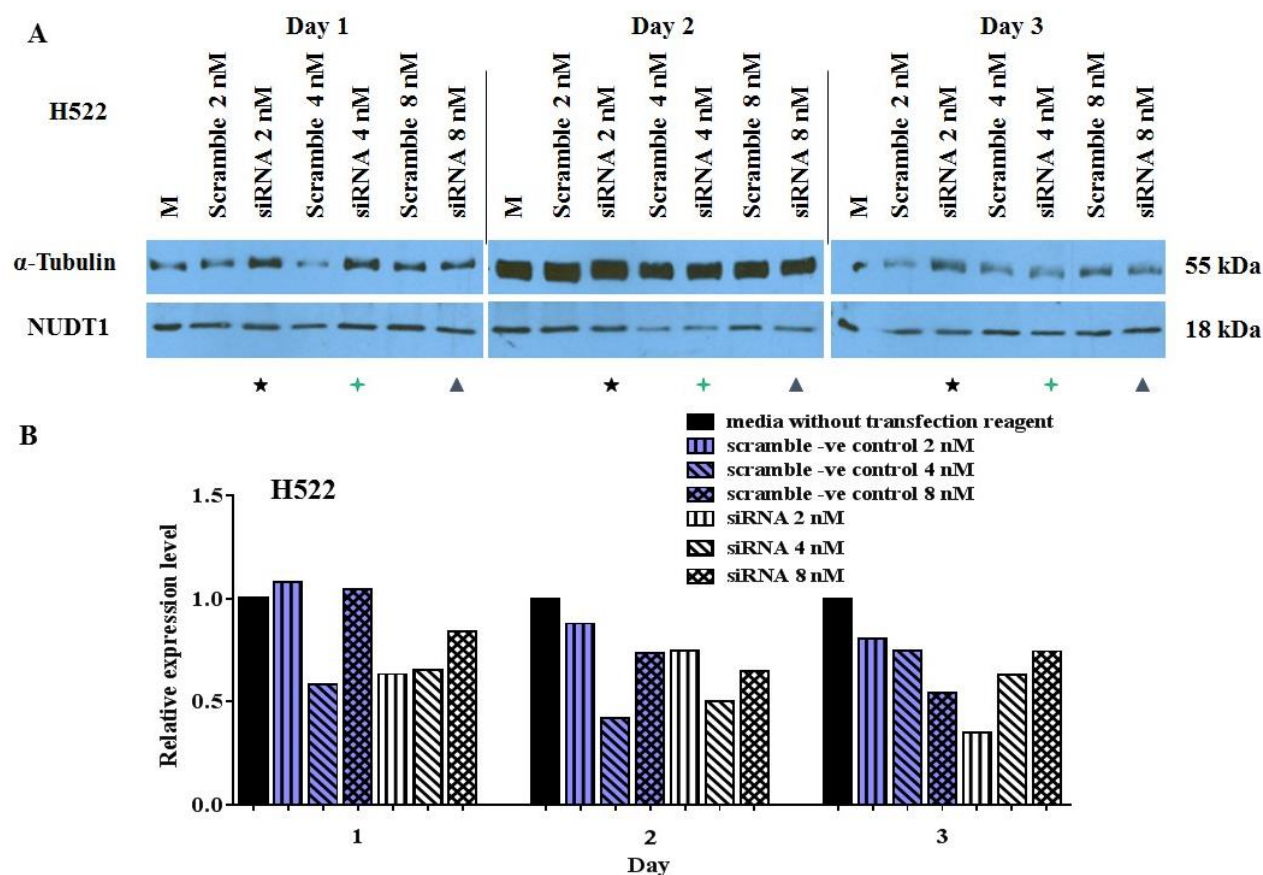


Figure 3-7 NUDT1 is slightly knocked down in H522 cell line after transfection with the lower NUDT1 siRNA (s194633) concentrations.

Western blots to determine NUDT1 protein levels. [A] H522 cells were grown in media (M) without transfection reagent/siRNA, or transfected for 3 days with NUDT1 siRNA (s194633) (2 [★], 4 [+], or 8 [▲] nM), or silencer select -ve control siRNA (2, 4, or 8 nM (Scramble)). [B] Bands intensities were initially quantitated, normalized with the corresponding loading control α -Tubulin bands, and then siRNA samples for each day were normalized to the corresponding band of media without transfection reagent nor siRNA. The number of individual experiments (n) = 1.

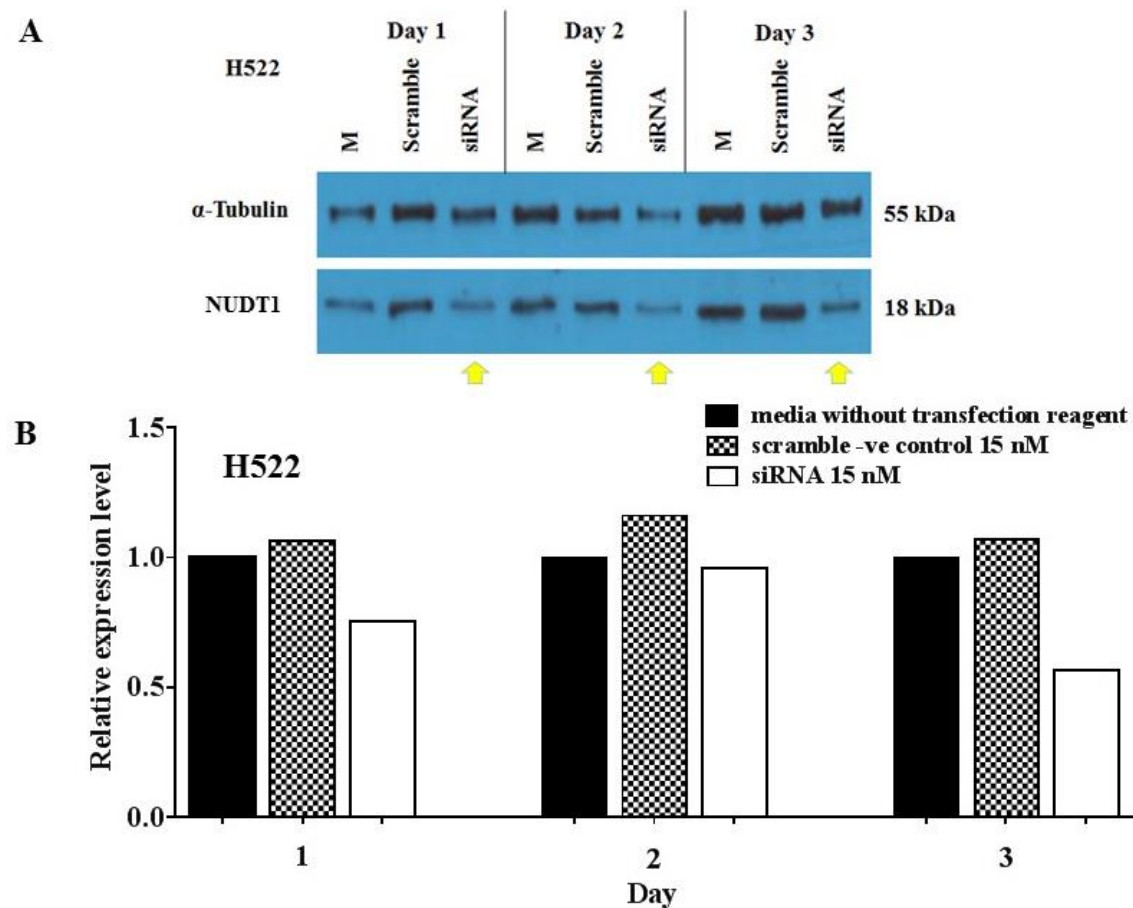


Figure 3-8 NUDT1 is slightly knocked down in H522 cell line after transfection with 15 nM NUDT1 siRNA (s194633).

Western blots to determine NUDT1 protein levels. [A] H522 cells were grown in media (M) without transfection reagent/siRNA, or transfected for 3 days with NUDT1 siRNA (s194633) (15 nM [↑]), or silencer select -ve control siRNA 15 nM (Scramble). [B] Bands intensities were initially quantitated, normalized with the corresponding loading control α -Tubulin, and then siRNA samples for each day were normalized to the corresponding band of media without transfection reagent nor siRNA. The number of individual experiments (n) = 1.

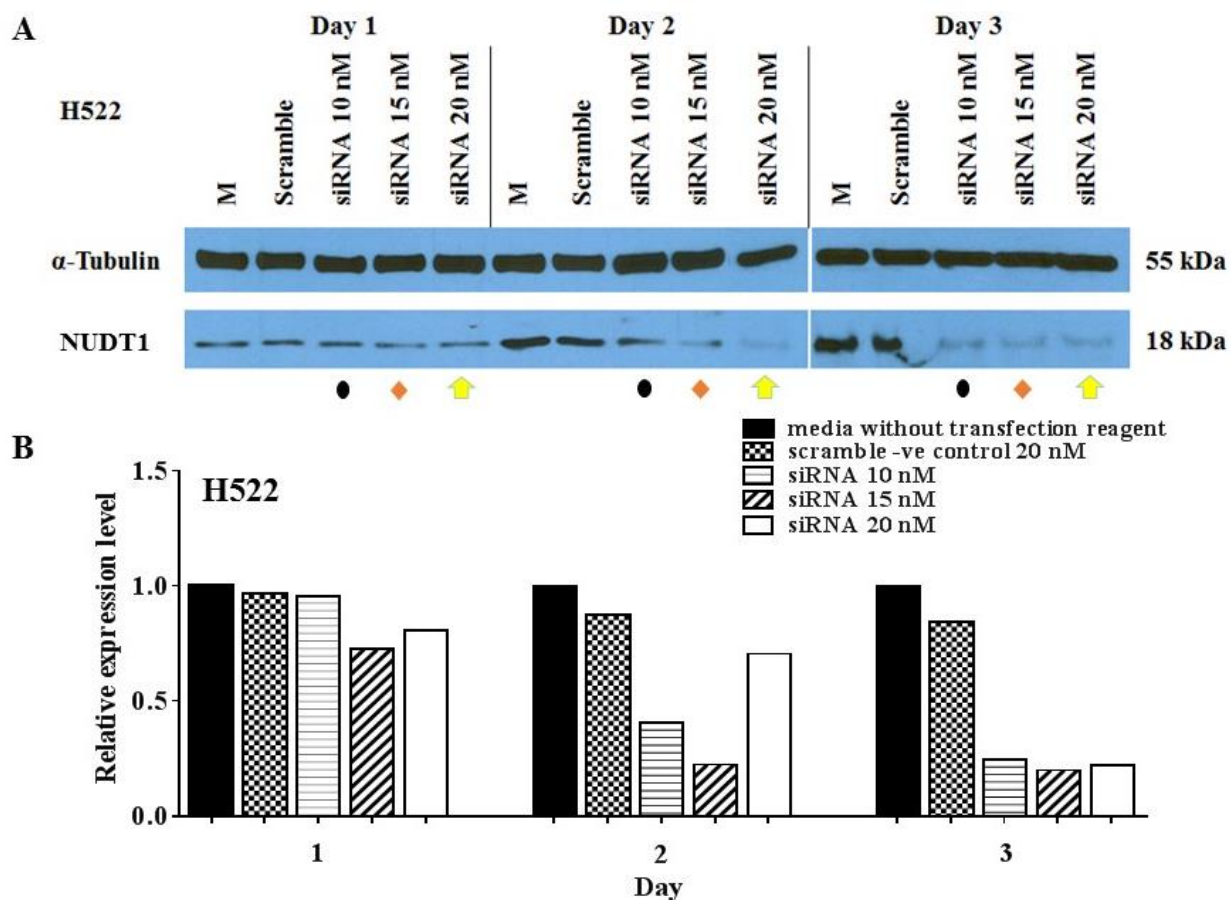


Figure 3-9 Efficient knockdown of NUDT1 in H522 cell line for up to 3 days after transfection with 20 nM NUDT1 siRNA (s9030).

Western blots to determine NUDT1 protein levels. [A] H522 cells were grown in media (M) without transfection reagent/siRNA, or transfected for 3 days with NUDT1 siRNA (s9030) (10 [●], 15 [◆], and 20 [▲] nM), or silencer select -ve control siRNA 20 nM (Scramble). [B] Bands intensities were initially quantitated, normalized with the corresponding loading control α -Tubulin bands, and then siRNA samples for each day were normalized to the corresponding band of media without transfection reagent nor siRNA. The number of individual experiments (n) = 1.

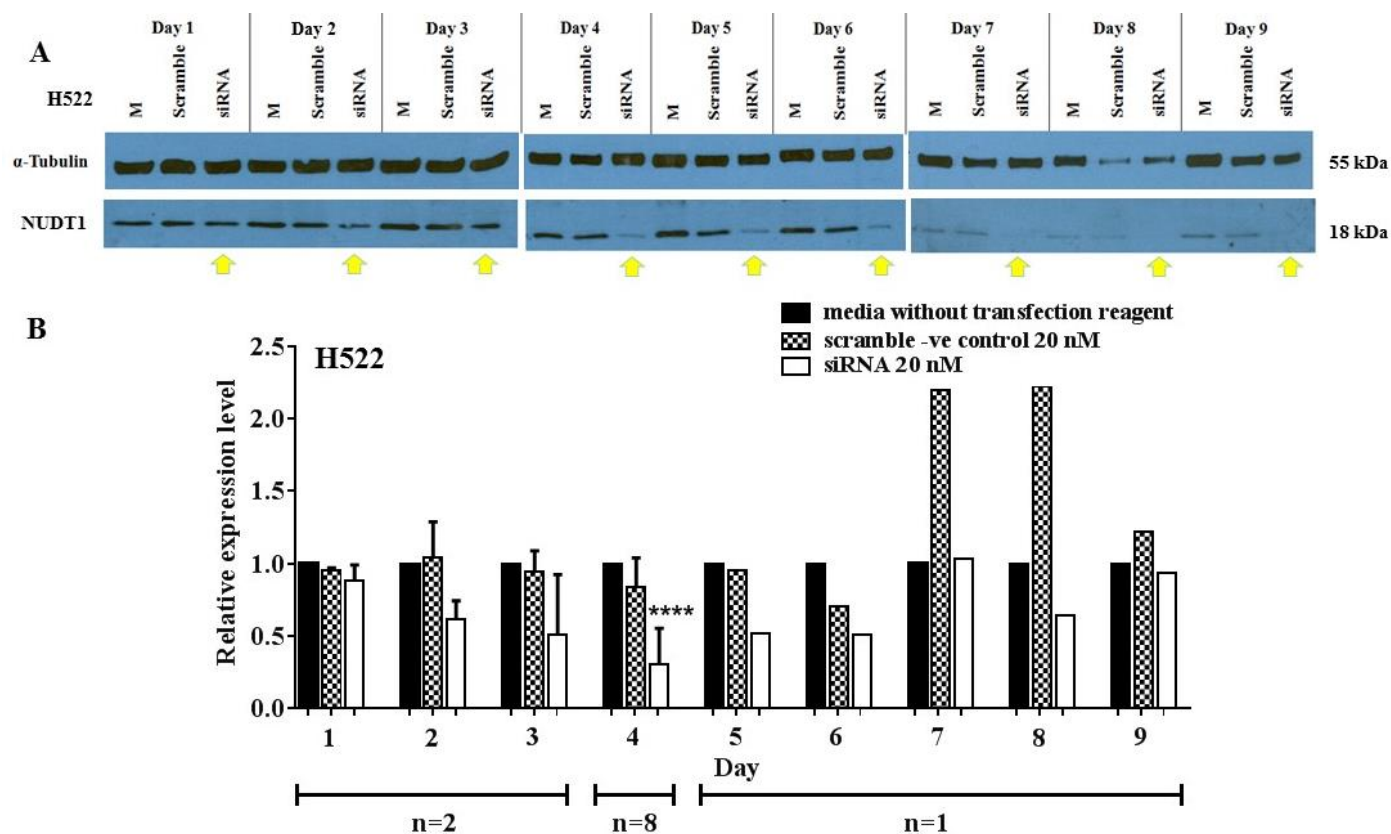


Figure 3-10 Successful knockdown of NUDT1 in H522 cell line for up to 6 days after transfection with NUDT1 siRNA (s9030).

Western blots to determine NUDT1 protein levels. [A] H522 cells were grown in media (M) without transfection reagent/siRNA, or transfected for 9 days in total with NUDT1 siRNA (s9030) (20 nM [⬆]), or silencer select -ve control siRNA 20 nM (Scramble). [B] Bands intensities were initially quantitated, normalized with the corresponding loading control α -Tubulin bands, and then siRNA samples for each day were normalized to the corresponding band of media without transfection reagent nor siRNA. Asterisks represent a significant difference relative to corresponding untransfected (no transfection reagent/siRNA) control cells (**** $P < 0.0001$). The number of individual experiments (n) are indicated.

3.1.3 A549 knockdown using NUDT1 siRNA (s9030)

Similar to the other NSCLC cell lines, optimization of NUDT1 knockdown was carefully considered in A549 cells to facilitate a robust delivery of siRNA. In this case, the gene silencing was carried out using NUDT1 siRNA (s9030). As illustrated in Figure 3-11, two different siRNA concentrations were used, 10 and 15 nM. Silencer select -ve control siRNA (scramble siRNA), and untreated samples with media (M) without transfection reagent or siRNA were also included as a control. Overall, a reduction in gene expression consistently exceeded 75% only 3 days after both concentrations of NUDT1 siRNA, and remained low for at least 6 days. Specifically, the average levels of NUDT1 knockdown on day 3 were 91% for 10 nM and 83% for 15 nM concentrations; while on day 4 they were 55% and 71% for either concentration, respectively. The reduction trends of NUDT1 expression were continued at lower levels, reaching on day 6, 90% for 10 nM and 83% for 15 nM concentrations. This result suggests a greater potency in inhibiting NUDT1 protein by using 15 nM NUDT1 siRNA (s9030) than the lower used concentration, 10 nM. In addition, these tested siRNA amounts might affect α -tubulin levels especially on day 4, at least in the shown data (Figure 3-11A). However, a minimal variation in α -tubulin expression was detected at protein level during the same time interval with other passive transfection experiments, Figure 3-11B. Collectively, the above results suggest an efficient passive transfection of A549 cells for 6 days following the intake of NUDT1 siRNA, and it also adopted the usage of 15 nM siRNA (s9030) to carry out further transfection in such cell line, and hence, by using siRNA it was able to later study the role of NUDT1 in the A549 cell line.

3.1.4 MRC-5 knockdown using NUDT1 siRNA (s9030)

Normal human lung fibroblast, MRC-5 cells, were also knocked down with NUDT1 siRNA (s9030), in which successful transfection requires careful optimization of the applied condition. Herein, two siRNA (s9030) concentrations (10 and 15 nM) were used for MRC-5 cells transfection. Silencer select -ve control siRNA (Scramble), and untreated samples with media (M) without transfection reagent or siRNA were also included as a control. As indicated in Figure 3-12, the siRNA-mediated knockdown of NUDT1 gene showed a dose-dependent response. By using 10 and 15 nM siRNA (s9030), they had a consistent reduction in gene expression for at least 75% only 3 days

after NUDT1 siRNA transfection, and remained low for at least 6 days. Specifically, the levels of NUDT1 knockdown on day 3 were 80% for 10 nM and 76% for 15 nM concentrations; while on day 4 they were 70% and 73% for either concentration, respectively. The reduction trends of NUDT1 expression were continued at lower levels, reaching on day 5, 78% for 10 nM and 87% for 15 nM concentrations. On the final day of verified time interval (day 6), the NUDT1 level after 15 nM NUDT1 siRNA transfection was as low as 10%, and still greater than the NUDT1 knockdown efficiency (69%) which was attained by the lower used concentration. Despite the NUDT1 protein samples of scrambled siRNA and that grown in media (M) without transfection reagent or siRNA exhibited faint band intensities especially on day 4 (Figure 3-12A), other NUDT1 knockdown experiment was shown, (Figure 3-12B) with a minimal variation in NUDT1 expression at protein level during the same time interval.

Overall, this result suggests a greater efficiency for inhibiting NUDT1 protein by using 15 nM NUDT1 siRNA (s9030) relative to the lower used concentration. In addition, the above findings also indicate an efficient NUDT1 siRNA (s9030) intake that applied for transient transfection of MRC-5 cells for 6 days, and recommended the usage of 15 nM siRNA (s9030) to carry out further transfection in such cell line. Hence, using siRNA enabled the study of the role of NUDT1 in MRC-5 cell line.

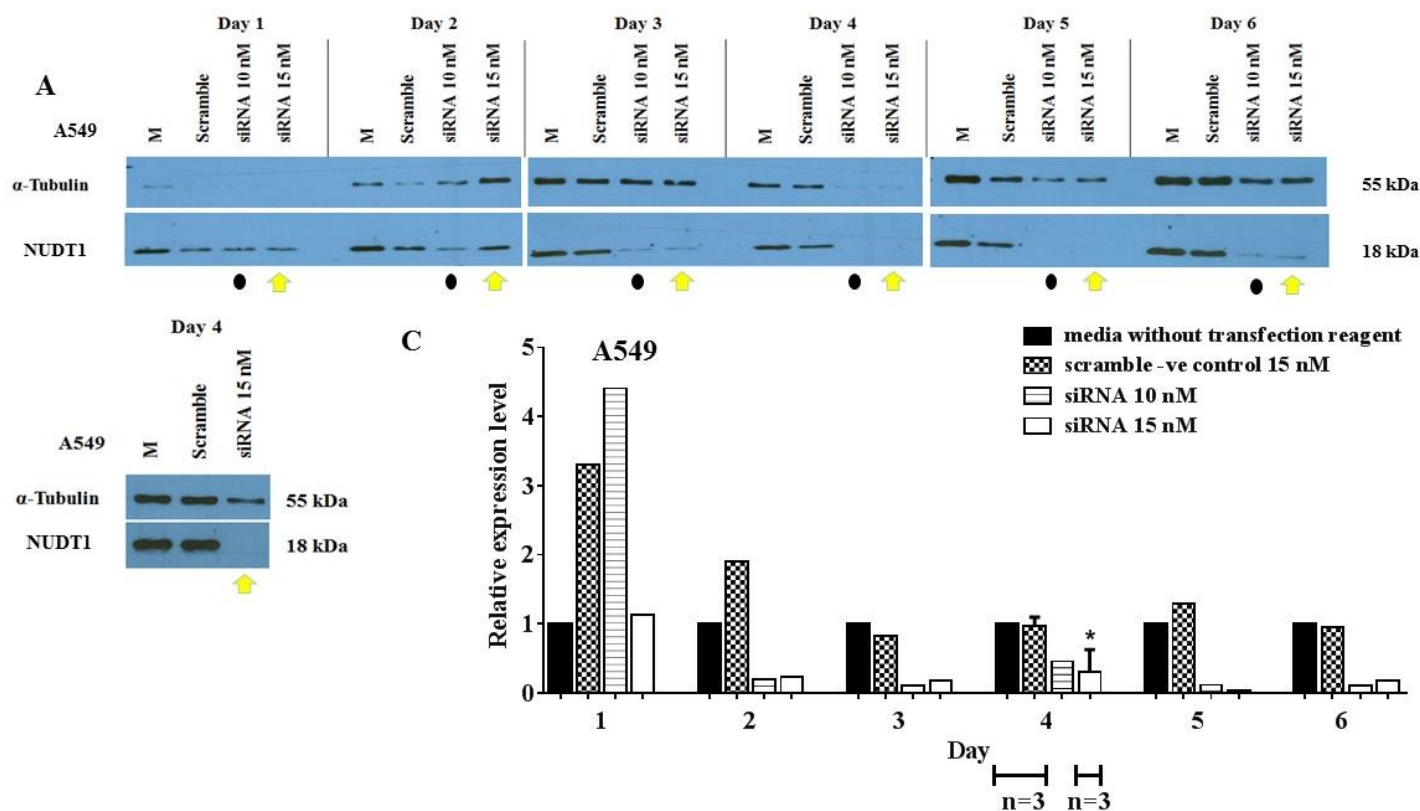


Figure 3-11 Successful knockdown of NUDT1 in A549 cell line for up to 6 days.

Western blots to determine NUDT1 protein levels. [A] A549 cells were grown in media (M) without transfection reagent/siRNA, or transfected for 6 days in total with NUDT1 siRNA (s9030) (10 [●] or 15 [➤] nM), or silencer select -ve control siRNA 15 nM (Scramble). [B] Representative Western blot for NUDT1 knockdown on day 4 shown from another experiment. [C] Bands intensities were initially quantitated, normalized with the corresponding loading control α -Tubulin bands, and then siRNA samples for each day were normalized to the corresponding band of media without transfection reagent nor siRNA. Asterisks represent a significant difference relative to corresponding untransfected (media without transfection reagent/siRNA) control cells (* $P < 0.05$). The number of individual experiments (n) = 1 or as indicated.

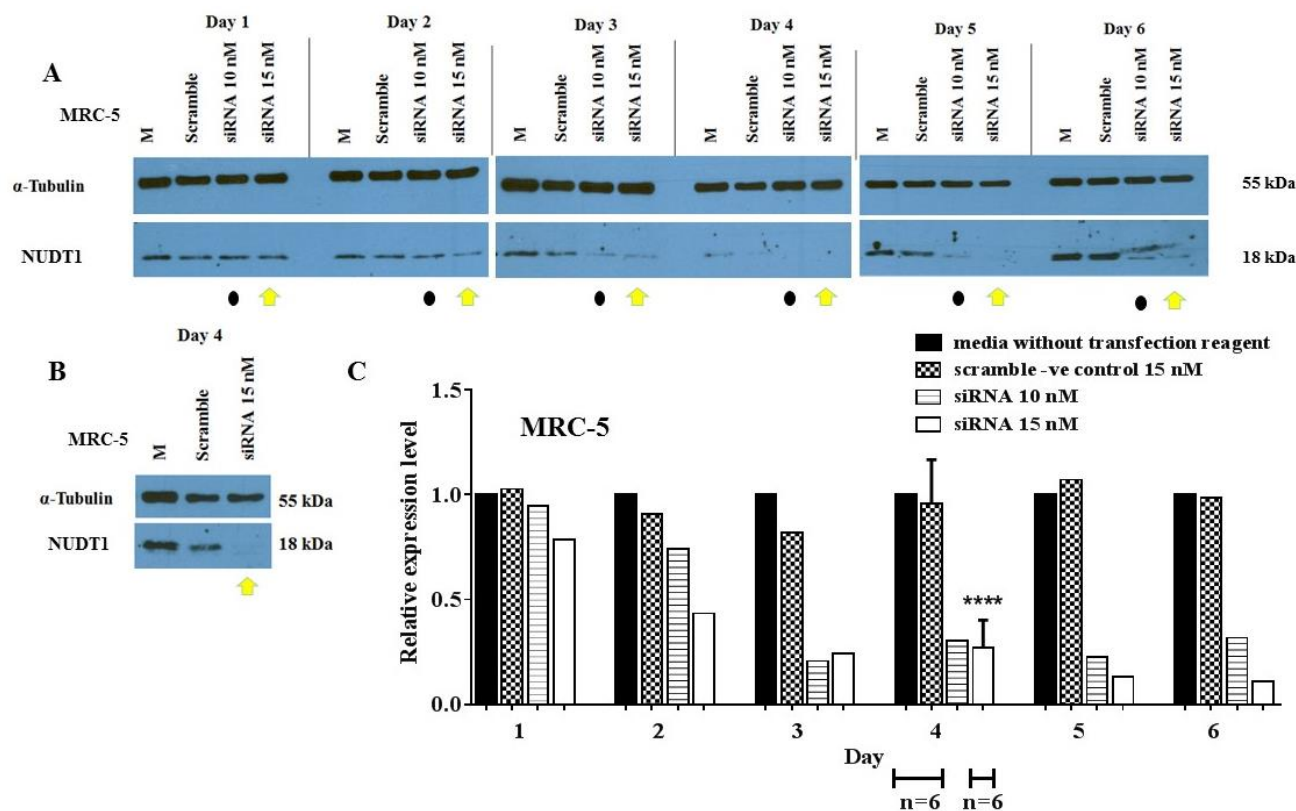


Figure 3-12 Successful knockdown of NUDT1 in MRC-5 normal human lung fibroblasts cells for up to 6 days.

Western blots to determine NUDT1 protein levels. [A] MRC-5 cells were grown in media (M) without transfection reagent/siRNA, or transfected for 6 days in total with NUDT1 siRNA (s9030) (10 [●] or 15 nM [▲]), or silencer select -ve control siRNA 15 nM (Scramble). [B] Representative Western blot for NUDT1 knockdown on day 4 shown from another experiment. [C] Bands intensities were initially quantitated, normalized with the corresponding loading control α -Tubulin bands, and then siRNA samples for each day were normalized to the corresponding band of media without transfection reagent nor siRNA. Asterisks represent a significant difference relative to corresponding untransfected (no transfection reagent/siRNA) control cells (**** $P < 0.0001$). The number of individual experiments (n) = 1 or as indicated.

3.2 The expression level of NUDT15 after NUDT1 knockdown

NUDT15 is another Nudix hydrolase family member, which also hydrolyses 8-oxodGTP similar to NUDT1. In order to determine whether any compensatory activity or alteration in the expression level of NUDT15 occurs after a transient NUDT1 knockdown, the NUDT15 levels were assessed after transfection of H23 cell line with 15 nM NUDT1 siRNA (S9030). The cells were then allowed to continue to grow and subcultured up to 6 days. Samples of -ve control scramble siRNA, and untreated media without siRNA or transfection reagent were also applied.

During this time interval, successful NUDT1 depletion in H23 cell line did not increase the levels of NUDT15, suggesting that NUDT15 does not act to compensate for the NUDT1 loss, at least for the verified duration, as confirmed by Western blot, Figure 3-13.

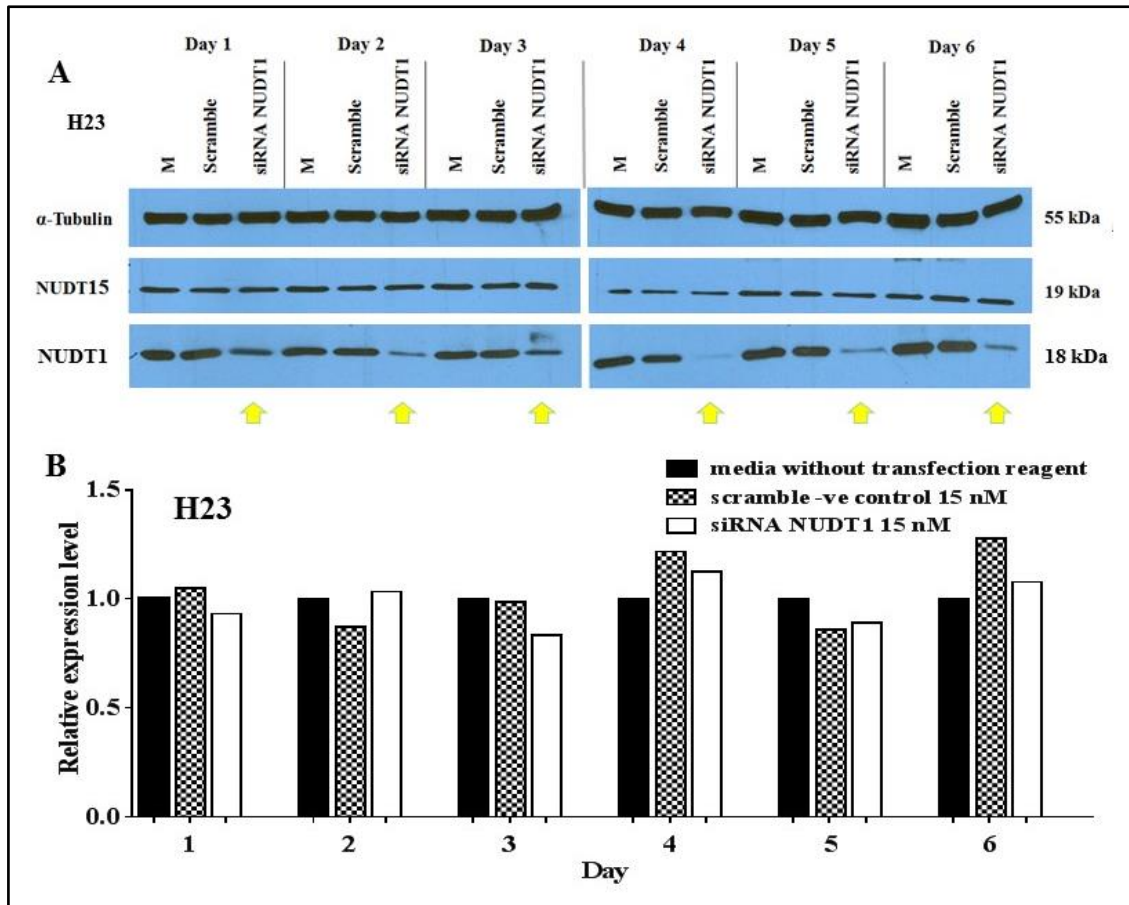


Figure 3-13 NUDT15 levels remain stable following transfection with NUDT1 siRNA for up to 6 days.

Western blots to determine NUDT15 and NUDT1 protein levels. [A] H23 cells were grown in media (M) without transfection reagent/siRNA, or transfected for 6 days in total with NUDT1 siRNA (s9030) (15 nM [⬆]), or silencer select -ve control siRNA 15 nM (Scramble). [B] Bands intensities were initially quantitated, normalized with the corresponding loading control α -Tubulin bands, and then siRNA samples for each day were normalized to the corresponding band of media without transfection reagent nor siRNA. The number of individual experiments (n) = 1.

3.3 Discussion

Transfection conditions differ between cell lines, especially for those hard-to-transfect lines. Such variation is due to the characteristic features of each cell, as well as the actual applied conditions that require optimization before the start of any research work.

Here, it has been shown that siRNA transfection can potently inhibit NUDT1 enzyme in normal human lung fibroblasts and NSCLC panel cell lines. Consistent NUDT1 knockdown was achieved using siRNA via lipofection with reverse transfection method. Among two tested siRNA, NUDT1 siRNA (s9030) in particular was more effective in transient knockdown of NUDT1 at the protein level in all used cells. Given that the amount of delivered siRNA was optimised, this would allow extending the knockdown transfection period for at least 6 days. The observed results hereby might provide a basis for further analysis of the effect of NUDT1 depletion.

Previous publications suggest the high-throughput efficiency of reverse transfection method (Ovcharenko et al., 2005, Amarzguioui, 2004). Similar to our observation, it facilitates a fast and robust intake of siRNA compared to the standard plated transfection. During the latter technique, the adherent cells might display decreased compatibility with lipid-induced siRNA delivery, as the cellular membrane exposure to transfection complexes is likely minimised in the surrounding medium (Ovcharenko et al., 2005). Easier cell transfection possibly occurs in the presence of such complexes/cells in suspension at the time when morphological cellular changes might accompany the attachment to a surface of growing plates or dishes (Amarzguioui, 2004).

In addition, the reproducibility of transfection is another required factor for successful siRNA delivery. This might be attributed to the characteristic features of the reverse transfection method that enables a reduction in the well-to-well variability such as the uses of master mixes of cells and transfection complex, as well as fewer pipettings and manipulations. The reverse transfection also allowed an efficient reduction of the target gene expression by using lower siRNA concentration relative to corresponding standard transfection approach. Similar observation was noticed previously (Ovcharenko et al., 2005) with almost negligible or slight induction of cytotoxicity by the used siRNA concentrations. In this case, the transfection could be provided with more specificity and consistent phenotypic results.

The amount of siRNA was optimized for this study in order to make it possible to obtain an efficient knockdown of NUDT1 enzyme for all used cells. Interestingly, the transfection of cells in suspension permits high silencing efficiency for 6 days, or even up to 9 days with H23 cells. Here, NUDT1 siRNA (s9030) in particular, transiently knocked down of NUDT1 protein level in all cells, giving promising results and in some cases even better transfection efficacy values than the other used siRNA. By this way, this siRNA could be used to study the role of NUDT1 depletion in those transfected cells.

For H522, the downregulation of NUDT1 expression was about 75% at day 4. An extended NUDT1 knockdown was noticed up to 6 days, albeit with lower extent (Figure 3-10). This suggests that the tested conditions of reverse transfection might be less efficient for delivering NUDT1 siRNA (s9030) to H522 in primary culture than other cell lines. It has been stated that electroporation could be an alternate useful method for cells relatively refractory to transfection, making it possible susceptible to the siRNA for those none or slow dividing cells (Ovcharenko et al., 2005). However, more siRNA concentration is needed for the latter approach to making successful gene silencing with an apparent shorter extended period. In addition, optimal electroporation conditions including peak voltage, pulse-length, the number of pulses, and time between consecutive pulses are usually considered for each cell type, as essential parameters to obtain an efficient electroporation (Ovcharenko et al., 2005).

The observed no change in a level of NUDT15 expression in H23 cells following NUDT1 knockdown is consistent with an earlier published finding, although the qRT-PCR technique was used to quantify such NUDT15 expression in that case (Gad et al., 2014). In the same study, no alterations in the level of MUTYH or OGG1 expressions were also determined after shRNA-mediated NUDT1 depletion. In addition, neither MUTYH nor OGG1 overexpression could cause any change in the elevated cytotoxic action of synthetic small molecule NUDT1 inhibitors (Gad et al., 2014). This observation might be explained by an overload of DNA genome with the oxidized bases, BER system overwhelming, or even 8-oxodGTP/2-OHdATP, perhaps, act as signaling for cell death (Gad et al., 2014). A recent publication suggested NUDT15 has a preference for nucleotide substrates different to those of NUDT1, and also showed that depletion of NUDT15 has no impact on clonogenic survival of several cancer cell lines, even without an occurrence of any additive or synergistic action when combined

with siRNA NUDT1-mediated knockdown (Carter et al., 2015). Furthermore, neither progression of cell cycle, DDR markers of DNA DSBs (RPA/53BP1 foci formation), nor 8-oxo-dG DNA content alter following NUDT15 knockdown (Carter et al., 2015).

Overall, the siRNA was successfully used to knockdown NUDT1 and that enabled studies on the role of NUDT1 in various NSCLC cell lines along with normal lung fibroblasts cells. In addition, the level of another Nudix hydrolase family enzyme member, NUDT15, did not rise after the siRNA-mediated NUDT1 knockdown, suggesting it does not to compensate for the NUDT1 loss. This is concordant with a recent study that found NUDT15 prefers nucleotide substrates different to those of NUDT1 (Carter et al., 2015).

Chapter 4: Genotoxic and cytotoxic effects of NUDT1 knockdown in NSCLC cell lines

4.1 Introduction

Nucleotide precursors (d)NTPs exist free within nucleotide pools. Similar to any cellular biomolecules, they are vulnerable to damaging ROS formed both as a by-product of intracellular metabolism and from other genotoxic agents, including ionising radiation and chemotherapeutic drugs. Consequently, oxidatively modified (d)NTPs are cleared from nucleotide pools by Nudix hydrolase family enzymes; such as NUDT1, to prevent their mis-incorporation into DNA genome or RNA by converting them into a mono-phosphate product and PPi (Mildvan et al., 2005).

Overexpression of NUDT1 protein has been recognized in several tumours with RAS gene mutation including NSCLC. Interestingly, such elevation continues to increase even in high-grade NSCLC adenocarcinoma compared to surrounding normal tissue. This is in favour, perhaps, the adaptive mechanism during cancer progression rather than compensatory effect to counteract oxidative stress induced by RAS oncogene (Rai, 2010).

Indeed, NUDT1 overexpression may be necessary for tumour cell proliferation and survival to compensate for oncogenic RAS-mediated DDR and ROS formation, leading to avoidance of RAS-induced senescence outcome (Rai et al., 2011). This could be attributed to the ability of NUDT1 to eliminate oxidized nucleotides as oncogenic RAS mutation increases intracellular level of ROS via enhancement of NADPH oxidase activity and disturbance of mitochondrial function (Rai, 2012). However, it is unlikely that normal untransformed cells rely on such processes of elevated NUDT1 for survival, as these cells possess a rigid redox regulation status and/or have an intact cell cycle checkpoints response to oxidative stress relative to cancer cells (Gad et al., 2014, Guo et al., 2010).

Oxidation of DNA components by ROS is regarded as one of the major routes for the induction of endogenous DNA lesions. This role might involve oxygen free radicals [superoxide radical anion ($O_2^{\cdot-}$) and hydroxyl radical (HO^{\cdot})] or non-radical oxidants including H_2O_2 and singlet oxygen (1O_2) (Kawanishi et al., 2001, Altieri et al., 2008). Disturbance in ROS level in a situation exceeding the cellular ability to counteract their deleterious effect by antioxidant defence mechanisms is described as “oxidative stress”. To such a degree, the intermediates of oxygen molecule reduction mediate DNA damage, generating oxidized base modification (e.g. 8-oxoGua), AP sites, DNA strand

breaks, and DNA-protein adducts (Altieri et al., 2008, Collins et al., 1996). Failure to repair such DNA lesions, to some extent, has a potential for serious genomic instability consequence and/or cellular functions deregulation (Altieri et al., 2008). Therefore, evidence of oxidative DNA damage in the form of lesions, such as 8-oxo-Gua, is an indicator of oxidative stress. As a hallmark cancer trait, oxidative stress is often recognised in almost all cancer cells (Liou and Storz, 2010, Luo et al., 2009), and to great extent contributes to both initial malignant transformation and disease progression (Liou and Storz, 2010, Kumar et al., 2008). However, ROS are regarded as the key bases of the cytotoxicity induced by radiotherapy and other different chemotherapeutic treatments (Borek, 2004, Lomax et al., 2013, Conklin, 2004). Thus, there may be several normally non-essential oxidative stress response factors and pathways that become essential in cancer cells and/or significantly affect responses to cancer therapies.

It is understood that AP sites occur as an intermediate during the early step of BER process, following the excision of damaged bases and cleavage of N-glycoside bond by DNA glycosylase enzymes (Collins et al., 2008). Furthermore, abasic sites and DNA strand breaks with non-ligatable ends are also generated by the abstraction of the hydrogen atom by hydroxyl radical, mainly at C-4' and C-5' positions of deoxyribose or ribose. This progress of hydrogen abstraction forms carbon central radicals, which then convert to peroxy radicals in the presence of oxygen, and finally, undergo several reactions leading to DNA strand breaks formation in most cases (Nakamura et al., 2000, Altieri et al., 2008).

The sequence specificity for direct DNA base damage is suggested to depend on ROS redox potentials, DNA bases oxidation potentials, as well as the distribution of highest occupied molecular orbital (HOMO) on DNA bases. It seems that guanine has the lowest oxidation potential (1.29 V) than other three bases of DNA, and the 5'-G position of GG sequence in B-form double-stranded DNA mostly has the greatest extent of electrons of HOMO (Kawanishi et al., 2001). Therefore, the generation of (8-oxoGua) lesion could arise from two possible ways either by misincorporation of oxidized nucleotide precursors into DNA sequence or from the further oxidation of guanine DNA base as a direct consequence of ROS. Whilst DNA damage has been widely investigated in terms of mutation and tumourigenesis, ROS can play a crucial role in the therapeutic actions of radiotherapy and selected chemotherapeutic agents.

Oxidative modification of DNA synthesis precursors (d)NTPs has previously received less attention than oxidation of DNA, despite the ability of the former to induce mutation, invoke DDR and promote apoptosis or senescence by virtue of their inevitable misincorporation into DNA and RNA by polymerases.

Recently, it has been proposed that first-in-class selective NUDT1 small molecule inhibitors as a promising general treatment for cancer due to the concept of non-oncogene addiction with cancer phenotype lethality strategy (Helleday, 2014). This approach is to target factors and cell processes that are non-essential in normal cells but that become essential for cell growth following the acquisition of hallmark cancer traits (Helleday, 2014, Liou and Storz, 2010, Toledo et al., 2011, Puigvert et al., 2016). Thus, targeting of NUDT1 has indicated a new therapeutic approach which could achieve the conversion of oxidative stress into cytotoxic DNA damage with eventual cancer cell death (Gad et al., 2014). By this way, it may overcome the problem of intra-tumour heterogeneity as well as becoming more applicable to broad tumours range (Gad et al., 2014). In addition, upregulated NUDT1 expression was observed in cancers with RAS mutation such as NSCLC and renal cell carcinoma, supporting the notion of oncogenic transformation coupled with oxidative stress (Huber et al., 2014, Kennedy et al., 2003, Speina et al., 2005, Okamoto et al., 1996). The further global role of NUDT1 in tumorigenesis is probably reinforced by the anti-proliferative effects of SCH51344 small molecule and (S)-enantiomer crizotinib, identified as selective inhibitors to target NUDT1 catalytic activity. Such anti-proliferative findings were remarked in cancer cells undergoing transformation by mechanisms other than mutations of RAS oncogene (Huber et al., 2014).

It was the aim of this chapter to investigate the effect of NUDT1 knockdown in normal human lung fibroblast and NSCLC panel of cell lines; whether it could lead to any cellular alteration in respect to DNA damage, proliferation and/or apoptotic death patterns; and whether this is specific to cancer cells (Figure 1-13). In addition, it attempted to inspect if any induction of DDR signaling markers occurs in response to NUDT1 knockdown.

4.2 Determination of DNA damage induced by NUDT1 knockdown

To determine if targeting NUDT1 has functional effects in NSCLC cells, and whether any consequences were variable between various NSCLC cell lines and/or normal control counterpart's cells, the level of DNA oxidation was first assessed after an efficient knockdown of NUDT1 for 4 days. This duration allows the cells a sufficient time to undergo DNA replication in the existence of significantly lower levels of NUDT1. Herein, the formation of DNA damage in normal human lung fibroblast (MRC-5 cells) along with the panel of NSCLC cell lines (H23, H522, and A549 cells) was investigated, by means of Fpg-modified alkaline comet assay. As described in materials and methods section (2.2.3), Fpg enzyme was used to detect oxidatively damaged purine lesions mainly 8-oxoGua. Nevertheless, the comet assay when analysed in the absence of Fpg allows recognition of DNA SSBs and, even at an alkaline condition with $\text{pH} > 13$, alkali-labile sites (ALS) could also be identified. The latter may contain apurinic/apyrimidinic (AP) sites, oxidised AP sites and modified bases (Cadet et al., 2000, Cooke et al., 2008).

Mock transfection samples (media without siRNA or transfection reagent) were incubated with or without Fpg repair enzyme and processed in every experiment to evaluate an endogenous DNA damage, as well as, any unintended damage that might occur during the sample preparation. Silencer select –ve control siRNA (Scramble) slides were also included. In our laboratory, the final concentration of Fpg enzyme, 0.8 U/Gel (at 1:500 dilution), along with incubation period, 30 min, were established previously. These optimal conditions were adopted during this project, despite the optimization procedure was carried out at that time using different cell line, SK23 melanoma cancer cells treated with H_2O_2 .

An efficient transient depletion of NUDT1 protein was established for 4 days amongst different NSCLC cell lines. As previously mentioned, those NSCLC cells with mutated p53 status (H23, and H522 cells) were successfully transfected using 15 or 20 nM NUDT1 siRNA (s9030), respectively. The former siRNA concentration (15 nM) was also applied for A549 lung carcinoma (wild-type p53) NSCLC cell line along with MRC-5 normal lung cells, which acts as a control to determine if the outcome effect is cancer specific.

As illustrated in Figures 4-1, 4-2, and 4-3, the panel of NSCLC cell lines (H23, H522, and A549) displayed a significant increase in Fpg sensitive sites after the knockdown of NUDT1 (P-value <0.0001, <0.001, and <0.05, respectively); without further addition of DNA SSBs or ALS. The inclusion of Fpg enzyme has a substantial effect, and the greatest increase in 8-oxoGua was noticed in H23 cells with a nearly two-fold rise in comparison with corresponding scrambled or untransfected cells. However, there was no change in Fpg sensitive sites and/or DNA SSBs observed in MRC-5 cells following 15 nM NUDT1 siRNA (s9030) transfection (Figure 4-4). Indeed, these findings suggest that knockdown of NUDT1 leads to an increase in genomic levels of 8-oxodG, the principle substrate of Fpg, specifically in NSCLC cell lines. This is consistent with the notion that the presence of NUDT1 enzyme is required to suppress the misincorporation of oxidized dNTPs formed at higher levels in cancer cells due to cancer-associated oxidative stress (Gad et al., 2014, Speina et al., 2005). However, successfully silencing of NUDT1 did not cause a rise in SSBs or ALS levels in any of the lung cell lines.

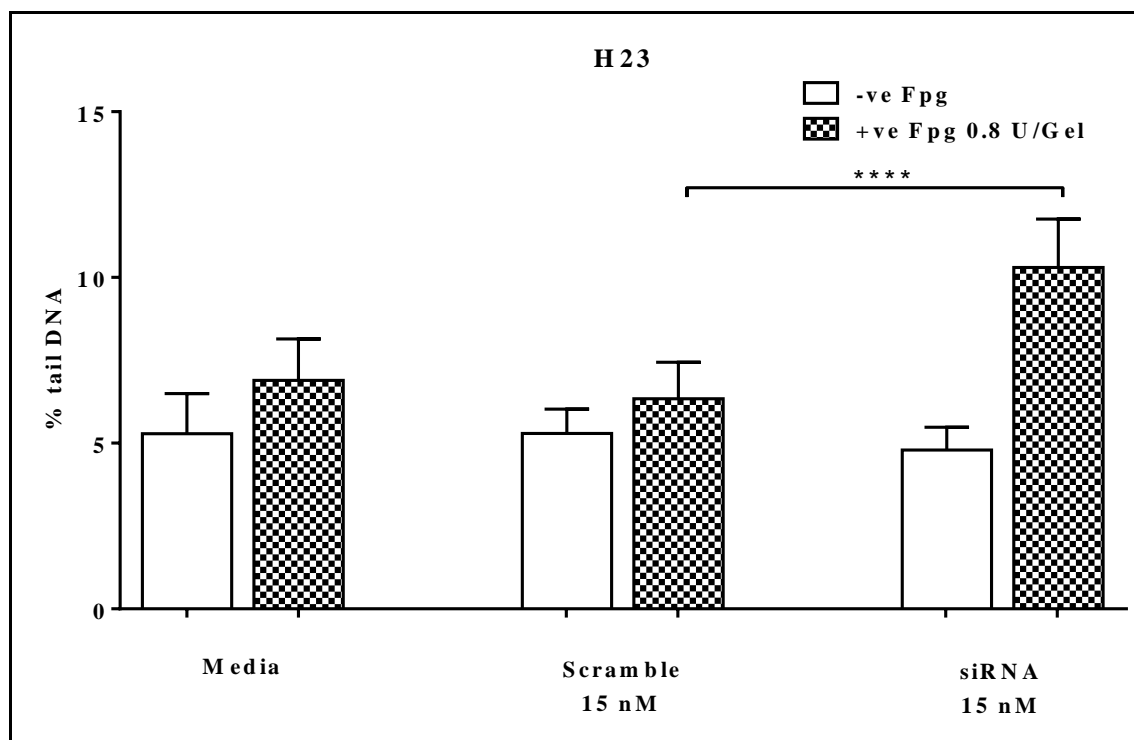


Figure 4-1 NUDT1 knockdown significantly increases Fpg sensitive sites of oxidised DNA bases within H23 cells.

Fpg-modified alkaline comet assay was applied to determine DNA damage levels in individual H23 cells after transfection for 4 days in total with 15 nM NUDT1 siRNA or silencer select -ve control siRNA (Scramble), or those grown in media without transfection reagent/siRNA. DNA damage levels were expressed as % tail DNA with [] or without [] Fpg repair enzyme treatment. These results represent mean \pm SD of eight independent experiments; at which 200 individual comets were scored for each sample to determine the experiment mean value. Asterisks indicate a significant difference relative to corresponding scrambled siRNA control (****P<0.0001).

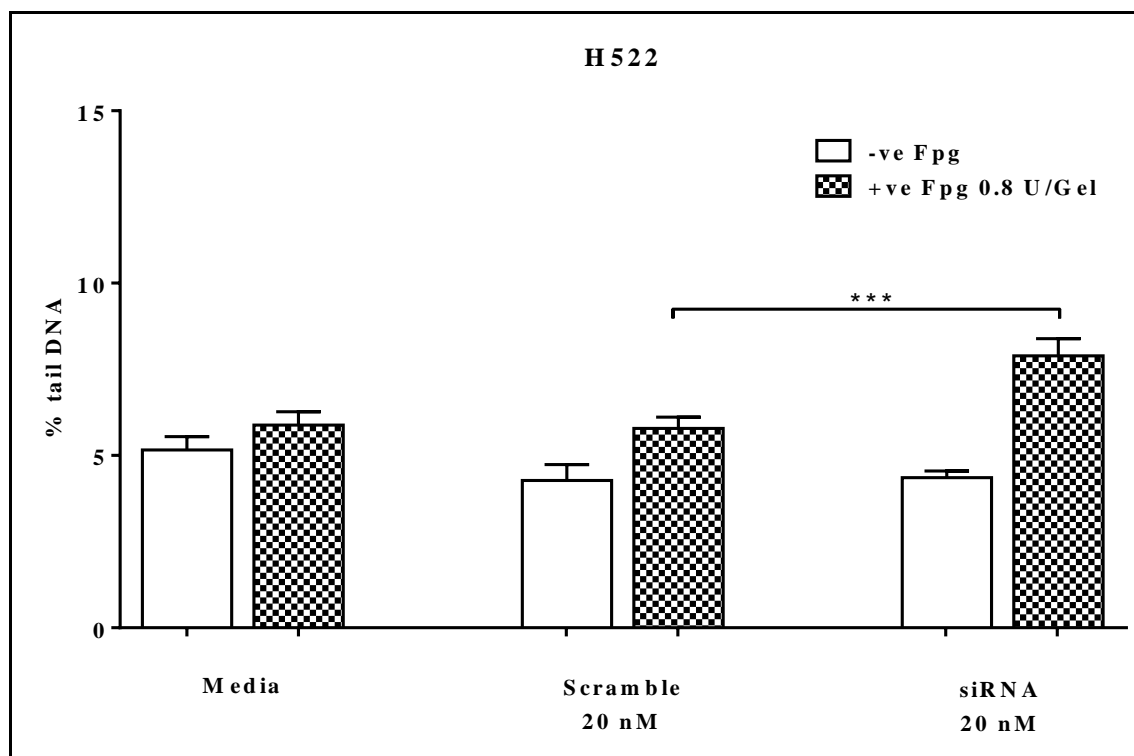


Figure 4-2 NUDT1 knockdown significantly increases Fpg sensitive sites of oxidised DNA bases within H522 cells.

Fpg-modified alkaline comet assay was applied to determine DNA damage levels in individual H522 cells after transfection for 4 days in total with 20 nM NUDT1 siRNA or silencer select -ve control siRNA (Scramble), or those grown in media without transfection reagent/siRNA. DNA damage levels were expressed as % tail DNA with [] or without [] Fpg repair enzyme treatment. These results represent mean \pm SD of four independent experiments; at which 200 individual comets were scored for each sample to determine the experiment mean value. Asterisks indicate a significant difference relative to corresponding scrambled siRNA control (***) $P < 0.001$.

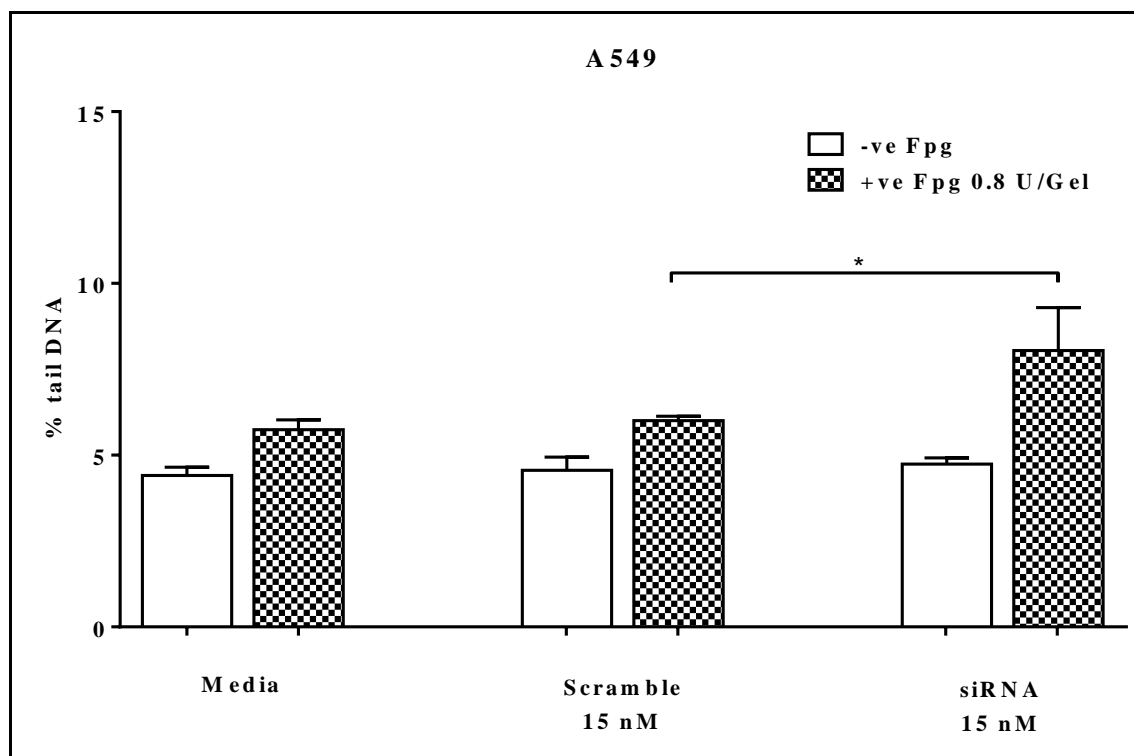


Figure 4-3 NUDT1 knockdown significantly increases Fpg sensitive sites of oxidised DNA bases within A549 cells.

Fpg-modified alkaline comet assay was applied to determine DNA damage levels in individual A549 cells after transfection for 4 days in total with 15 nM NUDT1 siRNA or silencer select -ve control siRNA (Scramble), or those grown in media without transfection reagent/siRNA. DNA damage levels were expressed as % tail DNA with [] or without [] Fpg repair enzyme treatment. These results represent mean \pm SD of three independent experiments; at which 200 individual comets were scored for each sample to determine the experiment mean value. Asterisks indicate a significant difference relative to corresponding scrambled siRNA control (* $P < 0.05$).

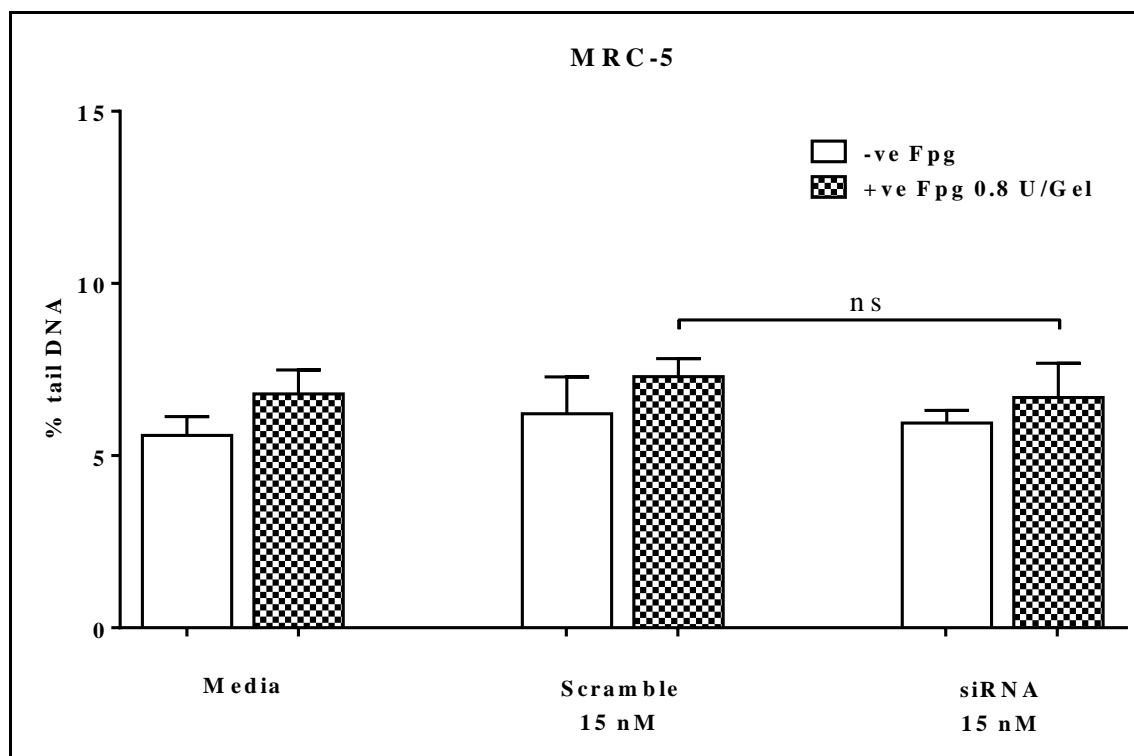


Figure 4-4 NUDT1 knockdown in MRC-5 cells does not lead to alteration level in Fpg sensitive sites of oxidised DNA bases

Fpg-modified alkaline comet assay was applied to determine DNA damage levels in individual MRC-5 cells after transfection for 4 days in total with 15 nM NUDT1 siRNA or silencer select -ve control siRNA (Scramble), or those grown in media without transfection reagent/siRNA. DNA damage levels were expressed as % tail DNA with [] or without [] Fpg repair enzyme treatment. These results represent mean \pm SD of three independent experiments; at which 200 individual comets were scored for each sample to determine the experiment mean value. No significant difference was observed relative to corresponding scrambled siRNA control (ns).

4.3 Endogenous ROS levels of NSCLC lines relative to MRC-5 cells

Given that the possible NUDT1 requirement in cancerous cells is suggested to occur due to high oxidative stress condition relative to normal cells (Gad et al 2014), the endogenous ROS level was assessed for different cell lines (H23, H522, A549, and MRC-5). Accordingly, the ROS detecting H2DCF-DA fluorescent probe was used alone with microplate reader for the measurement of samples relative fluorescence intensity. Treatment of the cells with freshly prepared H₂O₂ (9.8 mM) at room temperature was considered as a positive control. Here, 30,000 cells per well were chosen as the cell density required to reveal the level of intracellular ROS. Blank samples without seeded cells were also included.

As shown in Figure 4-5, despite H522 exhibiting lower ROS levels, the intracellular background ROS productions were similar for all of the cell lines, at a mean level around 25 relative fluorescence units. In addition, no significant changes have occurred within the panel of NSCLC (H23, H522, and A549) and also between normal human lung fibroblast (MRC-5). This finding is concordant with that being observed when no significant alteration occurs between any of the tested cell lines regarding the levels of endogenous DNA oxidation as well as SSBs (Figures 4-1, 4-2, 4-3, and 4-4). This indicates that NUDT1 requirement in NSCLC cells to protect against high oxidatively damaged DNA levels is not simply attributed to ROS levels and, perhaps, there is another basis for the cancer-specificity.

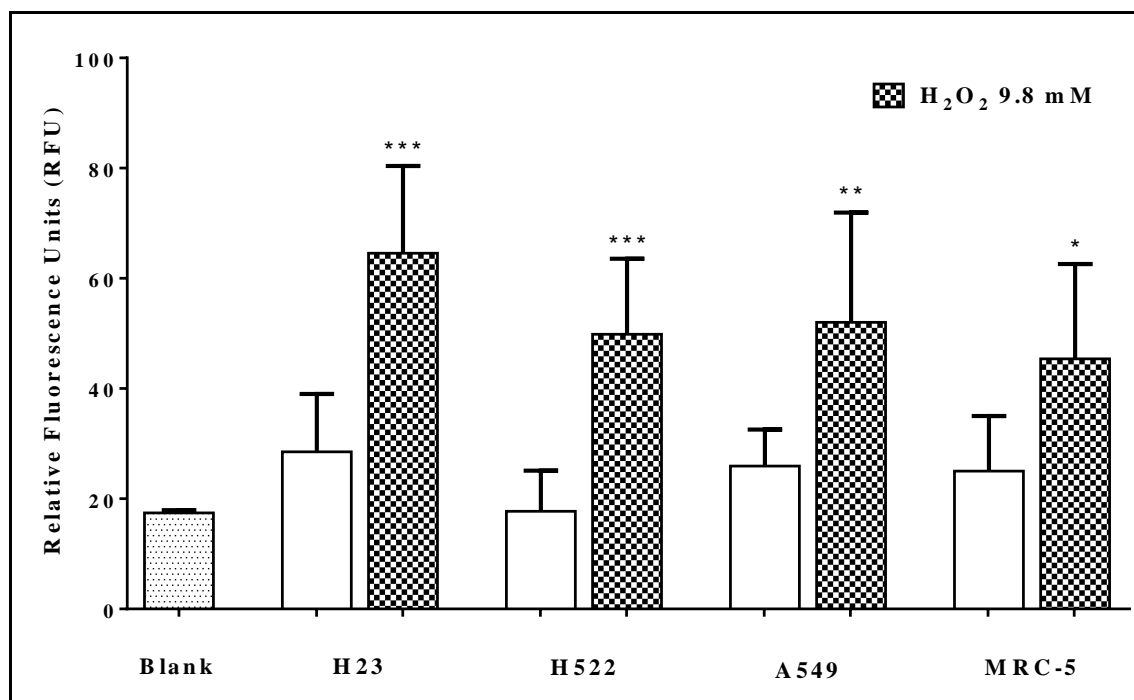


Figure 4-5 NSCLC cell lines generate endogenous ROS at levels similar to MRC-5 cells.

The endogenous background ROS levels were determined by measuring fluorescence signal induced by oxidation of non-fluorescent probe 2',7'-dichlorodihydrofluorescein diacetate (H₂DCF-DA), and expressed as relative fluorescence units (RFU). Pre-treatment of cells with 9.8 mM H₂O₂ was used as a positive control. Blank samples without seeded cells were also included. These results represent mean \pm SD of four independent experiments. Asterisks indicate a significant difference in H₂O₂-treated cells relative to corresponding untreated samples (***P<0.001, **P<0.01 and *P<0.05).

4.4 DNA damage response following NUDT1 knockdown

Here, it is proposed that the increase amounts of oxidised bases misincorporation due to NUDT1 depletion may lead to DNA replication stress in NSCLC cell lines, whereas normal cells would persist stable at the genomic level. The core mediator kinases in the DNA-replication-associated DDR are mainly ATR and ATM, which in turn activated in discrete pathways as a response to the existence of specific DNA damage (Marechal and Zou, 2013). By this mean, if the oxidatively damage DNA present in NUDT1 deficient NSCLC cells leads to the induction of DNA replication fork stalling and single-stranded DNA formation, it would be expected that ATR-Chk1 activation mainly occurs, whereas DSBs induction would cause ATM-Chk2 activation. However, it is worth to mention that an overlap between the roles for ATM and ATR could occur as ATM activation at DSBs can afterward lead to ATR activation if they are resected to

produce ssDNA overhangs (Shiotani and Zou, 2009), and processing of ATR-activating defective stalled forks can generate one-ended DSBs that subsequently activates ATM (Hanada et al., 2007).

Therefore, in this study as markers of induction of DDR signaling, the expression level of pChk2/pChk1 by Western blotting was assessed in the panel of NSCLC cell lines, as well as, normal human lung fibroblast following an efficient and transient knockdown of NUDT1 enzyme.

Treated cells with hydroxyurea (2 mM), etoposide or phleomycin (25 µg/ml) for 2 h at 37°C were considered as positive controls. Phleomycin is regarded as glycopeptide antibiotics similar to bleomycin could produce single or double-strands DNA breaks. Consequently, it can block the entry into S-phase of the cell cycle (He et al., 1996). Etoposide is a semisynthetic antimitotic agent and its cytotoxicity is initiated by affecting the cell-cycle regulated protein-DNA topoisomerase II (Calderon-Montano et al., 2014). In addition, hydroxyurea can stall replication fork progression, by inhibiting RNR enzyme via scavenged tyrosyl free radicals to decrease the production of deoxyribonucleotides (Cerqueira et al., 2007).

In addition, here, the cells were transfected with the optimal concentration of NUDT1 siRNA (s9030) in order to achieve an effective knockdown up to 4 days, and confirmed by Western blot as mentioned above. Silencer select -ve control siRNA (Scramble) along with mock transfection samples (media without siRNA and transfection reagent) were also processed after harvesting the cell lysates.

As shown in Figure 4-6, there was an approximate two-fold upregulation in the expression of phospho-Chk2 (Thr 68) for H522 cells after 4 days of NUDT1 protein depletion, relative to corresponding media without transfection reagent or scrambled samples. This might indicate the existence of DSBs and ATM activation. Such Chk2 phosphorylation at Thr68 was not detected in other cell lines, while increased levels noticed in topoisomerase II inhibitor (etoposide) and phleomycin treated cells as a positive control.

In addition, no evident change occurs in the expressions of phospho-Chk1 (Ser 345 or Ser 317) following 4 days of siRNA-mediated NUDT1 knockdown in all indicated cell lines, as seen by using etoposide and hydroxyurea exposure control samples (Figure 4-

7). However, Chk1 (2G1D5) recognizing an endogenous expression level of total Chk1 protein, was decreased after A549 and H23 cells transfected with NUDT1 siRNA during the same time interval relative to scrambled and no siRNA control. The exact basis for such down regulation of total Chk1 is not so evident. This might suggest an increase in DNA replication stress levels for NUDT1-deficient H23 and A549 cells, but that a selective pressure occurs in a way to quickly adapt and suppress the associated ATR-Chk1 activity in order to overwhelm growth arrest and allow the cells to continue their proliferation. Interestingly, MRC-5 cells did not display total Chk1 (2G1D5) protein in any verified cell samples (Figure 4-7), indicating to some extent a substantial defect in the expression of Chk1 of this cell line stock which, as far as we know, has not been described before. Thus, the above findings point to the alteration in DDR cascades in NSCLC cells lines after NUDT1 deficiency, suggesting a cellular response to some kind of secondary DNA damage. However, it is surprising that the affected DDR signaling pathways varied in different NSCLC cell lines with either activation or repression pattern.

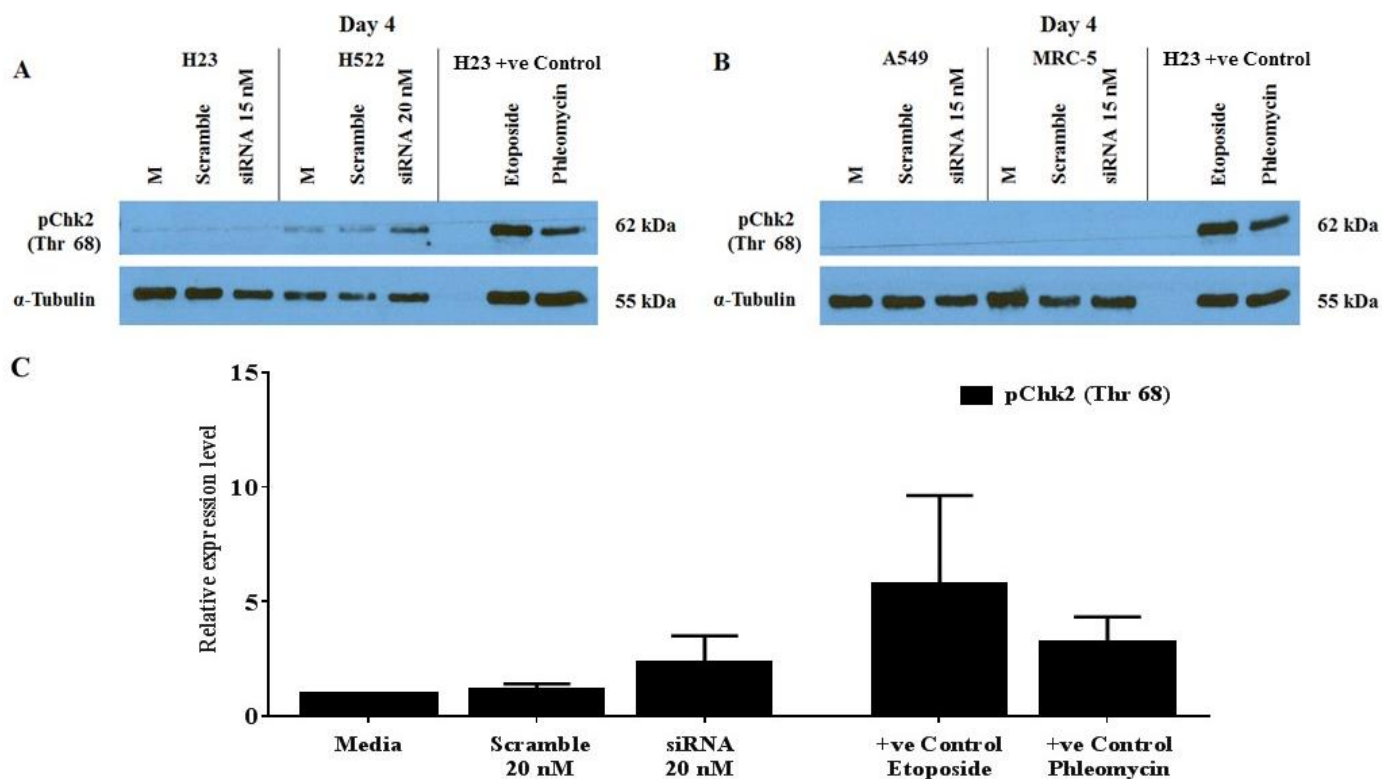


Figure 4-6 Alteration in phospho-Chk2 expression level 4 days after NUDT1 siRNA transfection in NSCLC cell lines.

Western blots were applied to determine phospho-Chk2 (Thr 68) expression levels. The cells were grown in media (M) without transfection reagent/siRNA, or transfected for 4 days in total with NUDT1 siRNA (s9030) (20 or 15 nM for H522 and other indicated cell lines, respectively), or silencer select -ve control siRNA (Scramble). Positive (+ve) control samples were H23 cells treated with etoposide (25 μ g/ml) or phleomycin (25 μ g/ml) at 37°C for 2 h. Subsequently, the collected cell lysate proteins were subjected to Western blotting with the indicated antibodies. [A] Representative Western blot on day 4 for H23 and H522 cell line. [B] Representative Western blot on day 4 for A549, and MRC-5 cell lines. [C] Western blot band intensities of pChk2 (Thr 68) were initially quantitated, normalized with the corresponding loading control α -Tubulin, and then established relative to the corresponding band of media without transfection reagent nor siRNA (n=3).

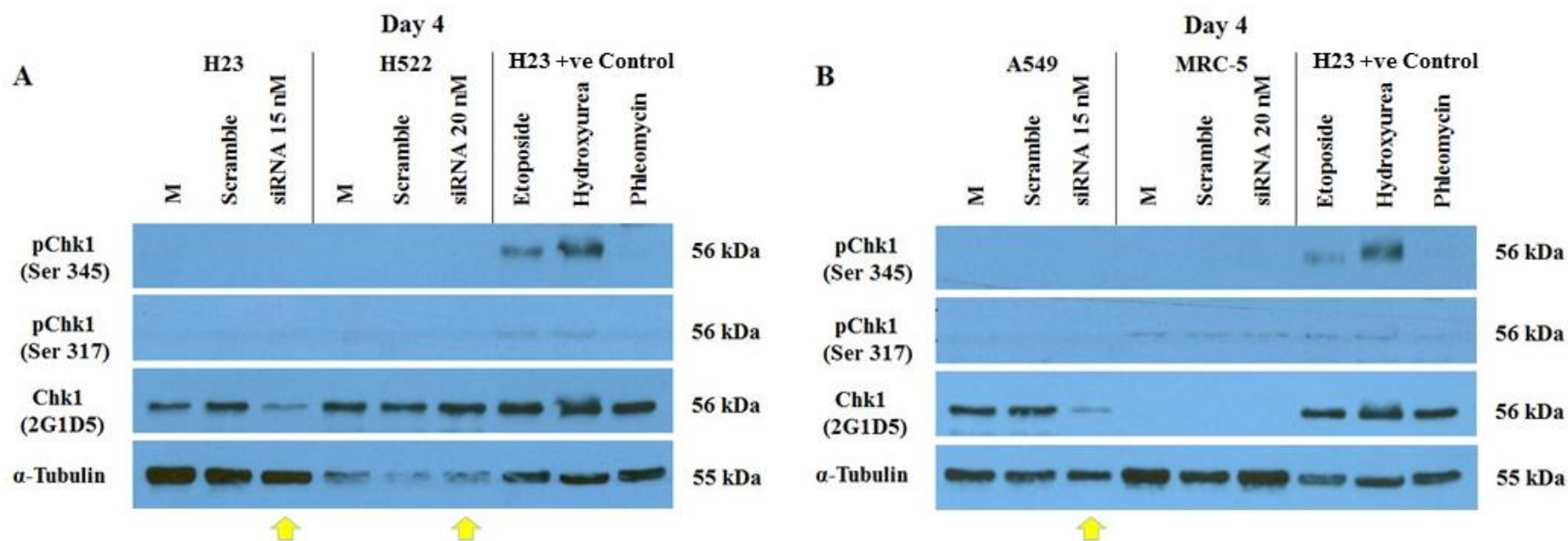


Figure 4-7 Alteration in total Chk1 expression level 4 days after NUDT1 siRNA transfection in NSCLC cell lines.

The cells were grown in media (M) without transfection reagent/siRNA, or transfected for 4 days in total with [👉] NUDT1 siRNA (s9030) (20 or 15 nM for H522 and other indicated cell lines, respectively), or silencer select -ve control siRNA (Scramble). Positive (+ve) control samples were H23 cells treated with etoposide (25 μ g/ml), phleomycin (25 μ g/ml) or hydroxyurea (2 mM) at 37°C for 2 h. Subsequently, the collected cell lysate proteins were subjected to Western blotting with phospho-Chk1 (pChk1 Ser 345 or Ser 317), total Chk1 (2G1D5) and loading control α -Tubulin antibodies. Representative Western blots on day 4 for [A] H23 and H522, or [B] A549 and MRC-5 cell lines (n=3).

4.5 Assessment of NUDT1 knockdown-induced apoptosis

Earlier studies suggest that NUDT1 deficiency is cytotoxic to different cancer cell lines in a selective manner (Gad et al 2014). Additionally, given that it was observed in previous sections accumulations of genomic oxidatively damaged DNA (Figures 4-1, 4-2, and 4-3) and evidence of secondary types of DNA damage (Figures 4-6, and 4-7) in all of the NSCLC cell lines after NUDT1 deficit, this firmly strengthened the notion that NUDT1 in NSCLC would be regarded as ‘conditionally essential’ enzyme. To examine this view, it was assessed whether targeting NUDT1 could induce apoptosis in the panel of NSCLC cell lines (H23, H522, and A549) relative to MRC-5 normal cell control. Here, early and late apoptotic cell fractions were determined by Annexin V-FITC / PI dual staining and then analysed using flow cytometry.

In order to achieve an efficient passive knockdown of NUDT1 up to 4 days, the cells were transfected with optimal concentrations of NUDT1 siRNA (s9030). In every experiment, silencer select -ve control siRNA (Scramble) along with mock transfection samples (media without siRNA and transfection reagent) were usually processed. Furthermore, etoposide (VP-16) at concentrations of 50-150 μ M for 24 h act as a positive control of apoptosis, and DMSO (0.5-1.5% v/v) treated samples were also included.

The reciprocal results of early and late apoptotic cells obtained following the NUDT1 knockdown are shown in Figures 4-8, 4-9, 4-10, and 4-11. For H23, etoposide (dissolved in DMSO, a final concentration of DMSO is 0.5% v/v) was chosen as a positive control for induction of apoptosis. Here, as shown in Figure 4-8, exposure to 50 μ M etoposide for 24 h exhibit 42.8% apoptotic cells, which was significantly higher than apoptotic cell fractions in untreated (4.6%) and cells treated with 0.5% v/v DMSO (5.1%) (P-value < 0.0001). In addition, it was noted that the apoptotic fractions rise almost two-fold in both scrambled (12.1%) and NUDT 1 knockdown transfected (10.9%) samples relative to corresponding untreated control cells.

For H522, exposure to etoposide (dissolved in DMSO, a final concentration of DMSO is 0.5-1.5% v/v), was introduced as a positive control for induction of apoptosis. No notable effect was observed for 48 h after 50 and 100 μ M etoposide treatment (data not shown), whereas, the percentage of apoptotic cells following 150 μ M etoposide for 24 h was 25.1%; significantly higher than untreated (2.6%) and treated cells with 1.5% v/v

DMSO (3.5%) (P-value < 0.0001, Figure 4-9). Therefore, the low responsiveness of H522 cells to etoposide was noticed with higher required dose exposure. Similar to H23 cells, H522 possessed three times higher percentage of early and late apoptotic cells in both scrambled (10.4%) and NUDT1 knockdown transfected (9.5%) samples relative to corresponding untreated control cells.

The above results suggest that (H23 and H522) cells are sensitive to sample transfection process with less viable cells relative to corresponding mock transfection control. However, as criteria for better transfection, the cell viability was still greater than 80% following the transfection of both scrambled and NUDT1 transfected samples. Thus, indeed, the above relative increase in apoptotic death levels did not relate to NUDT1 knockdown.

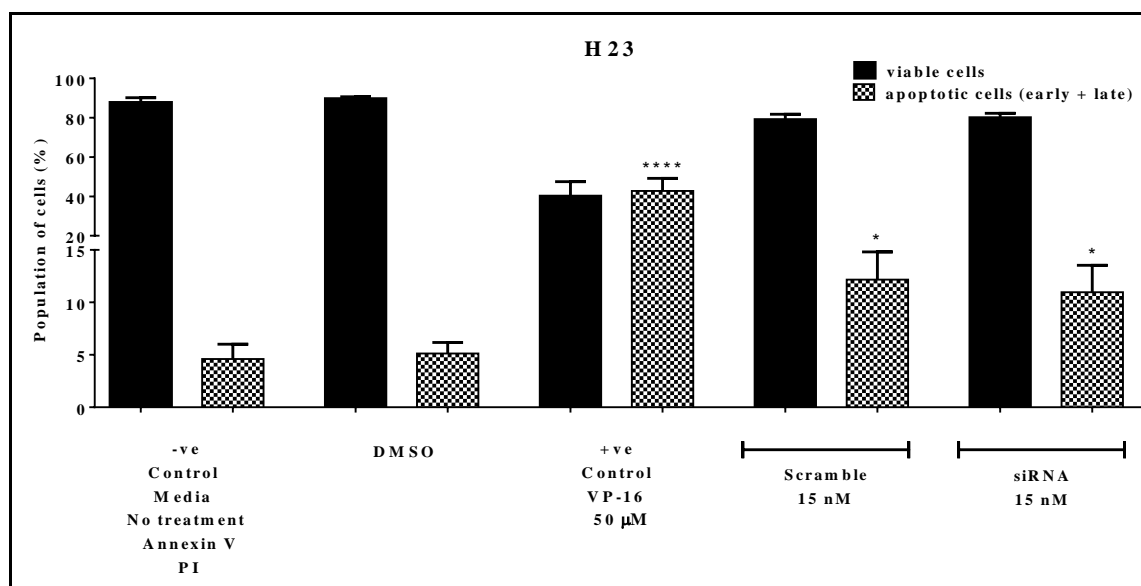


Figure 4-8 Transient NUDT1 knockdown does not enhance apoptotic death in H23 non-small-cell-lung cancer cells.

Annexin V–FITC/PI assay was applied to determine apoptotic cell deaths. H23 cells were grown in media without transfection reagent/siRNA, or transfected for 4 days in total with 15 nM NUDT1 siRNA or silencer select -ve control siRNA (Scramble). DMSO (0.5% v/v) and etoposide (VP-16); as a positive control of apoptosis; for 48 h were also applied. The harvested cells were then dual stained with annexin V-FITC/PI and assessed by flow cytometry. The shaded bars of detected apoptotic cells represent the result during both early and late apoptosis. These data were mean \pm SD of three individual experiments. Asterisks indicate a significant difference relative to corresponding control cells without transfection (****P<0.0001, *P<0.05).

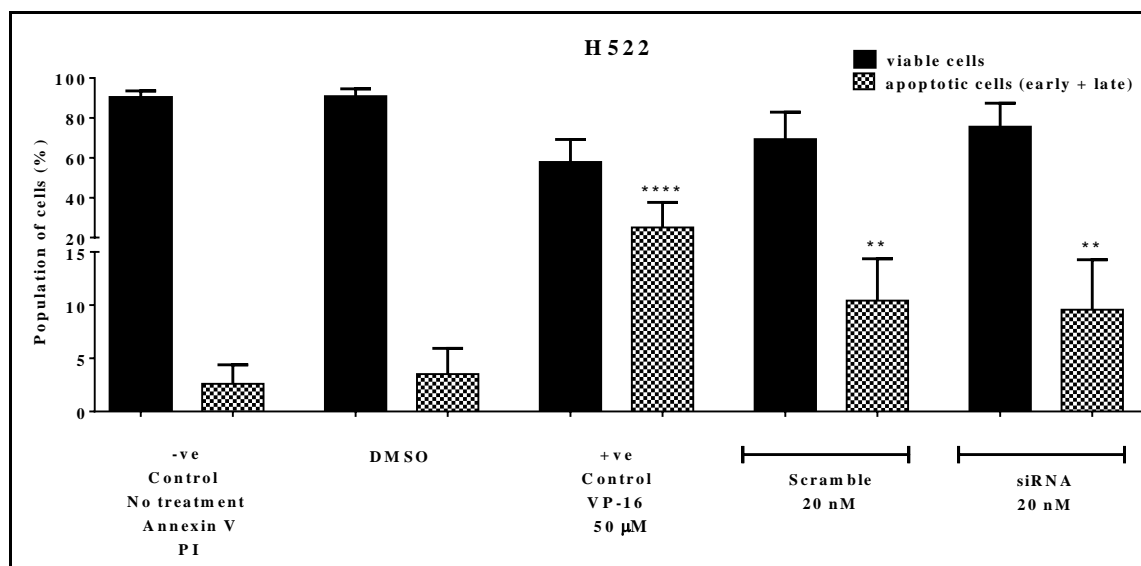


Figure 4-9 Transient NUDT1 knockdown does not enhance apoptotic death in H522 non-small-cell-lung cancer cells.

Annexin V–FITC/PI assay was applied to determine apoptotic cell deaths. H522 cells were grown in media without transfection reagent/siRNA, or transfected for 4 days in total with 20 nM NUDT1 siRNA or silencer select -ve control siRNA (Scramble). DMSO (1.5% v/v) and etoposide (VP-16); as a positive control of apoptosis; for 48 h were also applied. The harvested cells were then dual stained with annexin V-FITC/PI and assessed by flow cytometry. The shaded bars of detected apoptotic cells represent the result during both early and late apoptosis. These data were mean \pm SD of four individual experiments. Asterisks indicate a significant difference relative to corresponding control cells without transfection (**** P <0.0001, ** P <0.01).

As shown in Figure 4-10, A549, another NSCLC cell line with competent p53, displayed 34.5% early and late apoptotic cells after treatment with 50 μ M etoposide (dissolved in DMSO, a final concentration of DMSO is 0.5% v/v), as a positive control for 24 h. In addition, no significant change occurred in cell death pattern (apoptotic fractions) after both NUDT1 knockdown and silencer select -ve control siRNA (Scramble) transfected samples compared to corresponding untransfected control cells (P -value > 0.05).

A similar result was also observed for the MRC-5 cell, with no clear alteration in apoptotic cell death levels after 4 days of efficient delivery of NUDT1 siRNA and/or silencer select -ve control (Figure 4-11). As a positive control of apoptosis, 100 μ M etoposide (dissolved in DMSO, a final concentration of DMSO is 1% v/v) was applied for 24 h, showing a significant increase in apoptotic cell levels (P -value <0.01).

Overall, successfully transient NUDT1 knockdown for 4 days did not increase apoptosis levels in any of the normal and NSCLC cells relative to the scrambled siRNA controls, no matter the p53-status of the cell line. This raises the possibility that NUDT1 is not regarded as ‘conditionally essential’ in NSCLC. This observation contradicts previous suggestions that NUDT1 is potentially a highly effective therapeutic target (Helleday, 2014). Additionally, earlier reported data suggested dramatic drop in cell proliferation within 4 days in NUDT1-deficient A549 cells (wild-type p53) via cell counting with hemocytometer, which is also accompanied by elevation in senescence associated beta-galactosidase (SA-beta-gal) activity, whereas the stable NUDT1 knockdown of H23 (mutant p53) and H358 (p53 null) cells exhibited a lesser decrease in cell proliferation levels than A549 cells, but still significant, without upregulation of SA-beta-gal activity nor G1/S arrest (Patel et al., 2015). Despite all tested cell lines used in that previous study (Patel et al., 2015) have a negligible cell death outcomes upon shNUDT1 transduction which is consistent with our results, the notable reduction of NUDT1-deficient A549 cell proliferation was proposed to be due to p53 activity. Therefore, further experiments were performed to assess if NUDT1 was required for NSCLC cell proliferation.

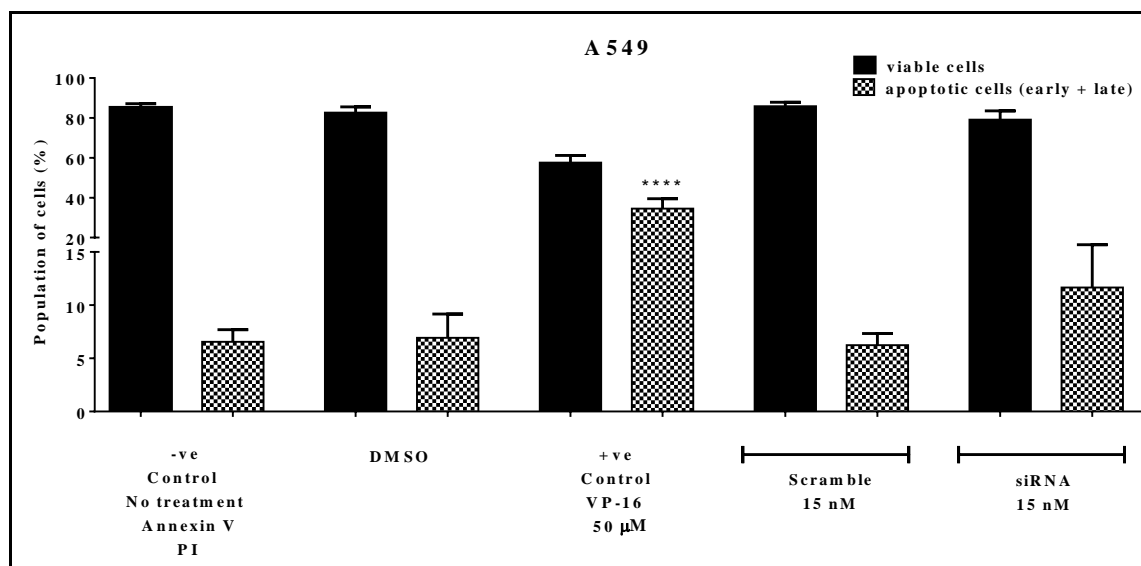


Figure 4-10 Transient NUDT1 knockdown does not enhance apoptotic death in A549 non-small-cell-lung cancer cells.

Annexin V–FITC/PI assay was applied to determine apoptotic cell deaths. A549 cells were grown in media without transfection reagent/siRNA, or transfected for 4 days in total with 15 nM NUDT1 siRNA or silencer select -ve control siRNA (Scramble). DMSO (0.5% v/v) and etoposide (VP-16); as a positive control of apoptosis; for 48 h were also applied. The harvested cells were then dual stained with annexin V-FITC/PI and assessed by flow cytometry. The shaded bars of detected apoptotic cells represent the result during both early and late apoptosis. These data were mean \pm SD of three individual experiments. Asterisks indicate a significant difference relative to corresponding control cells without transfection (****P<0.0001).

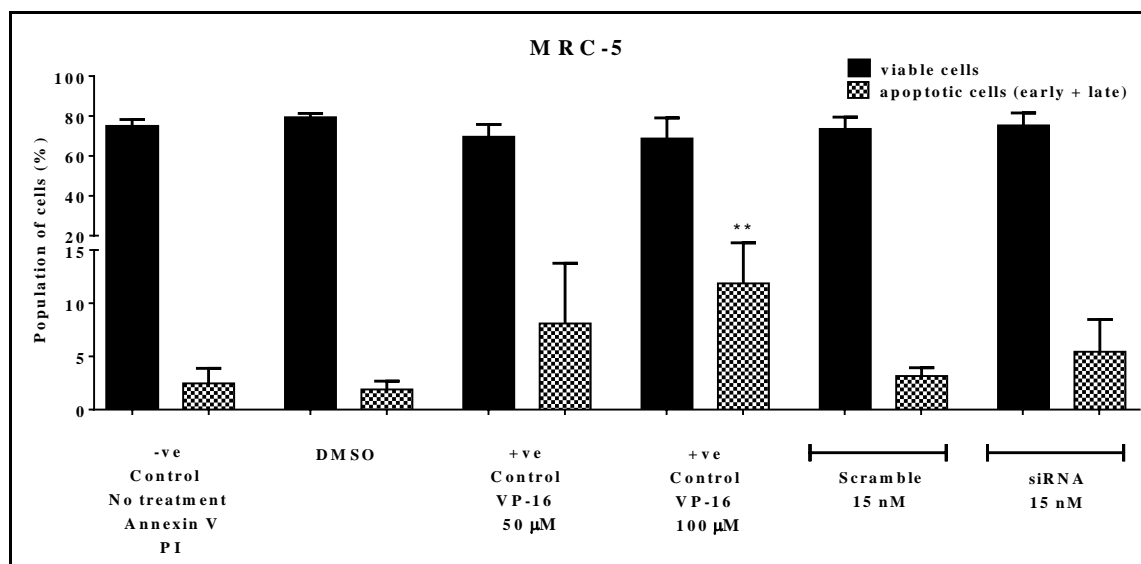


Figure 4-11 Transient NUDT1 knockdown does not enhance apoptotic death in normal human lung fibroblast cell line (MRC-5 cells).

Annexin V–FITC/PI assay was applied to determine apoptotic cell deaths. MRC-5 cells were grown in media without transfection reagent/siRNA, or transfected for 4 days in total with 15 nM NUDT1 siRNA or silencer select -ve control siRNA (Scramble). DMSO (0.5-1% v/v) and etoposide (VP-16); as a positive control of apoptosis; for 48 h were also applied. The harvested cells were then dual stained with annexin V-FITC/PI and assessed by flow cytometry. The shaded bars of detected apoptotic cells represent the result during both early and late apoptosis. These data were mean \pm SD of four individual experiments. Asterisks indicate a significant difference relative to corresponding control cells without transfection (**P<0.01).

4.6 Assessment of cellular viability following NUDT1 deficiency in NSCLC cell lines

Earlier studies propose the selective cytotoxicity following NUDT1 deficiency to various cancerous cell line (Gad et al., 2014, Patel et al., 2015). In addition, as observed in previous sections, there are increased levels of genomic DNA base oxidation and evidence of secondary types of DNA damage in the indicated NSCLC cell lines after NUDT1 deficit, although did not manifest an induction in term of apoptosis. Thereby, it is focused to detect whether targeting NUDT1 could influence NSCLC cell proliferation relative to MRC-5 normal cell control. To achieve this, transient knockdown of NUDT1 was obtained for 5 days in total and WST-1 assay, quantifying the metabolic activity of the cell culture, was then used to determine such relative cell proliferation.

Herein, to attain an efficient passive knockdown of NUDT1 up to 5 days, the cells were transfected with optimal concentrations of NUDT1 siRNA (s9030). In every experiment, silencer select -ve control siRNA (Scramble siRNA) along with mock transfection samples (media without siRNA and transfection reagent) were processed. Furthermore, treatment with etoposide (VP-16) at concentrations of 100-150 μ M for 48 h act as a positive control of growth inhibition. In this project, preliminary experiments were carried out to determine appropriate cell densities seeded for each cell line in 96-well plates, as well as, a series of cells incubation (between 30 min-4 h) in the presence of WST-1 reagent before reading samples absorbance. The absorbance values that ranged between (0.5-1.8) were considered as appropriate measures; regarding cell seeding density and incubation time period (Figures 8-1, 8-2, 8-3, and 8-4). For H23, A549, and MRC-5 cell lines, Cell density (1×10^4) per well were considered as well as an incubation time with a WST-1 reagent for (3 h or 30 min), respectively, before measuring the plate absorbance. However, higher sensitivity was achieved for H522 cells when seeded at 2×10^4 cell concentration instead and incubated for 1 h with the WST-1 reagent in 96- well plates.

The data for H23 adenocarcinoma cells (p53-mutated) in Figure 4-12, showed that transient NUDT1 knockdown for 5 days induced a 45.62% decrease in cell proliferation relative to untransfected control samples (P-value <0.0001). A reduction in cell proliferation was also noticed in siRNA scrambled samples (79.6%) (P-value > 0.05),

suggesting that H23 cells are sensitive to sample transfection process with less cell proliferation. Furthermore, 48 h treatment with etoposide (VP-16) at 100 and 150 μM suppressed the rate of cell proliferation to 32.81% and 43.32%, respectively, as a positive control (P-value <0.0001).

However, as shown in Figures 4-13, 4-14, and 4-15, 5 days after NUDT1 deficiency had no effect upon A549, H522 and MRC-5 cells proliferation relative to mock transfection and the scrambled controls. In H522 cells, another NSCLC cell line with mutated p53, using etoposide (VP-16) as a positive control dropped the cellular proliferation to 29.46% after exposure to 150 μM dose for 48 h (P-value <0.001) (Figure 4-13). Despite the decline in cellular proliferation for both siRNA scrambled (69.81%) and NUDT1 siRNA (82.19%) transfected samples, this did not lead to significant difference in comparison to corresponding untransfected control cells (P-value > 0.05). The sensitivity to sample transfection process might also be considered, by this way, but it is clear that NUDT1 knockdown did not induce growth inhibition.

For NUDT1-deficient A549 cells (wild-type p53), the percentage of proliferating cells remained approximately (106.58%) compared to untransfected (100%) and scrambled (106.76%) control, even 5 days' incubation period time following NUDT1 depletion (P-value > 0.05) (Figure 4-14). Furthermore, as a positive control, treatment of A549 cells with 100 and 150 μM etoposide for 48 h displayed 53.29% and 40.98% reduction in cellular proliferative capacity, respectively (P-value <0.01, and <0.001, respectively).

A similar result was also observed for MRC-5 normal cells, without an apparent alteration of cellular proliferation levels after 5 days of efficient delivery of NUDT1 siRNA (103.15%) and/or scrambled siRNA of silencer select -ve control (99.97%) (P-value > 0.05) (Figure 4-15). Treatment of MRC-5 cells with etoposide (VP-16) at 150 μM was applied for 48 h, showing a nearly two-fold significant decrease in relative cell proliferation (35.7%), as a positive control (P-value <0.0001). Thus, to some extent, these findings were contrary to previous data (Patel et al., 2015), especially for NUDT1-deficient A549 cells which showed a complete proliferative arrest (in G1/S). However, here, they did not exhibit any change in cell proliferation capacity when using WST-1 assay to measure metabolic activity of the cell culture.

Collectively, apart from a partial requirement for H23 cell proliferation, NUDT1 is ultimately not essential for cell viability and/or proliferation in any NSCLC no matter of the p53-status of the cell lines.

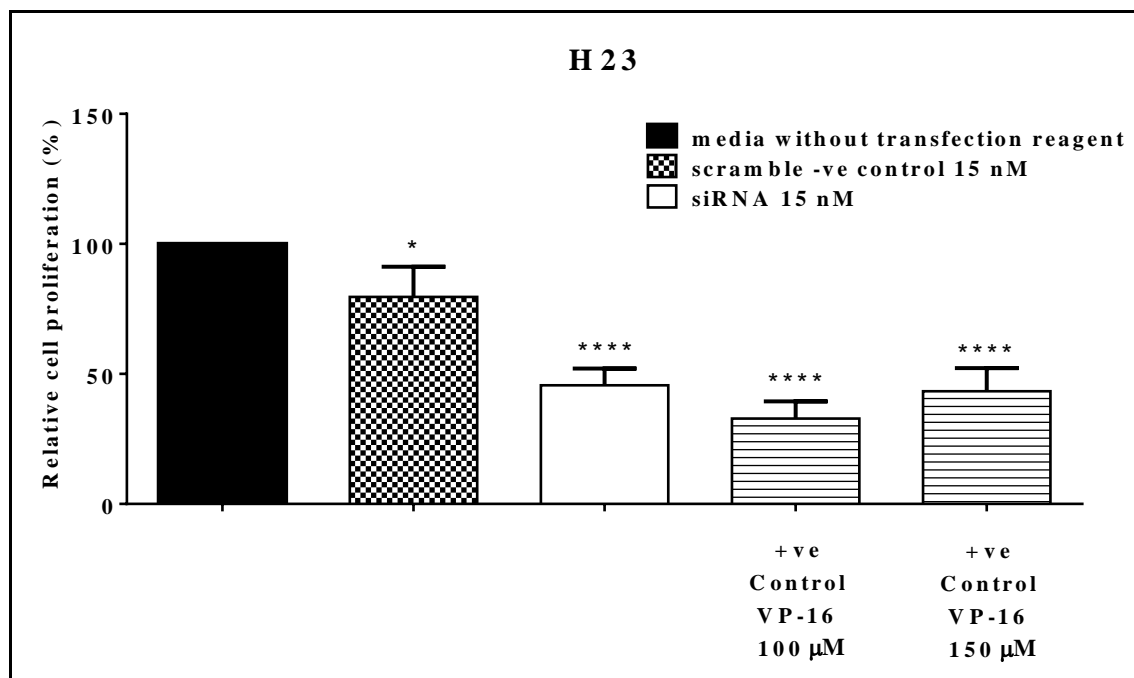


Figure 4-12 Transient NUDT1 knockdown reduces cell proliferation in H23 non-small-cell-lung cancer cells.

WST-1 assay was applied to determine cell viability. H23 cells were grown in media without transfection reagent or transfected for 5 days in total with either 15 nM NUDT1 siRNA or silencer select -ve control siRNA (scramble). Two days after transfection, 1×10^4 cells per well were seeded overnight in triplicate in 96-well plates and then the cells continue growing in appropriate culture media for the remaining time. Etoposide (VP-16) (100 and 150 uM) was added on day 3 as a positive control. The samples absorbance were measured 3 h after an addition of WST-1 reagent against a blank control background, using plate reader at 450 nm wavelength. These results represent mean \pm SD of three independent experiments. Asterisks indicate a significant difference relative to corresponding untransfected control cells (**** $P < 0.0001$, * $P < 0.05$).

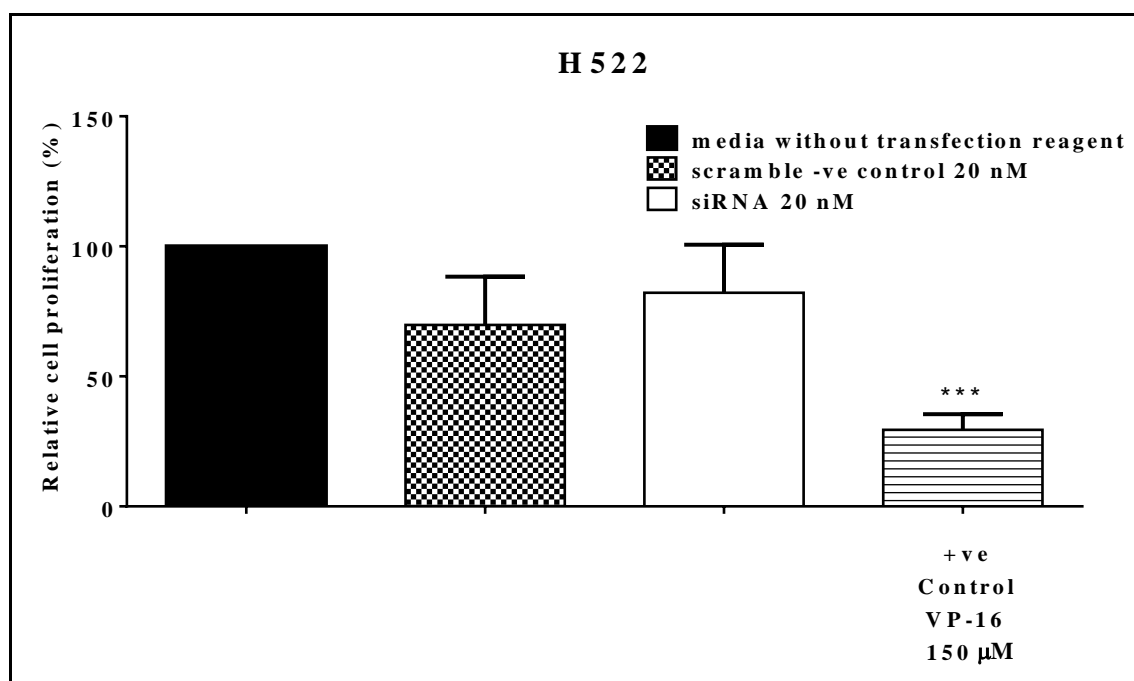


Figure 4-13 Transient NUDT1 knockdown does not reduce cell proliferation in H522 non-small-cell-lung cancer cells.

WST-1 assay was applied to determine cell viability. H522 cells were grown in media without transfection reagent or transfected for 5 days in total with either 20 nM NUDT1 siRNA or silencer select -ve control siRNA (scramble). Two days after transfection, 2×10^4 cells per well were seeded overnight in triplicate in 96-well plates and then the cells continue growing in appropriate culture media for the remaining time. Etoposide (VP-16) (150 μ M) was added on day 3 as a positive control. The samples absorbance were measured 1 h after addition of WST-1 reagent against a blank control background, using plate reader at 450 nm wavelength. These results represent mean \pm SD of three independent experiments. Asterisks indicate a significant difference relative to corresponding untransfected control cells (*** $P < 0.001$).

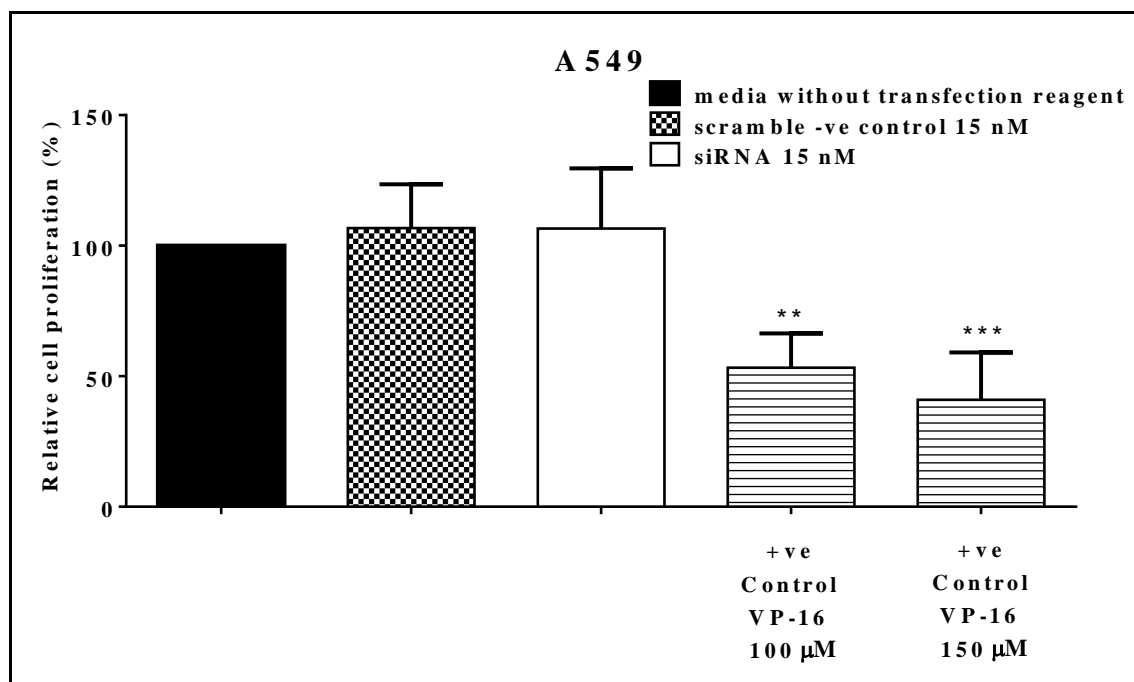


Figure 4-14 Transient NUDT1 knockdown does not reduce cell proliferation in A549 non-small-cell-lung cancer cells.

WST-1 assay was applied to determine cell viability. A549 cells were grown in media without transfection reagent or transfected for 5 days in total with either 15 nM NUDT1 siRNA or silencer select -ve control siRNA (scramble). Two days after transfection, 1×10^4 cells per well were seeded overnight in triplicate in 96-well plates and then the cells continue growing in appropriate culture media for the remaining time. Etoposide (VP-16) (100 and 150 μ M) was added on day 3 as a positive control. The samples absorbance were measured 30 min after addition of WST-1 reagent against a blank control background, using plate reader at 450 nm wavelength. These results represent mean \pm SD of four independent experiments. Asterisks indicate a significant difference relative to corresponding untransfected control cells (*** $P < 0.001$, ** $P < 0.01$).

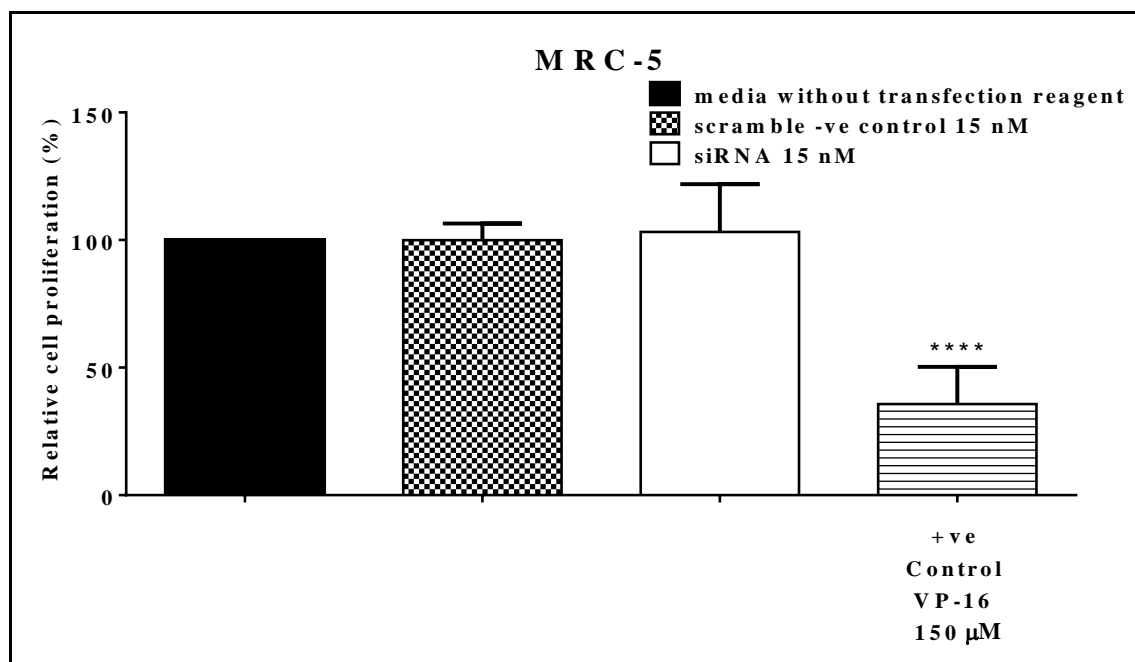


Figure 4-15 Transient NUDT1 knockdown does not reduce cell proliferation in normal human lung fibroblast cell line (MRC-5).

WST-1 assay was applied to determine cell viability. MRC-5 cells were grown in media without transfection reagent or transfected for 5 days in total with either 15 nM NUDT1 siRNA or silencer select -ve control siRNA (scramble). Two days after transfection, 1×10^4 cells per well were seeded overnight in triplicate in 96-well plates and then the cells continue growing in appropriate culture media for the remaining time. Etoposide (VP-16) (150 uM) was added on day 3 as a positive control. The samples absorbance were measured 30 min after addition of WST-1 reagent against a blank control background, using plate reader at 450 nm wavelength. These results represent mean \pm SD of four independent experiments. Asterisks indicate a significant difference relative to corresponding untransfected control cells (**** $P < 0.0001$).

4.7 Discussion

Targeting NUDT1 enzyme is a potentially promising novel approach to selectively kill cancer cells, whereas it is thought to have a non-essential role inside untransformed cells (Gad et al., 2014). However, with contradictory data being reported relating to the impact of NUDT1 deficiency on cancer cell growth, our study aims to shed new light regarding the role of NUDT1 in NSCLC. Here, it is assessed for the first time the effect of NUDT1 knockdown in a panel of NSCLC cell lines relative to normal lung cells, and determined how effective targeting NUDT1 enzyme is as ‘conditionally essential’ therapeutic approach; also assessed the role of p53 in altering such effects. In the previous chapter, it has been shown that NUDT1 siRNA (s9030) can be efficiently delivered to both normal and cancer cells by lipofection with reverse transfection method. To some extent, this transfection system allows suppression of NUDT1 protein in a robust manner.

Upon transfection with NUDT1 siRNA, it does indeed promote 8-oxodG level through increasing the incorporation of 8-oxodGTP into genomic DNA of different NSCLC cell lines, as detected by Fpg modified alkaline comet assay. However, such observation is unlikely to occur in normal human lung fibroblast cells under similar condition. This is consistent with an earlier published findings which show similar enhancement of 8-oxodG incorporation into DNA genome of U2OS human osteosarcoma cells, recognized by OGG1 modified comet assay, albeit to a higher degree (Gad et al., 2014). In the same study, the latter method also disclosed a build-up of 2-OH-dA level detected by using MUTYH repair enzyme. However, a conformational increase in 8-oxodG incorporated into DNA was not possible at that time, using liquid chromatography-mass spectrometry (LC-MSS/MS) due to the broad spectrum of oxidized bases yield during a preparation of samples (Gad et al., 2014).

Despite large agreement with other work regarding the specific requirement that is herein demonstrated for NUDT1 in protecting against the oxidised DNA base misincorporation into the cellular genomes (Gad et al., 2014, Yoshimura et al., 2003, Speina et al., 2005), our modified comet assay results observed no further addition of DNA SSBs or ALS in both normal and NSCLC cells. A similar finding was previously observed after NUDT1-siRNA knockdown of normal fibroblast cells (GM00637), whereas, H₂O₂ exposure sensitized these NUDT1-depleted cells, showing an additional

increase in DNA SSBs compared to control untransfected cells (Youn et al., 2008). To some extent, this suggests NUDT1 is not required unless there is oxidative stress. This is not the case with another reported study at which 4 times cells with intense comet tails (i.e. DNA SSBs or ALS) were observed for human BJ fibroblasts shNUDT1 infected cells (Rai et al., 2009). An induction in DNA SSBs was also stated in U2OS cancer cells following siRNA-mediated NUDT1 depletion and/or other determined selective inhibitors of NUDT1 catalytic activity, such as SCH51344 and (S)-crizotinib (Huber et al., 2014). In U2OS cells, (S)-enantiomer crizotinib could also lead to augmentation in 8-oxoG and 2-OH-A levels identified by modified alkaline comet assay (Huber et al., 2014). It was suggested that the induction of DNA SSBs is attributed to activation of BER system to remove the accumulated 8-oxoGua by DNA glycosylase (Huber et al., 2014). In addition, overexpression of NUDT1 could impair DNA SSBs formation in the cells treated by SCH51344 or (S)-crizotinib, but not by H₂O₂, suggesting NUDT1 as the functional relevant target (Huber et al., 2014). However, here no generation of SSBs nor impact on cell viability were found following siRNA-mediated NUDT1 knockdown in NSCLC. This raises the possibility of a nonspecific effect of the initially (Huber et al., 2014) published siRNA oligonucleotides.

It has been reported that stable NUDT1 modulation through retroviral overexpression or lentiviral small-hairpin RNA was performed in a panel of K-RAS mutated NSCLC cells (H358, H23, A549) with a null, mutated, or wild-type p53 state, respectively. The stable knockdown NUDT1 expression in non-functional p53 cells (H358 or H23) induced decreased cell proliferation, without upregulation of senescence-associated beta-galactosidase activity nor G1/S arrest, whereas, a complete proliferative arrest was observed in A549 after NUDT1 loss (Patel et al., 2015). The latter also underwent persistent DNA DSB gamma-H2AX/53BP1 foci formation which was not the case for H358 and H23 cells. In addition, upon shNUDT1 transduction, all cell lines have a negligible cell death outcome. In accordance with our result, NUDT1 depletion in p53-deficient H358 and H23 cells did not change the extent of DNA strand breaks detected by the alkaline comet assay. However, shNUDT1-transduced A549 cells could induce a significant increase in the percent of total cells displaying long comet tails (Patel et al., 2015). Altogether, our results and that of others strongly supported the view that

NUDT1 is necessary to suppress oxidatively damaged DNA levels specifically in a spectrum of cancer cell types.

The exact basis of such NUDT1 cancer-specific role is unclear. One possible explanation is simply that cancerous cells build-up higher levels of endogenous oxidative stress with subsequent accumulation of oxidised dNTPs within the pool, and that leads to raising the likelihood of oxidised precursor's misincorporation. Despite this, the intracellular ROS levels seem to be similar within the panel of NSCLC cell lines (H23, H522, and A549) and relative to normal human lung fibroblasts (MRC-5). The lack of ROS differences is consistent with finding from another report in which cells with high RAS and NUDT1 overexpression had no change in ROS levels relative to the control cells (Giribaldi et al., 2015). However, it was stated that many cancer types suffer from oxidative stress status as great amounts of H₂O₂ might be produced (Szatrowski and Nathan, 1991, Brautigam et al., 2016). In addition to increase production of ROS, altered redox state has commonly been detected in malignant cells, suggesting that this property can be exploited for treatment benefits (Trachootham et al., 2009). However, as an adaptive mechanism to the endogenous oxidative stress condition, upregulation in cellular antioxidant capacity could occur and confer drug resistance (Trachootham et al., 2009). Therefore, redox modulation to abrogate such drug-resistant mechanisms might have a potential therapeutic approach in cancer (Trachootham et al., 2009).

Depending on the endogenous level of H₂O₂, various cellular responses are observed. this is caused by the requirement for H₂O₂ in several pathways signaling inside the cell as part of a normal cellular homeostatic condition or associated with a defined pathological outcome (Huang et al., 2016). *In vivo* production of H₂O₂ is continuous and maintained in an apparent steady state within normal functioning cells, at which H₂O₂ concentration alters in a time scale slower than its turnover (Antunes and Cadenas, 2001). In addition, it was suggested that H₂O₂ at low level could induce cell survival, proliferation, and differentiation, whereas, it's higher ranges lead to genomic instability, tumorigenesis, and likely eventual cellular death (Huang et al., 2016). The redox environment of cancer cells is distinctive from the healthy corresponding part, representing an essential element to manifest malignant growth and metastasis. In parallel with oncogene (e.g. RAS) redox system, they act together to adjust the cellular metabolism in a way to meet cancer cell demands in order to maintain tumour growth,

spread, and angiogenesis process (Brautigam et al., 2016). However, the cost is an elevation in oxidative pressure upon cancer cell via over activation of NADPH oxidases which ultimately needs the antioxidant systems to be upregulated along with other non-oncogenic addiction enzymes.

Deregulated hypoxic signaling (VHL/HIF1 α axis) in cancer cell could also rise the redox burden pressure (Brautigam et al., 2016). It has been reported that enhancement of oxidative stress status in noncancerous cells by non-alkylating oxidation agents (KBrO₃) could sensitize the cells to the effect of small molecule inhibitor of NUDT1 (TH588). In malignant cells, however, pre-treatment with glutathione precursor (N-acetyl-L-cysteine) or PEG-catalase reduced the oxidative pressure, and that could protect against the inhibitory effect of TH588 exposure, as well as, decrease the incorporation of 8-oxo-dGTP into DNA genome following the inhibition of NUDT1 catalytic enzyme activity by TH588 (Brautigam et al., 2016). To some extent, activation of VHL/HIF1 α axis was commonly observed in several cancers and associated with poor prognosis. It was noticed in zebrafish that ectopic stimulus, to mimic hypoxic signaling by prolyl hydroxylases inhibitor (DMOG), exhibits further dramatic inhibition of embryo viability when combined with TH588, whereas, pre-treatment with N-acetyl-L-cysteine or PEG-catalase for those DMOG-treated zebrafish embryos, has a protective effect against NUDT1 inhibitor (Brautigam et al., 2016). In addition, up to 6 days, no alteration in cellular total ROS level following stable NUDT1 knockdown has previously been observed, whereas, it starts to rise about 11 days after shNUDT1-infected cells as a senescent cellular phenotype state occur (Rai et al., 2009). Acute oxidative stress marker, etheno adducts, and major cellular antioxidant proteins (catalase and superoxide dismutase) were also not changed by such stable knockdown process (Rai et al., 2009). Collectively, it is denoted that the basis of the cancer specificity for NUDT1 expression to protect against oxidatively damaged DNA is not simply attributed to higher ROS levels. Given all the disturbances in genetic burden and signaling cascades within cancerous cells, there may perhaps be other causes for such NUDT1 dependency that are elusive at present.

The rising level of oxidatively damaged DNA in NSCLC cell lines post NUDT1 knockdown was relatively small, about 1.5- to 2-fold increase (Figures 4-1, 4-2, and 4-3). Conversely, the changes in DDR signaling (Figures 4-6, and 4-7) indicate that this was still enough to promote secondary DNA damage, suggesting such slight elevation

is sufficient to disrupt DNA replication. The basis of DNA replication stress induction by oxidised DNA bases that lead to further DNA damage remains uncertain, and more work is still required to interpret these issues.

Interestingly, there was an up-regulation of the expression of pChk2 (Thr 68) after H522 cell knockdown, with a decrease in total Chk1 expression after siRNA-mediated NUDT1 depletion in A549 and H23 cells. Therefore, the type of DDR altered in our experiments between different NSCLC cell lines, with either activated DDR in H522 or DDR inhibition in the other two NSCLC cells.

Chk2 amino-terminal domain consists of seven serine or threonine residues (Ser19, Thr26, Ser28, Ser33, Ser35, Ser50, and Thr68) each of them is followed by glutamine (SQ or TQ cluster domain) which appears to possess a regulatory function. These sites are phosphorylated by ATM/ATR kinases following DNA damage caused by irradiation exposure (ionizing or ultraviolet radiations) or treatment with hydroxyurea (Kastan and Lim, 2000, Matsuoka et al., 2000, Melchionna et al., 2000, Ahn et al., 2000). Residue Thr68 phosphorylation is necessitated for the subsequent step activation, that is attributed to Chk2 autophosphorylation on Thr383 and Thr387 sites in the activation loop of the kinase domain (Lee and Chung, 2001). In our study, the induction of Chk2 phosphorylation in H522 cells (Figure 4-6), perhaps, suggests DNA DSBs formation, thereby activate the ATM/Chk2-mediated pathway.

It was indicated the direct activation of ATM by ROS also occurs in the absence of DNA DSBs and MRN complex, at which disulfide-cross-linked dimers of oxidized ATM was formed and contributed to a cysteine residue in ATM (Guo et al., 2010). However, here, it did not detect any difference in ROS levels between the NSCLC cell lines relative to MRC-5 (Figure 4-5).

Activation of DDR after siRNA-mediated NUDT1 depletion has been previously observed, including activation of RAD51/DNA-PKcs-mediated DSBs repair (homologous recombination/non-homologous end-joining pathways, respectively), ATM-dependent p53 phosphorylation as well as p21 upregulation (Gad et al., 2014). However, Kettle et. al. have seen no effect on DDR markers (p-Ser1981 ATM, p-Ser15 p53) after repeating the above experiment by using the same NUDT1-siRNA oligonucleotide and cell line (U2OS) (Kettle et al., 2016). Stable knockdown by infection with shNUDT1 vector also shown higher cells number containing gamma-

H2AX and 53BP1 foci, which are identified to bind DNA DSBs sites and involved in DDR signaling through ATM/Chk2 pathway (Rai et al., 2009). Recently, A549 (wild-type p53) cells exhibited an increase in (gamma-H2AX/53BP1) foci formation following the stable NUDT1 knockdown, whereas, such rise in DNA DSB co-localized foci was not seen in H23 (p53-mutated) and H358 (p53 null) cells (Patel et al., 2015). Here, there was no change in the expression of pChk2 (Thr 68) observed after siRNA-mediated NUDT1 depletion in A549 and H23 cells. In addition, it has been reported that the sensitivity of SW480 cells to ATM or ATR kinase inhibitors did not differentially change during stable NUDT1 knockdown (Huber et al., 2014). Furthermore, regulation of cell cycle events occurs in response to DNA damage by Chk1 and Chk2 as regulators of cyclin-dependent kinases. Essentially, both have major roles in G2 DNA damage checkpoint through inhibiting Cdc25C activity with a subsequent mitotic blockage (Stanford and Ruderman, 2005, Gautier et al., 1991).

Chk1 (2G1D5) antibody was applied herein to identify total Chk1 endogenous protein level. In A549 and H23 cells, although the reason for decreased total Chk1 level is uncertain (Figure 4-7), downregulation of total Chk1 could allow the cells to re-enter the cell cycle despite the existent of DNA damage, leading to eventual chromosome instability. So far, to our knowledge, this is the first time such switch off DDR has been detected following NUDT1 knockdown.

It is known that upstream ATR kinase activation occurs in response to DNA replication fork stalling, thereby activation of Chk1 which involves phosphorylation at Ser 345 or Ser 317 sites (Zhao and Piwnica-Worms, 2001). The phosphorylation at Ser 345 allows the nuclear localization of Chk1 after activation of the checkpoint (Jiang et al., 2003), whereas phosphorylation at Ser 317 as well as site-specific phosphorylation of PTEN permits re-entry into cell cycle after stalled DNA replication (Martin and Ouchi, 2008). On the cell cycle, Chk1 exerts its checkpoint action partly by regulating cdc25 phosphatases family. Activated Chk1 could result in Cdc25C inactivation through phosphorylation at Ser 216, leading to block in Cdc2 activation and transition into mitosis (Zeng et al., 1998). In addition, it was shown that Chk1 centrosome could phosphorylate cdc25B, causing inhibition of its activation to cyclin B/Cdk1 and subsequently abrogate mitotic spindle assembly and chromatin condensation (Loffler et al., 2006). In this study, after siRNA-mediated NUDT1 depletion, the phosphorylation

of Chk1 at Ser 345 or Ser 317 sites was not observed (Figure 4-7). This suggests no activation of ATR kinase might occur in response to NUDT1 knockdown.

A critical finding in this work relates to the apoptotic cell death/cell viability data. Our original hypothesis was that NUDT1 protein depletion would kill NSCLC cells in selective manner, based both on our observation of increase in genomic 8-oxodG levels in NSCLC cells as discussed above, and on earlier findings relating to cell growth in various cancerous cells (Gad et al., 2014, Rai et al., 2011, Giribaldi et al., 2015). However, successfully NUDT1 knockdown does not lead to induction of cellular apoptosis. Moreover, by using WST-1 assay to assess metabolic activity of the cell culture, NUDT1-deficient H23 cells slowed down its cellular proliferation, but have not seen for other cells. Lack of proliferation without apoptotic cell death has previously been reported following stable NUDT1 knockdown in human BJ fibroblasts, as analysed by Annexin V/PI staining (Rai et al., 2009). shNUDT1 infected cells (H23, H358, and A549) have also shown negligible cell death induction, with reducing cell proliferation (H23 and H358 cells), or complete proliferative arrest (G1/S) seen in A549 cells that retain competent p53 (Patel et al., 2015). The latter cell line also exhibited an increase in SA-beta-gal staining as well as DNA DSB foci formation (gamma-H2AX/53BP1) following stable NUDT1 knockdown (Patel et al., 2015). Recent publications have indicated that by inhibiting NUDT1 in cancer cells, there is increased incorporation of 8-oxodGTP and 2-OHdATP into DNA genome, leading to replication fork stalling and DSBs formations with ultimate apoptotic cell death (Gad et al., 2014, Huber et al., 2014, Puigvert et al., 2016). They demonstrate that three different siRNA were able to reduce the viability and clonogenic survival in NUDT1-deficient U2OS cells with no attenuation in a survival of VH10 normal cells (Gad et al., 2014). Large variability in response to siRNA was observed in the above study and attributed to passive and incomplete depletion of NUDT1, as even low level of NUDT1 protein remains was possibly sufficient to maintain the survival of cells (Gad et al., 2014). In addition, small molecule NUDT1 inhibitors (TH588, TH287) as well as other determined selective inhibitors of NUDT1 catalytic activity, such as, SCH51344 and (S)-crizotinib, exerted an effective cytotoxicity towards certain cancer cells with considerable less impact on primary and immortalized cells (Gad et al., 2014, Huber et al., 2014).

Using U2OS cancer cells, a team from Astra Zeneca tried to revalidate siRNA knockdown experiments with another commercially available, different, and a distinctive sequence NUDT1-targeting oligonucleotide from previously reported. Complete knockdown was observed at that time and no alteration on clonogenic survival of NUDT1-deficient cells. However, when repeating the experiment with the same reported Gad et al. siRNA sequence, it exhibited a profound effect on cell viability (Kettle et al., 2016). These data are in line with our results at which siRNA-mediated NUDT1 depletion was ineffective to induce cancer cell killing. Another study also supports this finding, when siRNA targeting NUDT1 proficiently knocked down of HeLa cells for 96 h, failed to suppress cell growth as well as the progression of the cell cycle (Kawamura et al., 2016). The differences in siRNA influences suggest the possibility of a nonspecific effect of the Gad et al. reported siRNA oligonucleotide; and such results should be interpreted with caution especially when cell death is the main focus (Kettle et al., 2016). In addition, SW480 colorectal adenocarcinoma stable clones, lacking NUDT1 expression were generated by CRISPR technology. These clones were able to continue growing efficiently as their wild-types counterpart; and both cell line types show similar growth rate reduction upon treatment with TH588 and (S)-crizotinib, suggesting the off-target activity of these compounds (Kettle et al., 2016). In addition, it has been previously noticed *in vivo* that (H358, H23, and A549) cells transduced with constitutive shNUDT1 could induce a significant reduction in xenograft tumor formation. This was not related to a rise of *in vivo* cell death pattern, as no perceptible alteration in caspase-3 cleaved stain was distinguished between shNUDT1 and control shGFP xenograft sections (Patel et al., 2015).

It was proposed that depending on the p53 state, NUDT1 suppression elicits a molecular basis for distinctive cell cycle inhibitors response. In A549 cells, transduction with shNUDT1 upregulates p53 and p21^{cip/waf1} protein expressions that suggest the onset of RAS oncogene induce senescence. However, NUDT1 loss leads to an elevation in p27^{kip1} expression level in non-functional p53 cells (H358, and H23), lacking p21^{cip/waf1}, which was not seen in A549 shNUDT1 cells. In addition, the cells transduced with constitutive shNUDT1 could reduce phospho-Akt protein level, without exhibiting any change in phospho-Erk1/2 expressions that indicates an inhibition of PI3K/Akt signaling pathway. The latter finding seems to be strengthened in p53-nonfunctional cell lines (Patel et al., 2015). Moreover, chronic loss of NUDT1 reduces the expression

of oncogenic KRAS and ROS levels in H358 and H23 cells within 14 days as an adaptive mechanism, but not in wild-type p53 A549 cells. The ROS stimulates and is known to produce by Akt signaling. In general, these results suggest the idea that non-functional p53 with mutated KRAS NSCLC cells adapt to NUDT1 suppression by downregulation of ROS-generating mechanism, including oncogenic RAS levels and Akt signaling. Such adjustment might allow the cells to persist their proliferation ability, albeit at a lower degree. However, the contribution of another redox-regulatory pathway along with additional stress response process cannot be excluded, in order to maintain the proliferation downstream to NUDT1 as an adaptive response (Patel et al., 2015). However, in this study, it is worth to mention that all NSCLC cell lines responded similarly to the NUDT1 enzyme depletion in terms of increased oxidation of DNA and without apoptotic cell death enhancement. In addition, to some extent our cell proliferation findings are in contradictory to previous assertion in the literature (Patel et al., 2015), especially for NUDT1-deficient A549, as here it did not exhibit any change in cell proliferation and/or viability, suggesting that the status of p53 does not impact on such outcomes.

In summary, NUDT1 has a NSCLC-specific p53-independent role for suppressing oxidative DNA damage levels and genomic instability, though surprisingly the basis of this may not be related to ROS levels. However, it is shown here that targeting NUDT1 is not an effective therapeutic approach; rather it induces non-cytotoxic DNA damage that could promote cancer heterogeneity and evolution.

Chapter 5: Effect of NUDT1 knockdown on sensitization to current treatment agents

5.1 Introduction

Chemotherapy and radiotherapy have key roles for the treatments of many cancers. Ionizing radiation exerts its action by damaging cancerous tissue DNA with subsequent cellular death, either directly or via indirect interaction with water molecules to yield hydroxyl free radicals (HO[•]) (Nikitaki et al., 2016, Desouky et al., 2015), whereas, cytotoxic drugs are classified according to their mechanism of action (crosslinking agent, alkylating agents etc.).

In addition to a role for nucleotide pool sanitizing enzyme NUDT1 in processing oxidised nucleotide precursors that are produced endogenously within tumor cells, we proposed it might also be required for reduction of mis-incorporated DNA damage bases after exogenous exposure to oxidative stress sources and chemotherapeutic agents.

In this chapter, the exogenous oxidant treatments (H₂O₂ and ionizing radiation) were applied on a panel of NSCLC cell lines along with certain drugs, namely, cisplatin and gemcitabine that are considered as the first-line treatment for NSCLC. Gemcitabine inhibits an enzyme RNR, leading to a suppression of the available deoxyribonucleotides required for DNA synthesis (Oguri et al., 2006). Cisplatin reacts inside the cell in a way that allows to bind DNA at N⁷ position purine bases, causing DNA strand crosslinks (Basu and Krishnamurthy, 2010, Un, 2007). However, it is recognised that most chemotherapeutic agents depend on ROS generation and oxidative damage to attain effective tumor eradication (Panieri et al., 2013, Tu et al., 2016), including cisplatin and maybe gemcitabine as discussed thoroughly in section 1.9. Among the many sources of ionizing radiation are traditional X-rays, also involved in lung cancer therapy.

H₂O₂ is regarded as an oxidant that has long been applied as a study model related to oxidative stress conditions in different cell types (Coyle and Kader, 2007, Meneghini, 1997, Barbouti et al., 2002, Garcia et al., 2006). It is characterized by stability, less reactive and highly diffusible structure, as it readily passes through cell membrane and ultimately forms a more potent and highly reactive hydroxyl radical (HO[•]) (Potts et al., 2001, Panieri et al., 2013, Mishina et al., 2011), that has the capacity to interact with contents of DNA at or near diffusion-controlled rates, thereby giving rise to DNA lesions (Zastawny et al., 1995). Once within the cell, the H₂O₂ is reduced by the most abundant transition metal ion in biological systems, iron ions, to produce hydroxyl

radical (HO[•]) via a Fenton-and Haber-Weiss-type reactions, and subsequently causes DNA damage, including strand breaks, depurination/depyrimidination, or modification of DNA bases or sugars (Duarte and Jones, 2007). Oxidation of lipids or proteins could also be produced by such iron-mediated processes (Duarte and Jones, 2007, Welch et al., 2002).

Despite the lack of NSCLC cytotoxicity observed in the previous chapter after NUDT1 knockdown, it is still suggested that targeting NUDT1 enzyme could be an effective way to augment current therapeutic approaches that promote DNA damage and replication stress of DNA particularly if they are associated with generating oxidative stress, which would be discussed in this section.

5.2 Exposure to H₂O₂ insult

As an exogenous source of oxidative stress, H₂O₂ was applied on NSCLC cell lines, H23 and H522.

5.2.1 Determination of apoptotic cell killing and sensitivity of NSCLC cells exposed to H₂O₂

The sensitivity of NSCLC cells to H₂O₂ was assessed by determining their apoptotic dose response curves following exposure to different concentrations of H₂O₂ (50, 100, 200, 400, and 800 μM). The cytotoxic effect of H₂O₂ was observed at two-time points (24 and 48 h), and the early and late apoptotic fractions were determined by Annexin V-FITC/PI assay. Herein, the harvested cells were dual staining with Annexin V-FITC/PI and assessed by flow cytometry. As a positive control of apoptosis, H23 and H522 cells were treated with etoposide at concentrations of 50 or 150 μM, respectively. DMSO (0.5-1.5% v/v) and no treatment negative control (-ve) samples were also included.

As shown in Figures 5-1, and 5-2, the exposure of H23 cells to 50 μM etoposide for 24 and 48 h exhibit 35.5, and 65.1% apoptotic cells, respectively, which was more significant than apoptotic cell fractions in untreated and treated samples with 0.5% v/v DMSO (almost 5% apoptotic cells) (P-value < 0.0001). For H522 cells, no significant change in apoptotic cell fractions was observed after 24 h treatment with 150 μM etoposide, whereas, using the same dose for 48 h induced a nearly 5-fold higher apoptotic cell level than untreated (4.2%) and DMSO 1.5% v/v treated cells (5.5%) (P-

value < 0.0001) (Figures 5-3, and 5-4). Therefore, the low responsiveness and resistance of H522 cells to etoposide was observed, relative to H23 cells, with much higher doses required.

An incremental rise in the rate of early and late apoptotic H23 cells was obtained in a dose dependent manner for both (24 and 48 h) time points, with a trend toward significance occurring at 400 μM H_2O_2 (P-value < 0.05 , and < 0.0001 , respectively) (Figures 5-1, and 5-2). This increase in apoptotic cell death percentages seemingly arises at late rather than early apoptotic stage after 48 h (Figure 5-1). Specifically, following 48 h treatment with H_2O_2 , the percentage of apoptotic cell death on early stage were 4.2% for 400 μM , 5.1% for 600 μM and 8.6% for 800 μM H_2O_2 ; while at late stage they were 11.5%, 20.7% and 30.2%, respectively (Figure 5-1). Interestingly, the H522 cells did not exhibit any H_2O_2 -induced early or late apoptosis up to 800 μM after both 24 and 48 h of the treatment (Figures 5-3, and 5-4), indicative that H23 cells are more sensitive to H_2O_2 in term of induction of apoptotic cell death.

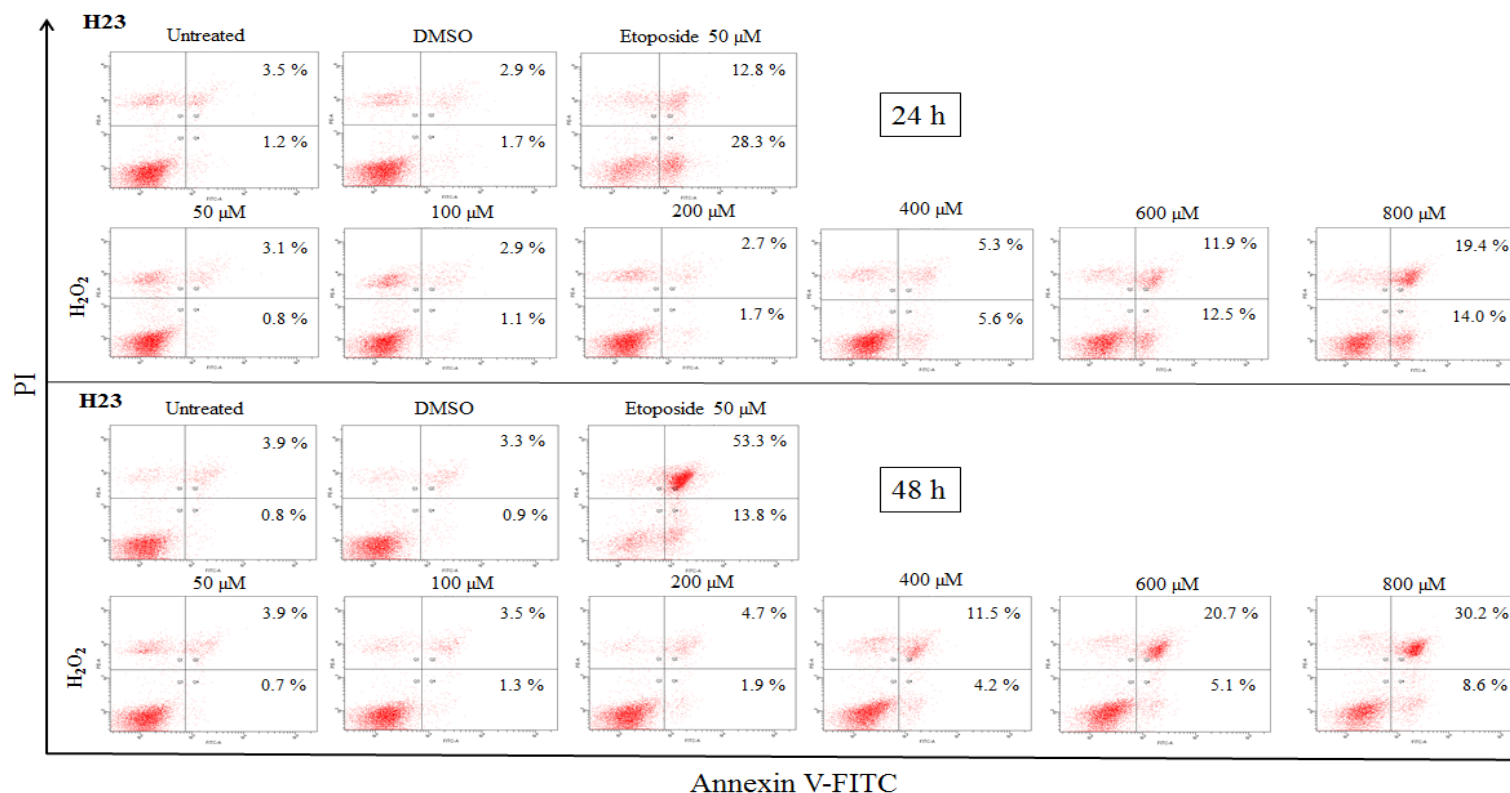


Figure 5-1 Bivariate plots of Annexin V-FITC and propidium iodide staining following H₂O₂ treatment of H23 cell.

The H23 cells were either untreated or exposed to increasing doses of H₂O₂ for 24 and 48 h. Etoposide (VP-16) treatment was also included as a positive control of apoptosis, and its vehicle control was DMSO (0.5% v/v). To discriminate apoptotic cells proportions, the harvested cells were dual stained with annexin V/PI and assessed by flow cytometry. For each dot plot, percentages shown in the bottom and top right quadrants are correspondent with early apoptosis (annexin +/PI -) and late apoptosis/necrosis (annexin +/PI +), respectively. In addition, viable cells (annexin -/PI -) are represented at low left quadrant while nuclear fragments dead cells (annexin -/PI +) are represented at upper left quadrant. An incremental rise in the rate of early and late apoptotic cells was obtained in a dose dependent manner, yet several differences existed.

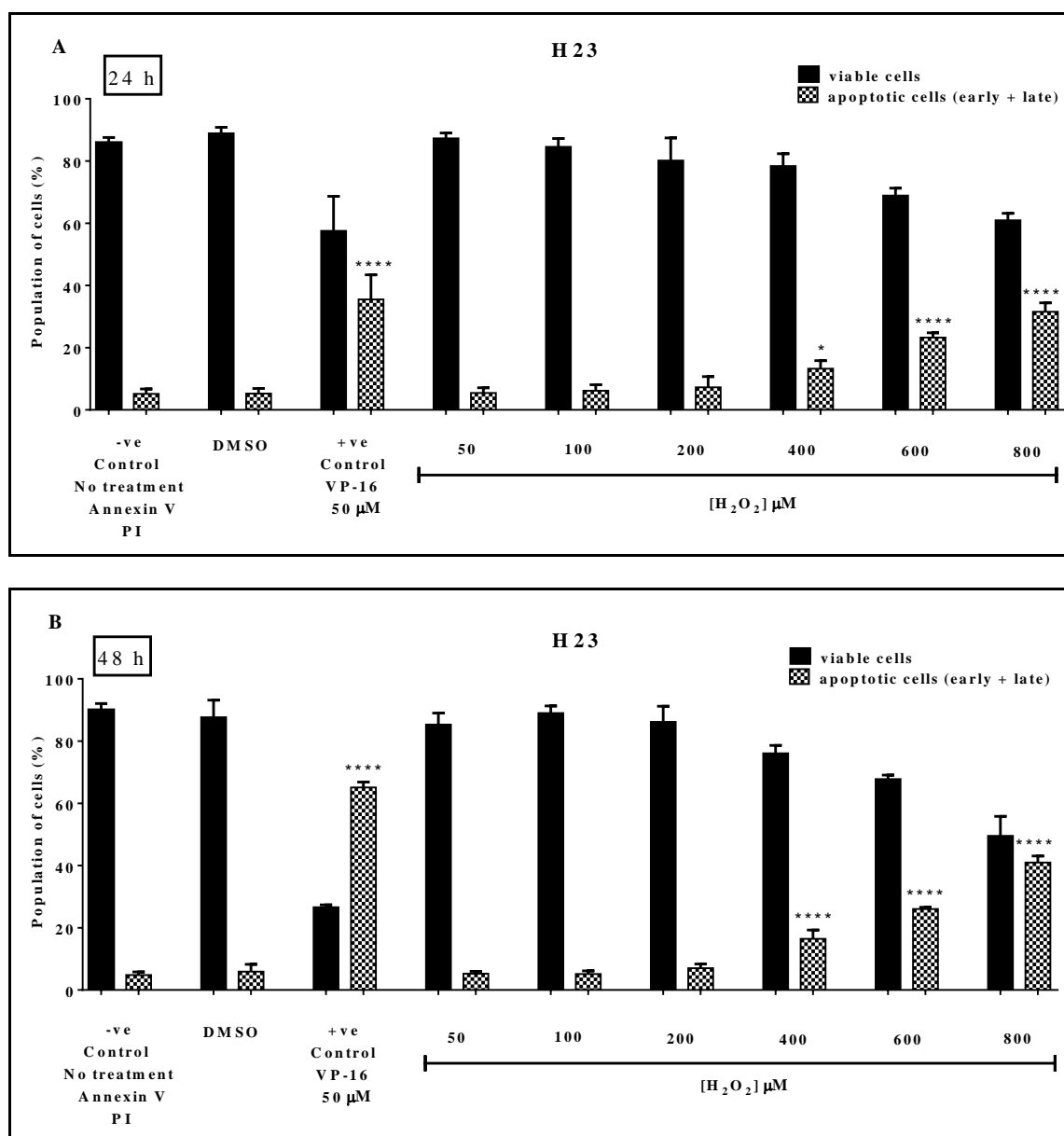


Figure 5-2 Apoptotic dose response curves in H23 cells following H₂O₂ treatment.

Annexin V–FITC/PI assay was applied to determine apoptotic cell deaths following [A] 24 and [B] 48 h exposure of H23 cells to different concentrations of H₂O₂ up to 800 μM. In addition, the cells were treated with etoposide (VP-16) as a positive control of apoptosis, along with DMSO (0.5% v/v) and no treatment (-ve control) samples. The harvested cells were then dual stained with annexin V-FITC/PI and finally assessed by flow cytometry. The shaded bars of detected apoptotic cells represent the result during both early and late apoptosis. These data were mean ± SD of three individual experiments. Asterisks indicate a significant difference relative to corresponding untreated control cells (****P<0.0001, *P<0.05).

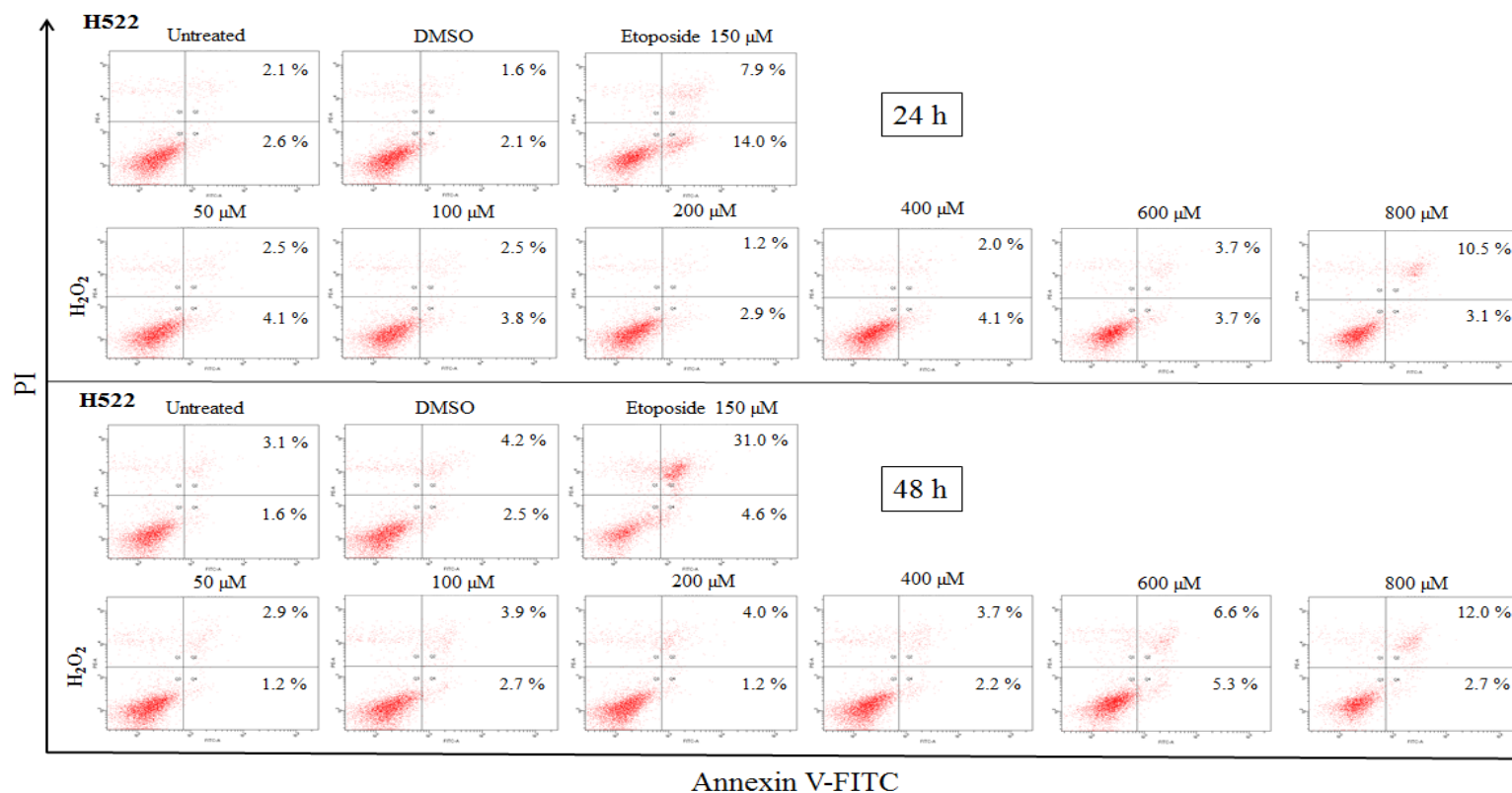


Figure 5-3 Bivariate plots of Annexin V-FITC and propidium iodide staining following H₂O₂ treatment of H522 cell.

H522 cells were either untreated or exposed to increasing doses of H₂O₂ for 24 and 48 h. Etoposide (VP-16) treatment was also included as a positive control of apoptosis, and its vehicle control was DMSO (1.5% v/v). To discriminate apoptotic cells proportions, the harvested cells were dual stained with annexin V/PI and assessed by flow cytometry. For each dot plot, percentages shown in the bottom and top right quadrants are correspondent with early apoptosis (annexin +/PI -) and late apoptosis/necrosis (annexin +/PI +), respectively. In addition, viable cells (annexin -/PI -) are represented at low left quadrant while nuclear fragments dead cells (annexin -/PI +) are represented at upper left quadrant. H₂O₂ treatments induce nearly similar apoptotic fractions to corresponding untreated cells up to 800 μM for both time points.

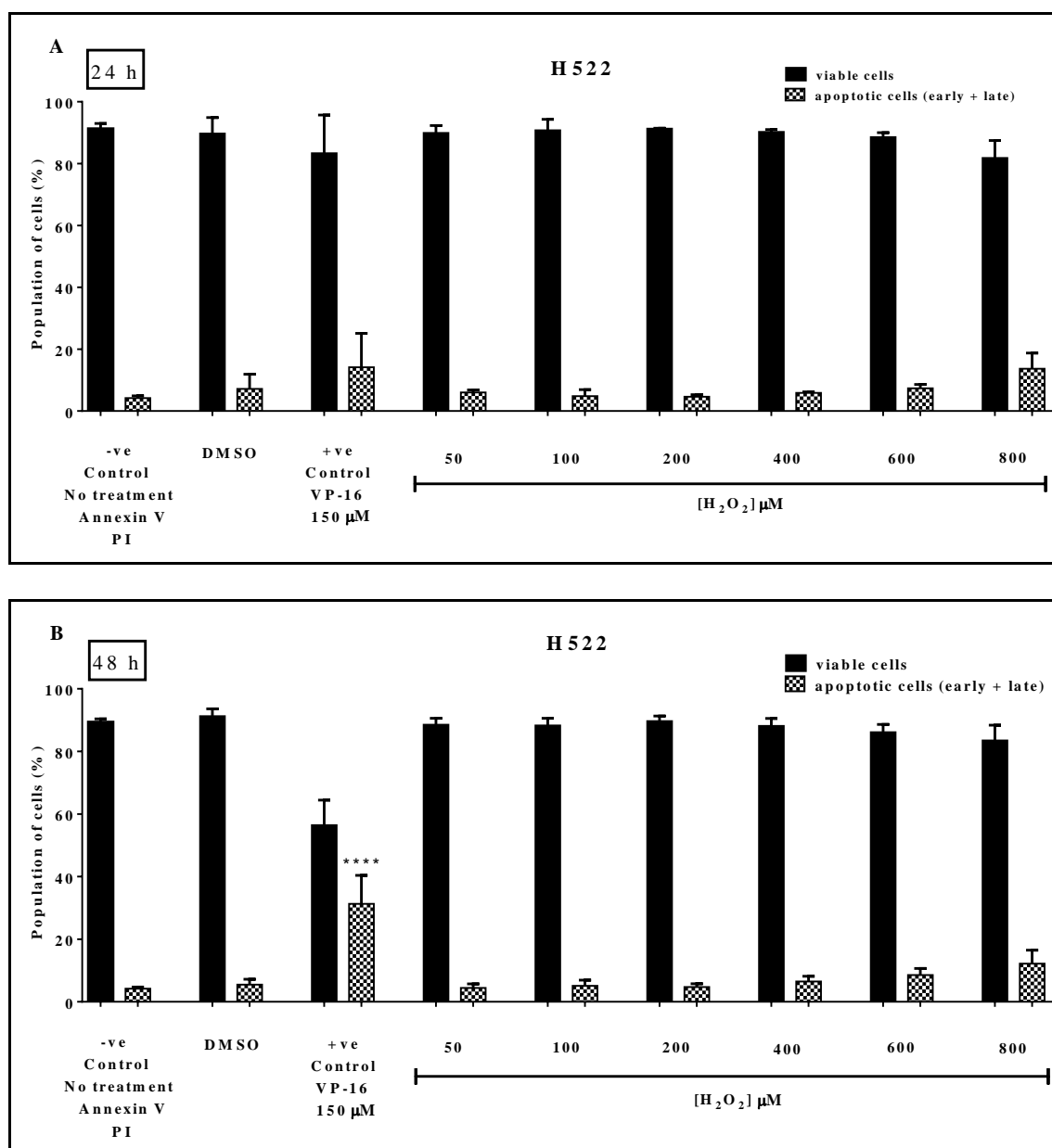


Figure 5-4 H522 cell line displays an apoptotic resistance to high doses of H₂O₂.

Annexin V–FITC/PI assay was applied to determine apoptotic cell deaths following [A] 24 and [B] 48 h exposure of H522 cells to different concentrations of H₂O₂ up to 800 μM. In addition, the cells were treated with etoposide (VP-16) as a positive control of apoptosis, along with DMSO (1.5% v/v) and no treatment (-ve control) samples. The harvested cells were then dual stained with annexin V-FITC/PI and finally assessed by flow cytometry. The shaded bars of detected apoptotic cells represent the result during both early and late apoptosis. These data were mean ± SD of three individual experiments. Asterisks indicate a significant difference relative to corresponding untreated control cells (****P<0.0001).

5.2.2 Determination of H₂O₂-induced DNA damage in NSCLC cells with and without NUDT1 knockdown

It is proposed that in addition to the role for NUDT1 in processing oxidised precursors of dNTPs that are produced endogenously within cancer cells, it would also be needed to prevent the misincorporation of damaged DNA bases after exposure to exogenous sources of oxidative stress and cancer therapeutic agents. H₂O₂, a well-known as non-radical ROS oxidant model, was assessed first.

To ensure which dose of H₂O₂ is applied to induce a notable DNA damage level, it is initially required to determine the dose-response curves of such modified DNA damage in NUDT1 proficient cells (without protein depletion). Different concentrations of H₂O₂ (50, 100, and 200 μ M) was introduced to NSCLC cell lines, mainly H23 and H522 cells.

For this condition, the formation of H₂O₂-induced DNA damage in the cells was investigated by mean of Fpg-modified comet assay, to detect DNA SSBs or ALS along with oxidised purine-derived lesions. The results showed a clear dose-dependent DNA damage induced by H₂O₂ in H23 and H522 cell lines for both SSBs or ALS and Fpg sensitive sites, measured as an increase in % tail DNA (Figures 5-5 and 5-6). Furthermore, the oxidative DNA modifications, mainly 8-oxodG, for both cell lines were significantly higher relative to SSBs or ALS at the indicated H₂O₂ treatment doses. Specifically, the average levels of oxidised DNA bases at H₂O₂ 50 μ M were 13.27% for H23 (P-value <0.05), and 12.54% for H522 (P-value <0.05); whereas at 100 μ M concentration they were 37.39% for H23 (P-value <0.01) and 19.91% for H522 (P-value <0.05). This oxidatively modified DNA were further increased at H₂O₂ 200 μ M for both H23 and H522 cells, reaching 67.51% (P-value <0.001) and 55.13% (P-value 0.05), respectively. In addition, it is indicated that the H23 cell line formed greater amounts of DNA damage at all used H₂O₂ concentrations when compared to H522 cells, correlating with the apoptosis data (Figures 5-2, and 5-4).

According to these data, 100 μ M H₂O₂ was selected for both H23 and H522 cell lines to carry out further experiments in combination with the NUDT1 knockdown. The H₂O₂ doses more than 100 μ M created higher levels of SSB (i.e. Fpg-independent percentage DNA in comet tail) and oxidatively damaged DNA (i.e. Fpg-dependent percentage DNA in comet tail) (Figures 5-5 and 5-6) (data of 400 and 600 μ M H₂O₂ are not shown)

that could mask any incremental rise in comet size that occurs following combination with NUDT1 knockdown. In contrast, lower exposure doses of H₂O₂ might not be enough to induce DNA damage with observable effect to discriminate between SSBs and oxidatively damaged DNA. Therefore, 100 µM H₂O₂ was considered to generate a substantial level of oxidatively damaged DNA to be detected by using Fpg repair enzyme, and utilised for further experiments in combination with NUDT1 deficiency.

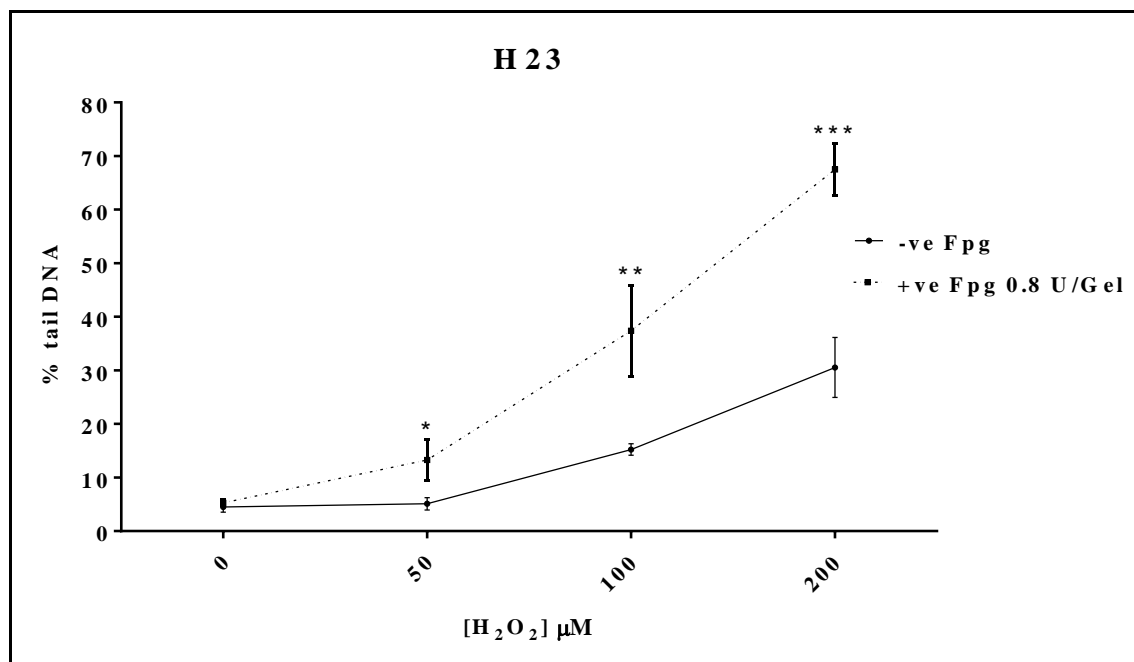


Figure 5-5 Dose response curves of oxidised DNA bases and SSB/ALS in H23 cells following H₂O₂ treatment.

Fpg-modified alkaline comet assay was applied to determine DNA damage levels in individual H23 cells treated with increasing dose of H₂O₂ up to 200 µM for 30 min on ice. DNA damage levels were expressed as % tail DNA after incubation for 30 min at 37°C with Fpg repair enzyme (0.8 U/Gel) or buffer alone (control). These results represent mean ± SD of three independent experiments; at which 100 individual comets were scored for each sample to determine the experiment mean value. Asterisks indicate a significant difference relative to corresponding without Fpg repair enzyme treatment (buffer alone control) (***P<0.001, **P<0.01 and *P<0.05).

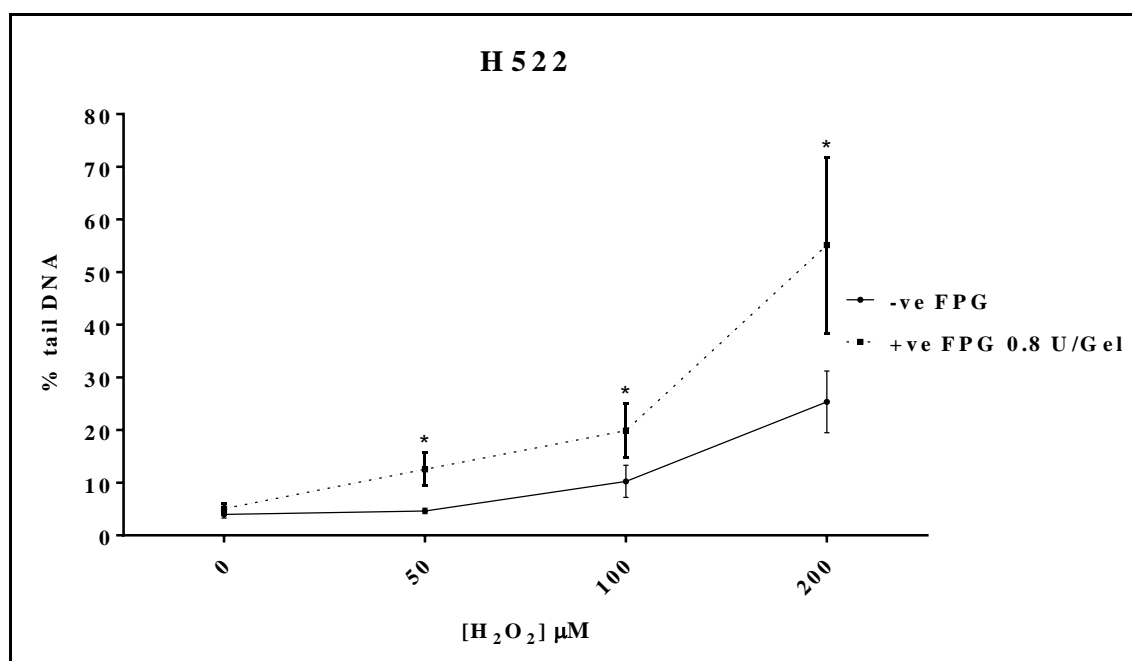


Figure 5-6 Dose response curves of oxidised DNA bases and SSB/ALS in H522 cells following H₂O₂ treatment.

Fpg-modified alkaline comet assay was applied to determine DNA damage levels in individual H522 cells treated with increasing dose of H₂O₂ up to 200 μM for 30 min on ice. DNA damage levels were expressed as % tail DNA after incubation for 30 min at 37°C with Fpg repair enzyme (0.8 U/Gel) or buffer alone (control). These results represent mean ± SD of three independent experiments; at which 100 individual comets were scored for each sample to determine the experiment mean value. Asterisks indicate a significant difference relative to corresponding without Fpg repair enzyme treatment (buffer alone control) (*P<0.05).

In order to assess whether higher DNA damage levels were detected in NUDT1-depleted NSCLC cells (H23 and H522) after H₂O₂ exposure, the Fpg-modified comet assay was applied. An efficient transient depletion of NUDT1 protein was established for 4 days in (H23 and H522 cells), by using the previously mentioned concentrations of NUDT1-siRNA (s9030) [15 and 20 nM, respectively]. Mock transfection (media without siRNA or transfection reagent) and silencer select -ve control siRNA (Scramble) samples were also included. Afterwards, the cells were treated with or without 100 μM H₂O₂ (30 min on ice), and then analysed immediately.

H23 (Figure 5-7), and H522 (Figure 5-8) cells without H₂O₂ treatment have 1.5 to 2-fold increase in Fpg sensitive sites (oxidatively damaged DNA) after NUDT1 knockdown; as previously shown in Figures 4-1, and 4-2, without any further additional DNA SSBs or ALS lesions (4.57% for H23 and 4.26% for H522) compared to

corresponding scramble siRNA controls (5.23% for H23 and 4.24% for H522). In addition, when the cell samples were analysed immediately after H₂O₂ exposure, the relative rise in DNA SSBs or ALS lesions, as well as Fpg-dependent percentage DNA in comet tail (oxidatively damaged DNA), did not change between NUDT1 siRNA transfected cells and silencer select -ve control siRNA (Scramble) samples. Specifically, the levels of SSBs or ALS directly after 100 µM H₂O₂ treatment of H23 and H522 cells were 22.71% and 19.02% for scramble control, and 21.44% and 15.28% for NUDT1-deficient cultures, respectively (Figures 5-7, and 5-8). In a similar pattern, the oxidatively damaged DNA immediately following the above-indicated treatment for H23 cells reached 40.81% for scramble control, and 42.89% for NUDT1-deficient cultures; while for H522 cell line they were 40.1% and 42.49%, respectively (Figures 5-7, and 5-8).

These findings suggest that NUDT1 does not have a role in altering oxidatively modified DNA levels following direct exposure to H₂O₂ as a model oxidant.

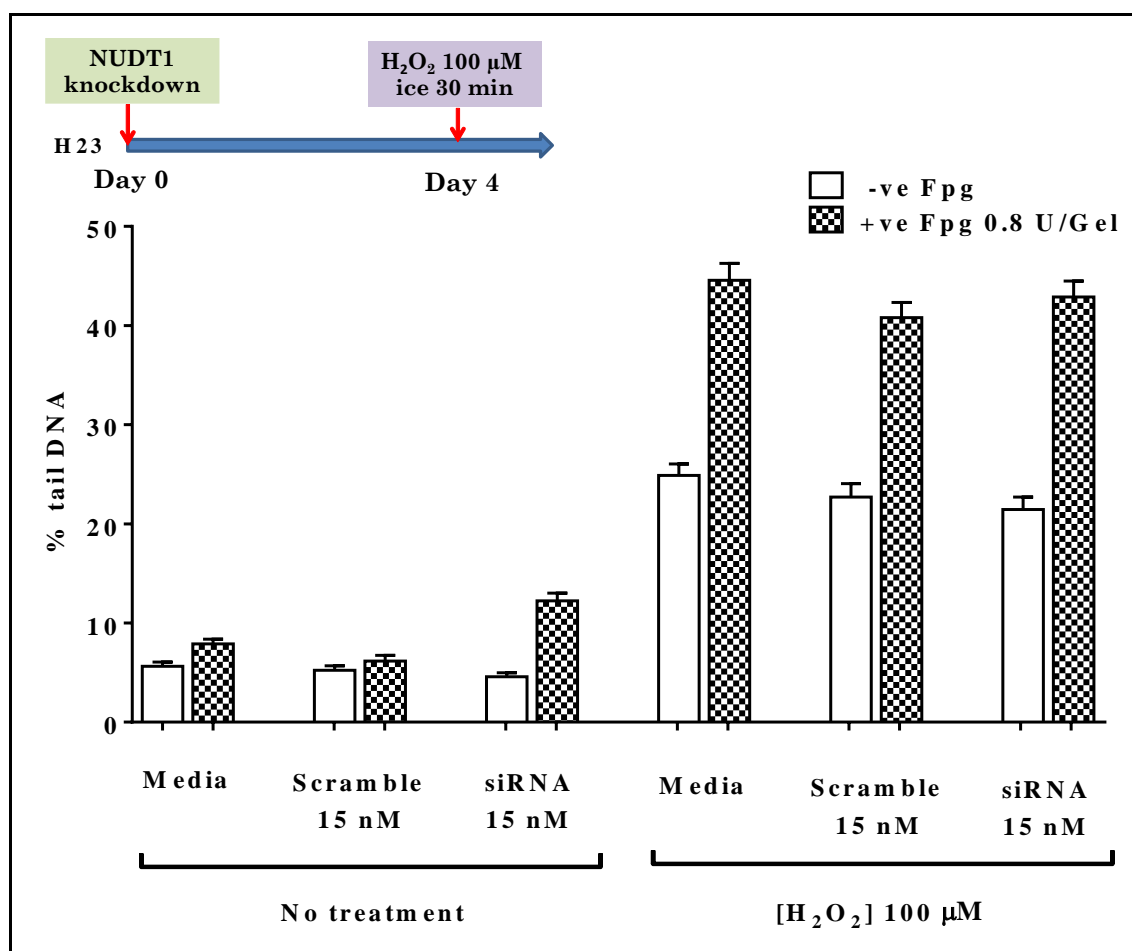


Figure 5-7 Transient NUDT1 knockdown does not lead to any alteration of oxidatively-modified DNA levels in H23 cells following H₂O₂ treatment.

Fpg-modified alkaline comet assay was applied to determine DNA damage levels in individual H23 cells 4 days after transfection with 15 nM NUDT1 siRNA or silencer select -ve control siRNA (Scramble), or those grown in media without transfection reagent/siRNA. At time point indicated, the cells were treated with 100 μM H₂O₂ for 30 min on ice or left untreated before proceeded with processing. DNA damage levels were expressed as % tail DNA with [▣] or without [□] Fpg repair enzyme treatment. These results represent mean ± SEM of 100 individual comets. (n=1).

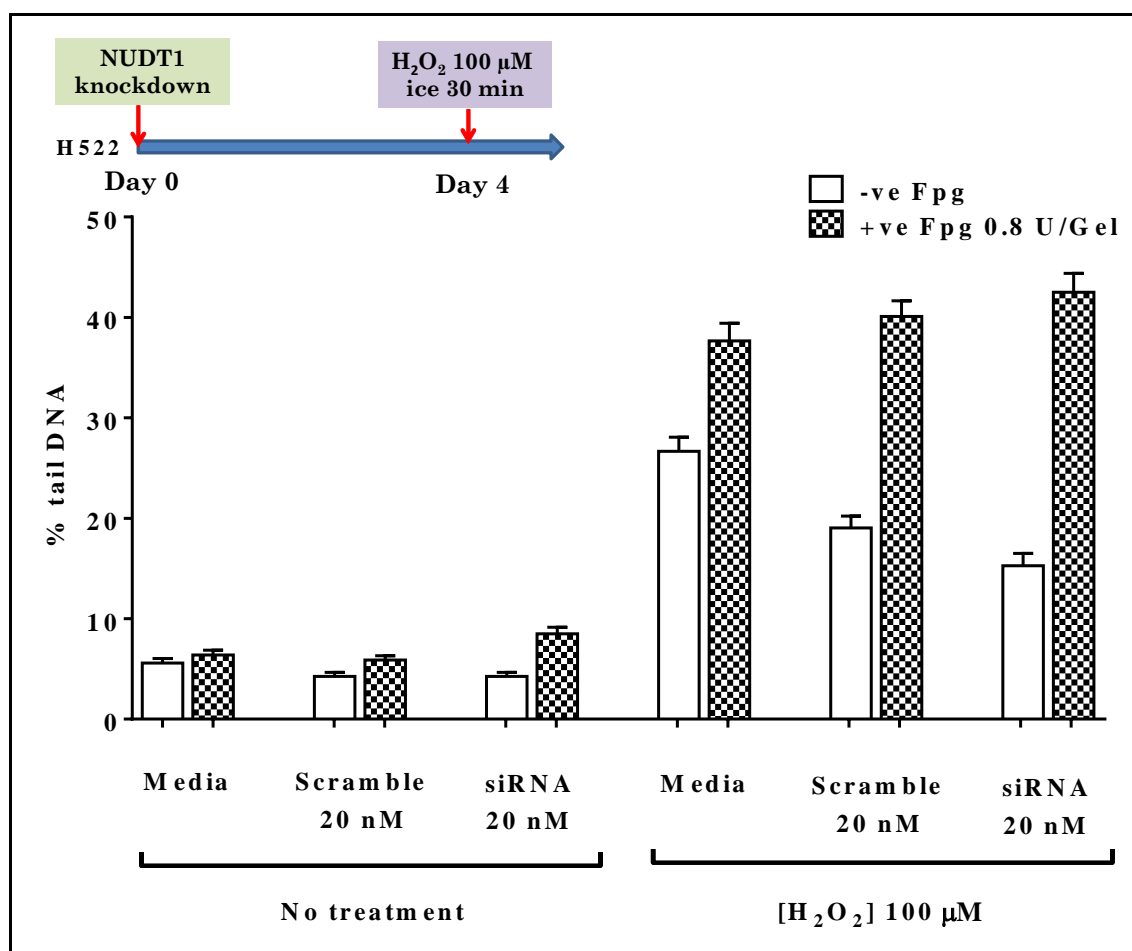


Figure 5-8 Transient NUDT1 knockdown does not lead to any alteration of oxidatively-modified DNA levels in H522 cells following H₂O₂ treatment.

Fpg-modified alkaline comet assay was applied to determine DNA damage levels in individual H522 cells 4 days after transfection with 20 nM NUDT1 siRNA or silencer select -ve control siRNA (Scramble), or those grown in media without transfection reagent/siRNA. At time point indicated, the cells were treated with 100 μM H₂O₂ for 30 min on ice or left untreated before proceeded with processing. DNA damage levels were expressed as % tail DNA with [▣] or without [□] Fpg repair enzyme treatment. These results represent mean ± SEM of 100 individual comets. (n=1).

A further experiment was performed to assess whether higher DNA damage levels were detected in NUDT1-depleted NSCLC cells (H23, and H522) after immediate H₂O₂ exposure (at 37°C) and following 24 h recovery period, in order to allow enough time for H₂O₂-induced oxidised nucleotide pool precursors to be incorporated into DNA genome during the replication process. To achieve this purpose, the Fpg-modified comet assay was also applied. An efficient transient depletion of NUDT1 protein was established for 4 days in (H23, and H522 cells), by using the previously mentioned concentrations of NUDT1-siRNA (s9030) [15 and 20 nM, respectively]. Mock transfection (media without siRNA or transfection reagent) and silencer select -ve control siRNA (Scramble) samples were also included. Consequently, the cells were analysed following immediate treatment with or without 100 µM H₂O₂ (30 min at 37°C), and after 24 h of cellular repair of DNA damage.

As seen in Figures (5-7, 5-8, 5-9, and 5-10), overall lower levels of DNA damage were observed by immediate exposure to H₂O₂ at 37°C than treatment on ice, including Fpg sensitive sites and DNA SSBs or ALS lesions. In addition, the results also indicated that H23 (Figure 5-9), and H522 (Figure 5-10) cells without H₂O₂ treatment, displayed 1.5 to 2-fold increase in Fpg sensitive sites after NUDT1 knockdown; as previously shown in Figures (4-1, 4-2, 5-7, and 5-8), without any further addition of DNA SSBs or ALS lesions (4.48% for H23, and 4.14% for H522) compared to corresponding scramble siRNA controls (4.47% for H23, and 4.62% for H522).

In addition, immediately after H₂O₂ exposure at 37°C, a similar pattern to H₂O₂ treatment on ice for induction of genomic DNA damage was observed. The relative rise in DNA SSBs or ALS lesions, as well as Fpg sensitive sites levels, did not change between NUDT1 siRNA transfected cells and silencer select -ve control siRNA (Scramble) samples. As seen in Figures 5-9, and 5-10, the levels of SSBs or ALS directly after 100 µM H₂O₂ treatment at 37°C of H23 and H522 cells were 7% and 4.61% for scramble control, and 8.69% and 5.84% for NUDT1-deficient cultures, respectively. The oxidatively damaged DNA levels also increased immediately following the above-indicated treatment with H₂O₂ at 37°C, but without exhibiting a difference between NUDT1 knockdown relative to those cells transfected with scrambled siRNA. For H23 cells, these levels of oxidised DNA bases reached 12.59% for scramble control, and 13.28% for NUDT1-deficient cultures; while for H522 cells

they were 22.25% and 17.69%, respectively (Figures 5-9, and 5-10). These findings also indicate that NUDT1 does not have a role in preventing direct oxidation of DNA.

The cell samples were also assessed at 24 h recovery point after treatment with or without 100 μ M H₂O₂ (at 37°C), in order to allow enough time for H₂O₂-induced oxidised dNTPs pool precursors to be incorporate into DNA genome during the replication process. Herein, those samples that were left untreated for both H23 (Figure 5-9), and H522 (Figure 5-10) cell lines still have 1.5 to 2-fold increase in Fpg sensitive sites after NUDT1 knockdown, which resemble the levels prior to treatment and those previously observed (Figures 4-1, 4-2, 5-7, and 5-8). Such accumulations of oxidatively damaged DNA occur without any further increase in DNA SSBs or ALS lesions (4.26% for NUDT1-deficient H23 cells, and 4.16% for NUDT1-deficient H522 cells) compared to corresponding scramble siRNA controls (5.46% for H23, and 4.9% for H522).

As seen in Figures (5-9, and 5-10) by 24 h recovery period, the remaining DNA damage levels induced following H₂O₂ treatment in all samples had returned to levels nearly equivalent to those prior to H₂O₂ exposure. Specifically, the levels of SSBs or ALS lesions for H23 and H522 cells were 6.79% and 4.64% for scramble control, and 6.63% and 5.3% for NUDT1-deficient cultures, respectively. In addition, the oxidatively damaged DNA levels following the indicated recovery duration in H23 cells reached 9.38% for scramble control, and 8.86% for NUDT1-deficient cultures; while for H522 cell line they were 6.28% and 7.75, respectively.

Overall, these findings suggest that NUDT1 does not have a role in altering oxidatively modified DNA levels following direct exposure to H₂O₂ as a model oxidant and even after 24 h recovery period.

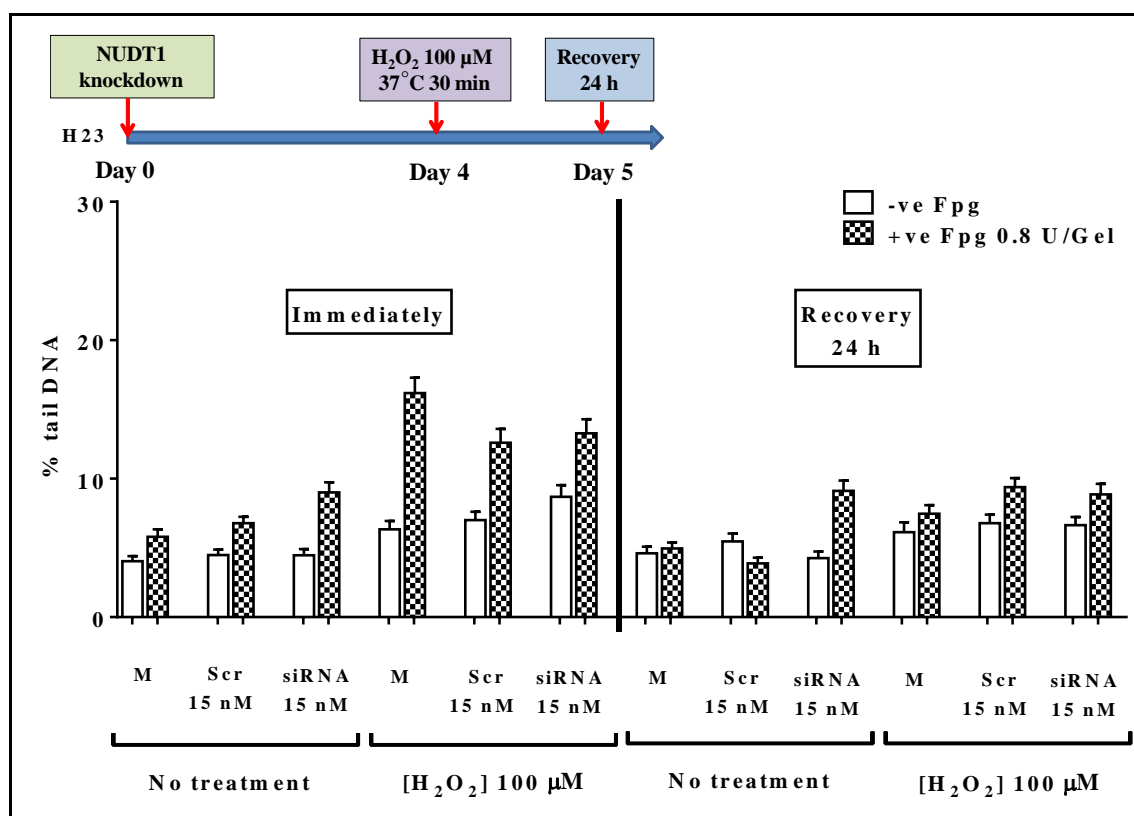


Figure 5-9 Transient NUDT1 knockdown in H23 cells does not alter oxidatively-modified DNA levels following both immediate and 24 h recovery of H₂O₂ treatment.

Fpg-modified alkaline comet assay was applied to determine DNA damage levels in individual H23 cells 4 days after transfection with 15 nM NUDT1 siRNA or silencer select -ve control siRNA (Scramble), or those grown in media (M) without transfection reagent/siRNA. After treatment with H₂O₂ (100 μM) for 30 min at 37° C, samples were collected either immediately or after 24 h recovery in fresh media. DNA damage levels were expressed as % tail DNA with [▣] or without [◻] Fpg repair enzyme treatment. These results represent mean ± SEM of 100 individual comets. (n=1).

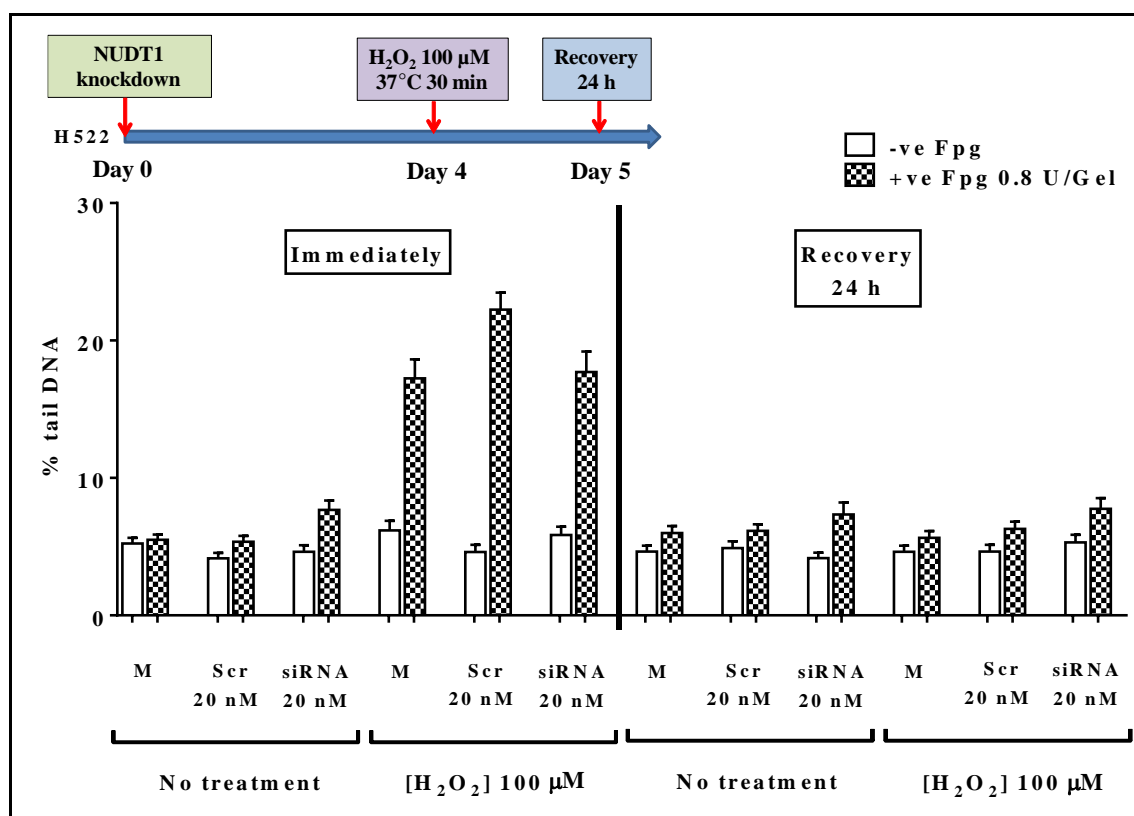


Figure 5-10 Transient NUDT1 knockdown in H522 cells does not alter oxidatively-modified DNA levels following both immediate and 24 h recovery of H₂O₂ treatment.

Fpg-modified alkaline comet assay was applied to determine DNA damage levels in individual H522 cells 4 days after transfection with 20 nM NUDT1 siRNA or silencer select -ve control siRNA (Scramble), or those grown in media (M) without transfection reagent/siRNA. After treatment with H₂O₂ (100 μM) for 30 min at 37° C, samples were collected either immediately or after 24 h recovery in fresh media. DNA damage levels were expressed as % tail DNA with [▣] or without [□] Fpg repair enzyme treatment. These results represent mean ± SEM of 100 individual comets. (n=1).

5.3 Exposure to ionising radiation

As mentioned in section (5.2.2), it is proposed that in addition to a role for NUDT1 in processing oxidised precursors of dNTPs that are produced endogenously within cancer cells, it would also be needed to prevent the misincorporation of damaged DNA bases after exposure to exogenous sources of oxidative stress and cancer therapeutic agents, thereby irradiation with X-ray was then assessed on the H23 NSCLC cell line as an exogenously oxidative stress source.

5.3.1 Determination of ionising radiation-induced DNA damage in NSCLC cells with and without NUDT1 knockdown

The formation of ionising radiation-induced DNA damage in H23 cells was investigated by means of Fpg-modified comet assay, to detect DNA SSBs or ALS along with oxidised purine-derived lesions.

Herein, a study was undertaken to assess whether higher DNA damage levels were recognised in NUDT1-depleted H23 cells after immediate ionising irradiation treatment (Haghdoost et al., 2005) and following 24 h recovery period. The latter duration allows enough time for ionising radiation-induced oxidised nucleotide pool precursors to be incorporated into DNA genome during the replication process. An efficient transient NUDT1 knockdown was established for 4 days by using 15 nM NUDT1-siRNA (s9030). Mock transfection (media without siRNA or transfection reagent) and silencer select -ve control siRNA (Scramble) samples were also included. Consequently, the cells were analysed following immediate exposure with or without 10 Gy X-ray, and after 24 h of cellular repair of DNA damage.

As shown in Figure 5-11, the H23 cell samples without exposure to irradiation had a 2-fold increase in Fpg sensitive sites after NUDT1 knockdown. This resembles the previous observations (Figures 4-1, 5-7, and 5-9) and occur without any further increase in DNA (SSBs/ALS) lesions (5.06% for NUDT1-deficient H23 cells) compared to corresponding untransfected (6.32%) and scramble siRNA controls (5.61%)

Similar to the H₂O₂ treatment observations, it was noticed that the relative rise in DNA (SSBs/ALS) lesions as well as Fpg sensitive sites levels immediately after X-ray irradiation did not change between NUDT1 siRNA transfected cells and silencer select -ve control siRNA (Scramble) samples. Specifically, as seen in Figure 5-11, the levels

of SSBs/ALS (Fpg-independent percentage DNA in comet tail) in H23 cells directly after 10 Gy X-ray ionising radiation were 20.35% for untransfected cells, 21.34% for scramble control, and 23.47% for NUDT1-deficient cultures; while the oxidatively damaged DNA (Fpg-dependent percentage DNA in comet tail) were 37%, 41.05%, and 33.91%, respectively. These findings also strongly indicate that NUDT1 does not have a role in preventing direct oxidation of DNA.

The H23 cell samples were also assessed at 24 h recovery point after X-irradiation treatment with or without 10 Gy. Herein, those samples that were left untreated (Figure 5-11) still have the 2-fold increase in Fpg sensitive sites after NUDT1 knockdown, which resembles the levels prior to treatment and those previously observed (Figures 4-1, 5-7, and 5-9). Such accumulations of oxidatively damaged DNA occur without any further increase in DNA (SSBs/ALS) lesions (5.59% for NUDT1-deficient H23 cells,) compared to corresponding untransfected (5.78%) and scramble siRNA controls (5.93%).

In addition, by 24 h post-ionising radiation (Figure 5-11), the remaining DNA damage levels in all samples had returned to levels nearly equivalent to those prior to X-ray irradiation exposure. Specifically, the levels of SSBs/ALS lesions were 5.61% for untransfected cells, 5.16% for scramble siRNA control, and 6.11% for NUDT1-deficient cultures. Moreover, for the oxidatively damage DNA levels, they were 7.43%, 7.85%, and 11.96%, respectively, at the end of the indicated recovery duration.

These findings indicate that NUDT1 does not have a role in altering oxidatively modified DNA levels following direct exposure to ionising radiation and even after 24 h recovery period. Overall, the above data of combined NUDT1 knockdown and H₂O₂ or ionising radiation treatments, suggest that NUDT1 does not act to protect against the dNTPs misincorporation that are oxidised via exogenous agents. Alternatively, there may be activation of other NUDT1-independent compensatory factors and/or activities have taken place, especially when very high damaged dNTPs levels are produced in an acute manner.

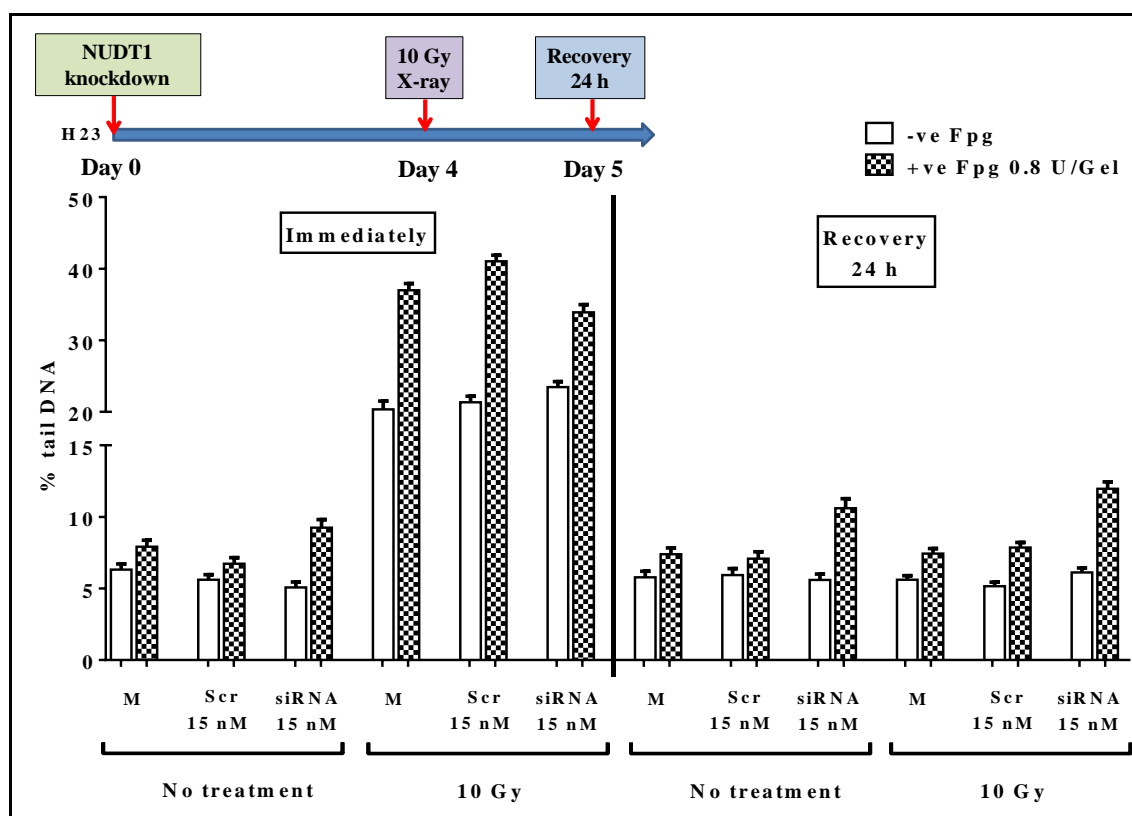


Figure 5-11 Transient NUDT1 knockdown in H23 cells does not alter oxidatively-modified DNA levels following both immediate and 24 h recovery of exposure to ionising radiation.

Fpg-modified alkaline comet assay was applied to determine DNA damage levels in individual H23 cells 4 days after transfection with 15 nM NUDT1 siRNA or silencer select -ve control siRNA (Scramble), or those grown in media (M) without transfection reagent/siRNA. For assessment of DNA damage levels immediately following irradiation, the cells embedded in LMP gels and irradiated with 10 Gy of X-rays or left untreated before proceeded with processing. Simultaneously, a set of cell cultures were irradiated with 10 Gy or left untreated before incubation at 37°C for 24 h, to allow for potential DNA repair prior to process proceeding. DNA damage levels were expressed as % tail DNA with [] or without [] Fpg repair enzyme treatment. These results represent mean \pm SEM of 400 individual comets from two independent experiments.

5.4 Exposure to gemcitabine and cisplatin

As described in the previous chapter, even though NUDT1 knockdown alone did not induce cytotoxic effects, it is proposed that it would still improve the targeting and effectiveness of current therapeutic agents and eventually help overcome frequent NSCLC therapy resistance. Gemcitabine and cisplatin are commonly used as first-line treatment for NSCLC and induce oxidative stress as well as DNA replication stress (Conklin, 2004, Donadelli et al., 2007). The basis of this study was that NUDT1 depletion promotes higher loads of oxidatively damaged DNA in NSCLC cells but not in normal cells, which once combined with therapy-induced effects selectively elevates the DNA damage levels over the threshold of cytotoxicity in NSCLC cells. To determine this, it was first required to assess the cytotoxic effect of such agents alone in NSCLC cells prior to combine with NUDT1 deficiency.

5.4.1 Sensitivity of NSCLC cells to gemcitabine induced-apoptosis (cellular viability)

To assess the sensitivity of NSCLC cell lines (H23 and H522 cells) to gemcitabine treatment and to determine which dose to apply to induce notable cytotoxic effects, the agent apoptotic dose-response curves were generated in NUDT1 proficient cells.

Herein, H522 cell lines were continuously treated with different doses of gemcitabine namely 1, 5, 10, 20, 40, 80 and 120 μM . The cytotoxic effect of gemcitabine was observed at two-time points (24 and 48 h), and the early and late apoptotic fractions were determined by Annexin V-FITC/PI apoptosis assay. As the former duration revealed no notable fraction of apoptotic cells (data not shown), 48 h incubation were selected for further experiments. In addition, the cells treated with etoposide were regarded as a positive control for induction of apoptosis. DMSO (0.5-2% v/v) and no treatment negative control (-ve) samples were also included.

After cellular exposure to 50 and 100 μM etoposide, no notable cytotoxic effects were observed for 48 h (data not shown), whereas the percentage of apoptotic cells following 150 and 200 μM etoposide were nearly 2.5 folds higher than untreated cells during the same treatment duration (P-value = 0.0021 and 0.0076, respectively) (Figure 5-13A). In addition, as shown in Figures 5-12, and 5-13A neither treatment with DMSO (0.5% v/v) nor gemcitabine up to 120 μM have evident effect compared to negative control,

untreated, cells (P-value > 0.9999). Hence, it is suggested that H522 cell line is possibly resistant to gemcitabine, at least for the applied doses.

For H23 cell line, treatment with lower concentrations of gemcitabine was evaluated (0.001, 0.01, 0.05, and 0.1 μM) as well as the above-mentioned doses for 48 h. Etoposide was also chosen as a positive control for induction of apoptosis. Here, as shown in Figures 5-12, and 5-13B etoposide exposure with 50 and 100 μM concentrations exhibited 61.12% and 65.63% apoptotic cells, respectively, and they were more significant than apoptotic cell fractions observed in untreated (4.72%) and treated cells with 0.5% v/v DMSO (5.2%) (P-value < 0.0001). Therefore, the responsiveness to etoposide was higher in H23 cells relative to H522 cell line sensitivity albeit at lower used doses. Moreover, there was a pattern of increased early and late apoptotic cell death after low concentrations of gemcitabine up to 0.05 μM (P-value < 0.05), indicative that H23 cells are to a great extent sensitive to gemcitabine. Interestingly, no further significant change was detected in the level of apoptotic fractions between all high doses up to 120 μM (Figures 5-12, and 5-13B).

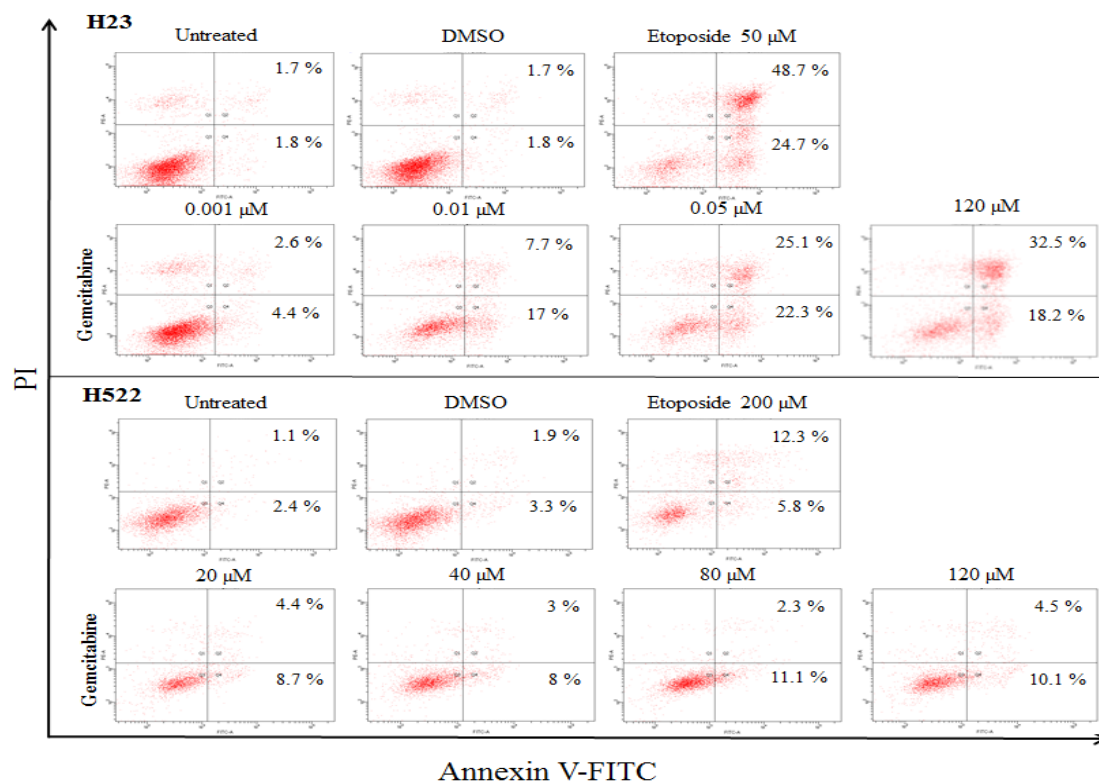


Figure 5-12 Bivariate plots of Annexin V-FITC and PI staining following gemcitabine treatment of H23 and H522 cell lines.

The indicated cells were either untreated or exposed for 48 h with increasing dose of gemcitabine. Etoposide (VP-16) treatment was also included as a positive control of apoptosis, and its vehicle control was DMSO (0.5-2% v/v). To discriminate apoptotic cells proportions, the harvested cells were dual stained with annexin V/PI and assessed by flow cytometry. For each dot plot, percentages shown in the bottom and top right quadrants are correspondent with early apoptotic cells (annexin +/PI -) and late apoptosis/necrosis (annexin +/PI +), respectively. In addition, viable cells (annexin -/PI -) are represented at low left quadrant while nuclear fragments dead cells (annexin -/PI +) are represented at upper left quadrant. No further notable increase was detected in the level of apoptotic cells induced between 0.05 and 120 μM for H23 cell line. Gemcitabine exposure for H522 cells induced nearly similar apoptotic fractions with corresponding untreated cells up to 120 μM.

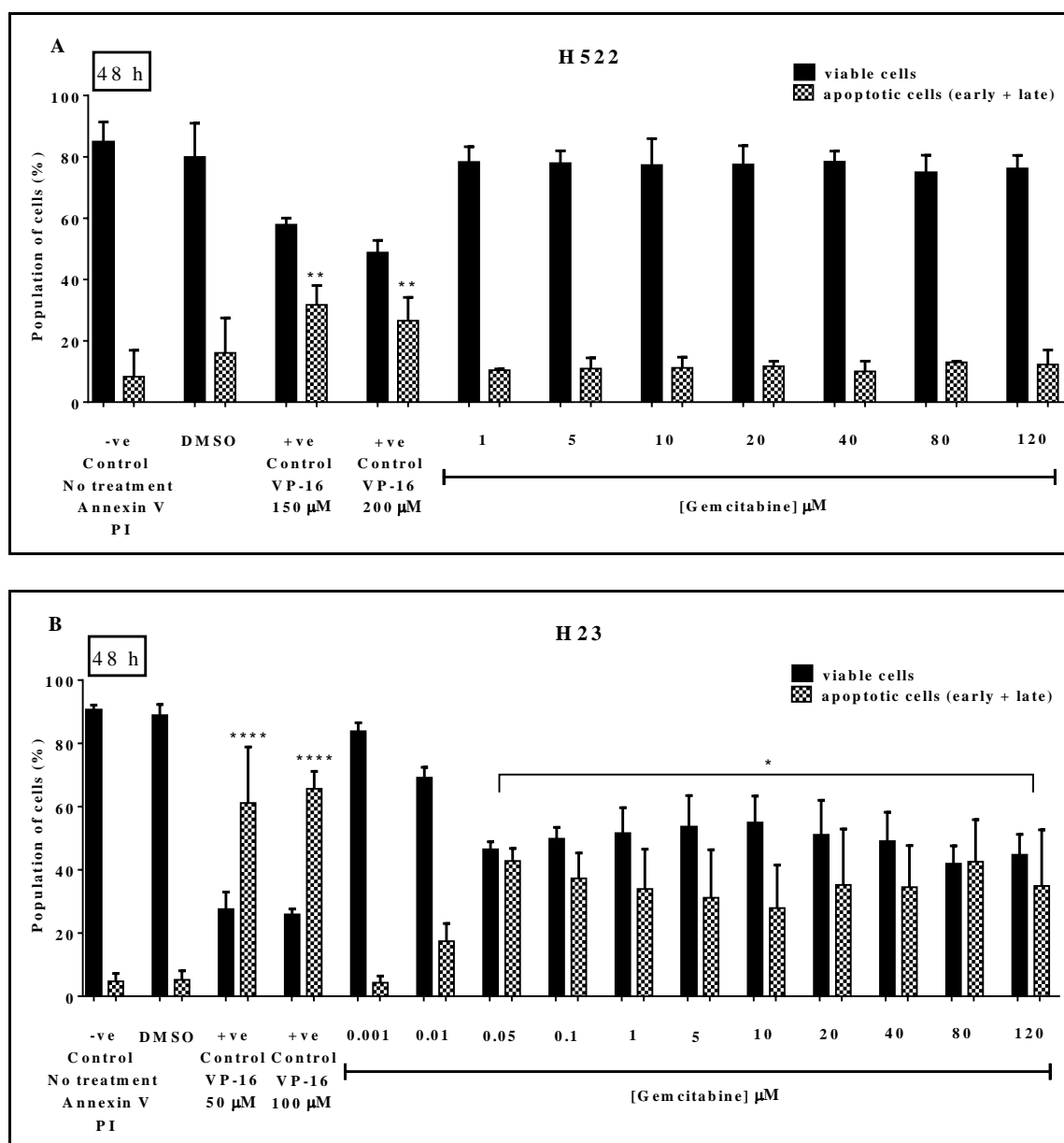


Figure 5-13 Apoptotic dose response curves to gemcitabine in H23 cells, while H522 cells are resistant to even high doses.

Annexin V–FITC/PI assay was applied to determine apoptotic cell deaths following 48 h treatment of [A] H522 and [B] H23 cells with increasing doses of gemcitabine up to 120 µM. In addition, the cells were treated with etoposide (VP-16) as a positive control of apoptosis, along with DMSO (0.5-2% v/v) and no treatment (-ve control) samples. The harvested cells were then dual stained with annexin V-FITC/PI and finally assessed by flow cytometry. The shaded bars of detected apoptotic cells represent the result during both early and late apoptosis. These data were mean \pm SD of more than three individual experiments. Asterisks indicate a significant difference relative to corresponding untreated control cells (**** P <0.0001, ** P <0.01, and * P <0.05).

5.4.2 Sensitivity of NSCLC cells to cisplatin-induced apoptosis (cellular viability)

To assess the sensitivity of NSCLC cells to cisplatin treatment and to determine which dose to apply to induce notable cytotoxic effects, the agent apoptotic dose response curves were generated in NUDT1 proficient cells.

Herein, H522 and H23 cell lines were continuously treated with increasing doses of cisplatin (1, 2, 5, 10, 20 and 50 μM). For discrimination of apoptotic cellular death (early and late apoptotic fractions), Annexin V-FITC/PI apoptosis assay was applied. Earlier experiments used DMSO as a solvent for cisplatin (data not shown), but this is known to diminish the cytotoxic action of this compound (Fischer et al., 2008), thereby, dissolving cisplatin in H_2O_2 was then considered for further experiments. Two-time points (24 and 48 h) were then observed for such drug treatment response. As the former duration revealed no notable fraction of apoptotic cells (data not shown), 48 h incubation were selected for further experiments. In addition, the cells treated with etoposide (dissolved in DMSO, final concentration of DMSO is 0.5-2% v/v) is regarded as a positive control for induction of apoptosis. DMSO (0.5-2% v/v) and no treatment negative control (-ve) samples were also included.

As described above in section 5.4.1, and 4.5, the sensitivity to etoposide was higher in H23 cells relative to H522, requiring lower doses to induce cell death (Figures 5-14, and 5-15). In addition, cisplatin treatments up to 20 μM have an incremental rise in the rate of early and late apoptotic cells, observed in a dose-dependent manner for both cell lines. Specifically, the average levels of apoptotic cells for H23 cells were 5.3% for 1 μM , 10.36% for 2 μM , 21.76% for 5%, 40.2% for 10 μM , and 61.3% for 20 μM ; while for H522 cell line they were 7.3%, 10.1%, 13.16%, 26.47%, and 36.73%, respectively. There was a trend toward significance taking place at a concentration of 5 μM for H23 cells (P value = 0.094) (Figures 5-14, and 5-15), the H522 cell line exhibited similar considerable elevation of apoptotic cells after 10 μM of cisplatin exposure compared with corresponding untreated cells (P value = 0.009) (Figure 5-15A). Despite no further H23 apoptotic cellular change with the higher dose (60.5%), apoptotic cell death still increased for H522 cells at 50 μM of cisplatin treatment (75.43%). Such build-up levels seem to occur at late rather than early apoptotic stage (Figure 5-14). It is worth to mention that inside the body, the peak plasma level of cisplatin (20 μM) accumulates instantly following recommended dose and then drops within 2 h to about 7 μM

concentration (Himmelstein et al., 1981). Therefore, an additional experiment was also performed (data not shown), during which the cells were exposed to 20 μ M cisplatin for 2 h and subsequently maintained in fresh media for further 48 h. Interestingly, about 20% increase in the level of apoptotic cells was induced in H23 cells, with no significant difference noticed for H522 cell line relative to corresponding untreated cells. The latter finding also confirms the sensitivity of H23 cells to cisplatin-induced apoptosis compared to H522 cells.

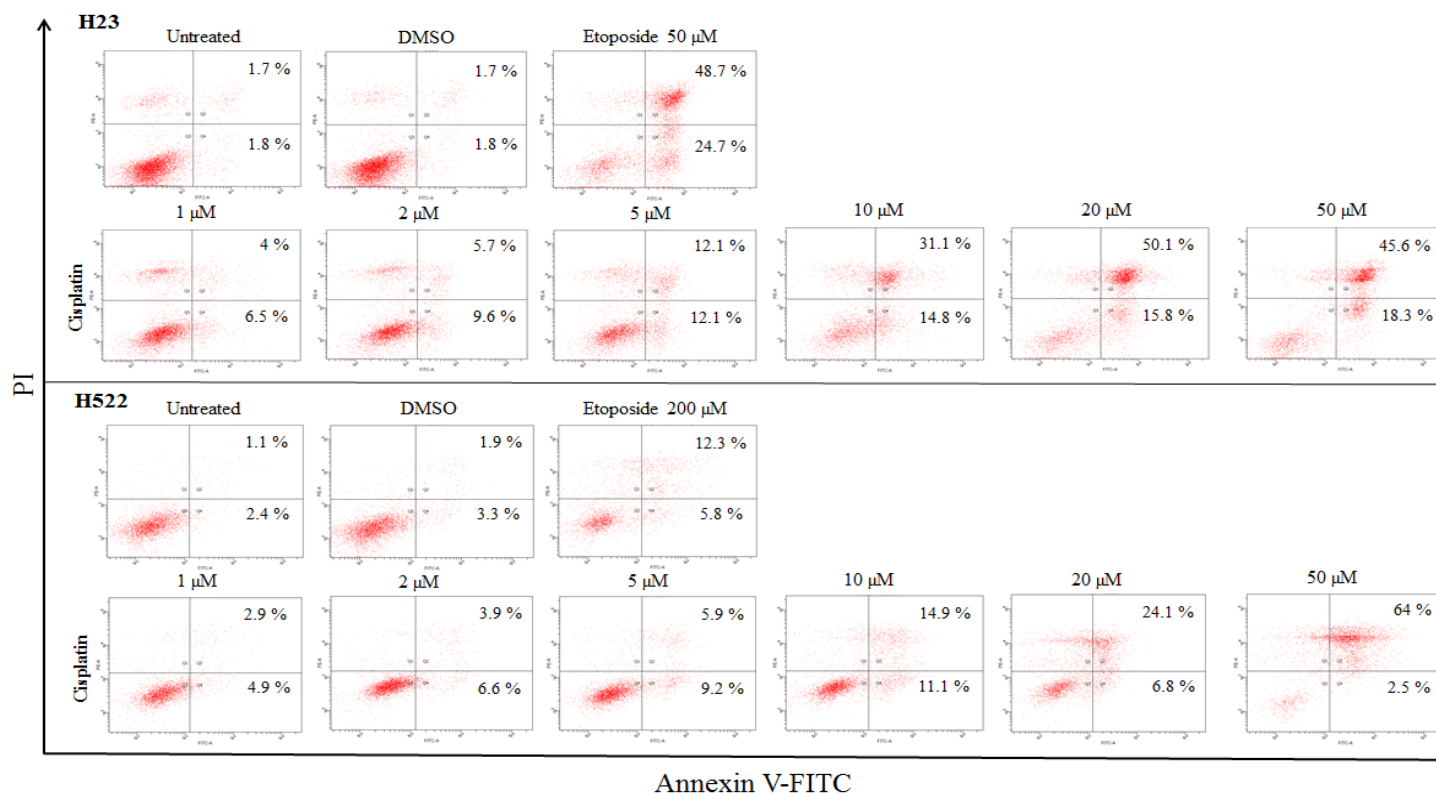


Figure 5-14 Bivariate plots of Annexin V-FITC and propidium iodide staining following cisplatin treatment of H23 and H522 cell lines.

The indicated cells were either untreated or exposed for 48 h with increasing dose of cisplatin. Etoposide (VP-16) treatment was also included as a positive control of apoptosis, and its vehicle control was DMSO (0.5-2% v/v). To discriminate apoptotic cells proportions, the harvested cells were dual stained with annexin V/PI and assessed by flow cytometry. For each dot plot, percentages shown in the bottom and top right quadrants are correspondent with early apoptotic cells (annexin +/PI -) and late apoptosis/necrosis (annexin +/PI +), respectively. In addition, viable cells (annexin -/PI -) are represented at low left quadrant while nuclear fragments dead cells (annexin -/PI +) are represented at upper left quadrant. An incremental rise in the rate of early and late apoptotic cells was obtained in a dose-dependent manner for both cell lines, yet several differences existed.

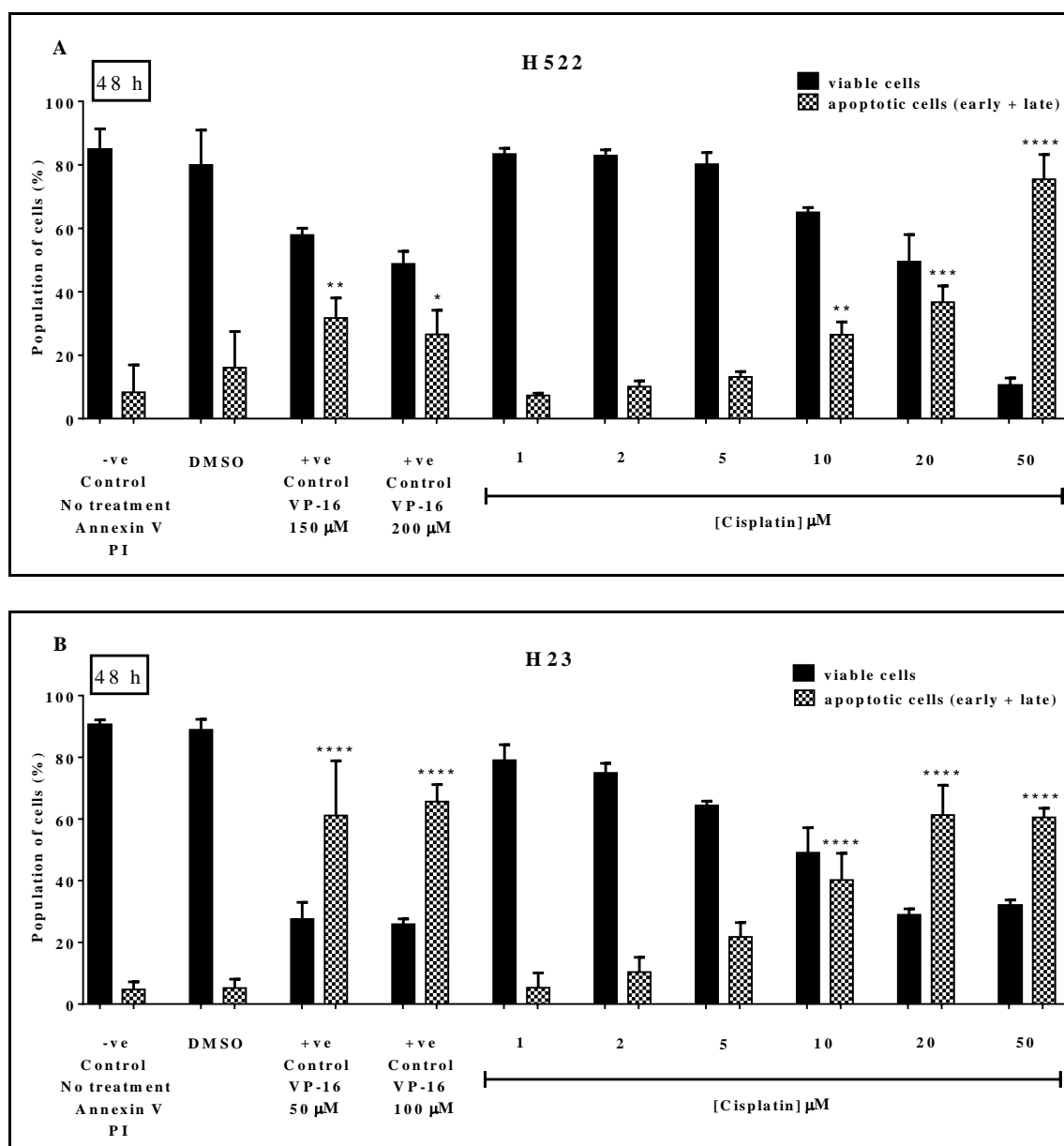


Figure 5-15 Apoptotic dose response curves to cisplatin in H522 and H23 cell lines.

Annexin V–FITC/PI assay was applied to determine apoptotic cell deaths following 48 h treatment of [A] H522 and [B] H23 cells with increasing doses of cisplatin up to 50 μM. In addition, the cells were treated with etoposide (VP-16) as a positive control of apoptosis, along with DMSO (0.5-2% v/v) and no treatment (-ve control) samples. The harvested cells were then dual stained with annexin V-FITC/PI and finally assessed by flow cytometry. The shaded bars of detected apoptotic cells represent the result during both early and late apoptosis. These data were mean ± SD of more than three individual experiments. Asterisks indicate a significant difference relative to corresponding untreated control cells (****P<0.0001, ***P<0.001, **P<0.01, and *P<0.05).

5.4.3 Potency of gemcitabine and cisplatin towards NSCLC cell lines

An achievement of dose response curve was essential for calculation of an agent concentration producing 50% response (EC_{50}). In this study, logarithmic measures for used concentrations were plotted against a drug effect.

The resistance of H522 cell line to gemcitabine perhaps prevents attainment of EC_{50} , at least for the applied doses. Although a dose-response was not forming a full sigmoidal curve after exposure of H522 to cisplatin, its EC_{50} of apoptosis was acquired by fitting to a normalized response model with variable slope ($24.66 \mu\text{M} \pm 0.0567$) (Figure 5-16A); suggesting that the introduction of cisplatin was required at higher concentration to get a maximum effective concentration.

For H23 cell line, the value of EC_{50} for apoptosis induced by gemcitabine and cisplatin was ($0.0052\mu\text{M} \pm 0.4165$) and ($7.969 \mu\text{M} \pm 0.059$), respectively. The former was estimated by using response (three parameters) model (Figure 5-16C); therefore, an introduction of extra lower doses of gemcitabine is recommended. As shown in Figure 5-16B, sufficient data points were available with clear sigmoidal shape response curve, therefore, the response with variable slope (four parameters) option was chosen to calculate EC_{50} of apoptosis for cisplatin-treated H23 cells.

This result indicated that gemcitabine and cisplatin are more potent towards H23 than H522 cell line, at least to some extent.

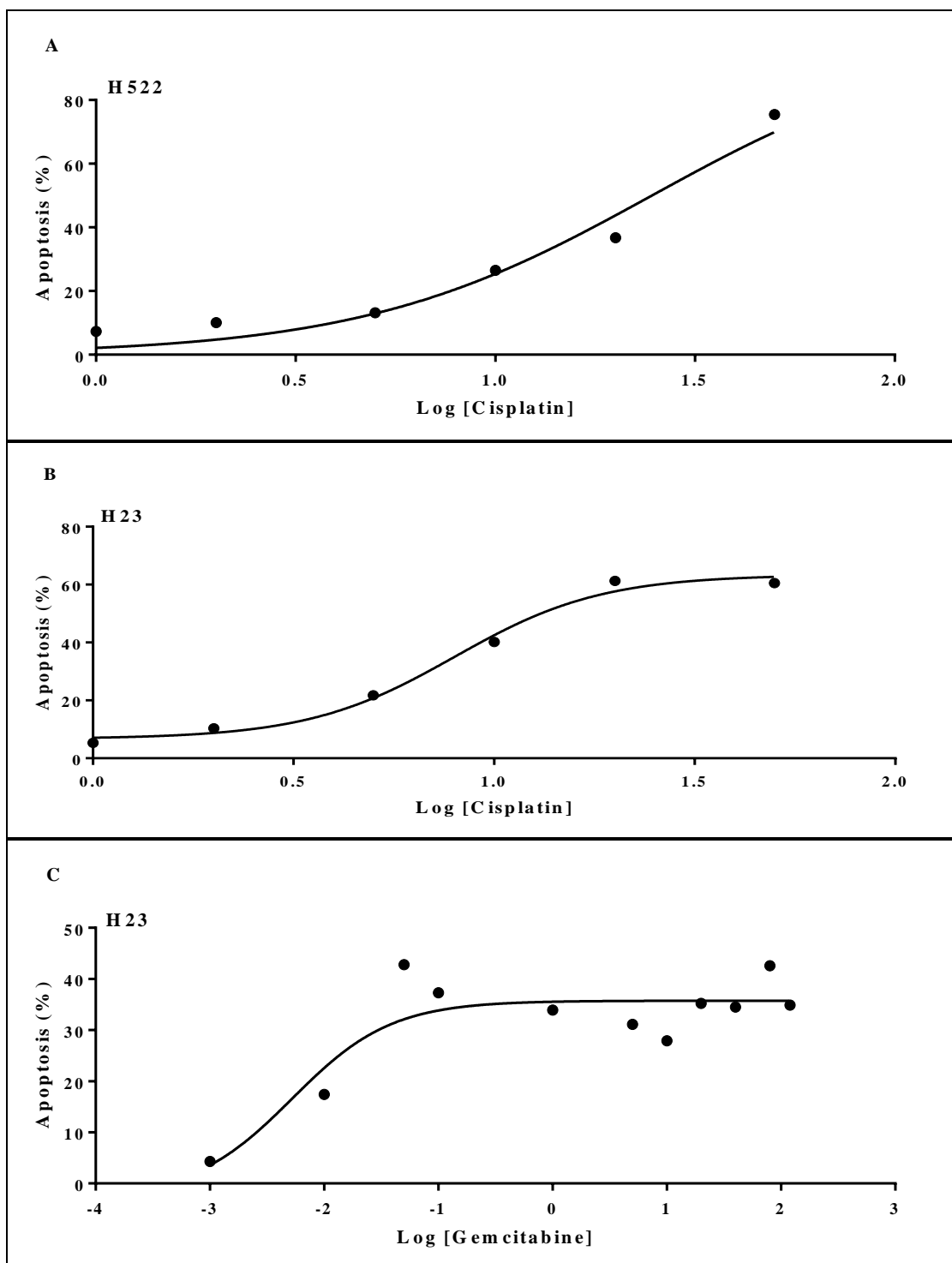


Figure 5-16 Dose-response curves for assessment of EC_{50} value of apoptosis.

Logarithmic measures for used concentrations were plotted against apoptosis response effect. The results show (A) EC_{50} of apoptosis for cisplatin of H522 was ($24.66 \mu\text{M} \pm 0.0567$), whereas for H23 cell line, the apoptosis EC_{50} values for (B) cisplatin and (C) gemcitabine were ($7.969 \mu\text{M} \pm 0.059$) and ($0.0052 \mu\text{M} \pm 0.4165$), respectively. The number of individual experiments ($n \geq 3$).

5.4.4 Determination of growth rate after cisplatin and gemcitabine exposure (growth inhibition)

The growth rate of H23 and H522 cell lines was studied and cell doubling times determined by Coulter counter. The growth assessed over three days interval by counting cell numbers at 24, 48 and 72 h. The doubling times for H23 and H522 cell lines were determined at the exponential phase of cell growth (Figures 5-17, and 5-18) as described in section 2.2.6. They were estimated to be 23.3 and 38.6 h for H23 and H522 cells, respectively.

Following cisplatin and gemcitabine treatment with indicated concentrations in section 2.2.6, H522 and H23 cell growth was determined using a Coulter counter as shown in Figures 5-17, and 5-18. Alteration in cell growth rates was more manifested at day three than other time points following exposure. In regard to H23 cells, the slow cell proliferation after cisplatin treatment was notable relative to untreated cells, with a significant reduction in growth at concentration $\geq 2 \mu\text{M}$ ($P\text{-value} \leq 0.001$) (Figure 5-17A). Gemcitabine at $0.001 \mu\text{M}$ showed no difference in growth compared with untreated H23 cells ($P\text{-value} = 0.1$) (Figure 5-17B). However, following higher doses up to $1 \mu\text{M}$, such cells exhibited significant growth cessation during the treatment period (at day 3, $P\text{-value} \leq 0.0001$). Similarly, cisplatin-induced growth inhibition was also detected in H522 cells with indicated doses (Figure 5-18A), almost one up to four-fold significant lower cell numbers at concentrations ($1\text{-}20 \mu\text{M}$) in day 3 relative to untreated cells ($P\text{-value} \leq 0.0188$). In addition, H522 cells did not proliferate after $0.01\text{-}80 \mu\text{M}$ gemcitabine, exhibiting plateau stasis during treatment interval for all used doses ($P\text{-value} \leq 0.0001$) (Figure 5-18B).

In order to assess the (IC_{50}), the drug dose which inhibits cell growth by 50%, the time point of 3 days was selected. The logarithm of used concentrations was plotted against the cell growth percentage versus untreated control cells. For H23 cells, as shown in Figure 5-17C, sigmoidal shape curves were obtained after both cisplatin and gemcitabine treatment with IC_{50} ($1.12 \pm 0.0838 \mu\text{M}$) and ($0.0035 \pm 12.74 \mu\text{M}$), respectively. These values were calculated by using the response with variable slope (four parameters) option to plot the inhibitory curves, whereas the cisplatin IC_{50} of H522 ($1.403 \pm 0.0548 \mu\text{M}$) was measured by fitting to a normalized response model, as data obtained was ineffective to form a full sigmoid curve (Figure 5-18C). Although

dramatic reductions were seen in H522 cell growth (52% for 0.001 μM and 70% for 0.01 up to 80 μM) following treatment with gemcitabine; the IC_{50} could not be established (Figure 5-18C). This finding was, perhaps, attributed to plateau inhibitory response at least for the applied gemcitabine doses, suggesting lower concentrations to be tested for further work. By this way, the results showed that cisplatin-induced notable proliferation reduction in H23 earlier than H522 cells. In addition, the growth reduction and cytostasis was exhibited at the lower used gemcitabine concentrations for H23 cells, or even at less doses for H522 cells.

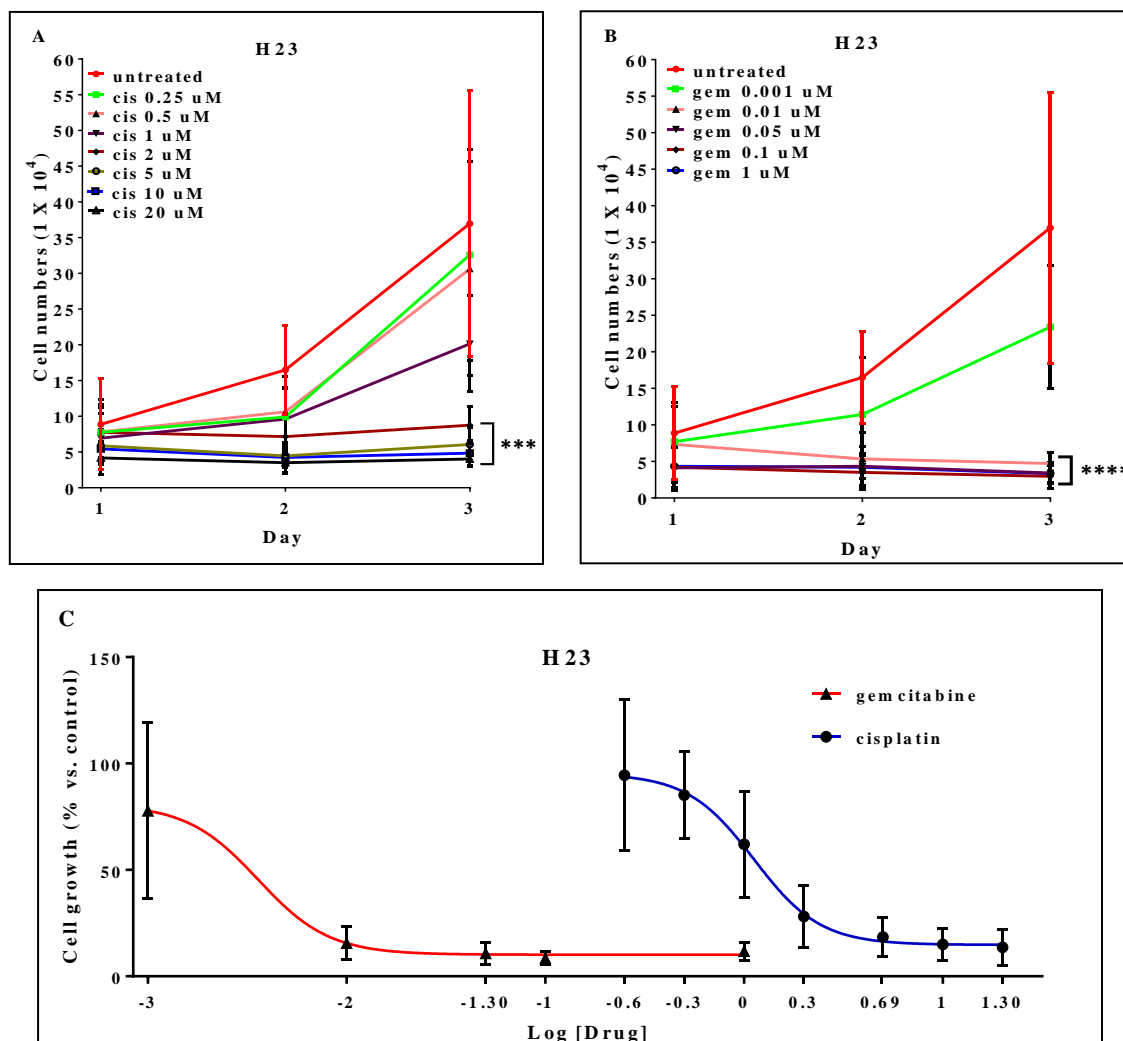


Figure 5-17 The growth inhibitory response following cisplatin and gemcitabine treatment in H23 cells.

Coulter counter was applied to determine the number of cells within the sample. The indicated cell was either untreated or exposed to (A) cisplatin or (B) gemcitabine for 24, 48 and 72 h with incremental doses. At day 3 time point, (C) logarithm of used concentrations was plotted against the cell growth percentage versus untreated control cells, wherein the obtained IC_{50} of cisplatin and gemcitabine were $(1.12 \pm 0.0838 \mu\text{M})$ and $(0.0035 \pm 12.74 \mu\text{M})$, respectively. These data were mean \pm SD of five individual experiments. Asterisk indicates a significant difference relative to corresponding untreated control cells (** $P < 0.001$, and **** $P < 0.0001$).

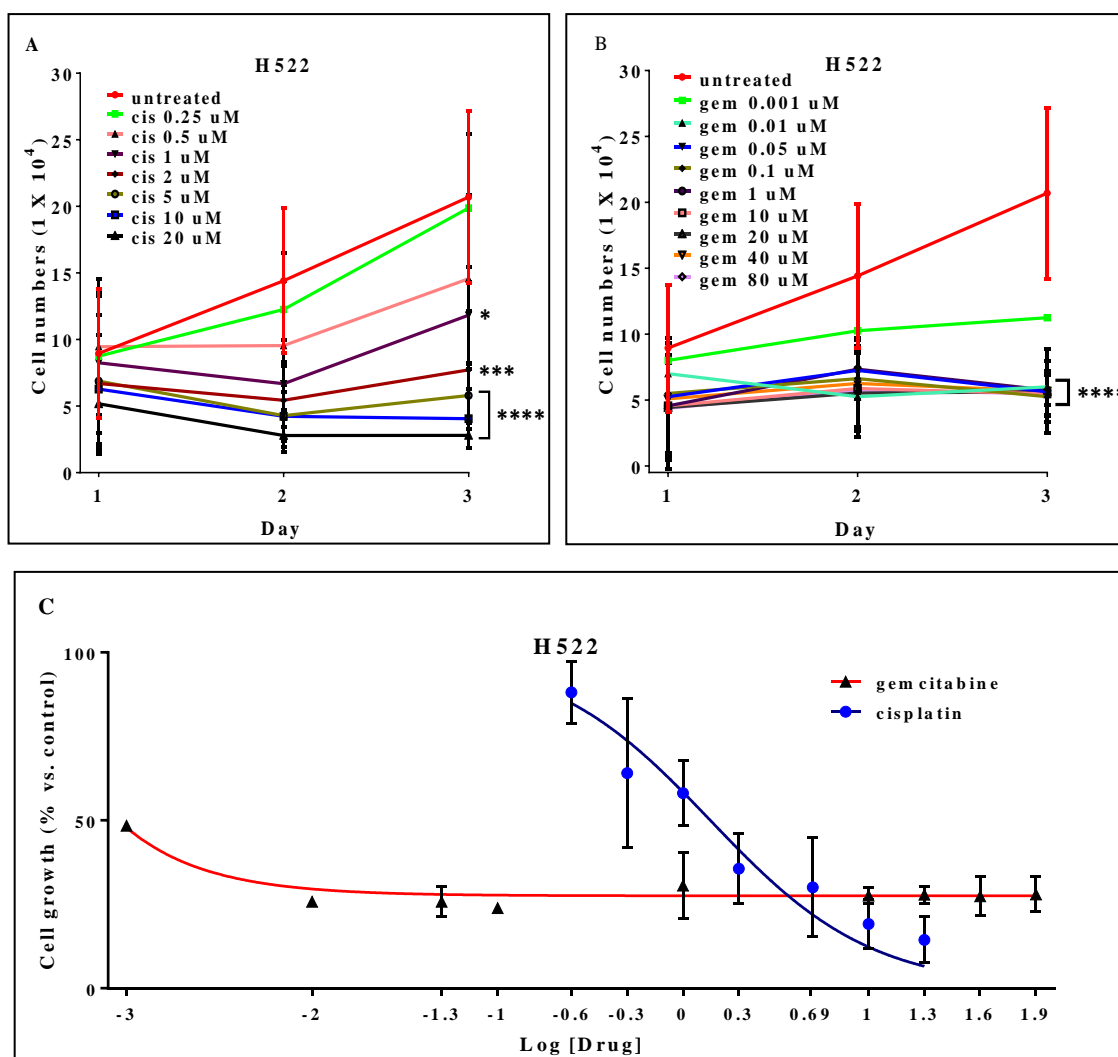


Figure 5-18 The growth inhibitory response following cisplatin and gemcitabine treatment in H522 cells.

Coulter counter was applied to determine the number of cells within the sample. The indicated cell was either untreated or exposed to (A) cisplatin or (B) gemcitabine for 24, 48 and 72 h with incremental doses. At day 3-time point, (C) logarithm of used concentrations was plotted against the cell growth percentage versus untreated control cells, wherein the obtained IC_{50} of cisplatin was $(1.403 \pm 0.0548 \mu\text{M})$. Gemcitabine exhibited a constant 70% growth inhibition at all concentrations with nearly 70% growth reduction (0.01 up to 80 μM). These data were mean \pm SD of at least four individual experiments; except for gemcitabine 0.001, 0.01, 0.05, and 0.1 μM ($n = 1$ or 2 experiments). Asterisk indicates a significant difference relative to corresponding untreated control cells (* $P < 0.05$, *** $P < 0.001$, and **** $P < 0.0001$).

5.4.5 Determination of apoptotic effect induced by gemcitabine or cisplatin when combined with NUDT1 knockdown in NSCLC cells

To conduct combination experiments of therapeutic agent treatments with the NUDT1 knockdown, the tested drug concentrations were selected from the apoptotic dose response curves (Figures 5-13, and 5-15) that gave equivalent effects between cell lines, inducing 20-25 % apoptosis as a single agent. Therefore, according to the previous results in section 5.4.1, and 5.4.2, it seemed that 48 h treatment with 5 and 10 μM cisplatin were appropriate to carry out further experiments for H23 and H522 cell lines, respectively. In addition, H23 treated cells with gemcitabine at 0.01 μM for 48 h induced the significant apoptotic cellular effect. Although H522 cells are resistant to even very high doses of gemcitabine during the above period; 40 μM concentration was chosen for these experiments.

Cells were exposed to the indicated drug concentrations following transient NUDT1 protein depletion. Herein, H23 and H522 cells were transfected with 15 and 20 nM NUDT1 siRNA (s9030), respectively, for 2 days prior to drug treatment with further 48 h. Another NUDT1 siRNA (s194633) was also verified in H23 cells by transfection with 15 nM for 3 days before therapeutic agent exposures with selected time points.

In every experiment, the cells transfected with corresponding concentrations of silencer select -ve control siRNA (Scramble) along with mock transfection samples (growing cells in media without siRNA and transfection reagent) were usually processed with and without the indicated drugs treatment. Furthermore, etoposide (VP-16) at concentrations of 50-150 μM for 48 h act as a positive control of apoptosis. DMSO (0.5-1.5% v/v) treated samples were also included. An early and late apoptotic fraction were determined after dual staining with Annexin V-FITC / PI and analysed using flow cytometry.

As shown in Figure 5-19, the exposure of H23 cells to 50 μM etoposide for 48 h exhibited 42.8% apoptotic cells, which was more significant than apoptotic cell fractions in untreated (4.6%) and treated samples with 0.5% v/v DMSO (5.1% apoptotic cells) (P-value < 0.0001). Moreover, there was a rise in cellular apoptotic levels for both scramble (12.16%) and NUDT1 siRNA (10.96%) transfected samples without any treatment relative to corresponding no siRNA negative control sample (4.6%), like the previous observations in Figures 4-6, and 4-7. In addition, the average levels of

apoptotic cell death after the combination of NUDT1 knockdown with either gemcitabine (16.13%) or cisplatin (16.3%) treatments did not display any considerable increase in cellular death, relative to their corresponding scramble siRNA control and treatments (23.86%, and 25.7%, respectively) or no siRNA treated samples (15.71%, and 16.21%, respectively) (Figure 5-19).

The low responsiveness and resistance of H522 cells to etoposide was also noticed with the higher treatment dose required as a positive control of apoptosis. As shown in Figure 5-20, the apoptotic fractions level following 48 h exposure to 150 μ M etoposide was 25.1%; and significantly higher than untreated (2.6%) and treated cells with 1.5% v/v DMSO (3.5%) (P-value < 0.0001). Similar to the previous observations in Figures 4-6, 4-7, and 5-19, the rise in cellular apoptotic levels occurred in both scramble (10.42%) and NUDT1 siRNA (9.57%) transfected samples without any treatment relative to corresponding no siRNA negative control sample (2.6%). In addition, there was no observable augmentation of current therapies following NUDT1 inhibition (Figure 5-20), as a combination of NUDT1 knockdown with either gemcitabine or cisplatin treatments did not cause a significant additional increase in H522 cell death levels (33.36%, 36.23%, respectively) relative to their corresponding scramble siRNA control and treatments (34.2%, and 50.83%, respectively). However, following such gemcitabine or cisplatin treatments, the above average result levels of apoptotic cell death for both NUDT1siRNA and scramble siRNA transfection were considerably 2- to 3-fold higher than the corresponding no siRNA treated samples (10.6% for no siRNA and gemcitabine treatment, and 9.76% for no siRNA and cisplatin). These results suggest that H522 cells are sensitive to sample transfection process with consecutive less viable cells outcome relative to corresponding untransfected cells when combined with gemcitabine and cisplatin treatments.

To confirm the result, a similar finding was observed when another NUDT1 siRNA (s194633) was tested in H23 cells, in combination with/without cisplatin or gemcitabine treatments (Figure 5-21). Specifically, there was an increase in cellular apoptotic levels for both scramble (8%) and NUDT1 siRNA (8.4%) transfected samples without any treatment relative to corresponding no siRNA negative control sample (4.1%). Moreover, the average levels of apoptotic cell death after the combination of NUDT1 knockdown with either gemcitabine (30.5%) or cisplatin (37.3%) treatments did not exhibit any considerable increase in cellular death, relative to their corresponding

scramble siRNA control and treatments (27.9%, and 34.9%, respectively) (Figure 5-21). However, following such gemcitabine or cisplatin treatments, the above average result levels of apoptotic cell death for both NUDT1siRNA and scramble siRNA transfection were considerably 2-fold higher than the corresponding no siRNA treated samples (15.71% for no siRNA and gemcitabine treatment, and 16.21% for no siRNA and cisplatin treatment), which are similar findings to the other used siRNA (Figure 5-19) to great extent.

Overall, NUDT1 knockdown alone does not induce apoptotic cell death, which was described thoroughly in the previous chapter. Despite our predictions, the above data also show that no augmentation in gemcitabine or cisplatin cytotoxicity occur after targeting NUDT1 enzyme in NSCLC cells, suggesting the NUDT1 inhibition does not sufficiently sensitise to the effects of such therapeutic agents.

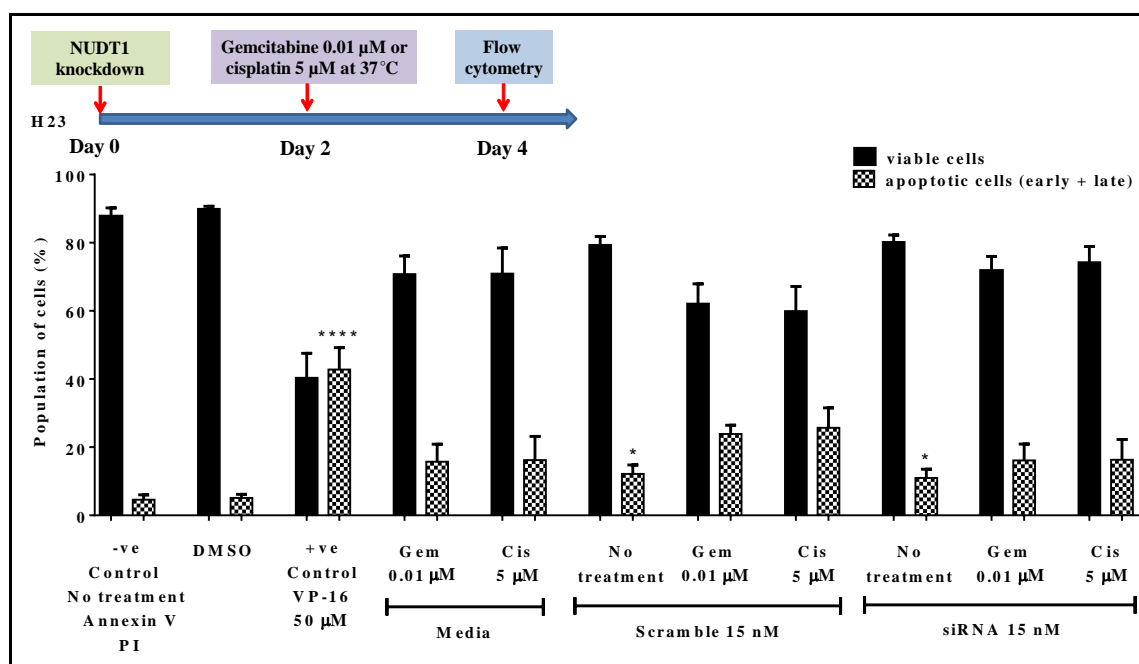


Figure 5-19 Transient NUDT1 knockdown does not enhance the cytotoxicity of gemcitabine and cisplatin treatments in H23 cells.

Annexin V–FITC/PI assay was applied to determine apoptotic cell deaths. H23 cells were grown in media without transfection reagent/treatment exposure, or transfected for 4 days in total with 15 nM NUDT1 siRNA or silencer select -ve control siRNA (Scramble). Two days after transfection, gemcitabine (Gem 0.01 μM) or cisplatin (Cis 5 μM) were added to the appropriate cultures for the remaining time interval. DMSO (0.5% v/v) and etoposide (VP-16); as a positive control of apoptosis; for 48 h were also applied. The harvested cells were then dual stained with annexin V-FITC/PI and assessed by flow cytometry. The shaded bars of detected apoptotic cells represent the result during both early and late apoptosis. These data were mean ± SD of more than three individual experiments. Asterisks indicate a significant difference relative to corresponding untreated control cells without transfection (****P<0.0001, *P<0.05).

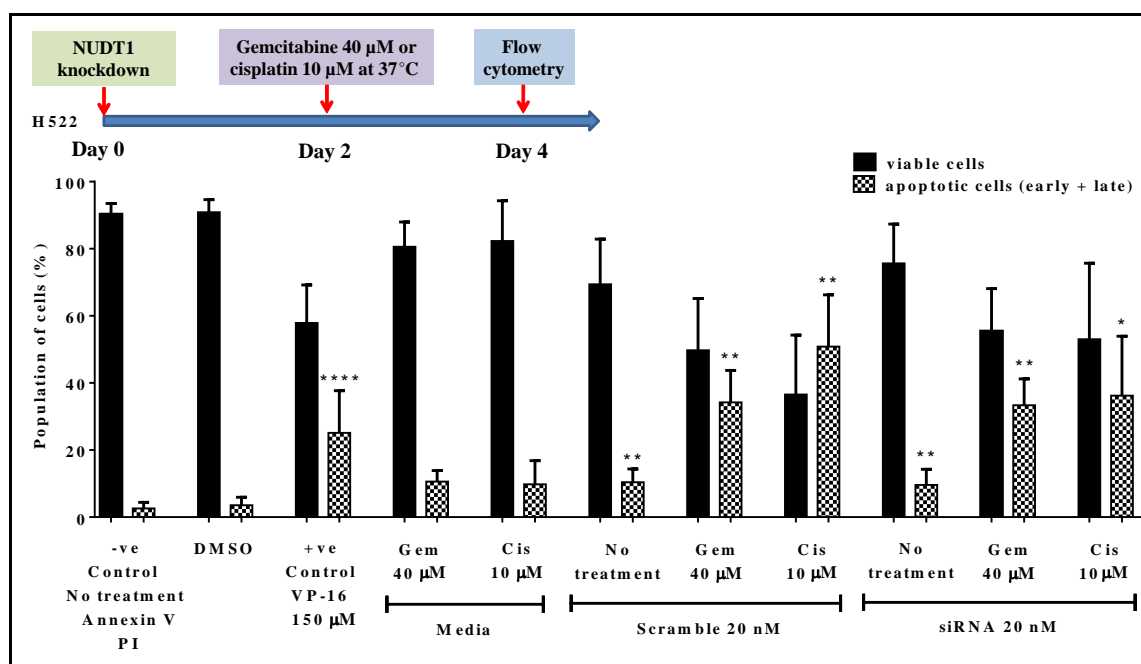


Figure 5-20 Transient NUDT1 knockdown does not enhance the cytotoxicity of gemcitabine and cisplatin treatments in H522 cells.

Annexin V–FITC/PI assay was applied to determine apoptotic cell deaths. H522 cells were grown in media without transfection reagent/treatment exposure, or transfected for 4 days in total with 20 nM NUDT1 siRNA or silencer select -ve control siRNA (Scramble). Two days after transfection, gemcitabine (Gem 40 μM) or cisplatin (Cis 10 μM) were added to the appropriate cultures for the remaining time interval. DMSO (1.5% v/v) and etoposide (VP-16); as a positive control of apoptosis; for 48 h were also applied. The harvested cells were then dual stained with annexin V-FITC/PI and assessed by flow cytometry. The shaded bars of detected apoptotic cells represent the result during both early and late apoptosis. These data were mean \pm SD of more than four individual experiments. Asterisks indicate a significant difference relative to corresponding untreated or treated cells without transfection (**** $P < 0.0001$, ** $P < 0.01$, * $P < 0.05$).

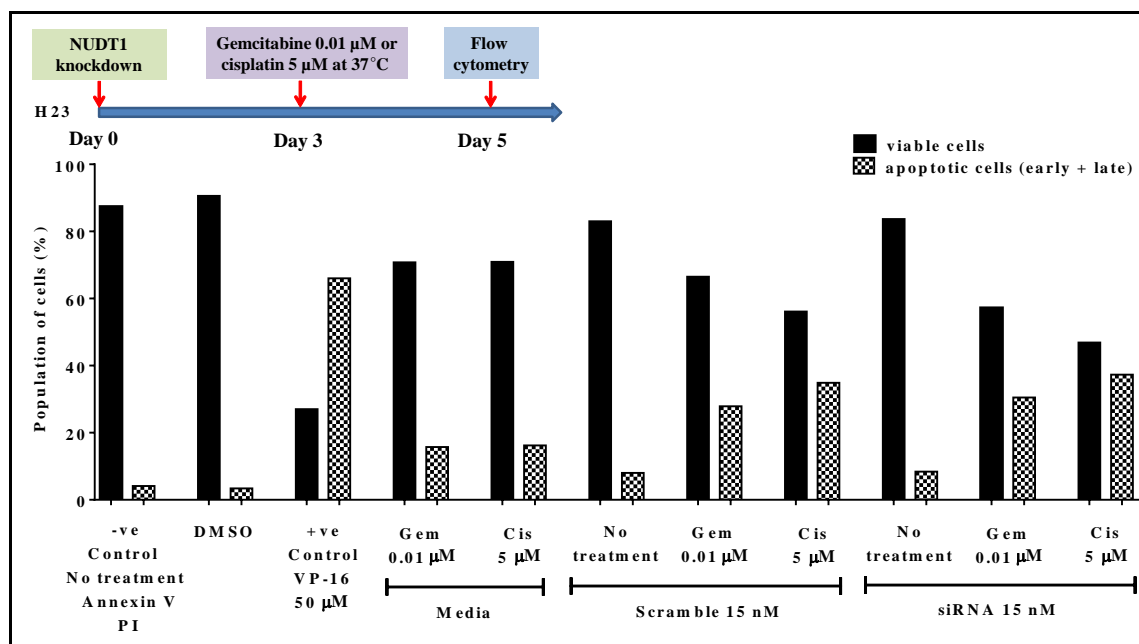


Figure 5-21 Transient NUDT1 knockdown does not enhance the cytotoxicity of gemcitabine and cisplatin treatments, confirmed by transfecting H23 cells with other NUDT1 siRNA.

Annexin V–FITC/PI assay was applied to determine apoptotic cell deaths. H23 cells were grown in media without transfection reagent/treatment exposure, or transfected for 5 days in total with 15 nM NUDT1 siRNA (s194633) or silencer select -ve control siRNA (Scramble). Three days after transfection, gemcitabine (Gem 0.01 μM) or cisplatin (Cis 5 μM) were added to the appropriate cultures for the remaining time interval. DMSO (0.5% v/v) and etoposide (VP-16); as a positive control of apoptosis; for 48 h were also applied. The harvested cells were then dual stained with annexin V-FITC/PI and assessed by flow cytometry. The shaded bars of detected apoptotic cells represent the result during both early and late apoptosis (n=1).

5.5 Discussion

Regardless of the absence of NSCLC cytotoxicity after NUDT1 knockdown, as observed in the last chapter, it was still proposed that targeting NUDT1 enzyme might be an effective way when combined with exogenous oxidative stress sources or chemotherapeutic agents, promoting additional DNA damage and ultimately apoptotic cell death. To determine this, it was first undertaken to assess the sensitivity of NSCLC cell lines (H23 and H522 cells) to such agents prior to protein depletion.

The cytotoxic effect on p53-deficient H522 cells was of particular interest, as relative to H23 and A549 this cell line seems highly resistant to etoposide and cisplatin, and is resistant to even very high doses of gemcitabine and H₂O₂. Additionally, in H23 cell line, gemcitabine engendered a saturation dose response curve with a plateau of apoptotic cells at nearly 40% (Figures 5-12, and 5-13). As expected, the growth reduction and cytostasis were exhibited at the lower used gemcitabine doses for both H23 and H522 cell lines (Figures 5-17, and 5-18). At the low concentration, gemcitabine produces rapid depletion of deoxyribonucleotide pools, subsequent inhibition of DNA synthesis and extended S phase arrest without activation of checkpoint 1 (Chk1) (Montano et al., 2013). Once adequate cells accumulate at S/G2 and initiate homologous recombination, a delay administration of a Chk1 inhibitor could provoke gemcitabine sensitivity; as arrested cells become Chk1 dependent with subsiding of replication forks and cell death (Montano et al., 2013).

The plateau pattern of survival was also observed previously in pancreatic cells with p53 mutations, suggesting the occurrence of drug resistance mechanism in comparison with another compound that elicited an entire growth inhibition response (Donadelli et al., 2007). Different mechanisms might describe the sensitivity to gemcitabine that involved its transport, activation, and metabolism as well as alteration of genes that regulate apoptosis (Bepler et al., 2006, Donadelli et al., 2007).

Recently, the basal expression of human equilibrative nucleoside transporter 1 (*hENT1*) gene has noticed to be high in H23 cells with low IC₅₀ value (0.051 μM) which directly correlated with sensitivity to gemcitabine in NSCLC (Achiwa et al., 2004). Moreover, reduced level of deoxycytidine kinase (*dCK*) expression was associated with gemcitabine acquired resistance model (Achiwa et al., 2004). However, another protein transporter which is encoded by multidrug resistance protein 5 (*ABCC5*) gene, seems to

be low in H23 cells and its level inversely associated with gemcitabine sensitivity (Oguri et al., 2006). It is also noteworthy that the ribonucleotide reductase subunit M1 (*RRM1*) gene has a role in determining gemcitabine efficacy, as an inverse correlation existed between its expression and sensitivity to gemcitabine along with apoptosis in knocked-in and knocked-out transfect H23 cells (Bepler et al., 2006). Lung cancer patients with low expression of *RRM1* and excision repair cross-complementation group 1 (*ERCC1*) genes, have shown better prognosis and tumour response to gemcitabine (Bepler et al., 2006). Although the accountability of K-RAS mutation was not established previously, other factors, such as extended doubling time in H522 cells [108 h (Zhou et al., 2010), 38.6 h in our study] and its deletion status of p53 were addressed and might contribute to gemcitabine resistance (IC_{50} value 1000 μ M) irrespective of the *RRM1* level (Zhou et al., 2010). Furthermore, a recent study in colonic and pancreatic cancer cell lines has shown that apoptosis mediated by gemcitabine is mainly depended on p53 and proapoptotic p53 upregulated modulator of apoptosis (PUMA) transcriptions, coexisted with a remarkable decline in p21 and 14-3-3 sigma proteins (Hill et al., 2013). In NSCLC, gemcitabine-induced apoptosis has been achieved after inhibition of NF- κ B with the release of cytochrome c followed by caspases 9 and 3 activations (Jones et al., 2002). If this is the case, the molecular action behind gemcitabine-induced apoptosis needs to be clarified, yet its correspondence was attained with activation of extracellular signal-regulated kinases (ERK), and inhibition of both AKT and anti-apoptotic Bcl-2 with caspase 9 activation, in p53 independent manner (Chang et al., 2004). p38 MAP kinase signaling might also contribute to cellular execution induced by gemcitabine (Habiro et al., 2004).

H522 cells were also exhibited lower sensitivity to etoposide relative to other cell lines, requiring higher doses to be used as a positive control for apoptosis. It was suggested that an absence of endogenous protein in H522 cells known as Transforming growth factor-beta-induced protein ig-h3 (Beta ig-h3), perhaps, was attributed to such resistance of etoposide-induced cell death (Zhao et al., 2006). However, higher sensitivity in H23 and A549 NSCLC cell lines was observed to etoposide-induced apoptosis when used as a positive control, compared to MRC-5 cells. This may be due to inherent DDR defects or elevated levels of endogenous DNA replication stress leading to an increased vulnerability to further DNA damage in some NSCLC cell lines.

This study also provides some evidence for the resistance of H522 cells to cisplatin-induced apoptosis, as well as growth inhibition, in comparison with H23 cells. The low level of dihydrodiol dehydrogenase (DDH) enzyme, especially isoform 1, was mentioned as a possible responsible factor for the sensitivity of H23 cells to cisplatin, with no correlation in regard to ERCC1 level (Chen et al., 2010). However, a clinical study conducted for patients suffer from NSCLC has recognized the benefit of adjuvant cisplatin therapy in those with low ERCC1 level (Olaussen et al., 2006). In addition, it was observed that there were high level of ERCC1 in H522 compared with H23 cells (Zhou et al., 2010). ERCC1 is involved in DNA repair of an interstrand cross-linked. Therefore, this may be the basis of the relative resistance of H522 cells, to some degree. The role of another repair enzyme (Rad51), implicated in homologous recombination DNA repair, was also mentioned as a determinant marker of cisplatin resistance (Takenaka et al., 2007). According to a current study, an essential meiotic structure-specific endonuclease 1 (Eme 1) which forms a complex with Mus81 protein, has anticipated as a more accurate measure than ERCC1 or Rad51. Those cells with low level of Eme1, which involved in replication-coupled DNA repair of interstrand crosslinked, were more sensitive to cisplatin (Tomoda et al., 2009). H522 cells seem to have moderate to low level of Eme1. Furthermore, a protein that forms a tight junction linking epithelial cells, claudin-7, has undetected expression level in H522 cells. A dramatic increase in the proportion of cisplatin-induced apoptotic cells was pronounced previously, once transfecting caludin-7 into H522 cells. This has been accompanied by activation of caspases 8 and 3 with increased expression of a cleaved poly adenosine 5'-diphosphate ribose polymerase (PARP) (Hoggard et al., 2013). Collectively, these results are consistent with previous observations for apoptosis and inhibition of growth, at least to some degree; nevertheless, different administration time points, applied techniques, and obtained value magnitudes were recognized relative to the majority of the others. In addition, the obtained data in this project further support the resistance of H522 NSCLC cell line to various genotoxic agents

Unexpectedly, there was no further increase in oxidatively damaged DNA in NUDTI depleted NSCLC cells both immediately and 24 h recovery after exposure to H₂O₂ or ionizing radiation. This observation suggests that NUDT1 enzyme is not needed to prevent genomic instability during the induction of exogenous oxidative stress, even though such treatments could generate free radicals which are vulnerably attacked the

nucleotide pool (Topal and Baker, 1982, Haghdoost et al., 2005). By this way, it is uncertain why NUDT1 would protect against misincorporation of endogenously-induced oxidized nucleotide precursors in cancer cells but not dNTPs damaged through exogenous agents. One possible suggestion is that the induction of acute oxidative stress in NUDT1 deficient cells might cause compensatory pathways activation which are not induced during the lesser stressful conditions initiated within cancer cells. Such compensatory outcomes might be obtained by either other currently undetermined 8-oxodGTPase activities, or possibly hOGG1 that was reported earlier to compensate for NUDT1 activity after H₂O₂-induced oxidative DNA bases damage (Ke et al., 2014). At that time, strong compensation was provided for NUDT1 knocked down in a human embryonic pulmonary fibroblast cell line (HFL) following H₂O₂ treatment as the levels of hOGG1 mRNA raised about 52%, leading to unaltered accumulation of 8-oxodG levels relative to those corresponding untransfected cells (Ke et al., 2014). The second alternative explanation is that the available small amount of residual NUDT1, perhaps, allow responding to acute oxidative stress enhanced by exogenous source, whereas, insufficiently remains during long terms of chronic stressful condition.

In term of cell viability, H23 and H522 cell lines have responded similarly to NUDT1 deficiency without any significant change in the induction of cellular apoptosis, as already discussed thoroughly in the previous chapter. However, it was still proposed that targeting NUDT1 could be an effective approach to enhance current therapeutic strategies that induce oxidative stress, DNA replication stress, as well as DNA damage. Surprisingly, it is again demonstrated that NUDT1 depletion in H23 and H522 cells does not increase the apoptotic death levels when combined with cisplatin and gemcitabine treatments (Figures 5-19, and 5-20). These findings were in support with similar observations when a different siRNA directed against human NUDT1 was also used in H23 cells (Figure 5-21). To our knowledge, this is the first time that such combined treatments with NUDT1 inhibition have been tested. Collectively, these findings are unexpected, yet still of particular interest in the cancer field, as they suggest that inhibiting NUDT1 has possibly no effective therapeutic role for NSCLC patients even if utilized in combination treatments.

Here, perhaps, several reasons might explain why the anticipated effects of NUDT1 knockdown on cancer cell viability were observed, as well as, the contradiction between our data and previous literature observations. Simply, the NUDT1 knockdown levels in

this study were not sufficient enough to elicit NUDT1 deficiency, leading to subsequent cellular apoptosis. Alternatively, the presence of other factors such as currently undefined 8-oxodGTPase activities that may be able to sufficiently compensate for NUDT1 activity; or even by hOGG1 which previously shown to compensate for NUDT1 to suppress the levels of oxidised DNA base after H₂O₂ treatment (Ke et al., 2014). Nevertheless, this is not the case of notice disparities to be certain, as shown in Figures (4-1, 4-2, 4-3, 5-7, 5-8, 5-9, 5-10, and 5-11), the increased levels of oxidised DNA bases were 1.5 to 2-fold in NSCLC cell lines which seem comparable to that in earlier studies that did determine loss of cellular viability (Rai et al., 2009, Gad et al., 2014, Giribaldi et al., 2015). On the other hand, the discrepancy in obtained results may be due to the use of different techniques to detect cell viability in current study when compared to most other publications. Here, the annexin V/PI apoptosis assay was applied to quantify the apoptotic cell levels, whereas the majority of past work used cell growth and/or senescence assay including calculation of population doubling time, colony formation ability, and detection of senescence-associated beta-galactosidase activity.

A clonogenic assay is a standard technique to determine the effectiveness of specific agents on the cells proliferation and survival. It is considered as most intensively used *in vitro* method in cancer research laboratories to test the proliferative capacity of tumour cells following radiation or anticancer drug treatments (Hoffman, 1991, Buch et al., 2012). Despite it has been proven to correlate with clinical response, there are certain drawbacks for the clonogenic assay usage. Accordingly, it was found low cellular plating efficiency, almost 30% out of 14000 involved patients with tumours had valuable results (Von Hoff, 1990). These data also showed that cancers of ovary, uterus, kidney, brain, and mesothelioma are best in term of growth in a culture system. In addition, the assay is time-consuming, can take several weeks to set up before obtaining the results (Hoffman, 1993). Another disadvantage arises during the use of multiple drugs in the verified process as it is difficult to add drugs sequentially to the clonogenic assay (Hoffman, 1993). Furthermore, the discrimination between cell death and senescence is difficult by using clonogenic assay, yet it still the gold standard method to determine anticancer cytotoxicity (Galluzzi et al., 2009). Thus, the clonogenic assay is not ideal per se to assess pure cell death (Galluzzi et al., 2009).

Different techniques have been developed to allow more rapid evaluation of drug sensitivity, including colorimetric methods. MTT assay, similar to WST-1 assay, depends on metabolically active cells to reduce tetrazolium salt MTT to form dark coloured formazan dye. A single point MTT assay applied after a defined time of insult exposure, might result in loss of certain information related to cell growth behaviour such as doubling time, and lag phase (Buch et al., 2012). By this way, the clonogenic assay is determined more accurate in the assessment of chemosensitivity since it considers the cellular proliferative capacity for several days after the treatment, long-term cells fate (Galluzzi et al., 2009), and not only the inhibition of cell proliferation following a short time interval. However, a strong linear correlation exists with survival data between clonogenic and multiple MTT assay, suggesting the latter method as a surrogate of clonogenic assay in determining the irradiated cancer cells survival (Buch et al., 2012). It is worth to mention that by using multiple MTT assay, slightly higher activity was observed compared to clonogenic assay, which perhaps explained by the existence of cells being alive with metabolic activity, but show poor or lack of cellular proliferation (Buch et al., 2012). It has also been recognized that failure to establish a direct correlation between radiation-induced apoptosis and loss of clonogenicity with solid tumours, as late apoptosis (postmitotic cell death) could occur (Balcer-Kubiczek, 2012). Accordingly, the MTT/WST-1 assays are considered as the first rounds of high-throughput cell death studies assessment, relatively inexpensive procedures, allow to simultaneously analyse multiple samples without prior processing requirement such as cell lysis, and also based on the availability of standard laboratory equipment (Galluzzi et al., 2009). However, they have considerable drawbacks. The mitochondrial enzyme activity could be shut down in conditions unrelated to cell death such as overconsumption of growing media and/or cells being over confluence, leads to underestimation of the total living cells number (Galluzzi et al., 2009). Moreover, an optimization process is required, as the MTT/WST-1 conversion efficiency varies in distinct cell lines (Galluzzi et al., 2009). Collectively, the colorimetric tests could be applied only for the preliminary part of cell death study, when several other conditions should be screened (Galluzzi et al., 2009). Therefore, integration of these assays with one another is regarded as a valuable approach, enabling for cross-confirmation of the cytotoxic and proliferation effects of insult exposure (Galluzzi et al., 2009).

However, more recent studies have also revealed a difference between their findings and those of past work, where no growth inhibition was observed in U2OS and HeLa cancer cells knocked down for NUDT1 (Kettle et al., 2016, Kawamura et al., 2016). These more recent data are in agreement with our observations least some of the contradicting observations are likely attributed to off-target, nonspecific effects of the siRNA that was utilised in the original study rather than NUDT1 deficiency itself (Kettle et al., 2016), as discussed in the previous chapter. After the complete knocked out of NUDT1 by CRISPR technique, it was also denoted that the colorectal adenocarcinoma cell line (SW480 cells) remained as viable as their wild-type counterparts (Kettle et al., 2016). Recently, another study (Wang et al., 2016) observed that NUDT1-deficient melanoma cell lines [by shRNA and two published siRNA sequences (Gad et al., 2014)] did not detect any reduction in cell viability or affect the clonogenic potential formation. However, they induced DNA DSBs in melanoma cells with mutations in BRAF (IgR3 cells) or NRAS (Mel-RM cells), but not in wild-type cells (Mel-FH cells) (Wang et al., 2016). The latter melanoma cells have low endogenous ROS level relative to the other indicated cell lines. Interestingly, the silencing of NUDT1 enzyme left melanoma cells more sensitive to apoptotic effects triggered by the oxidative stress inducer of ROS productions, elesclomol (Wang et al., 2016). However, another recent independent study (Tu et al., 2016) has successfully confirmed NUDT1 role in malignant glioma cell survival, as a reduction of its expression inhibited colony formation and *in vivo* xenograft tumor growth. A further critical finding was a significant drop of glioma cells viability after a combination of NUDT1 knockdown with H₂O₂ treatment relative to corresponding control (Tu et al., 2016). Here, in contrast, there was no further accumulation of neither oxidized DNA bases nor DNA SSBs observed in NUDT1-deficient NSCLC cell cultures (both immediately, and 24 h) post H₂O₂ or X-irradiation treatments (Figures 5-9, 5-10, and 5-11), suggesting a debatable role of NUDT1 in protection against genomic instability during extrinsically-induced oxidative stress, at least for NSCLC cells. This is in line with the literature notice that overexpression of NUDT1 impaired DNA SSBs formation in U2OS cancerous cells treated by SCH51344 or (S)-crizotinib, but not by H₂O₂ (Huber et al., 2014).

Chapter 6: Genotoxic and cytotoxic effects of NUDT1 small molecule inhibitors on NSCLC cell lines

6.1 Introduction

Gad with co-workers' team have purified the MTH1 protein, then the compound libraries have been screened and led to identifying the compounds, namely TH287 and TH588 (Figure 6-1). These selectively bind the NUDT1 active site as demonstrated by the protein co-crystal structures (Gad et al., 2014). They are first-in-class small molecules NUDT1 inhibitors with IC_{50} of 0.8 nM and 5 nM, respectively, that in selective and active manner kill U2OS cells along with other cancer cell lines, but not primary or immortalized cells. Despite the methyl group being replaced by a cyclopropyl molecule in TH588, the aminopyrimidine moieties of both compounds bind into Asn 33, Asp 119 and Asp 120; the active site of NUDT1, with hydrogen bonds. Such cyclopropyl replacement leads to 180-degree rotation of dichlorophenyl ring between TH287 and TH588 (Gad et al., 2014). The aminomethyl substituent and the corresponding amino group in TH287 and TH588, respectively, seem to take main part responsible for NUDT1 affinity and specificity, as the hydrogen bond between NH and Asp 119 perhaps mimic the specific role of previously reported 6-enol state of 8-oxodGTP (Gad et al., 2014, Svensson et al., 2011).

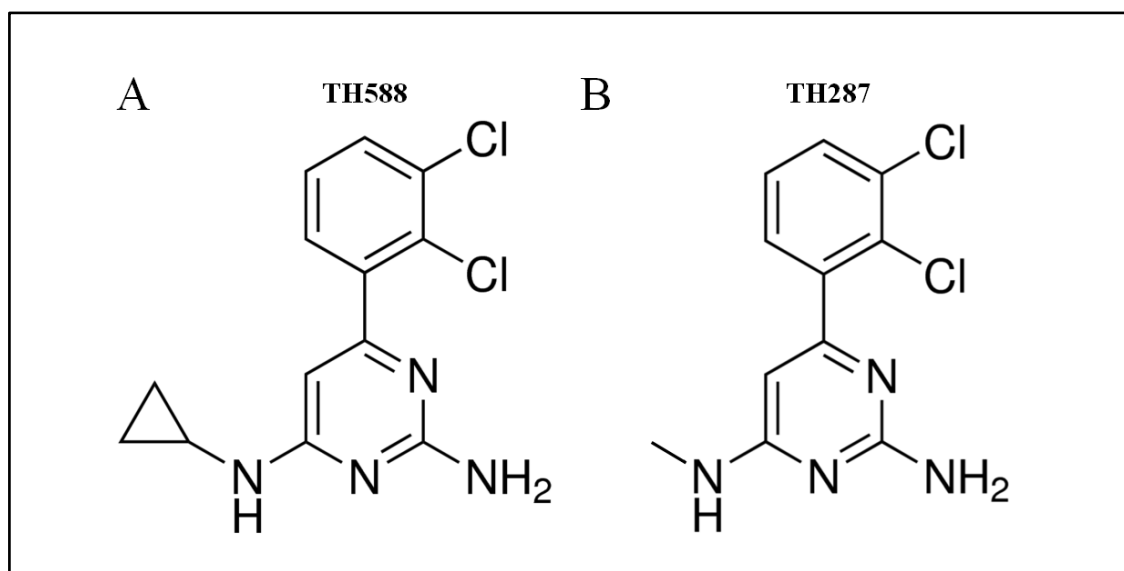


Figure 6-1 The chemical structure of small molecule NUDT1 inhibitors, (A) TH588 and (B) TH287 compounds. [The Figure adapted from (Gad et al., 2014).

It is stated that NUDT1 inhibition by TH287 or TH588 increase incorporation of oxidized dNTP precursors in cancer cells during DNA replication, causing DNA damage and cytotoxicity (Gad et al., 2014). By this way, TH287 and TH588 cause 53BP1, RPA, and DNA-PKcs foci formations, and trigger the DDR (through ATM Ps 1981, p53 Ps15, and p21 upregulations) and apoptosis (increase cleaved caspase 3 and cells in sub-G1 phase). The induction of apoptosis indicated DNA damage, and ATM-p53-mediated cell death response occurs in U2OS cancer cells, with considerably less effect towards primary VH10 cells (Gad et al., 2014). In addition, the cytotoxicity of TH287 and TH588 NUDT1 inhibitors were observed independent of Ras or p53 status, suggesting their possible activity towards diverse types of cancer (Gad et al., 2014, Huber et al., 2014). Despite poorly sustained serum levels, TH588 has an anti-tumour therapeutic response in patient-derived mouse xenografts, when inoculated once daily for treatment of mice with BRAF^{V600E} mutated tumour from a malignant melanoma patient developing resistance to carboplatin, dacarbazine and vemurafenib. Moreover, TH588 subcutaneous administration once per day, leading to suppression of tumour growth rates in SW480 colorectal and MCF7 breast cancer xenografts models. This in line with the notion of targeting NUDT1 enzyme is regarded as a potentially useful way for a variety of tumour types (Gad et al., 2014).

These small molecules NUDT1 inhibitors (TH287 and TH588) are highly selective, with no relevant inhibitory effect against other tested members of the nudix hydrolase protein family, such as NUDT15, NUDT5, NUDT12, NUDT14, and NUDT16, nor any of the nucleoside triphosphate pyrophosphatases (dUTPase, dCTPase, and ITPA). Selectivity data of TH588 (10 μ M) had shown little activity towards a panel of 87 enzymes (G-protein-coupled receptors, ion channels, transporters, and kinases), with few exemptions (Gad et al., 2014). In addition, it was observed that low-nanomolar enzymatic inhibitory action exhibited by NUDT1 inhibitor compounds, causing cancer cell cytotoxicity at micromolar ranges. This notable criterion might be clarified by the characteristic pharmacokinetic and/or pharmacological compounds behaviour including high protein binding property, low permeability and efflux in tumour cells (Gad et al., 2014). *In vivo* and *in vitro* rapid metabolism of TH287 has also been determined in human and mouse liver microsomes through N-dealkylation of the aminomethyl substituent (Gad et al., 2014). However, substitution of the methyl group by a cyclopropyl molecule in TH588 (Figure 6-1A), in comparison to TH287 (Figure 6-1B),

enhanced *in vitro* / *in vivo* metabolic stability with preserving potency against NUDT1 (Gad et al., 2014). TH588 and TH287 NUDT1 inhibitors have stated to produce the same metabolite (TH586) and their pharmacokinetic property was reported in an earlier literature (Saleh et al., 2015).

Notably, after exposure to such small molecules NUDT1 inhibitors, ectopic expression of *E. coli* MutT partially rescued toxicity of the TH588 compound in those passive transfected U2OS cells (Gad et al., 2014).

However, recent evidence has raised questions about the potential of NUDT1 inhibition in cancer-killing ability as a therapeutic target, and the specificity of such existing NUDT1 inhibitors (Kawamura et al., 2016, Petrocchi et al., 2016, Kettle et al., 2016).

The aim of this chapter was to further understand the role of NUDT1 enzyme in regard to oxidatively damaged DNA levels and cytotoxicity of NSCLC. This would be achieved by applying an earlier reported small molecules NUDT1 inhibitors, TH287 and TH588 (Gad et al., 2014).

6.2 Protein expression following treatment with small molecule NUDT1 inhibitors

In order to determine the effect following treatment with NUDT1 small molecule inhibitors (TH287 and TH588), the expression level of NUDT1 protein was assessed by Western blotting in a panel of NSCLC cell lines (H23, H522, and A549 cells), as well as, normal human lung fibroblast (MRC-5 cells).

The cells were treated with 10 μ M of either TH287 or TH588 and incubated for 24 h at 37°C in a humidified atmosphere, 95% air/5% CO₂. Exposure of the cells to DMSO (0.066% v/v) was also included as a vehicle control.

As expected, the treatment with NUDT1 small molecule inhibitors (TH287 and TH588 compounds) did not lead to apparent changes in the expression of NUDT1 protein relative to DMSO exposure for all indicated cell lines (H23, H522, A549, and MRC-5 cells). This result indicates that TH287 and TH588 compounds possibly inhibit the catalytic activity of NUDT1 enzyme (Gad et al., 2014), but not its expression level (Figure 6-2). However, the extracted protein of MRC-5 cell lysates have no loading control bands (α -Tubulin) in DMSO lane as well as TH287-treated samples, suggesting an issue might happen during or even after Western blot transfer, such as the presence

of trapped air bubbles; this possibly prevent the transfer of the proteins with consecutive blank areas formed on the developed blot.

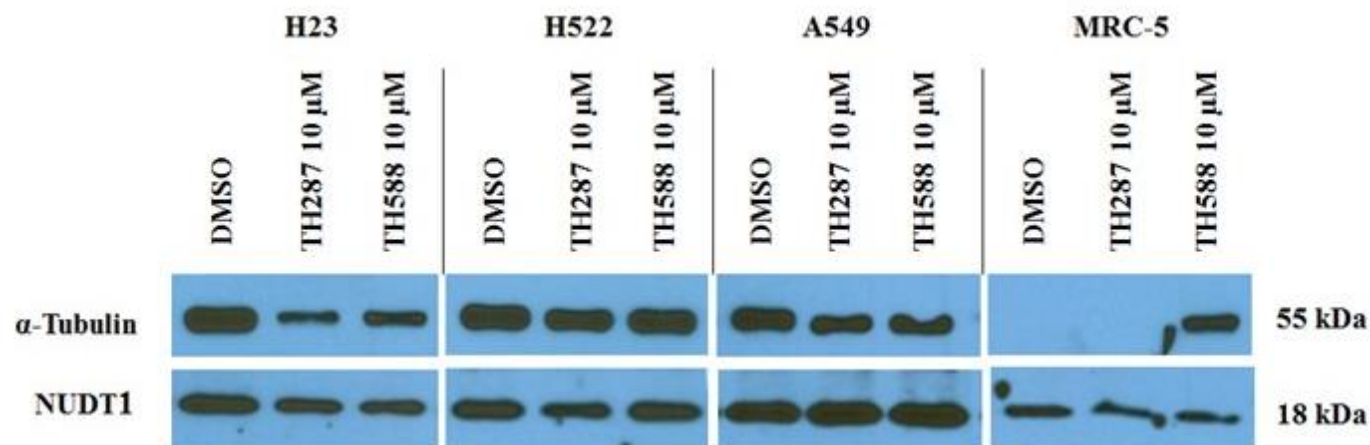


Figure 6-2 TH287 and TH588 NUDT1 small molecule inhibitors do not alter the expression levels of NUDT1 protein.

Western blots was applied to determine NUDT1 protein levels. The indicated cell lines (H23, H522, A549, and MRC-5) were exposed to 10 μ M of either TH287 or TH588 compounds at 37°C for 24 h. DMSO (0.066% v/v), as a vehicle control, was also applied. Subsequently, the collected cell lysate proteins were subjected to Western blot with NUDT1 and loading control α -Tubulin antibodies (n=1).

6.3 Determination of small molecule NUDT1 inhibitors-induced DNA damage in NSCLC cell lines

The use of siRNA for an assessment of NUDT1 depletion influences on lung cell lines had revealed some observations that agreed with our predictions based on previous studies, but also exposed other unexpected findings that suggest NUDT1 is not required for cellular viability of NSCLC. In order to further explore the observed surprising results and to understand the role of NUDT1 enzyme in a regulation of oxidatively damaged DNA levels and cell viability, herein, it is similarly utilised the small molecule NUDT1 inhibitors (TH287, and TH588) were studied (Gad et al., 2014). They were applied using the same earlier reported dose and duration of treatments (Gad et al., 2014), albeit for different cell types.

It is worth to mention that these compounds (TH287 and TH588) were previously shown to lead to a dramatic rise in oxidatively damaged DNA levels along with a loss of cellular viability selectively in cancer cells (Gad et al., 2014). Interestingly, in U2OS cancerous cell line, they also induced an accumulation of DNA SSBs, suggesting such inhibitors may have additional effects distinct from NUDT1 inhibition.

In this study, the formation of DNA damage induced by small molecule NUDT1 inhibitors in normal human lung fibroblast (MRC-5 cells) and the panel of NSCLC cell lines (H23, H522, and A549 cells) was examined, using the Fpg-modified alkaline comet assay. The latter can recognise DNA (SSBs/ALS) along with oxidised purine-derived lesions. Here, the cells were treated with 10 μ M of either TH287 or TH588 for 24 h at 37°C in a humidified atmosphere, 95% air/5% CO₂. Exposure to DMSO (0.066% v/v) was also included as a vehicle control, and usually processed in every experiment.

As shown in Figure 6-3, treatment of H23 cells with TH287 or TH588 induced a small but observable increase in the levels of oxidatively damaged DNA without any further rise in DNA SSBs. Specifically, there was about 1.5-fold rise in the average oxidised DNA bases levels following TH287 (7.98%) and TH588 (7.97%) treatments relative to corresponding DMSO control samples (6.1%). This result implies an evidence of small accumulation of such DNA lesions upon treatment with TH287 and TH588 NUDT1 inhibitors, which seems at a lower level than the H23 transfected cells with NUDT1 siRNA (Figures 4-1, 5-7, 5-9, and 5-11). However, the average levels of DNA

(SSBs/ALS) did not alter between DMSO (0.066% v/v) exposure samples (4.89%), and the cells treated with TH287 or TH588 small molecule NUDT1 inhibitors (5.04% and 5.45%, respectively) (Figure 6-3). Thus, these NUDT1 inhibitors compounds do not lead to increase in DNA SSBs in H23 cells.

For the other indicated NSCLC cell lines (H522 and A549), the treatment with small molecule NUDT1 inhibitors (TH287, and TH588) did not lead to significant alteration in Fpg sensitive sites (oxidatively damaged DNA levels) in comparison to corresponding DMSO (0.066% v/v) exposed cells (Figures 6-4, and 6-5). Specifically, the average levels of Fpg-dependent percentage DNA in comet tail after TH287 treatments were 6.43% for H522 and 6.17% for A549; while after TH588 treatments they were 6.66% for H522 and 6.44% for A549. Comparable average levels of Fpg sensitive sites were also observed in corresponding DMSO control samples (6.56, and 7.46%) for H522 and A549 cells, respectively. However, this is not the case after targeting NUDT1 using siRNA which induced oxidatively damaged DNA in all verified NSCLC cell lines, as previously described (Figures 4-1, 4-2, and 4-3), suggesting that the used published doses of TH287 and TH588 compounds might not completely inhibit NUDT1 in NSCLC cell lines. Another possible explanation is that a substitution of NUDT1 could occur during the small molecule inhibitor treatments by yet undescribed enzyme activities. In addition, as shown in Figures 6-4 and 6-5, both H522 and A549 cell lines did not display any significant increase in DNA SSBs or ALS levels following treatment with TH287 (5.02 and 4.82%, respectively) or TH588 (5.14 and 4.79%, respectively), compared to corresponding DMSO (0.066% v/v) treated cells as vehicle controls [DNA (SSBs/ALS) levels was 5.3% for H522 cells and 6.14% for A549 cells].

A similar pattern as H522 and A549 cells of DNA damage lesions was also noticed in normal human lung fibroblast (MRC-5 cells), when treated with small molecule NUDT1 inhibitors. For MRC-5 cell line, Figure 6-6 demonstrates that DMSO (0.066 % v/v) treated cells as a vehicle control exhibit oxidatively damaged DNA and DNA SSBs/ALS levels of 7.26 and 5.4%, respectively. In addition, the treatment with TH287 or TH588 did not induce any change in either Fpg sensitive sites (7.53 and 7.99%, respectively), nor DNA SSBs (5.6 and 6.2%, respectively), relative to the corresponding DMSO (0.066 % v/v) exposed cells (Figure 6-6). This phenotypic finding was also observed after siRNA targeting NUDT1 enzyme in MRC-5 cells, without any

detectable difference in the levels of DNA oxidised bases or DNA SSBs/ALS, as described previously (Figure 4-4). Overall, these findings suggest that small molecule NUDT1 inhibitors (TH287 and TH588) treatments do not lead to a detectable increase in the misincorporation of oxidised dNTPs precursors in H522, A549 or MRC-5 cell lines. Indeed, from the above-shown results, it also implies that there are variable effects of such inhibitory compounds (TH287 and TH588) concerning oxidatively damaged DNA levels in various NSCLC cell lines.

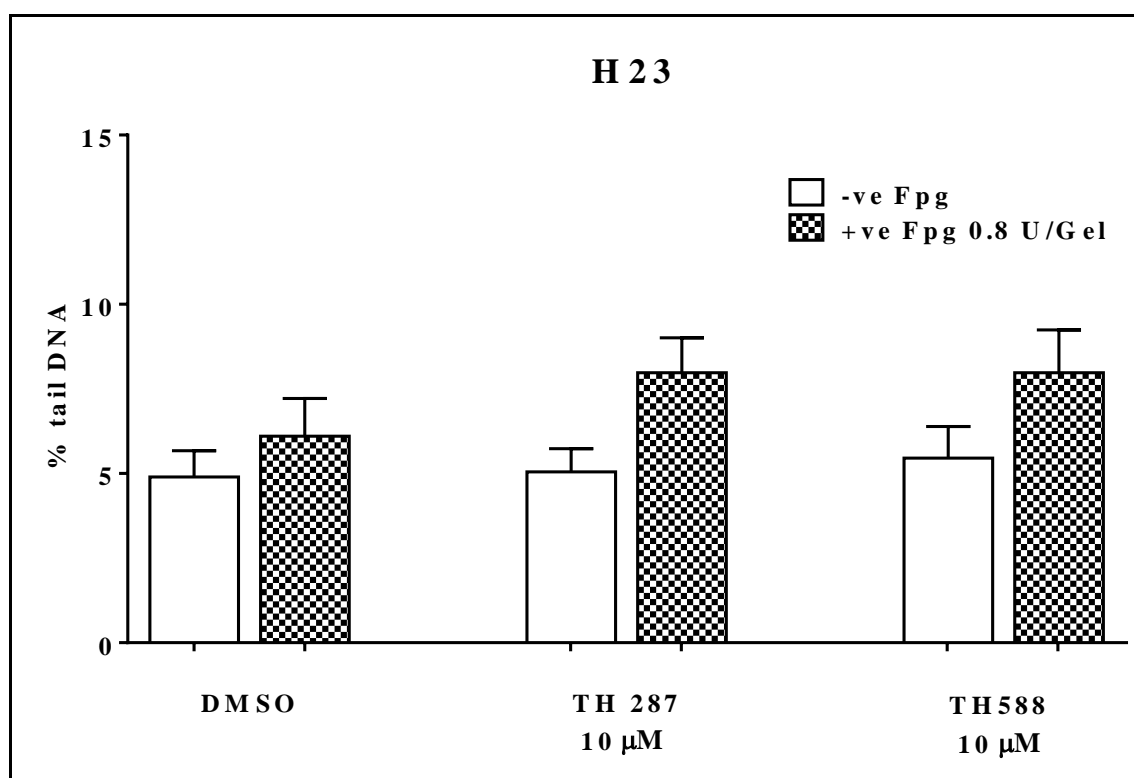


Figure 6-3 TH287 and TH588 NUDT1 small molecule inhibitors increase the oxidised DNA bases levels in H23 cell line.

Fpg-modified alkaline comet assay was applied to determine DNA damage levels in individual H23 cells after exposure for 24 h with 10 μM TH287 or TH588 compounds. DMSO (0.066% v/v), as a vehicle control sample, was also included. DNA damage levels were expressed as % tail DNA with [checkered] or without [white] Fpg repair enzyme treatment. These results represent mean ± SD of three independent experiments; at which 200 individual comets were scored for each sample to determine the experiment mean value.

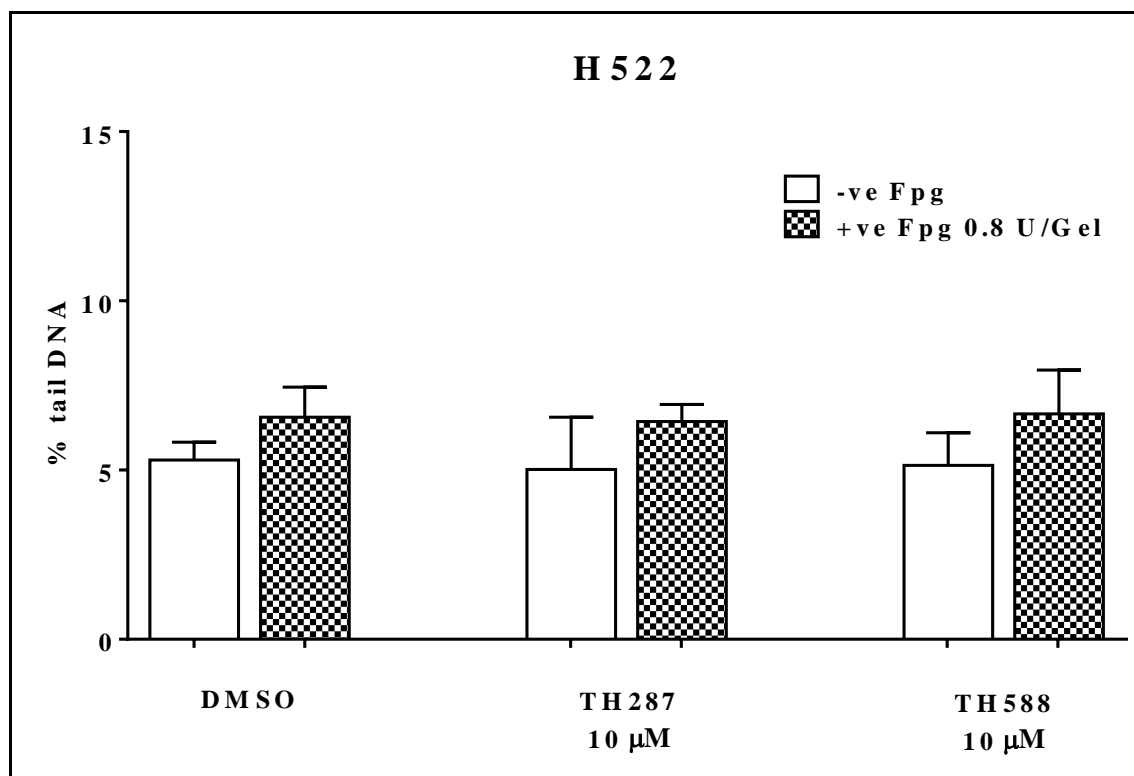


Figure 6-4 TH287 and TH588 NUDT1 small molecule inhibitors do not alter the oxidised DNA bases levels in H522 cell line.

Fpg-modified alkaline comet assay was applied to determine DNA damage levels in individual H522 cells after exposure for 24 h to 10 μM TH287 or TH588 compounds. DMSO (0.066% v/v), as a vehicle control sample, was also included. DNA damage levels were expressed as % tail DNA with [checkered] or without [white] Fpg repair enzyme treatment. These results represent mean ± SD of three independent experiments; at which 200 individual comets were scored for each sample to determine the experiment mean value.

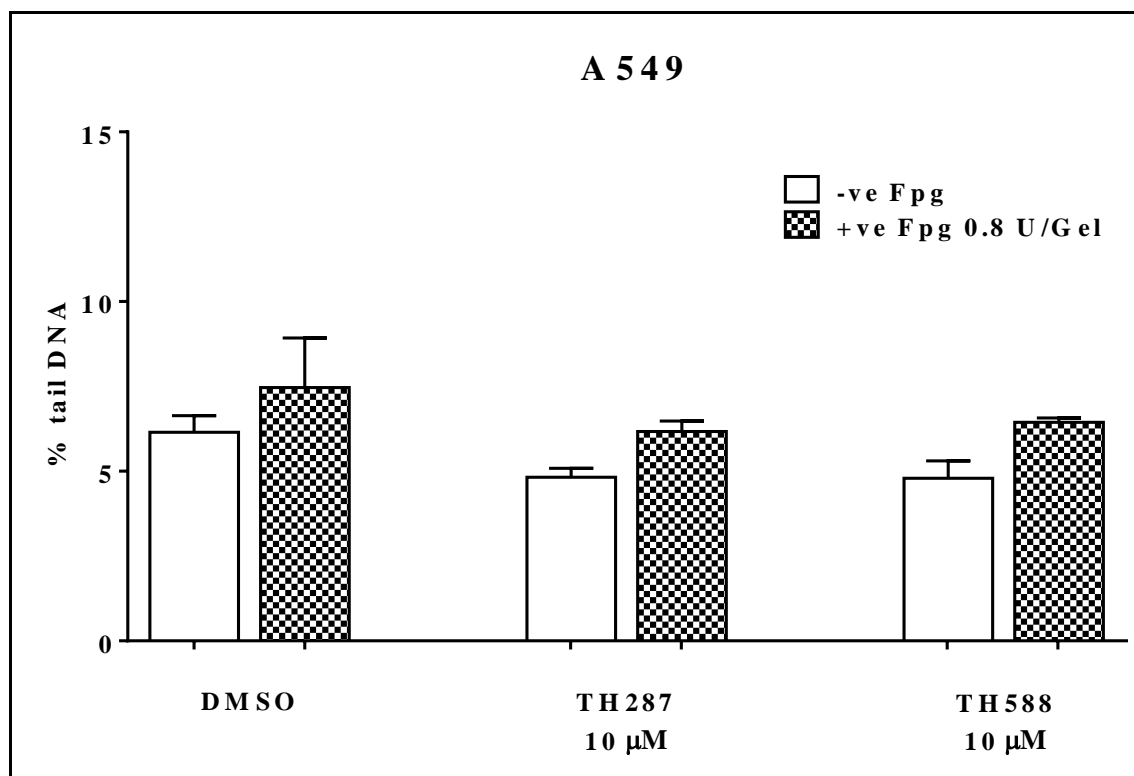


Figure 6-5 TH287 and TH588 NUDT1 small molecule inhibitors do not alter the oxidised DNA bases levels in A549 cell line.

Fpg-modified alkaline comet assay was applied to determine DNA damage levels in individual A549 cells after exposure for 24 h to 10 μM TH287 or TH588 compounds. DMSO (0.066% v/v), as a vehicle control sample, was also included. DNA damage levels were expressed as % tail DNA with [checkered] or without [white] Fpg repair enzyme treatment. These results represent mean ± SD of three independent experiments; at which 200 individual comets were scored for each sample to determine the experiment mean value.

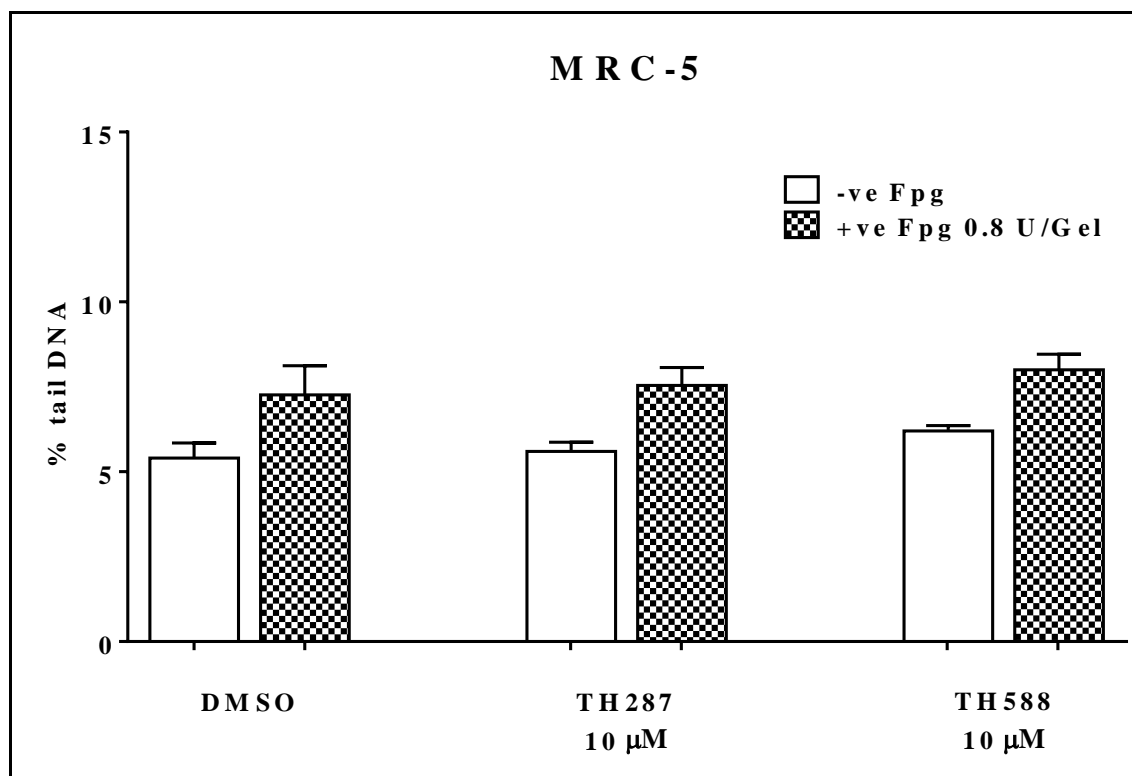


Figure 6-6 TH287 and TH588 NUDT1 small molecule inhibitors do not alter the oxidised DNA bases levels in MRC-5 cell line.

Fpg-modified alkaline comet assay was applied to determine DNA damage levels in individual MRC-5 cells after exposure for 24 h to 10 μM TH287 or TH588 compounds. DMSO (0.066% v/v), as a vehicle control sample, was also included. DNA damage levels were expressed as % tail DNA with [checkered] or without [white] Fpg repair enzyme treatment. These results represent mean ± SD of three independent experiments; at which 200 individual comets were scored for each sample to determine the experiment mean value.

6.4 Determination of apoptotic effect induced by small molecule NUDT1 inhibitors in NSCLC cell lines

Further assessment was performed to determine whether the small molecule NUDT1 inhibitor-induced apoptosis, and whether this correlated with oxidatively damaged DNA levels in different NSCLC cells. Herein, the apoptotic cell death induced by small molecule NUDT1 inhibitors (TH287 and TH588) was studied in a panel of NSCLC cell lines (H23, H522, and A549), as well as in normal human lung fibroblast cells (MRC-5).

The same doses and duration of treatments with NUDT1 inhibitory compounds were used as when determining DNA damage accumulation in the previous section (6.3). The cells were treated with 10 μ M of either TH287 or TH588 compounds for 24 h at 37°C in a humidified atmosphere, 95% air/5% CO₂. DMSO (0.5-1.5% v/v) exposure and untreated negative control (-ve) samples were also included. As a positive control for induction of apoptosis, the cells were treated with 50-150 μ M etoposide. In this study, the early and late apoptotic fractions were determined by Annexin V-FITC/PI dual staining and analysed using flow cytometry.

It was observed that the cellular apoptotic fractions levels in H23 cells rise almost 3 to 3.5-fold following NUDT1 inhibitor treatments for both TH287 (25.86%) and TH588 (24.46%) compounds relative to the corresponding untreated control samples (P-value < 0.0001) (Figure 6-7). Moreover, the exposure of H23 cells to 50 μ M etoposide for 24 h exhibited 28.56% of mutual early and late apoptotic cells levels, which was more significant than apoptotic cell fractions in untreated samples (8.06%) and those cells exposed to 0.5% v/v DMSO (5.76% apoptotic cells) (P-value < 0.0001).

TH287 and TH588 compounds induced 2.8 and 3.5-fold increases in apoptosis levels in H522 cells, respectively. In more specific detail, there was a significant rise in apoptotic cell death levels detected in H522 cells treated with small molecule NUDT1 inhibitors for both TH287 (9.4%) and TH588 (11.8%) compounds relative to the corresponding untreated control samples (P-value < 0.05) (Figure 6-8). The low responsiveness and resistance of H522 cells to etoposide was also observed, as previously described (Figures 4-9, 5-4, 5-13A, 5-15A, and 5-20); with higher treatment doses required as a positive control of apoptosis. Herein, after 24 h exposure to 150 μ M etoposide, the H522 apoptotic cell fractions was 14.76%; and significantly higher than the

corresponding untreated (3.35%) and treated cells with 1.5% v/v DMSO (5.75%) (P-value < 0.01) (Figure 6-8). These observations indicate that oxidatively damaged DNA levels were not the only basis responsible for the cytotoxic influence of small molecule NUDT1 inhibitors (TH287, and TH588), and they might act through inhibiting other factors than the NUDT1 enzyme. Perhaps, this suggests that TH287 and TH588 compounds may kill cancer cells via 'off-target effect' rather than the inhibition of NUDT1.

For A549 cells, NSCLC cells with proficient p53, there was no alteration in cell death pattern (early and late apoptosis) after both TH287 (6.83%) and TH588 (5.83%) exposures compared to the corresponding untreated control samples (Figure 6-9). In addition, the percentage of apoptotic cellular death 24 h after exposure to 50 and 150 μ M etoposide were 15.46% and 27.5%, respectively. Such finding as a positive control of apoptosis were significantly higher than untreated (4.96% apoptotic fractions) and those samples exposed to 1.5% v/v DMSO (4.4% apoptotic fractions) (Figure 6-9). This observation indicates that such small molecule NUDT1 inhibitors are ineffective in killing NSCLC cells with competent p53, at least with the indicated dose and duration of exposure.

Similarly, the non-cytotoxicity of small molecule NUDT1 inhibitors was also tested in normal human lung fibroblast cells (MRC-5). Specifically, neither TH287 (apoptotic fractions of 4.73%) nor TH588 (apoptotic fractions of 4.33%) treatments were considered toxic to MRC-5 cells relative to their corresponding untreated and those cells exposed to 1.5% v/v DMSO (1.93 and 3.1%, respectively) (Figure 6-10). As a positive control, an exposure to etoposide for 24 h at concentrations of 100 and 150 μ M induced significant MRC-5 apoptotic cell deaths of 14.83% and 22.63%, respectively (P-value < 0.0001) (Figure 6-10). These findings agree with the original suggestion that TH287 and TH588 small molecule NUDT1 inhibitor are not considered as cytotoxic to normal cells (Gad et al., 2014).

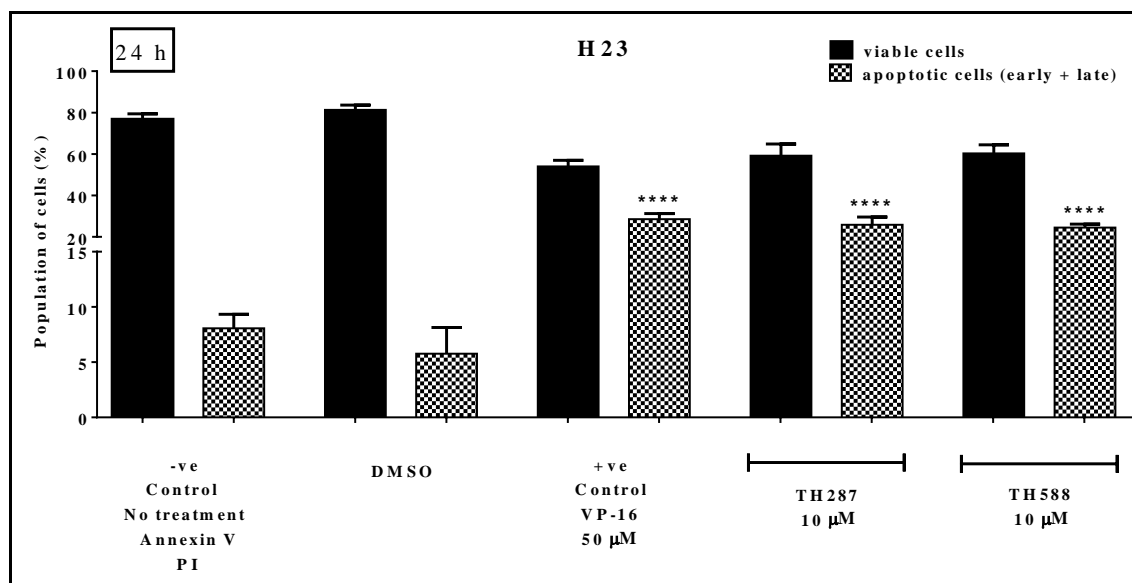


Figure 6-7 TH287 and TH588 NUDT1 small molecule inhibitors induce apoptotic death in H23 non-small-cell-lung cancer cells.

Annexin V–FITC/PI assay was applied to determine apoptotic cell deaths. H23 cells were treated with 10 μM of either TH287 or TH588 compounds for 24 h. In addition, DMSO (0.5% v/v) and etoposide (VP-16 50 μM) were acted as a vehicle control and a positive control of apoptosis, respectively. Subsequently, the cells were harvested, dual stained with annexin V-FITC/PI and assessed by flow cytometry. The shaded bars of detected apoptotic cells represent the result during both early and late apoptosis. These data were mean \pm SD of three individual experiments. Asterisks indicate a significant difference relative to corresponding untreated control cells (**** $P < 0.0001$).

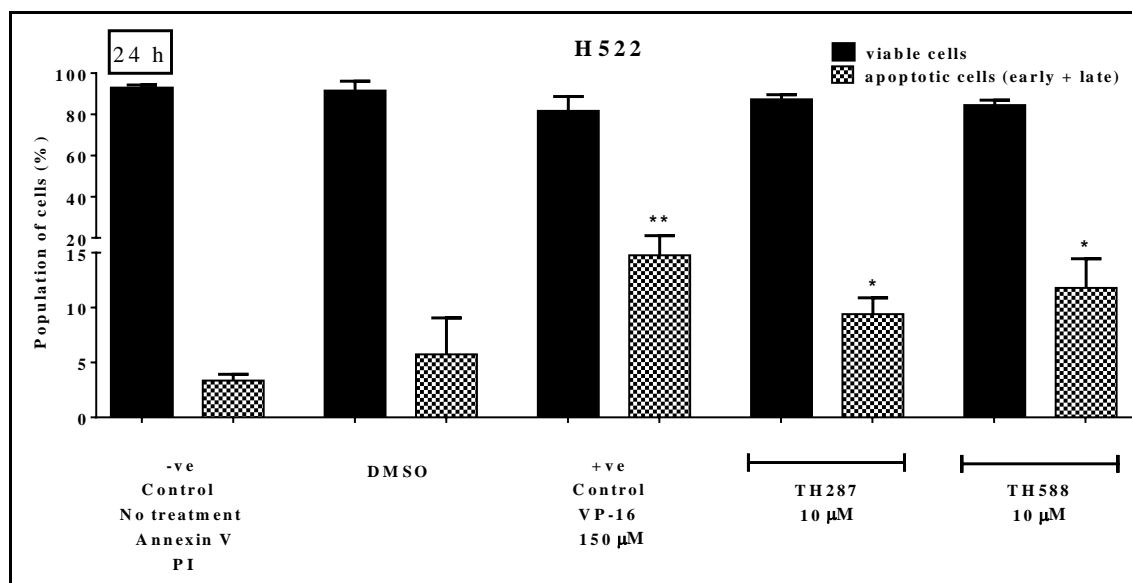


Figure 6-8 TH287 and TH588 NUDT1 small molecule inhibitors induce apoptotic death in H522 non-small-cell-lung cancer cells.

Annexin V–FITC/PI assay was applied to determine apoptotic cell deaths. H522 cells were treated with 10 μM of either TH287 or TH588 compounds for 24 h. In addition, DMSO (1.5% v/v) and etoposide (VP-16 150 μM) were acted as a vehicle control and a positive control of apoptosis, respectively. Subsequently, the cells were harvested, dual stained with annexin V-FITC/PI and assessed by flow cytometry. The shaded bars of detected apoptotic cells represent the result during both early and late apoptosis. These data were mean \pm SD of four individual experiments. Asterisks indicate a significant difference relative to corresponding untreated control cells (** $P < 0.01$, * $P < 0.05$).

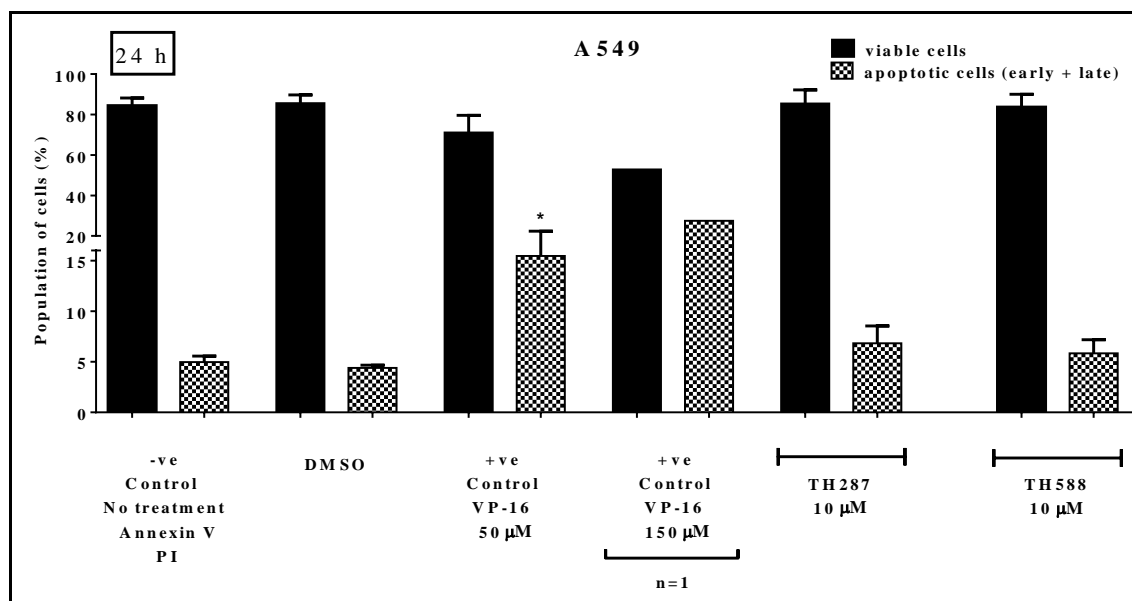


Figure 6-9 TH287 and TH588 NUDT1 small molecule inhibitors do not induce apoptotic death in A549 non-small-cell-lung cancer cells.

Annexin V–FITC/PI assay was applied to determine apoptotic cell deaths. A549 cells were treated with 10 μM of either TH287 or TH588 compounds for 24 h. In addition, DMSO (0.5-1.5% v/v) and etoposide (VP-16 50 or 150 μM) were acted as a vehicle control and a positive control of apoptosis, respectively. Subsequently, the cells were harvested, dual stained with annexin V-FITC/PI and assessed by flow cytometry. The shaded bars of detected apoptotic cells represent the result during both early and late apoptosis. These data were mean ± SD of three individual experiments or as indicated. Asterisks indicate a significant difference relative to corresponding untreated control cells (*P<0.05).

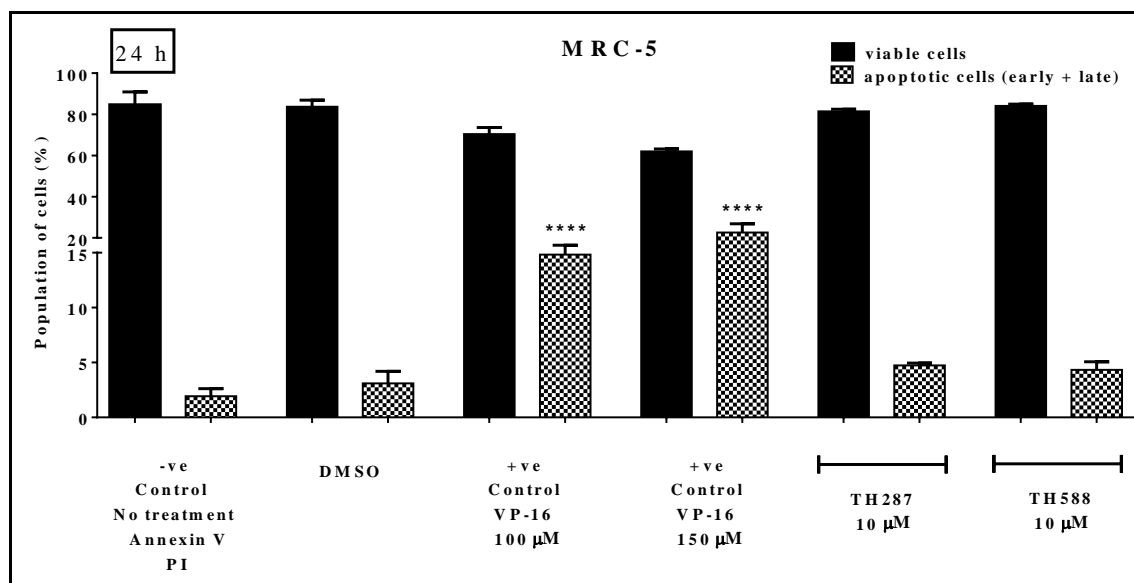


Figure 6-10 TH287 and TH588 NUDT1 small molecule inhibitors do not induce apoptotic death in normal human lung fibroblast cell line (MRC-5 cells).

Annexin V–FITC/PI assay was applied to determine apoptotic cell deaths. MRC-5 cells were treated with 10 μ M of either TH287 or TH588 compounds for 24 h. In addition, DMSO (1-1.5% v/v) and etoposide (VP-16 100 and 150 μ M) were acted as a vehicle control and a positive control of apoptosis, respectively. Subsequently, the cells were harvested, dual stained with annexin V-FITC/PI and assessed by flow cytometry. The shaded bars of detected apoptotic cells represent the result during both early and late apoptosis. These data were mean \pm SD of three individual experiments. Asterisks indicate a significant difference relative to corresponding untreated control cells (**** $P < 0.0001$).

6.5 Discussion

The use of siRNA for targeting NUDT1 enzyme in the previous chapter has revealed some unexpected findings that suggest NUDT1 is not entirely required to maintain cell proliferation or NUDT1 deficiency did not induce apoptotic cell death in NSCLC cells. In order to further explore the role of NUDT1 in regulating levels of oxidatively damaged DNA and NSCLC cell viability, small molecule NUDT1 inhibitors TH287 and TH588 were used, as these were previously reported to induce a dramatic accumulation of oxidised DNA bases and loss of viability selectively in cancer cells (Gad et al., 2014).

The most recent studies provide some clarification for our findings relating to the effect of small molecule NUDT1 inhibitors, TH287 and TH588. These compounds were proposed to be highly effective in killing cancer cells due to NUDT1 inhibition (Gad et al., 2014, Huber et al., 2014); however, herein, TH287 and TH588 only induced apoptotic cell deaths in a subset of NSCLC cell lines, mainly H23 and H522 cells (Figures 6-7, and 6-8) but not in A549 proficient-p53 cells (Figure 6-9). In addition, this enhancement in apoptosis levels did not entirely correlate with increases in oxidatively damaged DNA (Figures 6-3, 6-4, and 6-5). The above results suggest that the influences on cellular viability are likely distinct from NUDT1 inhibition. Accordingly, it was very recently proposed that both TH287 and TH588 compounds exert much of their cytotoxicity in HeLa cells primarily through tubulin polymerisation defects rather than NUDT1 inhibition (Kawamura et al., 2016), though this conclusion was subsequently confronted (Berglund et al., 2016).

Recently, TH287 in proteomic profiling analysis showed similarity with certain compounds that target tubulin, for example, nocodazole, vinblastine, and paclitaxel rather than other NUDT1 inhibitors (Kawamura et al., 2016). In addition, it was observed that both TH287 and the more metabolically stable TH588 analog promoted dose-dependent inhibition of tubulin polymerization in vitro, and lead to disruption of HeLa cells intracellular microtubule network with cellular shrinkage outcome (Kawamura et al., 2016). This is also supported as these compounds (TH287, and TH588) at their cytotoxic concentrations induced phosphorylation of Bcl-2, and cell cycle arrest in G2/M phase similar to tubulin-targeting agents, strengthening the suggestion that their cytotoxic effects are primarily through tubulin defects (Kawamura

et al., 2016). Interestingly, overexpression of NUDT1 did not rescue HeLa cells proliferation capacity after NUDT1 inhibitors treatments (Kawamura et al., 2016).

Similar observation was found in melanoma cell lines when overexpression of NUDT1 or introduction of ectopic bacterial homology of NUDT1 (MutT) with 8-oxodGTPase activity did not inhibit the cell viability against TH588 (Wang et al., 2016). This NUDT1 overexpression also did not reduce TH588-induced nuclear accumulation of 8-oxodGTP and formation of 53BP1 foci, indicating another mechanism than NUDT1 inhibition might be responsible for TH588-induced DNA damage and reduced viability in melanoma cells (Wang et al., 2016). Despite the sensitivity towards TH588 varying among melanoma cell lines, both endogenous ROS levels and its reflected carbonylated proteins have some positive correlations with the sensitivity of melanoma cells to apoptosis induced by TH588 (Wang et al., 2016).

Specifically, it was observed that TH588-induced apoptosis in those melanoma cell lines with relatively high endogenous ROS levels (IgR3, and Mel-RM), but not in Mel-FH cells with low ROS level background (Wang et al., 2016). This suggested to be mediated via activation of BAD and down-regulation of BCL-2 and MCL-1 proteins, although NUDT1 knockdown alone did not affect the cell viability nor generate any of such molecular changes (Wang et al., 2016). Perhaps, this is associated with high ROS levels which lead to inhibition of protein kinase B and induced c-Jun N-terminal kinase and p38 activation that subsequently contribute to the observed activation of BAD and down-regulation of BCL-2 and MCL-1 proteins produced by TH588. Another possible contribution is the inhibition of NF- κ B by high ROS levels which might also be considered (Wang et al., 2016). In this study, NSCLC cells responded differently to TH588 in term of apoptotic cell death induction (Figures 6-7, 6-8, and 6-9), while they exhibited equal low endogenous ROS levels similar to MRC-5 normal cells (Figure 4-5). This finding suggests no relationship exist between the sensitivity toward TH588 and the endogenous ROS level, at least in NSCLC cells, and might be other unidentified factors are responsible for such cellular sensitivity variation toward TH588 compound.

Concurrently, in the same study (Wang et al., 2016), there was an accumulation of 8-oxodGTP and triggering nuclear 53BP1 foci formation following TH588 treatment in IgR3 and Mel-RM, but not Mel-FH melanoma cells, suggesting DNA DSBs induction in these sensitive melanoma cells to TH588, which also associated with activation of

ATM-dependent phosphorylation of p53 (p53pS15) and its targeted protein, p21 (Wang et al., 2016). Despite the fact that NUDT1-deficient melanoma cell lines [by shRNA and two published siRNA sequences (Gad et al., 2014)] did not exhibit any reduction in cell viability or affect the clonogenic potential formation, it was still found further enhancement in DNA damage and cell death when combined NUDT1 silencing with TH588 treatment (Wang et al., 2016). The latter findings also suggest that TH588 may act via the inhibition of factors other than NUDT1.

Interestingly, exposure to exogenous oxidative stress inducer elesclomol did not alter the survival of melanoma cells, yet it leads to enhancement in TH588-induced apoptosis in both sensitive (IgR3, and Mel-RM) and resistant (Mel-FH) melanoma cells (Wang et al., 2016). On the other hand, the ROS scavenger (N-acetyl-L-cysteine) or an antioxidant (glutathione) agents attenuated the TH588-triggered cell death, and by this way protect the melanoma cells against TH588 effect (Wang et al., 2016). Therefore, it was suggested that the oxidative stress status determines the sensitivity to TH588, and it might be mediated by a mechanism interfering with the cellular ROS production/redox environment, at least in melanoma cells (Wang et al., 2016). Likewise, pre-treatment of U2OS osteosarcoma cells with glutathione precursor (N-acetyl-L-cysteine) or PEG-catalase protected the cell viability against TH588 exposure, as well as, decreased the incorporation of 8-oxo-dGTP into DNA genome (Brautigam et al., 2016). However, it has been shown in the present study that NUDT1 knockdown is likely not an effective therapeutic strategy for NSCLC even if used in combination treatments with agents induced oxidative stress as well as DNA damage and DNA replication stress, as discussed thoroughly in the previous chapters.

It is worth to mention that the experimental conditions were considerably varied among the reported studies (Brautigam et al., 2016, Kettle et al., 2016, Petrocchi et al., 2016, Kawamura et al., 2016, Gad et al., 2014, Huber et al., 2014). For example, herein, NSCLC cell cultures were not exposed long enough period to TH287 and TH588 compounds in order to establish their earlier reported cytotoxic effect (Gad et al 2014)

Unlike the first-in-class small molecule NUDT1 inhibitors (Gad et al., 2014), other newly synthesized and highly specific NUDT1 inhibitors independently were not found to be cytotoxic in cancer cells (Kettle et al., 2016, Petrocchi et al., 2016, Kawamura et al., 2016). Kettle with AstraZeneca team group has developed series of orthogonal and

chemically distinct compounds from those originally reported small molecules NUDT1 inhibitors (Gad et al., 2014). Their biochemical potency, selectivity and cellular engagement to NUDT1 were confirmed, but neither of these chemical series provoked appreciable cellular inhibitory phenotypic activity, as they did not have any impact on cancer cell viability. In addition, there was no modulation in the DDR signaling markers (p-Ser1981 ATM, p-Ser15 p53, γ H2AX, pSer4/8 RPA), or induction of caspase-3 mediated apoptosis was recognized at different time points after treatment of U2OS cells with one of the developed chemical when compared to TH588 (Kettle et al., 2016), which showed antiproliferative effect on a broad range of cancer cell lines (Gad et al., 2014). Other novel class series of aminopyrimidine NUDT1 inhibitors were structurally designed and identify compounds (IACS-4759, and IACS-4619) that are characterized as sub-nanomolar potent inhibitors of NUDT1, cell penetrant, metabolically stable, as well as the IACS-4759 has no effect against a panel of 97 kinases (Petrocchi et al., 2016). Likewise, these compounds also did not exert any cytotoxic or antiproliferative actions in the verified panel of cancer cells, being even tolerated by those cells with high intrinsic ROS levels. This latter finding raises the argument about the other reported observations (Wang et al., 2016) in concern of the sensitivity to TH588 agent as it is to be correlated with endogenous ROS levels in melanoma cells. In another independent recent study (Kawamura et al., 2016), it has been shown that different newly identified purine-based NUDT1 inhibitors (NPD7155, and NPD9948), by chemical array screening, exerted only weak cytotoxic potency towards HeLa cells and other tested cancer cell lines. In addition, they did not enhance any 8-oxo-dG accumulation in HeLa cells, even at the applied cytotoxic concentrations relative to that of TH287 compound. Taken together, these independent works and our results suggest that the cytotoxic and tumor growth suppression by knockdown/pharmacological inhibition of NUDT1 which was observed in previous studies (Gad et al., 2014, Huber et al., 2014), is likely attributed to off-target effects.

However, the conclusion of these independent studies (Kettle et al., 2016, Petrocchi et al., 2016, Kawamura et al., 2016) was subsequently challenged for the utility of NUDT1 inhibition as a therapeutic target of cancer (Berghlund et al., 2016). It was argued that the lack of cellular effect by three reported newly synthesis specific NUDT1 inhibitors could be attributed to their failure to the introduction of toxic oxidized nucleotides, 8-oxodG, into DNA genome. This is not the case in our study, as TH588

and TH287 compounds induced apoptosis in a subset of NSCLC cell lines, but this did not entirely correlate with increases in oxidatively damaged DNA levels. Therefore, it is still suggested that the effects on cell viability may have been distinct from NUDT1 inhibition. In contrast, an improved NUDT1 inhibitor (TH1579) has been described recently (Berglund et al., 2016), as an analogue of TH588 with potent and selective NUDT1 inhibitor characteristics, and orally available compound. Though it demonstrated *in vivo* acceptable pharmacokinetics and anti-cancer effects, its usefulness to validate NUDT1 inhibitor concept needs to be further verified.

Overall, regardless of at least some of the effects of TH287 and TH588 compounds are possibly independent of NUDT1 inhibition, this still does not explain why it is not observed any cytotoxic effects on NSCLC cell line (A549 cells) compared to results obtained from other cancerous cell lines (Gad et al., 2014, Huber et al., 2014, Kawamura et al., 2016, Petrocchi et al., 2016). In addition, the observation results of newly synthesized specific NUDT1 inhibitors not only support our NUDT1 knockdown data, but also strengthen the argument that NUDT1 inhibitors will not make effective therapeutic agents.

Chapter 7: General discussion and future directions

7.1 General discussion

In this study, the aim was to assess the potential of a new targeted therapeutic strategy for NSCLC, whilst simultaneously analysing contradictory opinions within the field regarding the conditionally essential requirements for NUDT1 in cancer cell growth and whether the current pursuit of development of NUDT1 inhibitors should continue (Helleday, 2014, Papeo, 2016). To shed new light regarding the role of NUDT1 in NSCLC; here, it is evaluated for the first time the genotoxic and cytotoxic effects of NUDT1 knockdown in a panel of NSCLC cell lines relative to normal lung cells. In addition, it is determined the effectiveness of targeting NUDT1 as a ‘conditionally essential’ (also known as ‘cancer phenotypic lethality’ (Helleday, 2014)) therapeutic approach, either as a single-agent strategy or for augmenting the cytotoxic effects of current therapies.

Our results show that NUDT1 does indeed have a NSCLC-specific role for maintaining genomic stability, as NUDT1 knockdown increased the levels of oxidised DNA bases in the genomes of all verified NSCLC cell lines and led to alterations in DDR signaling, but does not affect normal human lung fibroblasts. The basis of this cancer-specificity remains unclear since the oxidatively damaged DNA levels in NUDT1-deficient lung cells do not correlate with background ROS levels. Despite the functional role of NUDT1 in NSCLC cells, it is demonstrated that NUDT1 deficiency does not lead to NSCLC death either alone or when combined with other current NSCLC therapeutic agents. Hence, this work argues that NUDT1 inhibitors will likely not be an efficient therapeutic approach. Instead, given that our data show that NUDT1 depletion in NSCLC cells enhances non-cytotoxic DNA oxidation, it is proposed that treatment of NSCLC patients with NUDT1 inhibitors could actually promote an environment for further genetic mutational accumulation to drive the heterogeneity and evolution of cancer (Figure 7-1).

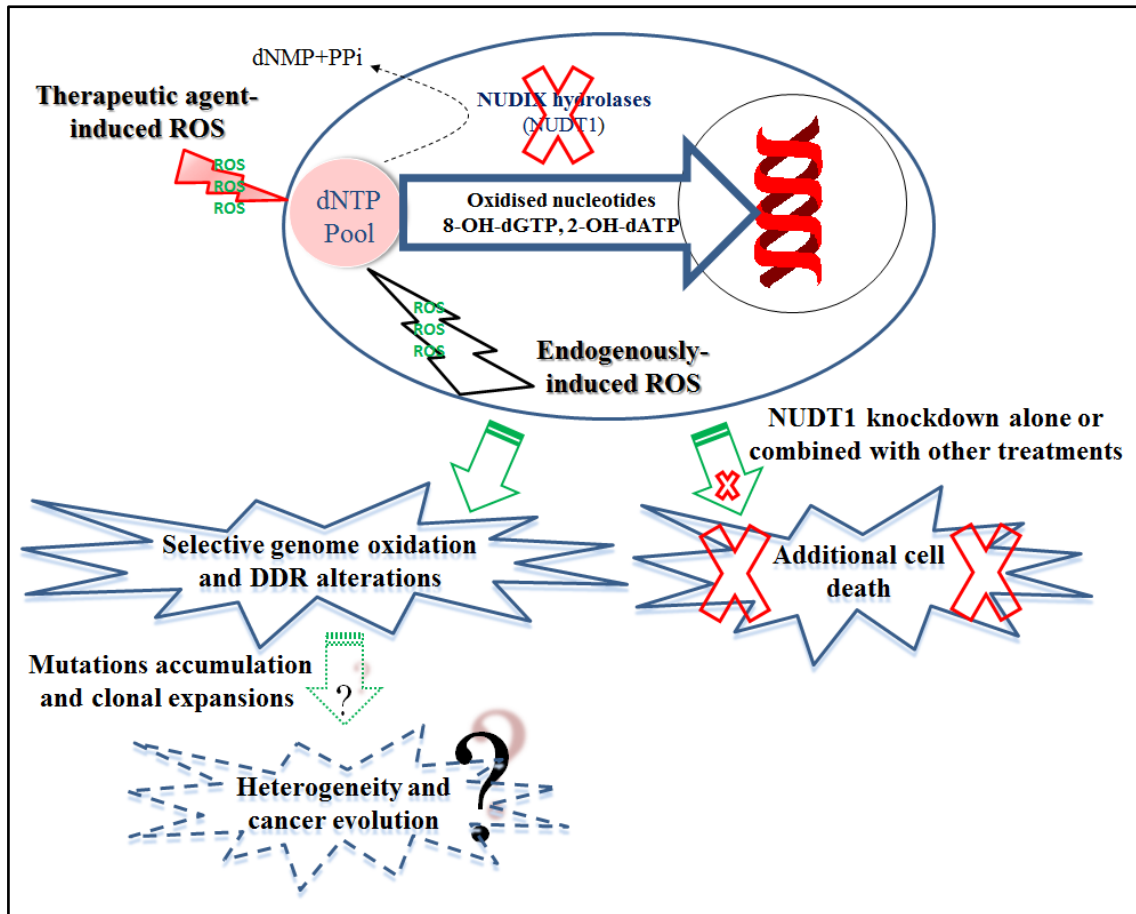


Figure 7-1 The model for targeting NUDT1 that does not induce apoptosis, but may lead to heterogeneity and cancer evolution.

Once exposed to ROS, the NUDT1-deficient cells would not be able to convert the oxidised dNTPs to their monophosphate products (dNMP) and inorganic pyrophosphate (PPi). By this way, NUDT1 targeting selectively increases non-cytotoxic oxidatively damaged DNA with alterations in DNA damage response (DDR) signaling; and during replication, it is proposed to provide an environment for further mutation accumulation to drive cancer heterogeneity and evolution. The smaller red arrow indicates that NUDT1 plays less or even no role in respect to exogenous ROS-inducing agents.

The heterogeneity of continuing mutation accumulation and clonal expansions leads tumor to possibly acquire new characteristics such as metastasis and therapeutic resistance. In accordance with this notion, NUDT1 knockdown in human B lymphoblastoid TK6 cells provides a higher mutation rate but not cell death following exposure to UVA-induced oxidative stress (Fotouhi et al., 2015, Fotouhi et al., 2011), whereas the overexpression of NUDT1 attenuated the DNA-replication-dependent mutator phenotype in MMR-deficient human colorectal carcinoma DLD-1 cells (Russo et al., 2004). In addition, following analysis of mutational frequencies at the endogenous *Thymidine kinase* gene, it is observed that NUDT1 in human lymphoblastoid cells is able to protect cells from UVA-induced base pair substitutions, mainly transitions at GC and AT base pairs (Fotouhi et al., 2013). Other previous studies also indicated an important role of NUDT1 in normal cells. A team work (Rai et al., 2009) has shown that the reduction of NUDT1 level in normal human diploid fibroblast cells lead to cellular senescence. Earlier studies also demonstrated a 2-fold increase of spontaneous mutations and more development of adenoma/adenocarcinoma in lung, liver, and stomach of 18-month-old NUDT1 knockout mice relative to wild-type animals (Tsuzuki et al., 2002, Tsuzuki et al., 2001), suggesting NUDT1 protein is important for both cancer and normal cells (Fotouhi et al., 2015). Here, it is shown selective genome oxidation and the normal human lung fibroblasts (MRC-5) exhibited continuing cell proliferation capacity after NUDT1 knockdown (Figure 4-15).

The specific requirement which is demonstrated here for NUDT1 in preventing the misincorporation of oxidised DNA bases into the genomes of NSCLC cell lines (Figures 4-1, 4-2, and 4-3) largely agrees with observations in other studies and various cancer cell lines (Gad et al., 2014, Speina et al., 2005, Yoshimura et al., 2003). However, our data did not observe any rise in DNA SSBs or ALS lesions after the NUDT1 knockdown, which conflicts with the influences of NUDT1 knockdown in A549 cells in an earlier study (Patel et al., 2015) as well as human BJ fibroblasts (Rai et al., 2009). The reasons for these inconsistent findings remain unclear. However, unless the cell line also harbours a BER defect that causes the generation of long-lived SSBs after the removal of damaged base, it would not be predicted an increase in SSBs following the knockdown of NUDT1. Thus, any effect on SSB levels induced by NUDT1 deficit may only occur in certain contexts or genetic backgrounds. Nevertheless, taken together our results and that of others strongly supported the view

that NUDT1 is required to overcome the oxidatively damaged DNA specifically in a range of cancer cell types, and this role likely derives during the early stages of malignant transformation.

The exact basis of such NUDT1 cancer-specific role is uncertain. One possibility is simply that cancerous cells build-up higher levels of endogenous oxidative stress, and this leads to the accumulation of oxidised dNTPs within the pool that increases the likelihood of subsequent oxidised precursors misincorporation. Indeed, though NUDT1 does not influence the ROS levels directly (Rai et al., 2009), NUDT1 levels were previously shown to correlate with ROS levels in NSCLC along with RAS-transformed cells (Giribaldi et al., 2015, Patel et al., 2015), suggesting that higher ROS levels leads to an adaptation over several passages to select for higher NUDT1 levels. Despite this, in our study it could not be able to detect any difference in ROS levels within a panel of NSCLC cell lines (H23, H522, and A549) and also between normal human lung fibroblast (MRC-5) (Figure 4-5), implying that the requirement for NUDT1 to protect against oxidatively damaged DNA is not simply attributed to higher ROS levels. Given all the disturbances in genetic burden and signaling cascades within cancer cells, there may be many other causes for such NUDT1 dependency that are still elusive at the present.

Unexpectedly, herein, there was no further increase in oxidatively damaged DNA levels in NUDT1-deficient NSCLC cells both immediately and 24 h recovery after exposure to H₂O₂ (Figures 5-7, 5-8, 5-9, and 5-10) or ionizing radiation (Figure 5-11). This observation indicates that NUDT1 enzyme is not essentially required to prevent genomic instability during exogenously-induced oxidative stress condition. This occurs even though the nucleotide pool is likely vulnerable to the attack of free radicals produced by such treatments (Topal and Baker, 1982, Haghdoost et al., 2005). It is unclear why NUDT1 would protect against the misincorporation of endogenously-induced oxidised dNTPs precursors in cancer cells but not that dNTPs damaged via exogenous agents. One possible suggestion is that the induction of acute oxidative stress in a NUDT1-deficient background might activate compensatory pathways that are not induced during the milder stressful conditions initiated within cancer cells. Such compensatory activity may be provided by either other currently indeterminate 8-oxodGTPase activities, or even by the potential effect of hOGG1 that was previously reported to compensate for NUDT1 activity after H₂O₂-induced oxidative DNA bases

damage (Ke et al., 2014). At that time, strong compensation was provided for NUDT1 knocked down human embryonic pulmonary fibroblast cell line (HFL) following H₂O₂ treatment as the levels of hOGG1 mRNA raised about 52%, leading to unaltered accumulation of 8-oxodG levels relative to those corresponding untransfected cells (Ke et al., 2014). Alternatively, the available small amount of residual NUDT1 enzyme may be sufficient to respond to acute oxidative stress enhanced by exogenous source, whereas, insufficiently remains during long terms of chronic stress condition.

The increased level of oxidatively damaged DNA in NSCLC cell lines after NUDT1 knockdown was relatively small, about 1.5- to 2-fold rise (Figures 4-1, 4-2, and 4-3). Conversely, the DDR signaling alterations (Figures 4-6, and 4-7) indicates that this was still enough to promote secondary types of DNA damage, implying this small elevation is sufficient to disrupt DNA replication. The mechanisms by which DNA replication stress is induced in response to oxidised DNA bases that lead to further DNA damage remain undefined, and more work is still needed to interpret these issues. Interestingly, in our experiments, the type of DDR changes differed depending on the NSCLC cell line, with DDR activation in H522 cells and DDR inactivation in the other two verified cell lines (H23, and A549). After NUDT1 knockdown, the up-regulation of pChk2 (Thr 68) expression in H522 cells (Figure 4-6) suggests that DNA DSBs arise and lead to activate the ATM/Chk2-mediated pathway, but the reasons for reduced total Chk1 levels in both H23 and A549 cell cultures are unclear (Figure 4-7). Though the activation of DDR after NUDT1 knockdown has previously been reported, including phosphorylation of H2AX, 53BP1, ATM and RAD51/DNA-PKcs (Gad et al., 2014, Huber et al., 2014, Rai et al., 2009, Patel et al., 2015), to our knowledge this is the first time that a NUDT1-knockdown-associated DDR ‘switch off’ has been detected. The induction of DDR factor deficiency may indicate that the knockdown of NUDT1 in H23 and A549 cells initially induces DNA replication fork stalling and ATR/Chk1 activation, but that the cell culture bulk efficiently turned off such cell cycle checkpoint signaling cascade by lowering Chk1 levels to continue proliferating. Given that the levels of Chk1 were reduced within 4 days of NUDT1 knockdown, this would not be enough for mutation and clonal expansion to occur within the population, suggesting that the suppression of Chk1 arises through another mechanism that may involve changes in gene expression (epigenetic), RNA processing, post-translational modifications and/or proteosomal degradation. Accordingly, various stresses have

previously been linked to degradation of Chk1 (Merry et al., 2010, Zhang and Hunter, 2014).

There may be several reasons to explain why the alteration in DDR signaling varied among the NUDT1-deficient NSCLC cell line, as one of them (H522 cells) initiate the ATM/Chk2 pathway and others (H23, and A549 cells) ATR/Chk1. The deficiency of NUDT1 enzyme along with its associated DNA oxidation could lead to differing types of secondary DNA damage lesions, perhaps, depending on the cell line and cancer type. Another possible explanation is that the type of DNA damage could be the same, but the ATM/Chk2 and ATR/Chk1 pathways are ultimately interlinked as ATM-activating DSBs can afterward lead to ATR activation if they are resected to produce ssDNA overhangs prior to homologous recombination-mediated DNA repair (Shiotani and Zou, 2009), and processing of ATR-activating stalled forks can generate one-ended DSBs that subsequently activates ATM (Hanada et al., 2007). Alternatively, given that different cancers already have many other genetic mutations and potentially DDR defects, the signaling variances by this mean may simply reflect the differing abilities and deficiencies in DDR functions and signaling capabilities in different cancers.

A critical finding in this work relates to the cell viability data. Our original hypothesis was that NUDT1 protein depletion would kill NSCLC cells in a selective manner, which was based both on our observation of higher oxidatively damaged DNA levels in NSCLC cells (Figures 4-1, 4-2, and 4-3) and on earlier findings relating to cell growth in various cancer cells (Gad et al., 2014, Rai et al., 2011, Rai et al., 2009, Giribaldi et al., 2015). In contrast to this expectation, successfully transient NUDT1 knockdown herein does not lead to induction levels of cellular apoptosis. Moreover, by using WST-1 assay to assess metabolic activity of the cell culture, NUDT1-deficient H23 cells slowed down its cellular proliferation, but this was not seen for other NSCLC cell lines. The lack of proliferation in H23 without apoptotic cell death has previously been reported following stable NUDT1 knockdown in human BJ fibroblasts, as analysed by Annexin V/PI staining (Rai et al., 2009). However, earlier study (Patel et al., 2015) has shown negligible cell death induction in shNUDT1 infected NSCLC cells (H23, H358, and A549), with reducing cell proliferation capacity in H23 and H358 cells, or even complete proliferative arrest (in G1/S) and senescence activation in A549 cells which retain competent p53 (Patel et al., 2015). Indeed, in this study, all NSCLC cell lines responded similarly to NUDT1 depletion in terms of increased DNA oxidation and

without apoptotic cell death enhancement. However, to some extent our cell proliferation findings are contradictory to previous assertions in the literature (Patel et al., 2015), especially for NUDT1-deficient A549, as they did not exhibit any change in cellular proliferation and/or viability, suggesting overall that the status of p53 does not impact on such outcomes.

Despite the lack of cytotoxicity in NSCLC cell lines following siRNA-mediated NUDT1 depletion, and given that a recent study suggested that NUDT1 acts to drop apoptosis levels in glioma cells during H₂O₂ treatment (Tu et al., 2016), it is still proposed that targeting NUDT1 could be an effective approach to enhance current therapeutic strategies which induce oxidative stress, DNA replication stress, as well as DNA damage. Unfortunately again, NUDT1 deficiency in H23 and H522 cells does not increase the apoptotic death levels when combined with cisplatin and gemcitabine treatments (Figures 5-19, and 5-20). Similar observation was seen with another siRNA directed against human NUDT1 that applied instead to transfect H23 cell line (Figure 5-21). To our knowledge, this is the first time that such combined treatments with NUDT1 inhibition have been tested. Collectively, these findings are unexpected, but are of interest in the cancer field, as they indicate that inhibiting NUDT1 is likely not an effective therapeutic strategy for NSCLC patients even if utilized in combination treatments.

There are several reasons for the contradictions between our data and previous literature observations and why it was not seen herein the anticipated NUDT1 knockdown effects on cancer cell viability. Simply, the NUDT1 knockdown levels in our experiments were not sufficient enough to induce NUDT1 enzyme deficiency and lead to subsequent cellular apoptosis. Or, as already discussed (Ke et al., 2014), the second explanation is that the presence of other factors may be able to sufficiently compensate for NUDT1. However, it is not believed this to be the basis of notice disparities, as shown in Figures (4-1, 4-2, 4-3, 5-7, 5-8, 5-9, 5-10, and 5-11), the levels of oxidised DNA bases were increased about 1.5 to 2-fold in NSCLC cell lines after NUDT1 deficiency which is comparable to that in earlier studies that did detect loss of cellular viability (Rai et al., 2009, Gad et al., 2014, Giribaldi et al., 2015). Alternatively, the discrepancy in obtained results and the difference in conclusions may be due to the application of different types of cell viability assays in current studies relative to majority of the others. Here, the annexin V/PI apoptosis assay was used to determining the apoptotic cell death levels,

whereas much of the past work used cell growth and senescence assays including calculation of population doubling time, colony formation ability, and detection of senescence-associated beta-galactosidase activity.

However, more recent new studies may shed some light on the inconsistencies between our findings and those past works. Two independent studies did not observe any growth inhibition in U2OS and HeLa cells knocked down for NUDT1 (Kettle et al., 2016, Kawamura et al., 2016). In addition, it has been suggested by Kettle et al., 2016, that at least some observations from the original previous work (Gad et al., 2014) were attributed to ‘off-target’, nonspecific effects of the utilised siRNA rather than NUDT1 knockdown itself (Kettle et al., 2016). After the complete knocked out of NUDT1 by CRISPR technique, the SW480 colorectal adenocarcinoma stable clones could also continue growing efficiently as proved to be viable as their wild-type counterparts (Kettle et al., 2016). However, it is mentioned that CRISPR/Cas9 mutant cells may adapt as happens in yeast after gene deletion and thereby phenotypes may change with the passage or not attributable to original mutants (Teng et al., 2013), thereby siRNA-mediated knockdown is applied here to study the role of NUDT1. Recently, another study (Wang et al., 2016) observed that NUDT1-deficient melanoma cell lines [by shRNA and two published siRNA sequences (Gad et al., 2014)] also did not detect any reduction in cell viability or affect the clonogenic potential formation. In contrast, they induced DNA DSBs in melanoma cells with mutations in BRAF (IgR3 cells) or NRAS (Mel-RM cells), but not in wild-type cells (Mel-FH cells) (Wang et al., 2016). The latter melanoma cells have low endogenous ROS level relative to the other indicated cell lines. Interestingly, the silencing of NUDT1 enzyme rendered melanoma cells more sensitive to apoptotic effect triggered by the oxidative stress inducer of ROS productions, elesclomol (Wang et al., 2016). On the other hand, very recent independent study (Tu et al., 2016) has successfully confirmed the NUDT1 role in malignant glioma cell survival, as a reduction of its expression inhibited colony formation and *in vivo* xenograft tumor growth.

These most recent independent studies also provide some explanation for our findings relating to the effect of small molecule NUDT1 inhibitors, TH287 and TH588. Despite these compounds being suggested as highly effective in killing cancer cells due to NUDT1 inhibition (Gad et al., 2014, Huber et al., 2014), in our studies TH287 and TH588 only induced an increase in apoptotic cell deaths in a subset of NSCLC cell

lines, H23 and H522 cells (Figures 6-7, and 6-8) but not in A549 proficient-p53 cells (Figure 6-9). Moreover, this enhancement in apoptosis levels did not entirely correlate with increases in oxidatively damaged DNA (Figures 6-3, 6-4, and 6-5). The above results suggest that the effects on cell viability may have been distinct from NUDT1 inhibition. Accordingly, it was very recently proposed that both TH287 and TH588 compounds exert much of their cytotoxicity in HeLa cells primarily through tubulin polymerisation defects rather than NUDT1 inhibition (Kawamura et al., 2016), though this conclusion was subsequently challenged (Berglund et al 2016). Interestingly, overexpression of NUDT1 or introduction of ectopic bacterial homology of NUDT1 (MutT) with 8-oxodGTPase activity did not rescue HeLa or melanoma cell lines proliferation capacity after NUDT1 inhibitors treatments (Kawamura et al., 2016, Wang et al., 2016). This NUDT1 overexpression also did not reduce TH588-induced nuclear accumulation of 8-oxodGTP and formation of 53BP1 foci, indicating another mechanism than NUDT1 inhibition might be responsible for TH588-induced DNA damage and reduced viability in melanoma cells (Wang et al., 2016). In addition, both endogenous ROS levels and its reflected carbonylated proteins have some positive correlations with the sensitivity of melanoma cells to apoptosis induced by TH588 (Wang et al., 2016). However, in this study, the data did not show similar relationship between endogenous ROS levels and sensitivity towards TH588 compound, as NSCLC cells were responded differently to TH588 in term of apoptotic cell death induction (Figures 6-7, 6-8, and 6-9), while they exhibited equal low endogenous ROS levels similar to MRC-5 normal cells (Figure 4-5). This suggests other unidentified factors might be responsible for the TH588 sensitivity variations, at least in NSCLC cells. Moreover, the further enhancement in DNA damage and cell death levels observed in melanoma cells when combined NUDT1 knockdown by shRNA or siRNA with TH588 treatments (Wang et al., 2016), indeed indicates that TH588 action on other pathways than NUDT1 inhibition cannot be excluded.

In addition, unlike the first-in-class small molecule NUDT1 inhibitors (Gad et al., 2014), other newly synthesized and highly specific NUDT1 inhibitors were found to not be cytotoxic in cancer cells (Kettle et al., 2016, Petrocchi et al., 2016, Kawamura et al., 2016). Despite their biochemical potency, selectivity and cellular engagement to NUDT1 were confirmed, these independently developed compounds did not elicit any cytotoxic effects or appreciable cellular inhibitory phenotype activity in the verified

panel of cancer cells. Taken together, these independent works and our results suggest that the cytotoxic and tumor growth suppression by knockdown/pharmacological inhibition of NUDT1 which was observed in previous studies (Gad et al., 2014, Huber et al., 2014), more likely attributed to off-target effects. Yet, an improved potent and selective NUDT1 inhibitor (TH1579) has been described recently as an analogue of TH588 and demonstrated *in vivo* an acceptable pharmacokinetics and anti-cancer effects (Berglund et al., 2016), its usefulness to validate NUDT1 inhibitor concept needs to be further verified.

7.2 Future directions

The regulation of oxidative stress status is still a crucial factor in both development of tumours as well as responses to anticancer therapies. Several signaling pathways that are linked to tumorigenesis could also modulate the ROS metabolism via direct or indirect mechanisms (Gorrini et al., 2013). Three main antioxidant pathways have previously been determined to drive ROS detoxification, including reduced glutathione, thioredoxin, and catalase. All these pathways have certain enzymes that could be specifically targeted in order to suppress the antioxidant capabilities within cancer cells, leading to induction of oxidative stress with a preferential killing of cancer (Gorrini et al., 2013). In the case of hypoxia and nutrient deprivation in solid tumors for example, glutathione metabolism that maintained a correct Redox balance has an essential role to ensure cancer cells survive in such extreme stressful environments. By this way, the strategy of combining glutathione inhibitors, or other antioxidant inhibitors, with ionising radiation or chemotherapeutic drugs that promote cell death by inducing oxidative stress conditions, possibly considered to be a useful approach for targeting cancer cells (Gorrini et al., 2013). In addition, this treatment strategy indeed stands in contrast to conventional way of targeting oncogenes and tumor suppressors genes which has emerged to be mostly ineffective due to presence of numerous oncogenes and tumor suppressors along with their ability to evoke compensatory pathways, for instance KRAS mutations that cause resistance to anti-epidermal growth factor receptor drugs (Gorrini et al., 2013). Therefore, these cancer cells are characterized by having a high antioxidant capacity required to modulate ROS to levels that are compatible with the biological functions within the cell but still higher than that in normal cells, to some extent. It has believed that by targeting such enhanced antioxidant defence mechanisms

might still represent an effective approach that can tackle cancer cells in specific manner, including tumor-initiating cells but not normal cells (Gorrini et al., 2013).

In conclusion, this work is an important contribution to the cancer field as it is shown that NUDT1 has a specific role in NSCLC cells for protection against the accumulation of oxidatively damaged DNA, but it is not regarded as ‘conditionally essential’ for the survival of NSCLC cells. In addition, the lack of cytotoxicity in the observed results of newly synthesis specific NUDT1 inhibitors support our NUDT1 knockdown data, and at the same time, strengthen the argument that NUDT1 inhibitors will not make effective therapeutic agents. Hence, we proposed that the notion to target NUDT1 as a potential therapeutic approach is not worth to pursue for NSCLC, even as an augementer of current therapies. On the contrary, our findings indicate that inhibiting NUDT1 leads to non-cytotoxic oxidative DNA damage, which may actually promote genomic instability and mutation accumulation that could ultimately contribute to tumour heterogeneity and evolution.

Appendix

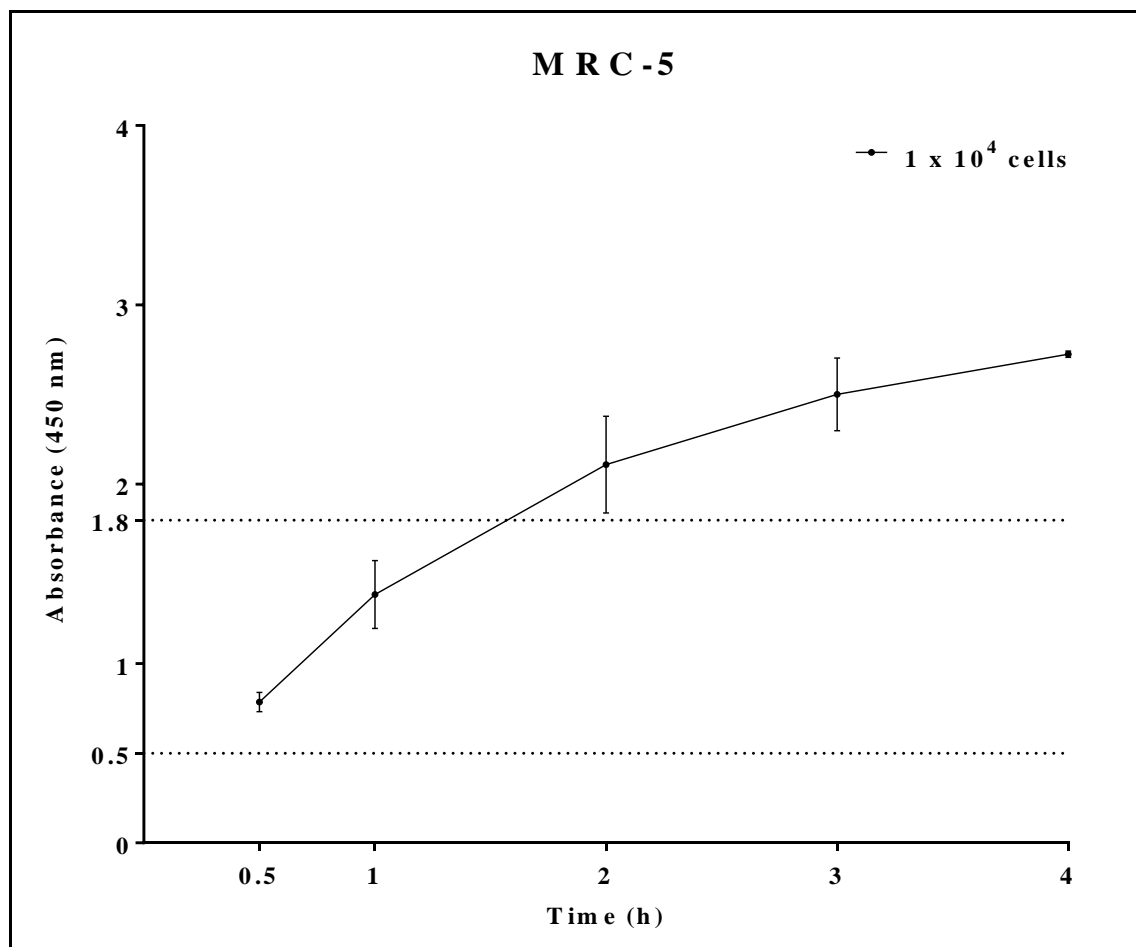


Figure 8-1 The metabolic kinetic of cell proliferation reagent WST-1 in MRC-5 cells cultured at a density of 1×10^4 cells.

MRC-5 cells were seeded (1×10^4 cells per well) in triplicate in 96-well plates and allowed to grow in corresponding culture media for 3 days. Serial samples measurement of absorbance (0.5, 1, 2, 3, and 4 h) were determined against a blank control background after the addition of WST-1 reagent, using plate reader at 450 nm wavelength. For any incubation time period of WST-1 reagent, the absorbance values that ranged between (0.5-1.8) were considered as appropriate measures; regarding cell seeding density and incubation time period. These data were mean \pm SD of four individual experiments.

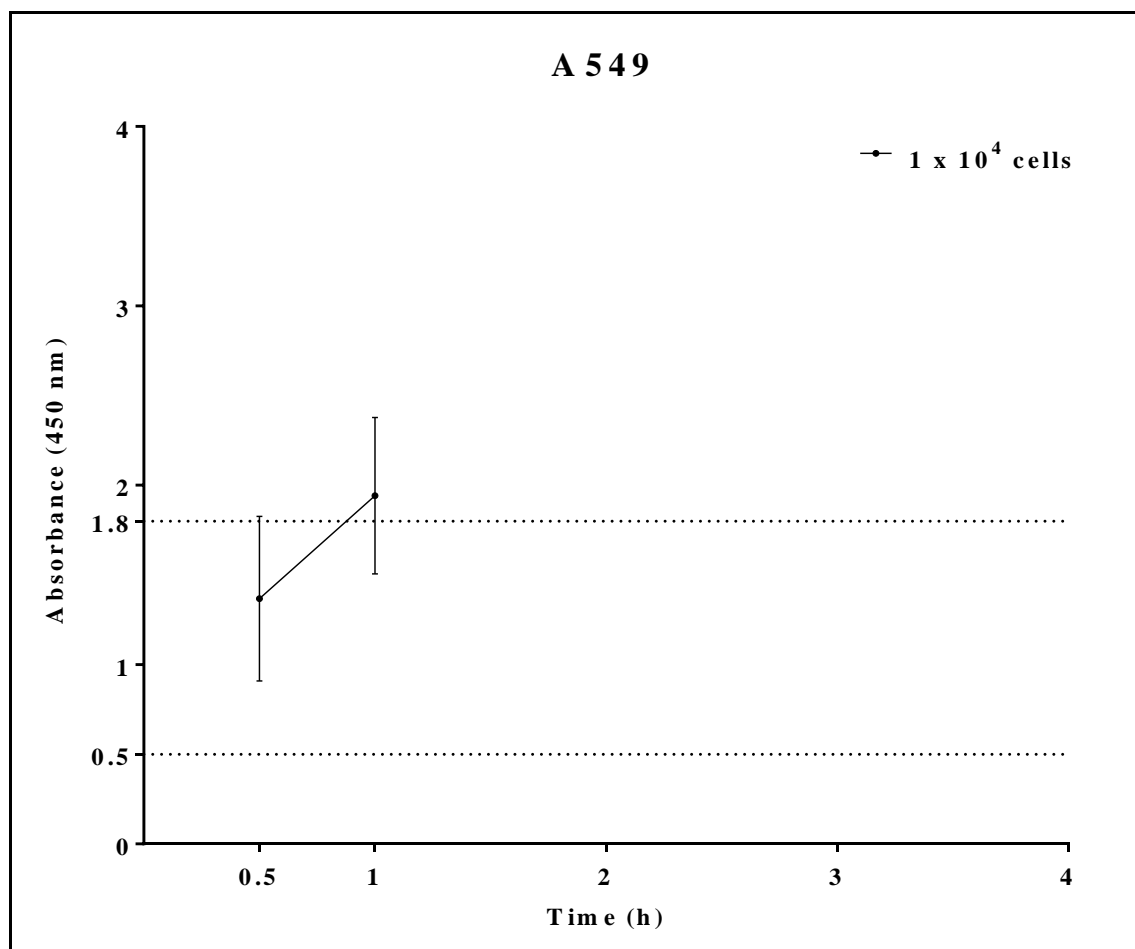


Figure 8-2 The metabolic kinetic of cell proliferation reagent WST-1 in A549 cells cultured at a density of 1×10^4 cells.

A549 cells were seeded (1×10^4 cells per well) in triplicate in 96-well plates and allowed to grow in corresponding culture media for 3 days. Serial samples measurement of absorbance (0.5, 1, 2, 3, and 4 h) were determined against a blank control background after the addition of WST-1 reagent, using plate reader at 450 nm wavelength. For any incubation time period of WST-1 reagent, the absorbance values that ranged between (0.5-1.8) were considered as appropriate measures; regarding cell seeding density and incubation time period. These data were mean \pm SD of four individual experiments.

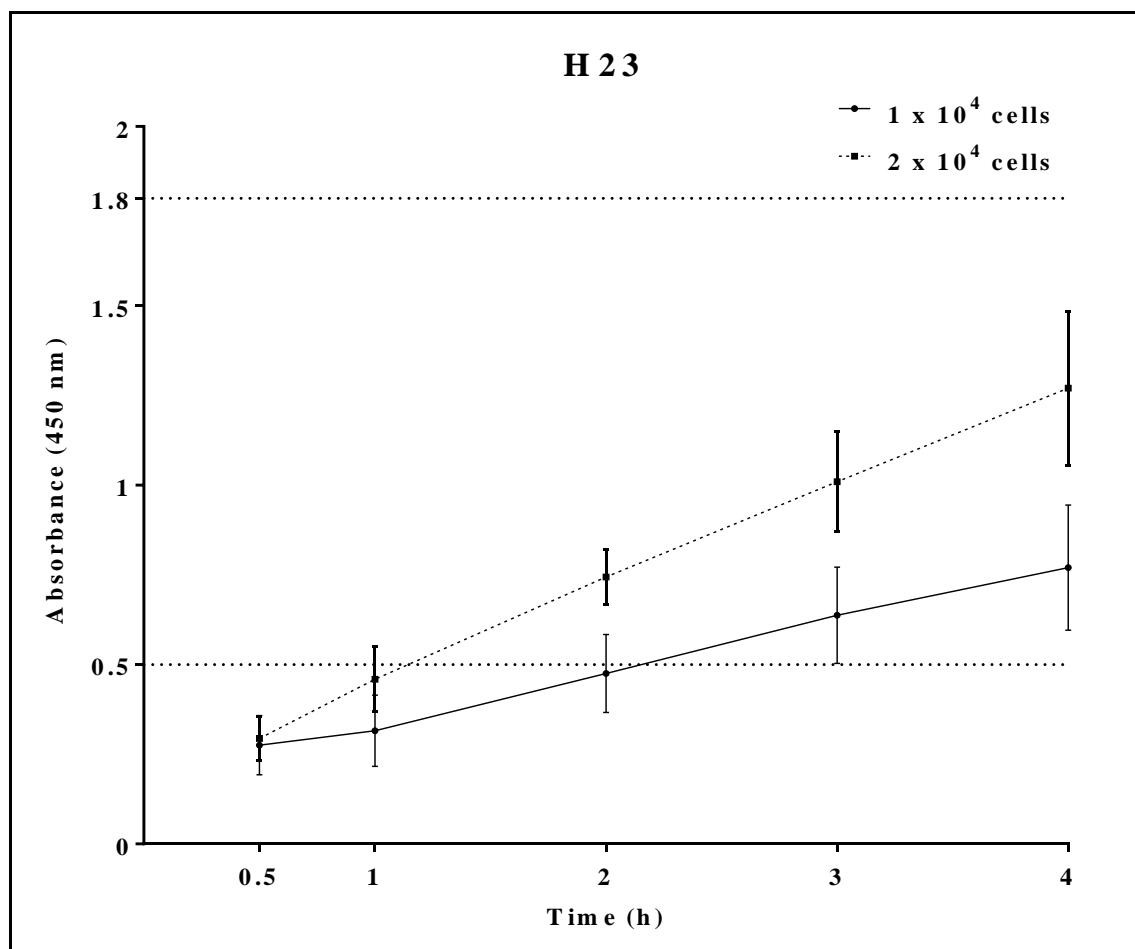


Figure 8-3 The metabolic kinetic of cell proliferation reagent WST-1 in H23 cells cultured at a density of 1 or 2 x 10⁴ cells.

H23 cells were seeded (1 or 2 x 10⁴ cells per well) in triplicate in 96-well plates and allowed to grow in corresponding culture media for 3 days. Serial samples measurement of absorbance (0.5, 1, 2, 3, and 4 h) were determined against a blank control background after the addition of WST-1 reagent, using plate reader at 450 nm wavelength. For any incubation time period of WST-1 reagent, the absorbance values that ranged between (0.5-1.8) were considered as appropriate measures; regarding cell seeding density and incubation time period. These data were mean \pm SD of more than three individual experiments.

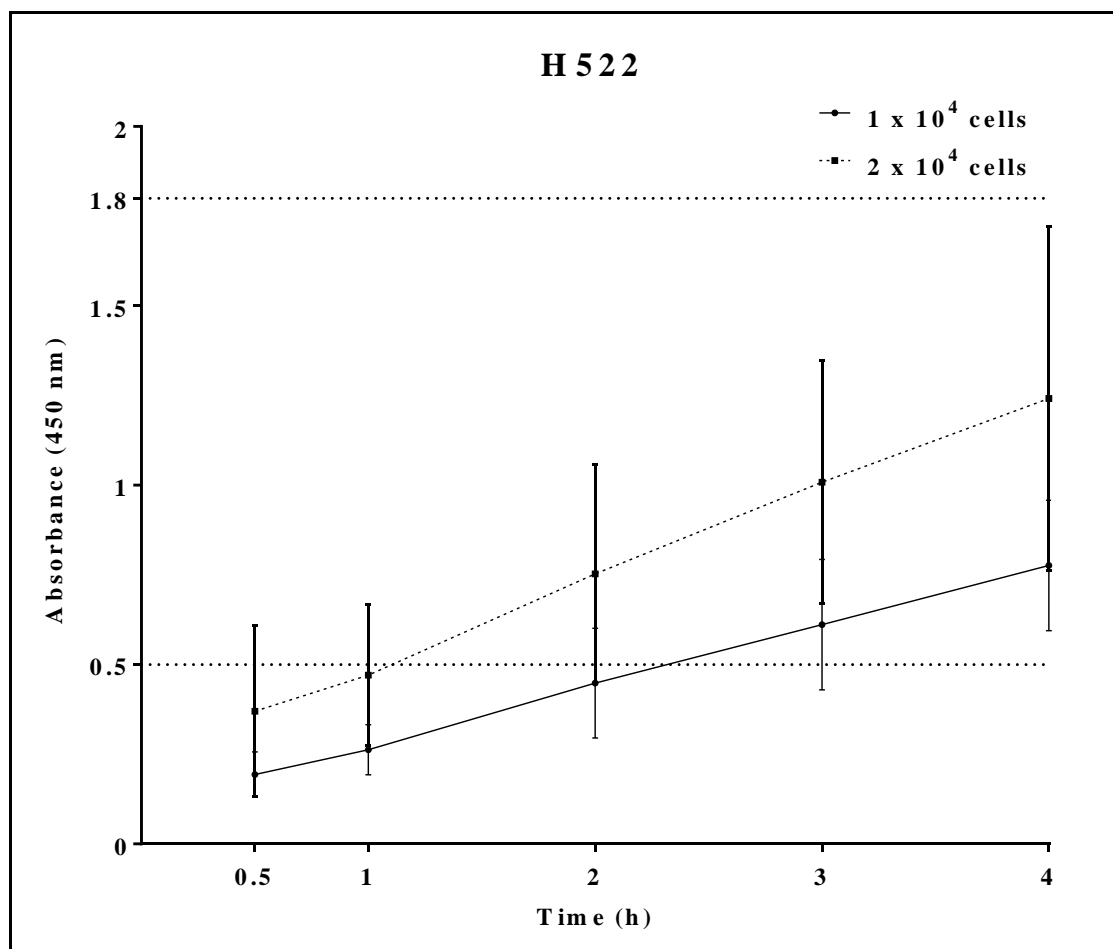


Figure 8-4 The metabolic kinetic of cell proliferation reagent WST-1 in H522 cells cultured at a density of 1 or 2 x 10⁴ cells.

H522 cells were seeded (1 or 2 x 10⁴ cells per well) in triplicate in 96-well plates and allowed to grow in corresponding culture media for 3 days. Serial samples measurement of absorbance (0.5, 1, 2, 3, and 4 h) were determined against a blank control background after the addition of WST-1 reagent, using plate reader at 450 nm wavelength. For any incubation time period of WST-1 reagent, the absorbance values that ranged between (0.5-1.8) were considered as appropriate measures; regarding cell seeding density and incubation time period. These data were mean \pm SD of more than three individual experiments.

References

- ACHIWA, H., OGURI, T., SATO, S., MAEDA, H., NIIMI, T. & UEDA, R. 2004. Determinants of sensitivity and resistance to gemcitabine: The roles of human equilibrative nucleoside transporter 1 and deoxycytidine kinase in non-small cell lung cancer. *Cancer Science*, 95, 753-757.
- AGUILERA, A. & GOMEZ-GONZALEZ, B. 2008. Genome instability: a mechanistic view of its causes and consequences. *Nature Reviews Genetics*, 9, 204-217.
- AHN, J.-Y., SCHWARZ, J. K., PIWNICA-WORMS, H. & CANMAN, C. E. 2000. Threonine 68 Phosphorylation by Ataxia Telangiectasia Mutated Is Required for Efficient Activation of Chk2 in Response to Ionizing Radiation. *Cancer Research*, 60, 5934-5936.
- ALTIERI, F., GRILLO, C., MACERONI, M. & CHICHIARELLI, S. 2008. DNA damage and repair: from molecular mechanisms to health implications. *Antioxid Redox Signal*, 10, 891-937.
- AMARZGUIOUI, M. 2004. Improved siRNA-mediated silencing in refractory adherent cell lines by detachment and transfection in suspension. *Biotechniques*, 36, 766-+.
- ANTUNES, F. & CADENAS, E. 2001. Cellular titration of apoptosis with steady state concentrations of H₂O₂: Submicromolar levels of H₂O₂ induce apoptosis through Fenton chemistry independent of the cellular thiol state. *Free Radical Biology and Medicine*, 30, 1008-1018.
- ARORA, S., BHARDWAJ, A., SINGH, S., SRIVASTAVA, S. K., MCCLELLAN, S., NIRODI, C. S., PIAZZA, G. A., GRIZZLE, W. E., OWEN, L. B. & SINGH, A. P. 2013. An Undesired Effect of Chemotherapy GEMCITABINE PROMOTES PANCREATIC CANCER CELL INVASIVENESS THROUGH REACTIVE OXYGEN SPECIES-DEPENDENT, NUCLEAR FACTOR kappa B- AND HYPOXIA-INDUCIBLE FACTOR 1 alpha-MEDIATED UP-REGULATION OF CXCR4. *Journal of Biological Chemistry*, 288, 21197-21207.

- AULA, S., LAKKIREDDY, S., JAMIL, K., KAPLEY, A., SWAMY, A. V. N. & LAKKIREDDY, H. R. 2015. Biophysical, biopharmaceutical and toxicological significance of biomedical nanoparticles. *Rsc Advances*, 5, 47830-47859.
- BALCER-KUBICZEK, E. K. 2012. Apoptosis in radiation therapy: a double-edged sword. *Exp Oncol*, 34, 277-85.
- BARBOUTI, A., DOULIAS, P.-T., NOUSIS, L., TENOPOULOU, M. & GALARIS, D. 2002. DNA damage and apoptosis in hydrogen peroxide-exposed Jurkat cells: bolus addition versus continuous generation of H₂O₂. *Free Radical Biology and Medicine*, 33, 691-702.
- BARTKOVA, J., HOREJSI, Z., KOED, K., KRAMER, A., TORT, F., ZIEGER, K., GULDBERG, P., SEHESTED, M., NESLAND, J. M., LUKAS, C., ORNTOFT, T., LUKAS, J. & BARTEK, J. 2005. DNA damage response as a candidate anti-cancer barrier in early human tumorigenesis. *Nature*, 434, 864-870.
- BASU, A. & KRISHNAMURTHY, S. 2010. Cellular responses to Cisplatin-induced DNA damage. *Journal of nucleic acids*, 2010.
- BEPLER, G., KUSMARTSEVA, I., SHARMA, S., GAUTAM, A., CANTOR, A., SHARMA, A. & SIMON, G. 2006. RRM1 modulated in vitro and in vivo efficacy of gemcitabine and platinum in non-small-cell lung cancer. *Journal of Clinical Oncology*, 24, 4731-4737.
- BERGLUND, U. W., SANJIV, K., GAD, H., KALDEREN, C., KOOLMEISTER, T., PHAM, T., GOKTURK, C., JAFARI, R., MADDALO, G., SEASHORE-LUDLOW, B., CHERNOBROVKIN, A., MANOILOV, A., PATERAS, I. S., RASTI, A., JEMTH, A. S., ALMLOF, I., LOSEVA, O., VISNES, T., EINARSDOTTIR, B. O., GAUGAZ, F. Z., SALEH, A., PLATZACK, B., WALLNER, O. A., VALLIN, K. S. A., HENRIKSSON, M., WAKCHAURE, P., BORHADE, S., HERR, P., KALLBERG, Y., BARANCZEWSKI, P., HOMAN, E. J., WIITA, E., NAGPAL, V., MEIJER, T., SCHIPPER, N., RUDD, S. G., BRAUTIGAM, L., LINDQVIST, A., FILPPULA, A., LEE, T. C., ARTURSSON, P., NILSSON, J. A., GORGOULIS, V. G., LEHTIO, J., ZUBAREV, R. A., SCOBIE, M. & HELLEDAY, T. 2016. Validation and

- development of MTH1 inhibitors for treatment of cancer. *Annals of Oncology*, 27, 2275-2283.
- BESSE, B. & RECK, M. 2014. Pharmacogenomics in NSCLC: mostly unsexy but desperately needed. *Annals of Oncology*, 25, 2099-2100.
- BIALKOWSKI, K. & KASPRZAK, K. S. 2004. Cellular 8-oxo-7,8-dihydro-2'-deoxyguanosine 5'-triphosphate pyrophosphohydrolase activity of human and mouse MTH1 proteins does not depend on the proliferation rate. *Free Radical Biology and Medicine*, 37, 1534-1541.
- BIALKOWSKI, K., SZPILA, A. & KASPRZAK, K. S. 2009. Up-regulation of 8-oxo-dGTPase Activity of MTH1 Protein in the Brain, Testes and Kidneys of Mice Exposed to Cs-137 gamma Radiation. *Radiation Research*, 172, 187-197.
- BOREK, C. 2004. Antioxidants and radiation therapy. *Journal of Nutrition*, 134, 3207S-3209S.
- BOYER, A. S., WALTER, D. & SORENSEN, C. S. 2016. DNA replication and cancer: From dysfunctional replication origin activities to therapeutic opportunities. *Seminars in Cancer Biology*, 37-38, 16-25.
- BRAUTIGAM, L., PUDELKO, L., JEMTH, A. S., GAD, H., NARWAL, M., GUSTAFSSON, R., KARSTEN, S., PUIGVERT, J. C., HOMAN, E., BERNDT, C., BERGLUND, U. W., STENMARK, P. & HELLEDAY, T. 2016. Hypoxic Signaling and the Cellular Redox Tumor Environment Determine Sensitivity to MTH1 Inhibition. *Cancer Research*, 76, 2366-2375.
- BRYANT, H. E., SCHULTZ, N., THOMAS, H. D., PARKER, K. M., FLOWER, D., LOPEZ, E., KYLE, S., MEUTH, M., CURTIN, N. J. & HELLEDAY, T. 2005. Specific killing of BRCA2-deficient tumours with inhibitors of poly(ADP-ribose) polymerase. *Nature*, 434, 913-917.
- BUCH, K., PETERS, T., NAWROTH, T., SANGER, M., SCHMIDBERGER, H. & LANGGUTH, P. 2012. Determination of cell survival after irradiation via clonogenic assay versus multiple MTT Assay - A comparative study. *Radiation Oncology*, 7, 6.

- BURRELL, R. A., MCCLELLAND, S. E., ENDEFELDER, D., GROTH, P., WELLER, M. C., SHAIKH, N., DOMINGO, E., KANU, N., DEWHURST, S. M., GRONROOS, E., CHEW, S. K., ROWAN, A. J., SCHENK, A., SHEFFER, M., HOWELL, M., KSCHISCHO, M., BEHRENS, A., HELLEDAY, T., BARTEK, J., TOMLINSON, I. R. & SWANTON, C. 2013a. Replication stress links structural and numerical cancer chromosomal instability. *Nature*, 494, 492-496.
- BURRELL, R. A., MCGRANAHAN, N., BARTEK, J. & SWANTON, C. 2013b. The causes and consequences of genetic heterogeneity in cancer evolution. *Nature*, 501, 338-345.
- CADET, J., BOURDAT, A. G., D'HAM, C., DUARTE, V., GASPARUTTO, D., ROMIEU, A. & RAVANAT, J. L. 2000. Oxidative base damage to DNA: specificity of base excision repair enzymes. *Mutation Research-Reviews in Mutation Research*, 462, 121-128.
- CALDERON-MONTANO, J. M., BURGOS-MORON, E., ORTA, M. L. & LOPEZ-LAZARO, M. 2014. Effect of DNA Repair Deficiencies on the Cytotoxicity of Drugs Used in Cancer Therapy - A Review. *Current Medicinal Chemistry*, 21, 3419-3454.
- CAMPISI, J. & DI FAGAGNA, F. D. 2007. Cellular senescence: when bad things happen to good cells. *Nature Reviews Molecular Cell Biology*, 8, 729-740.
- CARTER, M., JEMTH, A. S., HAGENKORT, A., PAGE, B. D. G., GUSTAFSSON, R., GRIESE, J. J., GAD, H., VALERIE, N. C. K., DESROSES, M., BOSTROM, J., BERGLUND, U. W., HELLEDAY, T. & STENMARK, P. 2015. Crystal structure, biochemical and cellular activities demonstrate separate functions of MTH1 and MTH2. *Nature Communications*, 6, 10.
- CASARES, C., RAMIREZ-CAMACHO, R., TRINIDAD, A., ROLDAN, A., JORGE, E. & GARCIA-BERROCAL, J. R. 2012. Reactive oxygen species in apoptosis induced by cisplatin: review of physiopathological mechanisms in animal models. *European Archives of Oto-Rhino-Laryngology*, 269, 2455-2459.

- CERQUEIRA, N., FERNANDES, P. A. & RAMOS, M. J. 2007. Ribonucleotide reductase: A critical enzyme for cancer chemotherapy and antiviral agents. *Recent Patents on Anti-Cancer Drug Discovery*, 2, 11-29.
- CHANG, G. C., HSU, S. L., TSAI, J. R., WU, W. J., CHEN, C. Y. & SHEU, G. T. 2004. Extracellular signal-regulated kinase activation and Bcl-2 downregulation mediate apoptosis after gemcitabine treatment partly via a p53-independent pathway. *European Journal of Pharmacology*, 502, 169-183.
- CHEN, J. L., EMARA, N., SOLOMIDES, C., PAREKH, H. & SIMPKINS, H. 2010. Resistance to platinum-based chemotherapy in lung cancer cell lines. *Cancer Chemotherapy and Pharmacology*, 66, 1103-1111.
- CICCIA, A. & ELLEDGE, S. J. 2010. The DNA Damage Response: Making It Safe to Play with Knives. *Molecular Cell*, 40, 179-204.
- COLEMAN, M. P., FORMAN, D., BRYANT, H., BUTLER, J., RACHET, B., MARINGE, C., NUR, U., TRACEY, E., COORY, M., HATCHER, J., MCGAHAN, C. E., TURNER, D., MARRETT, L., GJERSTORFF, M. L., JOHANNESSEN, T. B., ADOLFSSON, J., LAMBE, M., LAWRENCE, G., MEECHAN, D., MORRIS, E. J., MIDDLETON, R., STEWARD, J. & RICHARDS, M. A. 2011. Cancer survival in Australia, Canada, Denmark, Norway, Sweden, and the UK, 1995-2007 (the International Cancer Benchmarking Partnership): an analysis of population-based cancer registry data. *Lancet*, 377, 127-38.
- COLLINS, A. R., DUSINSKA, M., GEDIK, C. M. & STETINA, R. 1996. Oxidative damage to DNA: Do we have a reliable biomarker? *Environmental Health Perspectives*, 104, 465-469.
- COLLINS, A. R., OSCOZ, A. A., BRUNBORG, G., GAIVAO, I., GIOVANNELLI, L., KRUSZEWSKI, M., SMITH, C. C. & STETINA, R. 2008. The comet assay: topical issues. *Mutagenesis*, 23, 143-151.
- COLUSSI, C., PARLANTI, E., DEGAN, P., AQUILINA, G., BARNES, D., MACPHERSON, P., KARRAN, P., CRESCENZI, M., DOGLIOTTI, E. & BIGNAMI, M. 2002. The mammalian mismatch repair pathway removes DNA

- 8-oxodGMP incorporated from the oxidized dNTP pool. *Current Biology*, 12, 912-918.
- CONKLIN, K. A. 2004. Chemotherapy-associated oxidative stress: impact on chemotherapeutic effectiveness. *Integr Cancer Ther*, 3, 294-300.
- COOKE, M. S., DUARTE, T. L., COOPER, D., CHEN, J., NANDAGOPAL, S. & EVANS, M. D. 2008. Combination of azathioprine and UVA irradiation is a major source of cellular 8-oxo-7,8-dihydro-2'-deoxyguanosine. *DNA Repair*, 7, 1982-1989.
- COOKE, M. S., EVANS, M. D., DOVE, R., ROZALSKI, R., GACKOWSKI, D., SIOMEK, A., LUNEC, J. & OLINSKI, R. 2005. DNA repair is responsible for the presence of oxidatively damaged DNA lesions in urine. *Mutation Research-Fundamental and Molecular Mechanisms of Mutagenesis*, 574, 58-66.
- COOKE, M. S., HENDERSON, P. T. & EVANS, M. D. 2009. Sources of Extracellular, Oxidatively-Modified DNA Lesions: Implications for Their Measurement in Urine. *Journal of Clinical Biochemistry and Nutrition*, 45, 255-270.
- CORTES-LEDESMA, F. & AGUILERA, A. 2006. Double-strand breaks arising by replication through a nick are repaired by cohesin-dependent sister-chromatid exchange. *Embo Reports*, 7, 919-926.
- COYLE, C. H. & KADER, K. N. 2007. Mechanisms of H₂O₂-induced oxidative stress in endothelial cells exposed to physiologic shear stress. *ASAIO J*, 53, 17-22.
- CRESPAN, E., HUBSCHER, U. & MAGA, G. 2007. Error-free bypass of 2-hydroxyadenine by human DNA polymerase lambda with Proliferating Cell Nuclear Antigen and Replication Protein A in different sequence contexts. *Nucleic Acids Research*, 35, 5173-5181.
- DE CASTRO CARPEÑO, J. & BELDA-INIESTA, C. 2013. KRAS mutant NSCLC, a new opportunity for the synthetic lethality therapeutic approach. *Translational Lung Cancer Research*, 2, 142-151.

- DESOUKY, O., DING, N. & ZHOU, G. 2015. Targeted and non-targeted effects of ionizing radiation. *Journal of Radiation Research and Applied Sciences*, 8, 247-254.
- DIZDAROGLU, M. & JARUGA, P. 2012. Mechanisms of free radical-induced damage to DNA. *Free Radical Research*, 46, 382-419.
- DONADELLI, M., COSTANZO, C., BEGHELLI, S., SCUPOLI, M. T., DANDREA, M., BONORA, A., PIACENTINI, P., BUDILLON, A., CARAGLIA, M., SCARPA, A. & PALMIERI, M. 2007. Synergistic inhibition of pancreatic adenocarcinoma cell growth by trichostatin A and gemcitabine. *Biochimica Et Biophysica Acta-Molecular Cell Research*, 1773, 1095-1106.
- DUARTE, T. L. & JONES, G. D. D. 2007. Vitamin C modulation of H₂O₂-induced damage and iron homeostasis in human cells. *Free Radical Biology and Medicine*, 43, 1165-1175.
- EVANS, M. D. & COOKE, M. S. 2007. *Oxidative damage to nucleic acids*, New York, NY, Springer New York.
- EVANS, M. D., DIZDAROGLU, M. & COOKE, M. S. 2004. Oxidative DNA damage and disease: induction, repair and significance. *Mutation Research-Reviews in Mutation Research*, 567, 1-61.
- EVANS, M. D., SAPARBAEV, M. & COOKE, M. S. 2010. DNA repair and the origins of urinary oxidized 2'-deoxyribonucleosides. *Mutagenesis*, 25, 433-442.
- FARMER, H., MCCABE, N., LORD, C. J., TUTT, A. N. J., JOHNSON, D. A., RICHARDSON, T. B., SANTAROSA, M., DILLON, K. J., HICKSON, I., KNIGHTS, C., MARTIN, N. M. B., JACKSON, S. P., SMITH, G. C. M. & ASHWORTH, A. 2005. Targeting the DNA repair defect in BRCA mutant cells as a therapeutic strategy. *Nature*, 434, 917-921.
- FISCHER, S. J., BENSON, L. M., FAUQ, A., NAYLOR, S. & WINDEBANK, A. J. 2008. Cisplatin and dimethyl sulfoxide react to form an adducted compound with reduced cytotoxicity and neurotoxicity. *Neurotoxicology*, 29, 444-452.

- FOTOUHI, A., CORNELLA, N., RAMEZANI, M., WOJCIK, A. & HAGHDOOST, S. 2015. Investigation of micronucleus induction in MTH1 knockdown cells exposed to UVA, UVB or UVC. *Mutation Research-Genetic Toxicology and Environmental Mutagenesis*, 793, 161-165.
- FOTOUHI, A., HAGOS, W. W., ILIC, M., WOJCIK, A., HARMS-RINGDAHL, M., DE GRUIJ, F., MULLENDERS, L., JANSEN, J. G. & HAGHDOOST, S. 2013. Analysis of mutant frequencies and mutation spectra in hMTH1 knockdown TK6 cells exposed to UV radiation. *Mutation Research-Fundamental and Molecular Mechanisms of Mutagenesis*, 751, 8-14.
- FOTOUHI, A., SKIOLD, S., SHAKERI-MANESH, S., OSTERMAN-GOLKAR, S., WOJCIK, A., JENSSEN, D., HARMS-RINGDAHL, M. & HAGHDOOST, S. 2011. Reduction of 8-oxodGTP in the nucleotide pool by hMTH1 leads to reduction in mutations in the human lymphoblastoid cell line TK6 exposed to UVA. *Mutation Research-Fundamental and Molecular Mechanisms of Mutagenesis*, 715, 13-18.
- FUJIKAWA, K., KAMIYA, H., YAKUSHIJI, H., FUJII, Y., NAKABEPPU, Y. & KASAI, H. 1999. The oxidized forms of dATP are substrates for the human MutT homologue, the hMTH1 protein. *Journal of Biological Chemistry*, 274, 18201-18205.
- FUJIKAWA, K., KAMIYA, H., YAKUSHIJI, H., NAKABEPPU, Y. & KASAI, H. 2001. Human MTH1 protein hydrolyzes the oxidized ribonucleotide, 2-hydroxy-ATP. *Nucleic Acids Research*, 29, 449-454.
- GAD, H., KOOLMEISTER, T., JEMTH, A. S., ESHTAD, S., JACQUES, S. A., STROM, C. E., SVENSSON, L. M., SCHULTZ, N., LUNDBACK, T., EINARSDOTTIR, B. O., SALEH, A., GOKTURK, C., BARANCZEWSKI, P., SVENSSON, R., BERNTSSON, R. P. A., GUSTAFSSON, R., STROMBERG, K., SANJIV, K., JACQUES-CORDONNIER, M. C., DESROSES, M., GUSTAVSSON, A. L., OLOFSSON, R., JOHANSSON, F., HOMAN, E. J., LOSEVA, O., BRAUTIGAM, L., JOHANSSON, L., HOGLUND, A., HAGENKORT, A., PHAM, T., ALTUN, M., GAUGAZ, F. Z., VIKINGSSON, S., EVERS, B., HENRIKSSON, M., VALLIN, K. S. A., WALLNER, O. A.,

- HAMMARSTROM, L. G. J., WIITA, E., ALMLOF, I., KALDEREN, C., AXELSSON, H., DJUREINOVIC, T., PUIGVERT, J. C., HAGGBLAD, M., JEPPSSON, F., MARTENS, U., LUNDIN, C., LUNDGREN, B., GRANELLI, I., JENSEN, A. J., ARTURSSON, P., NILSSON, J. A., STENMARK, P., SCOBIE, M., BERGLUND, U. W. & HELLEDAY, T. 2014. MTH1 inhibition eradicates cancer by preventing sanitation of the dNTP pool. *Nature*, 508, 215-+.
- GAILLARD, H., GARCIA-MUSE, T. & AGUILERA, A. 2015. Replication stress and cancer. *Nature Reviews Cancer*, 15, 276-289.
- GALLUZZI, L., AARONSON, S. A., ABRAMS, J., ALNEMRI, E. S., ANDREWS, D. W., BAEHRECKE, E. H., BAZAN, N. G., BLAGOSKLONNY, M. V., BLOMGREN, K., BORNER, C., BREDESEN, D. E., BRENNER, C., CASTEDO, M., CIDLOWSKI, J. A., CIECHANOVER, A., COHEN, G. M., DE LAURENZI, V., DE MARIA, R., DESHMUKH, M., DYNLACHT, B. D., EL-DEIRY, W. S., FLAVELL, R. A., FULDA, S., GARRIDO, C., GOLSTEIN, P., GOUGEON, M. L., GREEN, D. R., GRONEMEYER, H., HAJNOCZKY, G., HARDWICK, J. M., HENGARTNER, M. O., ICHIJO, H., JAATTELA, M., KEPP, O., KIMCHI, A., KLIONSKY, D. J., KNIGHT, R. A., KORNBLUTH, S., KUMAR, S., LEVINE, B., LIPTON, S. A., LUGLI, E., MADEO, F., MALORNI, W., MARINE, J. C. W., MARTIN, S. J., MEDEMA, J. P., MEHLEN, P., MELINO, G., MOLL, U. M., MORSELLI, E., NAGATA, S., NICHOLSON, D. W., NICOTERA, P., NUNEZ, G., OREN, M., PENNINGER, J., PERVAIZ, S., PETER, M. E., PIACENTINI, M., PREHN, J. H. M., PUTHALAKATH, H., RABINOVICH, G. A., RIZZUTO, R., RODRIGUES, C. M. P., RUBINSZTEIN, D. C., RUDEL, T., SCORRANO, L., SIMON, H. U., STELLER, H., TSCHOPP, J., TSUJIMOTO, Y., VANDENABEELE, P., VITALE, I., VOUSDEN, K. H., YOULE, R. J., YUAN, J., ZHIVOTOVSKY, B. & KROEMER, G. 2009. Guidelines for the use and interpretation of assays for monitoring cell death in higher eukaryotes. *Cell Death and Differentiation*, 16, 1093-1107.
- GARCIA, C. L., FILIPPI, S., MOSESSO, P., CALVANI, M., NICOLAI, R., MOSCONI, L. & PALITTI, F. 2006. The protective effect of L-carnitine in

- peripheral blood human lymphocytes exposed to oxidative agents. *Mutagenesis*, 21, 21-7.
- GAUTIER, J., SOLOMON, M. J., BOOHER, R. N., BAZAN, J. F. & KIRSCHNER, M. W. 1991. cdc25 is a specific tyrosine phosphatase that directly activates p34cdc2. *Cell*, 67, 197-211.
- GIRIBALDI, M. G., MUNOZ, A., HALVORSEN, K., PATEL, A. & RAI, P. 2015. MTH1 expression is required for effective transformation by oncogenic HRAS. *Oncotarget*, 6, 11519-11529.
- GORGOULIS, V. G., VASSILIOU, L. V. F., KARAKAIDOS, P., ZACHARATOS, P., KOTSINAS, A., LILOGLOU, T., VENERE, M., DITULLIO, R. A., KASTRINAKIS, N. G., LEVY, B., KLETSAS, D., YONETA, A., HERLYN, M., KITTAS, C. & HALAZONETIS, T. D. 2005. Activation of the DNA damage checkpoint and genomic instability in human precancerous lesions. *Nature*, 434, 907-913.
- GORRINI, C., HARRIS, I. S. & MAK, T. W. 2013. Modulation of oxidative stress as an anticancer strategy. *Nature Reviews Drug Discovery*, 12, 931-947.
- GUILLOTIN, D. & MARTIN, S. A. 2014. Exploiting DNA mismatch repair deficiency as a therapeutic strategy. *Experimental Cell Research*, 329, 110-115.
- GUO, Z., KOZLOV, S., LAVIN, M. F., PERSON, M. D. & PAULL, T. T. 2010. ATM activation by oxidative stress. *Science*, 330, 517-21.
- HABIRO, A., TANNO, S., KOIZUMI, K., IZAWA, T., NAKANO, Y., OSANAI, M., MIZUKAMI, Y., OKUMURA, T. & KOHGO, Y. 2004. Involvement of p38 mitogen-activated protein kinase in gemcitabine-induced apoptosis in human pancreatic cancer cells. *Biochemical and Biophysical Research Communications*, 316, 71-77.
- HAGHDOOST, S., CZENE, S., NASLUND, I., SKOG, S. & HARMS-RINGDAHL, M. 2005. Extracellular 8-oxo-dG as a sensitive parameter for oxidative stress in vivo and in vitro. *Free Radical Research*, 39, 153-162.

- HANADA, K., BUDZOWSKA, M., DAVIES, S. L., VAN DRUNEN, E., ONIZAWA, H., BEVERLOO, H. B., MAAS, A., ESSERS, J., HICKSON, I. D. & KANAAR, R. 2007. The structure-specific endonuclease Mus81 contributes to replication restart by generating double-strand DNA breaks. *Nature Structural & Molecular Biology*, 14, 1096-1104.
- HANAHAN, D. & WEINBERG, R. A. 2011. Hallmarks of Cancer: The Next Generation. *Cell*, 144, 646-674.
- HASLETT, K., POTTGEN, C., STUSCHKE, M. & FAIVRE-FINN, C. 2014. Hyperfractionated and accelerated radiotherapy in non-small cell lung cancer. *Journal of Thoracic Disease*, 6, 328-335.
- HASTINGS, P. J., IRA, G. & LUPSKI, J. R. 2009. A Microhomology-Mediated Break-Induced Replication Model for the Origin of Human Copy Number Variation. *Plos Genetics*, 5, 9.
- HATAHET, Z., KOW, Y. W., PURMAL, A. A., CUNNINGHAM, R. P. & WALLACE, S. S. 1994. NEW SUBSTRATES FOR OLD ENZYMES - 5-HYDROXY-2'-DEOXYCYTIDINE AND 5-HYDROXY-2'-DEOXYURIDINE ARE SUBSTRATES FOR ESCHERICHIA-COLI ENDONUCLEASE-III AND FORMAMIDOPYRIMIDINE DNA N-GLYCOSYLASE, WHILE 5-HYDROXY-2'-DEOXYURIDINE IS A SUBSTRATE FOR URACIL DNA N-GLYCOSYLASE. *Journal of Biological Chemistry*, 269, 18814-18820.
- HE, C. H., MASSON, J. Y. & RAMOTAR, D. 1996. A *Saccharomyces cerevisiae* phleomycin-sensitive mutant, ph140, is defective in the RAD6 DNA repair gene. *Can J Microbiol*, 42, 1263-6.
- HELLEDAY, T. 2014. Cancer phenotypic lethality, exemplified by the non-essential MTH1 enzyme being required for cancer survival. *Annals of Oncology*, 25, 1253-1255.
- HENDERSON, P. T., EVANS, M. D. & COOKE, M. S. 2010. Salvage of oxidized guanine derivatives in the (2'-deoxy)ribonucleotide pool as source of mutations in DNA. *Mutation Research-Genetic Toxicology and Environmental Mutagenesis*, 703, 11-17.

- HILL, R., RABB, M., MADUREIRA, P. A., CLEMENTS, D., GUJAR, S. A., WAISMAN, D. M., GIACOMANTONIO, C. A. & LEE, P. W. K. 2013. Gemcitabine-mediated tumour regression and p53-dependent gene expression: implications for colon and pancreatic cancer therapy. *Cell Death & Disease*, 4.
- HIMMELSTEIN, K. J., PATTON, T. F., BELT, R. J., TAYLOR, S., REPTA, A. J. & STERNSON, L. A. 1981. CLINICAL KINETICS OF INTACT CISPLATIN AND SOME RELATED SPECIES. *Clinical Pharmacology and Therapeutics*, 29, 658-664.
- HIRSCH, F. R., SPREAFICO, A., NOVELLO, S., WOOD, M. D., SIMMS, L. & PAPOTTI, M. 2008. The Prognostic and Predictive Role of Histology in Advanced Non-small Cell Lung Cancer A Literature Review. *Journal of Thoracic Oncology*, 3, 1468-1481.
- HOFFMAN, R. M. 1991. INVITRO SENSITIVITY ASSAYS IN CANCER - A REVIEW, ANALYSIS, AND PROGNOSIS. *Journal of Clinical Laboratory Analysis*, 5, 133-143.
- HOFFMAN, R. M. 1993. IN-VITRO ASSAYS FOR CHEMOTHERAPY SENSITIVITY. *Critical Reviews in Oncology/Hematology*, 15, 99-111.
- HOGGARD, J., FAN, J. M., LU, Z., LU, Q., SUTTON, L. & CHEN, Y. H. 2013. Claudin-7 increases chemosensitivity to cisplatin through the upregulation of caspase pathway in human NCI-H522 lung cancer cells. *Cancer Science*, 104, 611-618.
- HORI, M., SATOU, K., HARASHIMA, H. & KAMIYA, H. 2010. Suppression of mutagenesis by 8-hydroxy-2'-deoxyguanosine 5'-triphosphate (7,8-dihydro-8-oxo-2'-deoxyguanosine 5'-triphosphate) by human MTH1, MTH2, and NUDT5. *Free Radical Biology and Medicine*, 48, 1197-1201.
- HUANG, B. K., STEIN, K. T. & SIKES, H. D. 2016. Modulating and Measuring Intracellular H₂O₂ Using Genetically Encoded Tools to Study Its Toxicity to Human Cells. *ACS Synth Biol*.
- HUBER, K. V. M., SALAH, E., RADIC, B., GRIDLING, M., ELKINS, J. M., STUKALOV, A., JEMTH, A. S., GOKTURK, C., SANJIV, K., STROMBERG,

- K., PHAM, T., BERGLUND, U. W., COLINGE, J., BENNETT, K. L., LOIZOU, J. I., HELLEDAY, T., KNAPP, S. & SUPERTI-FURGA, G. 2014. Stereospecific targeting of MTH1 by (S)-crizotinib as an anticancer strategy. *Nature*, 508, 222-+.
- IIDA, T., FURUTA, A., KAWASHIMA, M., NISHIDA, J., NAKABEPPU, Y. & IWAKI, T. 2001. Accumulation of 8-oxo-2'-deoxyguanosine and increased expression of hMTH1 protein in brain tumors. *Neuro-Oncology*, 3, 73-81.
- IRANI, K., XIA, Y., ZWEIER, J. L., SOLLOTT, S. J., DER, C. J., FEARON, E. R., SUNDARESAN, M., FINKEL, T. & GOLDSCHMIDTCLERMONT, P. J. 1997. Mitogenic signaling mediated by oxidants in ras-transformed fibroblasts. *Science*, 275, 1649-1652.
- ISHIBASHI, T., HAYAKAWA, H. & SEKIGUCHI, M. 2003. A novel mechanism for preventing mutations caused by oxidation of guanine nucleotides. *Embo Reports*, 4, 479-483.
- ITOH, T., TERAZAWA, R., KOJIMA, K., NAKANE, K., DEGUCHI, T., ANDO, M., TSUKAMASA, Y., ITO, M. & NOZAWA, Y. 2011. Cisplatin induces production of reactive oxygen species via NADPH oxidase activation in human prostate cancer cells. *Free Radical Research*, 45, 1033-1039.
- JACKSON, S. P. & BARTEK, J. 2009. The DNA-damage response in human biology and disease. *Nature*, 461, 1071-1078.
- JIANG, K., PEREIRA, E., MAXFIELD, M., RUSSELL, B., GOUDELOCK, D. M. & SANCHEZ, Y. 2003. Regulation of Chk1 includes chromatin association and 14-3-3 binding following phosphorylation on Ser-345. *J Biol Chem*, 278, 25207-17.
- JONES, D. R., BROAD, R. M., COMEAU, L. D., PARSONS, S. J. & MAYO, M. W. 2002. Inhibition of nuclear factor kappa B chemosensitizes non-small cell lung cancer through cytochrome c release and caspase activation. *Journal of Thoracic and Cardiovascular Surgery*, 123, 310-317.
- JOSSEN, R. & BERMEJO, R. 2013. The DNA damage checkpoint response to replication stress: A Game of Forks. *Frontiers in Genetics*, 4.

- KAMIYA, H., CADENA-AMARO, C., DUGUE, L., YAKUSHIJI, H., MINAKAWA, N., MATSUDA, A., POCHE, S., NAKABEPPU, Y. & HARASHIMA, H. 2006. Recognition of nucleotide analogs containing the 7,8-dihydro-8-oxo structure by the human MTH1 protein. *Journal of Biochemistry*, 140, 843-849.
- KAMIYA, H., HORI, M., ARIMORI, T., SEKIGUCHI, M., YAMAGATA, Y. & HARASHIMA, H. 2009. NUDT5 hydrolyzes oxidized deoxyribonucleoside diphosphates with broad substrate specificity. *DNA Repair*, 8, 1250-1254.
- KAMIYA, H. & KASAI, H. 1995. 2-Hydroxyadenine (isoguanine) as oxidative DNA damage: its formation and mutation inducibility. *Nucleic Acids Symp Ser*, 233-4.
- KASTAN, M. B. & LIM, D. S. 2000. The many substrates and functions of ATM. *Nat Rev Mol Cell Biol*, 1, 179-86.
- KAWAMURA, T., KAWATANI, M., MUROI, M., KONDOH, Y., FUTAMURA, Y., AONO, H., TANAKA, M., HONDA, K. & OSADA, H. 2016. Proteomic profiling of small-molecule inhibitors reveals dispensability of MTH1 for cancer cell survival. *Scientific Reports*, 6, 9.
- KAWANISHI, S., HIRAKU, Y. & OIKAWA, S. 2001. Mechanism of guanine-specific DNA damage by oxidative stress and its role in carcinogenesis and aging. *Mutation Research-Reviews in Mutation Research*, 488, 65-76.
- KE, Y. B., LV, Z. Q., YANG, X. F., ZHANG, J. Q., HUANG, J., WU, S. & LI, Y. R. 2014. Compensatory effects of hOGG1 for hMTH1 in oxidative DNA damage caused by hydrogen peroxide. *Toxicology Letters*, 230, 62-68.
- KENNEDY, C. H., PASS, H. I. & MITCHELL, J. B. 2003. Expression of human MutT homologue (hMTH1) protein in primary non-small-cell lung carcinomas and histologically normal surrounding tissue. *Free Radical Biology and Medicine*, 34, 1447-1457.
- KETTLE, J. G., ALWAN, H., BISTA, M., BREED, J., DAVIES, N. L., ECKERSLEY, K., FILLERY, S., FOOTE, K. M., GOODWIN, L., JONES, D. R., KACK, H., LAU, A., NISSINK, J. W. M., READ, J., SCOTT, J. S., TAYLOR, B., WALKER, G., WISSLER, L. & WYLOT, M. 2016. Potent and Selective

- Inhibitors of MTH1 Probe Its Role in Cancer Cell Survival. *Journal of Medicinal Chemistry*, 59, 2346-2361.
- KROKAN, H. E., NILSEN, H., SKORPEN, F., OTTERLEI, M. & SLUPPHAUG, G. 2000. Base excision repair of DNA in mammalian cells. *FEBS Lett*, 476, 73-7.
- KUMAR, B., KOUL, S., KHANDRIKA, L., MEACHAM, R. B. & KOUL, H. K. 2008. Oxidative stress is inherent in prostate cancer cells and is required for aggressive phenotype. *Cancer Research*, 68, 1777-1785.
- LANGER, C. J., BESSE, B., GUALBERTO, A., BRAMBILLA, E. & SORIA, J. C. 2010. The Evolving Role of Histology in the Management of Advanced Non-Small-Cell Lung Cancer. *Journal of Clinical Oncology*, 28, 5311-5320.
- LECHEVALIER, T., BRISGAND, D., DOUILLARD, J. Y., PUJOL, J. L., ALBEROLA, V., MONNIER, A., RIVIERE, A., LIANES, P., CHOMY, P., CIGOLARI, S., GOTTFRIED, M., RUFFIE, P., PANIZO, A., GASPARD, M. H., RAVAIOLI, A., BESEVAL, M., BESSEN, F., MARTINEZ, A., BERTHAUD, P. & TURSZ, T. 1994. RANDOMIZED STUDY OF VINOURELBINE AND CISPLATIN VERSUS VINDESINE AND CISPLATIN VERSUS VINOURELBINE ALONE IN ADVANCED NON-SMALL-CELL LUNG-CANCER - RESULTS OF A EUROPEAN MULTICENTER TRIAL INCLUDING 612 PATIENTS. *Journal of Clinical Oncology*, 12, 360-367.
- LEE, C. H. & CHUNG, J. H. 2001. The hCds1 (Chk2)-FHA domain is essential for a chain of phosphorylation events on hCds1 that is induced by ionizing radiation. *J Biol Chem*, 276, 30537-41.
- LEE, J. A., CARVALHO, C. M. B. & LUPSKI, J. R. 2007. A DNA replication mechanism for generating nonrecurrent rearrangements associated with genomic disorders. *Cell*, 131, 1235-1247.
- LI, C., TENG, R. H., TSAI, Y. C., KE, H. S., HUANG, J. Y., CHEN, C. C., KAO, Y. L., KUO, C. C., BELL, W. R. & SHIEH, B. 2005. H-Ras oncogene counteracts the growth-inhibitory effect of genistein in T24 bladder carcinoma cells. *British Journal of Cancer*, 92, 80-88.

- LIU, G.-Y. & STORZ, P. 2010. Reactive oxygen species in cancer. *Free Radical Research*, 44, 479-496.
- LIU, P. F., EREZ, A., NAGAMANI, S. C. S., DHAR, S. U., KOLODZIEJSKA, K. E., DHARMADHIKARI, A. V., COOPER, M. L., WISZNIEWSKA, J., ZHANG, F., WITHERS, M. A., BACINO, C. A., CAMPOS-ACEVEDO, L. D., DELGADO, M. R., FREEDENBERG, D., GARNICA, A., GREBE, T. A., HERNANDEZ-ALMAGUER, D., IMMKEN, L., LALANI, S. R., MCLEAN, S. D., NORTHRUP, H., SCAGLIA, F., STRATHEARN, L., TRAPANE, P., KANG, S. H. L., PATEL, A., CHEUNG, S. W., HASTINGS, P. J., STANKIEWICZ, P., LUPSKI, J. R. & BI, W. M. 2011. Chromosome Catastrophes Involve Replication Mechanisms Generating Complex Genomic Rearrangements. *Cell*, 146, 888-902.
- LOFFLER, H., REBACZ, B., HO, A. D., LUKAS, J., BARTEK, J. & KRAMER, A. 2006. Chk1-dependent regulation of Cdc25B functions to coordinate mitotic events. *Cell Cycle*, 5, 2543-7.
- LOMAX, M. E., FOLKES, L. K. & O'NEILL, P. 2013. Biological Consequences of Radiation-induced DNA Damage: Relevance to Radiotherapy. *Clinical Oncology*, 25, 578-585.
- LUO, J., SOLIMINI, N. L. & ELLEDGE, S. J. 2009. Principles of Cancer Therapy: Oncogene and Non-oncogene Addiction. *Cell*, 136, 823-837.
- MACPHERSON, P., BARONE, F., MAGA, G., MAZZEI, F., KARRAN, P. & BIGNAMI, M. 2005. 8-Oxoguanine incorporation into DNA repeats in vitro and mismatch recognition by MutS alpha. *Nucleic Acids Research*, 33, 5094-5105.
- MARECHAL, A. & ZOU, L. 2013. DNA Damage Sensing by the ATM and ATR Kinases. *Cold Spring Harbor Perspectives in Biology*, 5.
- MARTIN, S. A. & OUCHI, T. 2008. Cellular commitment to reentry into the cell cycle after stalled DNA is determined by site-specific phosphorylation of Chk1 and PTEN. *Mol Cancer Ther*, 7, 2509-16.
- MARULLO, R., WERNER, E., DEGTYAREVA, N., MOORE, B., ALTAVILLA, G., RAMALINGAM, S. S. & DOETSCH, P. W. 2013. Cisplatin Induces a

- Mitochondrial-ROS Response That Contributes to Cytotoxicity Depending on Mitochondrial Redox Status and Bioenergetic Functions. *PLoS One*, 8.
- MATSUOKA, S., ROTMAN, G., OGAWA, A., SHILOH, Y., TAMAI, K. & ELLEDGE, S. J. 2000. Ataxia telangiectasia-mutated phosphorylates Chk2 in vivo and in vitro. *Proc Natl Acad Sci U S A*, 97, 10389-94.
- MAZOUZI, A., VELIMEZI, G. & LOIZOU, J. I. 2014. DNA replication stress: Causes, resolution and disease. *Experimental Cell Research*, 329, 85-93.
- MAZUREK, A., BERARDINI, M. & FISHEL, R. 2002. Activation of human MutS homologs by 8-oxo-guanine DNA damage. *Journal of Biological Chemistry*, 277, 8260-8266.
- MCLENNAN, A. G. 2006. The Nudix hydrolase superfamily. *Cellular and Molecular Life Sciences*, 63, 123-143.
- MELCHIONNA, R., CHEN, X. B., BLASINA, A. & MCGOWAN, C. H. 2000. Threonine 68 is required for radiation-induced phosphorylation and activation of Cds1. *Nat Cell Biol*, 2, 762-5.
- MENEGHINI, R. 1997. Iron homeostasis, oxidative stress, and DNA damage. *Free Radic Biol Med*, 23, 783-92.
- MERRY, C., FU, K., WANG, J. N., YEH, I. J. & ZHANG, Y. W. 2010. Targeting the checkpoint kinase Chk1 in cancer therapy. *Cell Cycle*, 9, 279-283.
- MILDVAN, A. S., XIA, Z., AZURMENDI, H. F., SARASWAT, V., LEGLER, P. M., MASSIAH, M. A., GABELLI, S. B., BIANCHET, M. A., KANG, L. W. & AMZEL, L. M. 2005. Structures and mechanisms of Nudix hydrolases. *Archives of Biochemistry and Biophysics*, 433, 129-143.
- MISHINA, N. M., TYURIN-KUZMIN, P. A., MARKVICHEVA, K. N., VOROTNIKOV, A. V., TKACHUK, V. A., LAKETA, V., SCHULTZ, C., LUKYANOV, S. & BELOUSOV, V. V. 2011. Does Cellular Hydrogen Peroxide Diffuse or Act Locally? *Antioxidants & Redox Signaling*, 14, 1-7.

- MOISEEVA, O., BOURDEAU, V., ROUX, A., DESCHENES-SIMARD, X. & FERBEYRE, G. 2009. Mitochondrial Dysfunction Contributes to Oncogene-Induced Senescence. *Molecular and Cellular Biology*, 29, 4495-4507.
- MONTANO, R., THOMPSON, R., CHUNG, I., HOU, H., KHAN, N. & EASTMAN, A. 2013. Sensitization of human cancer cells to gemcitabine by the Chk1 inhibitor MK-8776: cell cycle perturbation and impact of administration schedule in vitro and in vivo. *BMC Cancer*, 13.
- MORGAN, M. A., PARSELS, L. A., MAYBAUM, J. & LAWRENCE, T. S. 2008. Improving Gemcitabine-Mediated Radiosensitization Using Molecularly Targeted Therapy: A Review. *Clinical Cancer Research*, 14, 6744-6750.
- NAKABEPPU, Y. 2001. Molecular genetics and structural biology of human MutT homolog, MTH1. *Mutation Research-Fundamental and Molecular Mechanisms of Mutagenesis*, 477, 59-70.
- NAKAMURA, J., LA, D. K. & SWENBERG, J. A. 2000. 5'-nicked apurinic/apyrimidinic sites are resistant to beta-elimination by beta-polymerase and are persistent in human cultured cells after oxidative stress. *Journal of Biological Chemistry*, 275, 5323-5328.
- NICKSON, C. M. & PARSONS, J. L. 2014. Monitoring regulation of DNA repair activities of cultured cells in-gel using the comet assay. *Frontiers in Genetics*, 5, 11.
- NIKITAKI, Z., MAVRAGANI, I. V., LASKARATOU, D. A., GIKA, V., MOSKVIN, V. P., THEOFILATOS, K., VOUGAS, K., STEWART, R. D. & GEORGAKILAS, A. G. 2016. Systemic mechanisms and effects of ionizing radiation: A new 'old' paradigm of how the bystanders and distant can become the players. *Seminars in Cancer Biology*, 37-38, 77-95.
- NISSINK, J. W. M., BISTA, M., BREED, J., CARTER, N., EMBREY, K., READ, J. & WINTER-HOLT, J. J. 2016. MTH1 Substrate Recognition-An Example of Specific Promiscuity. *Plos One*, 11, 16.
- ODA, H., TAKETOMI, A., MARUYAMA, R., ITOH, R., NISHIOKA, K., YAKUSHIJI, H., SUZUKI, T., SEKIGUCHI, M. & NAKABEPPU, Y. 1999.

- Multi-forms of human MTH1 polypeptides produced by alternative translation initiation and single nucleotide polymorphism. *Nucleic Acids Research*, 27, 4335-4343.
- OGURI, T., ACHIWA, H., SATO, S., BESSHO, Y., TAKANO, Y., MIYAZAKI, M., MURAMATSU, H., MAEDA, H., NIIMI, T. & UEDA, R. 2006. The determinants of sensitivity and acquired resistance to gemcitabine differ in non-small cell lung cancer: a role of ABCC5 in gemcitabine sensitivity. *Molecular Cancer Therapeutics*, 5, 1800-1806.
- OKA, S., OHNO, M., TSUCHIMOTO, D., SAKUMI, K., FURUICHI, M. & NAKABEPPU, Y. 2008. Two distinct pathways of cell death triggered by oxidative damage to nuclear and mitochondrial DNAs. *Embo Journal*, 27, 421-432.
- OKAMOTO, K., TOYOKUNI, S., KIM, W. J., OGAWA, O., KAKEHI, Y., ARAO, S., HIAI, H. & YOSHIDA, O. 1996. Overexpression of human mutT homologue gene messenger RNA in renal-cell carcinoma: Evidence of persistent oxidative stress in cancer. *International Journal of Cancer*, 65, 437-441.
- OLAUSSEN, K. A., DUNANT, A., FOURET, P., BRAMBILLA, E., ANDRÉ, F., HADDAD, V., TARANCHON, E., FILIPITS, M., PIRKER, R., POPPER, H. H., STAHEL, R., SABATIER, L., PIGNON, J.-P., TURSZ, T., LE CHEVALIER, T. & SORIA, J.-C. 2006. DNA Repair by ERCC1 in Non-Small-Cell Lung Cancer and Cisplatin-Based Adjuvant Chemotherapy. *New England Journal of Medicine*, 355, 983-991.
- OLINSKI, R., GACKOWSKI, D., ROZALSKI, R., FOKSINSKI, M. & BIALKOWSKI, K. 2003. Oxidative DNA damage in cancer patients: a cause or a consequence of the disease development? *Mutation Research-Fundamental and Molecular Mechanisms of Mutagenesis*, 531, 177-190.
- OVCHARENKO, D., JARVIS, R., HUNICKE-SMITH, S., KELNAR, K. & BROWN, D. 2005. High-throughput RNAi screening in vitro: From cell lines to primary cells. *Rna-a Publication of the Rna Society*, 11, 985-993.

- PANIERI, E., GOGVADZE, V., NORBERG, E., VENKATESH, R., ORRENIUS, S. & ZHIVOTOVSKY, B. 2013. Reactive oxygen species generated in different compartments induce cell death, survival, or senescence. *Free Radical Biology and Medicine*, 57, 176-187.
- PAPEO, G. 2016. MutT Homolog 1 (MTH1): The Silencing of a Target. *Journal of Medicinal Chemistry*, 59, 2343-2345.
- PATEL, A., BURTON, D. G. A., HALVORSEN, K., BALKAN, W., REINER, T., PEREZ-STABLE, C., COHEN, A., MUNOZ, A., GIRIBALDI, M. G., SINGH, S., ROBBINS, D. J., NGUYEN, D. M. & RAI, P. 2015. MutT Homolog 1 (MTH1) maintains multiple KRAS-driven pro-malignant pathways. *Oncogene*, 34, 2586-2596.
- PETROCCHI, A., LEO, E., REYNA, N. J., HAMILTON, M. M., SHI, X., PARKER, C. A., MSEEH, F., BARDENHAGEN, J. P., LEONARD, P., CROSS, J. B., HUANG, S., JIANG, Y. Y., CARDOZO, M., DRAETTA, G., MARSZALEK, J. R., TONIATTI, C., JONES, P. & LEWIS, R. T. 2016. Identification of potent and selective MTH1 inhibitors. *Bioorganic & Medicinal Chemistry Letters*, 26, 1503-1507.
- PETROS, J. A., BAUMANN, A. K., RUIZ-PESINI, E., AMIN, M. B., SUN, C. Q., HALL, J., LIM, S., ISSA, M. M., FLANDERS, W. D., HOSSEINI, S. H., MARSHALL, F. F. & WALLACE, D. C. 2005. mtDNA mutations increase tumorigenicity in prostate cancer. *Proceedings of the National Academy of Sciences of the United States of America*, 102, 719-724.
- POTTS, R. J., BESPALOV, I. A., WALLACE, S. S., MELAMEDE, R. J. & HART, B. A. 2001. Inhibition of oxidative DNA repair in cadmium-adapted alveolar epithelial cells and the potential involvement of metallothionein. *Toxicology*, 161, 25-38.
- PUIGVERT, J. C., SANJIV, K. & HELLEDAY, T. 2016. Targeting DNA repair, DNA metabolism and replication stress as anti-cancer strategies. *Febs Journal*, 283, 232-245.

- RAI, P. 2010. Oxidation in the nucleotide pool, the DNA damage response and cellular senescence: Defective bricks build a defective house. *Mutation Research-Genetic Toxicology and Environmental Mutagenesis*, 703, 71-81.
- RAI, P. 2012. Human Mut T Homolog 1 (MTH1): a roadblock for the tumor-suppressive effects of oncogenic RAS-induced ROS. *Small GTPases*, 3, 120-5.
- RAI, P., ONDER, T. T., YOUNG, J. J., MCFALINE, J. L., PANG, B., DEDON, P. C. & WEINBERG, R. A. 2009. Continuous elimination of oxidized nucleotides is necessary to prevent rapid onset of cellular senescence. *Proceedings of the National Academy of Sciences of the United States of America*, 106, 169-174.
- RAI, P., YOUNG, J. J., BURTON, D. G. A., GIRIBALDI, M. G., ONDER, T. T. & WEINBERG, R. A. 2011. Enhanced elimination of oxidized guanine nucleotides inhibits oncogenic RAS-induced DNA damage and premature senescence. *Oncogene*, 30, 1489-1496.
- RAMPAZZO, C., MIAZZI, C., FRANZOLIN, E., PONTARIN, G., FERRARO, P., FRANGINI, M., REICHARD, P. & BIANCHI, V. 2010. Regulation by degradation, a cellular defense against deoxyribonucleotide pool imbalances. *Mutation Research-Genetic Toxicology and Environmental Mutagenesis*, 703, 2-10.
- RAPONI, M., ZHANG, Y., YU, J., CHEN, G., LEE, G., TAYLOR, J. M. G., MACDONALD, J., THOMAS, D., MOSKALUK, C., WANG, Y. X. & BEER, D. G. 2006. Gene expression signatures for predicting prognosis of squamous cell and adenocarcinomas of the lung. *Cancer Research*, 66, 7466-7472.
- RECK, M., POPAT, S., REINMUTH, N., DE RUYSSCHER, D., KERR, K. M., PETERS, S. & GRP, E. G. W. 2014. Metastatic non-small-cell lung cancer (NSCLC): ESMO Clinical Practice Guidelines for diagnosis, treatment and follow-up. *Annals of Oncology*, 25, 27-39.
- REGAIRAZ, M., ZHANG, Y. W., FU, H. Q., AGAMA, K. K., TATA, N., AGRAWAL, S., ALADJEM, M. I. & POMMIER, Y. 2011. Mus81-mediated DNA cleavage resolves replication forks stalled by topoisomerase I-DNA complexes. *Journal of Cell Biology*, 195, 739-749.

- ROZALSKI, R., SIOMEK, A., GACKOWSKI, D., FOKSINSKI, M., GRAN, C., KLUNGLAND, A. & OLINSKI, R. 2005. Substantial decrease of urinary 8-oxo-7,8-dihydroguanine, a product of the base excision repair pathway, in DNA glycosylase defective mice. *International Journal of Biochemistry & Cell Biology*, 37, 1331-1336.
- RUSSO, M. T., BLASI, M. F., CHERA, F., FORTINI, P., DEGAN, P., MACPHERSON, P., FURUICHI, M., NAKABEPPU, Y., KARRAN, P., AQUILINA, G. & BIGNAMI, M. 2004. The oxidized deoxynucleoside triphosphate pool is a significant contributor to genetic instability in mismatch repair-deficient cells. *Molecular and Cellular Biology*, 24, 465-474.
- SAKUMI, K., FURUICHI, M., TSUZUKI, T., KAKUMA, T., KAWABATA, S., MAKI, H. & SEKIGUCHI, M. 1993. CLONING AND EXPRESSION OF CDNA FOR A HUMAN ENZYME THAT HYDROLYZES 8-OXO-DGTP, A MUTAGENIC SUBSTRATE FOR DNA-SYNTHESIS. *Journal of Biological Chemistry*, 268, 23524-23530.
- SAKUMI, K., TOMINAGA, Y., FURUICHI, M., XU, P., TSUZUKI, T., SEKIGUCHI, M. & NAKABEPPU, Y. 2003. Ogg1 knockout-associated lung tumorigenesis and its suppression by Mth1 gene disruption. *Cancer Research*, 63, 902-905.
- SALEH, A., GOKTURK, C., WARPMAN-BERGLUND, U., HELLEDAY, T. & GRANELLI, I. 2015. Development and validation of method for TH588 and TH287, potent MTH1 inhibitors and new anti-cancer agents, for pharmacokinetic studies in mice plasma. *Journal of Pharmaceutical and Biomedical Analysis*, 104, 1-11.
- SATOU, K., HARASHIMA, H. & KAMIYA, H. 2003. Mutagenic effects of 2-hydroxy-dATP on replication in a HeLa extract: induction of substitution and deletion mutations. *Nucleic Acids Research*, 31, 2570-2575.
- SATOU, K., KASAI, H., MASUTANI, C., HANAOKA, F., HARASHIMA, H. & KAMIYA, H. 2007a. 2-hydroxy-2'-deoxyadenosine 5'-triphosphate enhances A center dot T -> C center dot G mutations caused by 8-hydroxy-2'-deoxyguanosine 5'-triphosphate by suppressing its degradation upon replication in a HeLa extract. *Biochemistry*, 46, 6639-6646.

- SATOU, K., KAWAI, K., KASAI, H., HARASHIMA, H. & KAMIYA, H. 2007b. Mutagenic effects of 8-hydroxy-dGTP in live mammalian cells. *Free Radical Biology and Medicine*, 42, 1552-1560.
- SEKIGUCHI, M. 2006. Molecular devices for high fidelity of DNA replication and gene expression. *Proceedings of the Japan Academy Series B-Physical and Biological Sciences*, 82, 278-296.
- SETOYAMA, D., ITO, R., TAKAGI, Y. & SEKIGUCHI, M. 2011. Molecular actions of Escherichia coli MutT for control of spontaneous mutagenesis. *Mutation Research-Fundamental and Molecular Mechanisms of Mutagenesis*, 707, 9-14.
- SFIKAS, A., BATSI, C., TSELIKOU, E., VARTHOLOMATOS, G., MONOKROUSOS, N., PAPPAS, P., CHRISTOFORIDIS, S., TZAVARAS, T., KANAVAROS, P., GORGOULIS, V. G., MARCU, K. B. & KOLETTAS, E. 2012. The canonical NF-kappa B pathway differentially protects normal and human tumor cells from ROS-induced DNA damage. *Cellular Signalling*, 24, 2007-2023.
- SHENG, Z. J., OKA, S., TSUCHIMOTO, D., ABOLHASSANI, N., NOMARU, H., SAKUMI, K., YEMADA, H. & NAKABEPPU, Y. 2012. 8-Oxoguanine causes neurodegeneration during MUTYH-mediated DNA base excision repair. *Journal of Clinical Investigation*, 122, 4344-4361.
- SHIBUTANI, S., TAKESHITA, M. & GROLLMAN, A. P. 1991. Insertion of specific bases during DNA synthesis past the oxidation-damaged base 8-oxodG.
- SHIMIZU, M., GRUZ, P., KAMIYA, H., KIM, S. R., PISANI, F. M., MASUTANI, C., KANKE, Y., HARASHIMA, H., HANAOKA, F. & NOHMI, T. 2003. Erroneous incorporation of oxidized DNA precursors by Y-family DNA polymerases. *Embo Reports*, 4, 269-273.
- SHIOTANI, B. & ZOU, L. 2009. Single-Stranded DNA Orchestrates an ATM-to-ATR Switch at DNA Breaks. *Molecular Cell*, 33, 547-558.
- SINGH, N. P., MCCOY, M. T., TICE, R. R. & SCHNEIDER, E. L. 1988. A SIMPLE TECHNIQUE FOR QUANTITATION OF LOW-LEVELS OF DNA

- DAMAGE IN INDIVIDUAL CELLS. *Experimental Cell Research*, 175, 184-191.
- SPEINA, E., ARCZEWSKA, K. D., GACKOWSKI, D., ZIELINSKA, M., SIOMEK, A., KOWALEWSKI, J., OLINSKI, R., TUDEK, B. & KUSMIEREK, J. T. 2005. Contribution of hMTH1 to the maintenance of 8-oxoguanine levels in lung DNA of non-small-cell lung cancer patients. *Journal of the National Cancer Institute*, 97, 384-395.
- STANFORD, J. S. & RUDERMAN, J. V. 2005. Changes in regulatory phosphorylation of cdc25c Ser287 and wee1 Ser549 during normal cell cycle progression and checkpoint arrests. *Molecular Biology of the Cell*, 16, 5749-5760.
- STRUMBERG, D., PILON, A. A., SMITH, M., HICKEY, R., MALKAS, L. & POMMIER, Y. 2000. Conversion of Topoisomerase I Cleavage Complexes on the Leading Strand of Ribosomal DNA into 5'-Phosphorylated DNA Double-Strand Breaks by Replication Runoff. *Molecular and Cellular Biology*, 20, 3977-3987.
- SVENSSON, L. M., JEMTH, A. S., DESROSES, M., LOSEVA, O., HELLEDAY, T., HOGBOM, M. & STENMARK, P. 2011. Crystal structure of human MTH1 and the 8-oxo-dGMP product complex. *Febs Letters*, 585, 2617-2621.
- SZATROWSKI, T. P. & NATHAN, C. F. 1991. PRODUCTION OF LARGE AMOUNTS OF HYDROGEN-PEROXIDE BY HUMAN TUMOR-CELLS. *Cancer Research*, 51, 794-798.
- TAKAGI, Y., SETOYAMA, D., ITO, R., KAMIYA, H., YAMAGATA, Y. & SEKIGUCHI, M. 2012. Human MTH3 (NUDT18) Protein Hydrolyzes Oxidized Forms of Guanosine and Deoxyguanosine Diphosphates COMPARISON WITH MTH1 AND MTH2. *Journal of Biological Chemistry*, 287, 21541-21549.
- TAKENAKA, T., YOSHINO, I., KOUSO, H., OHBA, T., YOHENA, T., OSOEGAWA, A., SHOJI, F. & MAEHARA, Y. 2007. Combined evaluation of Rad51 and ERCC1 expressions for sensitivity to platinum agents in non-small cell lung cancer. *International Journal of Cancer*, 121, 895-900.

- TCHOU, J., BODEPUDI, V., SHIBUTANI, S., ANTOSHECHKIN, I., MILLER, J., GROLLMAN, A. P. & JOHNSON, F. 1994. SUBSTRATE-SPECIFICITY OF FPG PROTEIN - RECOGNITION AND CLEAVAGE OF OXIDATIVELY DAMAGED DNA. *Journal of Biological Chemistry*, 269, 15318-15324.
- TENG, X., DAYHOFF-BRANNIGAN, M., CHENG, W. C., GILBERT, C. E., SING, C. N., DINY, N. L., WHEELAN, S. J., DUNHAM, M. J., BOEKE, J. D., PINEDA, F. J. & HARDWICK, J. M. 2013. Genome-wide Consequences of Deleting Any Single Gene. *Molecular Cell*, 52, 485-494.
- TKESHELASHVILI, L. K., MCBRIDE, T., SPENCE, K. & LOEB, L. A. 1991. MUTATION SPECTRUM OF COPPER-INDUCED DNA DAMAGE. *Journal of Biological Chemistry*, 266, 6401-6406.
- TOLEDO, L. I., MURGA, M. & FERNANDEZ-CAPETILLO, O. 2011. Targeting ATR and Chk1 kinases for cancer treatment: A new model for new (and old) drugs. *Molecular Oncology*, 5, 368-373.
- TOMODA, Y., KATSURA, M., OKAJIMA, M., HOSOYA, N., KOHNO, N. & MIYAGAWA, K. 2009. Functional evidence for Eme1 as a marker of cisplatin resistance. *International Journal of Cancer*, 124, 2997-3001.
- TOPAL, M. D. & BAKER, M. S. 1982. DNA PRECURSOR POOL - A SIGNIFICANT TARGET FOR N-METHYL-N-NITROSOUREA IN C3H-10T1/2 CLONE 8 CELLS. *Proceedings of the National Academy of Sciences of the United States of America-Biological Sciences*, 79, 2211-2215.
- TOSCHI, L. & CAPPUZZO, F. 2009. Gemcitabine for the treatment of advanced nonsmall cell lung cancer. *OncoTargets and Therapy*, 2, 209-217.
- TOYOOKA, S., MARUYAMA, R., TOYOOKA, K. O., MCLERRAN, D., FENG, Z. D., FUKUYAMA, Y., VIRMANI, A. K., ZOCHBAUER-MULLER, S., TSUKUDA, K., SUGIO, K., SHIMIZU, N., SHIMIZU, K., LEE, H., CHEN, C. Y., FONG, K. M., GILCREASE, M., ROTH, J. A., MINNA, J. D. & GAZDAR, A. F. 2003. Smoke exposure, histologic type and geography-related differences in the methylation profiles of non-small cell lung cancer. *International Journal of Cancer*, 103, 153-160.

- TRACHOOTHAM, D., ALEXANDRE, J. & HUANG, P. 2009. Targeting cancer cells by ROS-mediated mechanisms: a radical therapeutic approach? *Nature Reviews Drug Discovery*, 8, 579-591.
- TSUZUKI, T., EGASHIRA, A. & KURA, S. 2001. Analysis of MTH1 gene function in mice with targeted mutagenesis. *Mutation Research-Fundamental and Molecular Mechanisms of Mutagenesis*, 477, 71-78.
- TSUZUKI, T., EGASHIRA, A., YAMAUCHI, K., YOSHIYAMA, K. & MAKI, H. 2002. Spontaneous tumorigenesis and mutagenesis in mice defective in the MTH1 gene encoding 8-oxo-dGTPase. In: SUGAHARA, T., NIKAIDO, O. & NIWA, O. (eds.) *Radiation and Homeostasis, Proceedings*.
- TU, Y. Y., WANG, Z., WANG, X., YANG, H. W., ZHANG, P. X., JOHNSON, M., LIU, N., LIU, H., JIN, W. L., ZHANG, Y. S. & CUI, D. X. 2016. Birth of MTH1 as a therapeutic target for glioblastoma: MTH1 is indispensable for gliomatumorigenesis. *American Journal of Translational Research*, 8, 2803-+.
- UN, F. 2007. G(1) arrest induction represents a critical determinant for cisplatin cytotoxicity in G(1) checkpoint-retaining human cancers. *Anti-Cancer Drugs*, 18, 411-417.
- USHIJIMA, Y., TOMINAGA, Y., MIURA, T., TSUCHIMOTO, D., SAKUMI, K. & NAKABEPPU, Y. 2005. A functional analysis of the DNA glycosylase activity of mouse MUTYH protein excising 2-hydroxyadenine opposite guanine in DNA. *Nucleic Acids Research*, 33, 672-682.
- VALKO, M., RHODES, C. J., MONCOL, J., IZAKOVIC, M. & MAZUR, M. 2006. Free radicals, metals and antioxidants in oxidative stress-induced cancer. *Chemico-Biological Interactions*, 160, 1-40.
- VAN ENGELAND, M., NIELAND, L. J. W., RAMAEKERS, F. C. S., SCHUTTE, B. & REUTELINGSPERGER, C. P. M. 1998. Annexin V-affinity assay: A review on an apoptosis detection system based on phosphatidylserine exposure. *Cytometry*, 31, 1-9.
- VON HOFF, D. D. 1990. He's not going to talk about in vitro predictive assays again, is he? *J Natl Cancer Inst*, 82, 96-101.

- WACHECK, V. & ZANGEMEISTER-WITTKE, U. 2006. Antisense molecules for targeted cancer therapy. *Crit Rev Oncol Hematol*, 59, 65-73.
- WANG, H. & HAYS, J. B. 2007. Human DNA mismatch repair: coupling of mismatch recognition to strand-specific excision. *Nucleic Acids Research*, 35, 6727-6739.
- WANG, J. Y., JIN, L., YAN, X. G., SHERWIN, S., FARRELLY, M., ZHANG, Y. Y., LIU, F., WANG, C. Y., GUO, S. T., YARI, H., LA, T., MCFARLANE, J., LEI, F. X., TABATABAEE, H., CHEN, J. Z., CROFT, A., JIANG, C. C. & ZHANG, X. D. 2016. REACTIVE OXYGEN SPECIES DICTATE THE APOPTOTIC RESPONSE OF MELANOMA CELLS TO TH588. *Asia-Pacific Journal of Clinical Oncology*, 12, 33-33.
- WANI, G., MILO, G. E. & D'AMBROSIO, S. M. 1998. Enhanced expression of the 8-oxo-7,8-dihydrodeoxyguanosine triphosphatase gene in human breast tumor cells. *Cancer Lett*, 125, 123-130.
- WELCH, K. D., DAVIS, T. Z., VAN EDEN, M. E. & AUST, S. D. 2002. Deleterious iron-mediated oxidation of biomolecules. *Free Radical Biology and Medicine*, 32, 577-583.
- WU, B. Y., LIU, R. Y., SO, K. L. & YU, A. C. H. 2000. Multi-lipofection efficiently transfected genes into astrocytes in primary culture. *Journal of Neuroscience Methods*, 102, 133-141.
- YOSHIMURA, D., SAKUMI, K., OHNO, M., SAKAI, Y., FURUICHI, M., IWAI, S. & NAKABEPPU, Y. 2003. An oxidized purine nucleoside triphosphatase, MTH1, suppresses cell death caused by oxidative stress. *Journal of Biological Chemistry*, 278, 37965-37973.
- YOUN, C. K., JUN, J. Y., HYUN, J. W., HWANG, G., LEE, B. R., CHUNG, M. H., CHANG, I. Y. & YOU, H. J. 2008. hMTH1 depletion promotes oxidative-stress-induced apoptosis through a Noxa- and caspase-3/7-mediated signaling pathway. *DNA Repair*, 7, 1809-1823.
- ZASTAWNY, T. H., ALTMAN, S. A., RANDERSEICHHORN, L., MADURAWA, R., LUMPKIN, J. A., DIZDAROGLU, M. & RAO, G. 1995. DNA-BASE MODIFICATIONS AND MEMBRANE DAMAGE IN CULTURED-

- MAMMALIAN-CELLS TREATED WITH IRON IONS. *Free Radical Biology and Medicine*, 18, 1013-1022.
- ZEMAN, M. K. & CIMPRICH, K. A. 2014. Causes and consequences of replication stress. *Nature Cell Biology*, 16, 2-9.
- ZENG, Y., FORBES, K. C., WU, Z., MORENO, S., PIWNICA-WORMS, H. & ENOCH, T. 1998. Replication checkpoint requires phosphorylation of the phosphatase Cdc25 by Cds1 or Chk1. *Nature*, 395, 507-10.
- ZHANG, F., KHAJAVI, M., CONNOLLY, A. M., TOWNE, C. F., BATISH, S. D. & LUPSKI, J. R. 2009. The DNA replication FoSTeS/MMBIR mechanism can generate genomic, genic and exonic complex rearrangements in humans. *Nature Genetics*, 41, 849-U115.
- ZHANG, Y. W. & HUNTER, T. 2014. Roles of Chk1 in cell biology and cancer therapy. *International Journal of Cancer*, 134, 1013-1023.
- ZHAO, H. & PIWNICA-WORMS, H. 2001. ATR-mediated checkpoint pathways regulate phosphorylation and activation of human Chk1. *Mol Cell Biol*, 21, 4129-39.
- ZHAO, Y. L., EL-GABRY, M. & HEI, T. K. 2006. Loss of Betaig-h3 protein is frequent in primary lung carcinoma and related to tumorigenic phenotype in lung cancer cells. *Molecular Carcinogenesis*, 45, 84-92.
- ZHENG, J. D., HEI, A. L., ZUO, P. P., DONG, Y. L., SONG, X. N., TAKAGI, Y., SEKIGUCHI, M. & CAI, J. P. 2009. Age-related alterations in the expression of MTH2 in the hippocampus of the SAMP8 mouse with learning and memory deterioration. *Journal of the Neurological Sciences*, 287, 188-196.
- ZHOU, J., OLIVEIRA, P., LI, X., CHEN, Z. & BEPLER, G. 2010. Modulation of the ribonucleotide reductase-antimetabolite drug interaction in cancer cell lines. *Journal of nucleic acids*, 2010, 597098.